The University Of Sheffield.

TMEM203 is a putative co-receptor of innate immune adaptor protein STING

Yang Li

A thesis submitted in partial fulfilment of the requirements for the degree of

Doctor of Philosophy

The University of Sheffield

Faculty of Medicine, Dentistry & Health,

Department of Infection, Immunity & Cardiovascular Disease (IICD)

Submission date: Jan 2019

Table of Contents

Table of Figures

Main thesis:

Paper 1:

Paper 2:

Paper 3:

Appendix:

Alternative Format Submission

This thesis is presented as an alternative thesis format to allow the incorporation of published works. This format consists of an introduction, a literature review, two result chapters presented in manuscript form and as an EMBO short-term fellowship end report, two chapters of discussion, references and appendices containing supplementary methods.

List of Publications

Paper 1:

Li Y, Wilson HL & Kiss-Toth E. Regulating STING in health and disease. *J Inflamm (Lond).* 2017; 14:11, eCollection 2017. doi: 10.1186/s12950-017-0159-2. Published.

This reviewed is presented on Page 38 and is presented as the format of accepted manuscript by the Journal.

Paper 2:

Li Y, James SJ, Wyllie DH, Wynne C, Czibula A, Pye K, Mustafah SMB, Fajka-Boja R, Angyal A, Hegedus Z, Kovacs L, Hill AVS, Jefferies CA, Wilson HL, Yongliang Z & Kiss-Toth E. TMEM203 is a novel binding partner and regulator of STING mediated inflammatory signalling in macrophages. PNAS, 2019. (In revision.)

This work is presented on Page 130 and is presented as the format of submitted manuscript.

Paper 3:

Li Y, Décembre E, Kiss-Toth E & Dreux M. STING regulation in response to Zika virus and Dengue virus infection in primary human monocyte-derived macrophages. EMBO Short Term Fellowship End Report. 2018. (Submitted to complete award requirement.)

This work is presented on Page 201 and is presented as the format of submitted manuscript to European Molecular Biology Organization as an End Report for the award of the fellowship.

Declaration

All the work presented in this thesis is my own unless otherwise stated. I confirm I have carried out over 90% of the experiments, with minor support from our technical staff and kind colleagues. Work produced in Paper 2 Fig 6C has been submitted in support of a Master's degree thesis to the University of Sheffield, UK, by Katherine Pye. I declare that no other work presented in this thesis has been used in application for another degree or qualification in this or any other educational institute.

Acknowledgements

I truly appreciate the support from Professor Yongliang Zhang's team at the National University of Singapore who helped us complete the manuscript (Paper 2) to characterise the role of TMEM203 in inflammatory signalling. Further appreciation is given to the following teams: MRC Harwell offered the *Tmem203* knockout mice hind limbs for isolation of bone marrow; David Borough's lab at University of Manchester produced and provided the immortalised murine bone marrow-derived macrophage (iBMDM) cell line; Dr Marlene Dreux's group acquired the human blood samples and carried out all the virus work at Level 3 bio-safety laboratory.

This PhD project was financially supported by the Faculty of Medicine, Dentistry and Health (The Medical School, University of Sheffield) who provided my scholarship and research funding. The collaborative work between our lab and Dr Marlene Dreux lab at ENS Lyon was supported by an EMBO short term fellowship award (ASTF_7459).

I wish to thank the following people for their support that underpins the enjoyment of my doctoral life:

Help is highly appreciated by Vera Kiss-Toth (cloning & microbiology), flow cytometry technicians, microscopy technician, NHS clinical research staffs, all our tissue culture technicians and core facility technicians.

I truly appreciate the support from my lab fellows Jess, Laura, Taewoo, Anjana and Merete, and many thanks to Katherine and Rosemary who put extensive effort into the Renilla PCA assay with me, you are all indispensable helpers and friends to me. Greatest thanks to my best friend and lab mate Chiara, for all your help, caring and concerns about me. I wish you a lucky future both in research and life.

I wish to thank my supervisors and “academic parents” Endre and Heather for giving me this opportunity. Your encouragement pushes me to surpass myself every day and made me confident to face very task. I hope your research advances steadily and rapidly.

I give my sincere thanks to my parents who gave me this life and supported me throughout the two decades. All my achievements sprout from you.

The final and wholehearted thanks is for my husband Zihao who has contributed extensively by keeping me surviving the past three years. You are the one that shares my happiness, understands my struggles, supports me in every pitfall and tolerates my every wrong. I cannot imagine a life without your love and accompany.

List of Abbreviations

(ds)DNA	(Double-stranded) deoxyribonucleic acid
(ss)RNA	(Single-stranded) Ribonucleic acid
2’-3’ cGAMP	2’-3’ Cyclic GMP-AMP
3’-3’ cGAMP	3’-3’ Cyclic GMP-AMP
AIM2	Absence in melanoma 2
AMP	Adenosine monophosphate
AP-1	Activator protein 1
ATP	Adenosine triphosphate
BCA	Bicinchoninic acid (assay)
BMDM	(Mouse) bone marrow-derived macrophage
CD14	Class of differentiation 14
CDN	Cyclic dinucleotide
cGAS	Cyclic di-GMP-AMP synthase
CLR	C-type Lectin receptor
DAMP	Danger associated molecular pattern
DDX41	DEAD-Box helicase 41
DENV	Dengue virus
DMXAA	5,6-Dimethylxanthenone-4-acetic acid
ER	Endoplasmic reticulum
FCL	Familial chilblain lupus
GAF	Gamma-interferon activating factor
GBP1	Guanylate-binding protein 1
GFP	Green fluorescent protein
GMP	Guanosine monophosphate
HAQ	STING variant R71H-G230A-R293Q
HCV	Hepatitis C virus
HIV	Human immunodeficiency virus
iBMDM	(Mouse) immortalised bone marrow-derived macrophage
IFI16	Interferon-gamma inducible protein 16
IFIT1	Interferon-induced protein with tetratricopeptide repeats 1

IFNAR	Interferon-α receptor
IFNGR	Interferon-γ receptor
IFN-I	Type I interferon
IFN-α	Interferon-α
IFN-β	Interferon-β
IFN-γ	Interferon-γ
IFN-λ	Interferon-λ
IKKs	IκB kinase
IL-1	Interleukin-1
iNOS	Inducible nitric oxide synthase
IP-30	Gamma-interferon-inducible protein 30
IP3R	Inositol 1, 4, 5-triphosphate receptor
IRAK	Interleukin-1 receptor-associated kinase 1
IRF3	Interferon regulatory factor 3
IRF9	Interferon regulatory factor 9
ISG	Interferon stimulating gene
ISG15	Interferon-stimulated gene 15
ISGF3	Interferon stimulating gene factor 3
ISRE	Interferon-stimulated response element
JAK	Janus kinase
JEV	Japanese encephalitis virus
KO	Knockout
LC	Langerhans cell
LCMV	Lymphocytic choriomeningitis virus
LGP2	Laboratory of genetics and physiology 2
LPS	Lipopolysaccharide
Mal	MyD88 associated protein
MAM	Mitochondria-associated membrane
MAPK	Mitogen-activated protein kinase
MAVS	Mitochondrial antiviral signalling protein
M-CSF	Macrophage-colony stimulating factor
MDA5	Melanoma differentiation associated factor 5

MDM	(Human) monocyte-derived macrophage
MET	Macrophage extracellular traps
MHC II	Major histocompatibility complex class II
MxA	Myxovirus resistance protein 1
MyD88	Myeloid differentiation primary response 88
NET	Neutrophil extracellular traps
NF-κB	Nuclear factor kappa-light-chain-enhancer of B cells
NLR	NOD-like receptor
OAS	Oligoadenylate synthase
PAMP	Pathogen associated molecular pattern
PCA	Protein complementation assay
PDHX	Pyruvate dehydrogenase complex component X
PKR	Protein kinase R
PRD	Positive regulatory domain
PRR	Pattern recognition receptor
RIG-I	Retinoic acid-inducible gene
RLR	RIG-I –like receptor
SAVI	STING-associated vasculopathy with onset in infancy
SERCA	Sarcoplasmic/endoplasmic reticulum calcium ATPase
SLE	Systemic lupus erythematosus
STAT	Signal transduces and activators of transcription
STIM1	Stromal interaction molecule 1
STING	Stimulator of Interferon Genes
TAB	TGF-beta activated kinase
TAK1	TGF beta-activated kinase 1
TBK1	TANK binding kinase
TGF-β	Transforming growth factor-β
TIRAP	Toll/interleukin-1 receptor domain-containing adaptor protein
TLR4	Toll-like receptor 4
TMEM203	Transmembrane protein 203
TNF-α	Tumour necrotic factor-α
TRAF	TNF receptor-associated factor

TRAM	Translocating chain-associated membrane protein 2
TRIF	TIR-domain-containing adaptor-inducing interferon-β
TyK	Tyrosin kinase
V1/V2	Venus1/Venus2
VSV	Vesicular stomatitis virus
WNV	West Nile virus
WT	Wildtype
YFP	Yellow fluorescent protein
YFV	Yellow Fever virus
ZIKV	Zika virus

Abstract

Acute inflammation is the innate immune defence against environmental disturbances. Macrophages are one of the central immune cells that react to infections and maintain tissue homeostasis, and they exhibit their functions via numerous inflammatory signalling regulators. In addition to previously identified immune mediators, novel proteins involved in inflammation continue to emerge.

A previous cDNA functional screening in murine macrophages has identified a novel protein named transmembrane protein 203 (Tmem203) displaying pro-inflammatory characteristics. Tmem203-promoted inflammatory activities were found to be TLR independent but dependent on STING, a cytosolic innate immune adaptor for DNA detection. STING responds to upstream DNA sensors and microbial cyclic dinucleotides, and instigates type I interferon response via TBK1-IRF3 axis.

The work in this thesis investigated the function of TMEM203 in STING-dependent type I interferon responses. TMEM203 has been found to colocalise, interact and migrate with STING. Further studies revealed a critical role for TMEM203 in STING-dependent type I interferon response in both human and mouse primary macrophages. We showed that TMEM203-STING association was highly dependent on STING's N-terminal transmembrane domains. Finally, TMEM203 showed a distinct regulation of STING-interferon signalling between stimulation by natural and synthetic STING ligands, and this difference was also reflected in TMEM203-STING interaction. Thus, this novel mechanism of TMEM203-dependent STING regulation has brought new insights to better understand critical regulators of pathogen infections and interferon-associated autoimmune diseases.

Additionally, a brief research was conducted to explore STING regulation in flavivirus infected primary macrophages. Flaviviruses Dengue virus and Zika virus infect humans to cause global pandemics. Dengue virus is known to specifically and potently interrupt STING-interferon pathway. The emerging flavivirus Zika virus is genetically-

closely related to Dengue virus and thus it has been hypothesised to adopt similar strategies in STING antagonism. We have investigated Dengue and Zika virus-induced type I interferon stimulated ISG response in the M-CSF differentiated primary macrophage model, and tested the role of STING in such conditions. Contradictory to previous report, our experiments showed a potent and persistent ISG induction in virus-infected macrophages. Prior virus infections were unable to intercept ISG induction cause by STING ligands, whereas the downregulation of STING dampens virus-induced ISG response. Therefore, this primary macrophage model highlights alternative regulatory mechanisms via STING in response to Dengue and Zika virus.

Chapter 1: Introduction

1.1 Inflammation

Inflammation is the response of the immune system to a variety of physiological disturbances, such as metabolic stress, damage, pathogen invasions, and senescence-associated cell and tissue failure. Our understanding of inflammation evolves with the discovery of novel diseases and the manifestations associated with them. Although inflammatory responses often result in irritations such as heat, pain, swelling, and sometimes the loss of mobility, it nonetheless has crucial roles in detecting, acting and restoring host immune homeostasis. The process of inflammation is evolved for two major functions, one is to limit infection by pathogens, predominantly bacteria and viruses, and another is to facilitate wound healing. The dysregulation of inflammatory response in diseases helped us to identify cellular and molecular components that composed the immune system and to understand how they are coordinated during disorders. Not only that the immune cells are capable of inflammatory activation, a variety of somatic cells are also able to respond to innate immune stimuli, including for instance endothelial and epithelial cells [1, 2].

The immune system can mount both the immediate innate response against stimuli encountered for the first time and the adaptive response to a recurrent challenge, both have been extensively reviewed in the past [3–6]. In comparison to adaptive immunity which protects host from a specific recurrent stimulus, innate immunity acts on a wide spectrum of antigens and the response is rapid and dynamic. Therefore, cells and molecules involved in an inflammatory response are diverse.

Myeloid cells are important regulators of inflammation, amongst which the neutrophils, monocytes, dendritic cells and macrophages, are the most predominant contributors. Not only do they express and secrete inflammatory signals (mostly cytokines) during the response, their responses also help alerting the surrounding tissue and cells when danger and damage appears. Some myeloid cells are specialised in certain environment or a period of inflammation, such as the immediate and short-lasting action of neutrophils to early infections, but macrophages are present throughout most inflammatory activities. These cells can engulf invading bacteria, present antigens to cytotoxic effector cells, release cytokines to induce or suppress further inflammatory

responses, and even regulate lipid and nutrients metabolism to adapt to the changing environment [7, 8]. Thus, comprehending the role of macrophages *in vivo* enables us to study a number of human pathologies and to develop novel therapeutics.

1.2 Macrophages

1.2.1 Macrophage Lineages

The macrophage is a cell of complex origins. Contrary to the traditional view that macrophages combat infections *in situ* and therefore are supplied from the differentiating monocytes in the circulation, recent observations showed that there are two lineages of macrophages. One adopts the known mechanism of replenishing “old” macrophages from monocytes produced from the bone marrow, while some macrophages emerged with the tissue during embryonic development and their survival is independent of monocyte-derived macrophages [9, 10]. Tissue-resident macrophages adapt to the niche-specific environment and predominantly respond to on-site infections and the homeostasis of the tissue [7, 11]. For instance, the central nerve system macrophage microglia combat infections in the brain and are actively involved in neuroinflammation and the removal of degenerated or damaged neurons [12, 13]. A summary of macrophage development is shown in Figure 1.

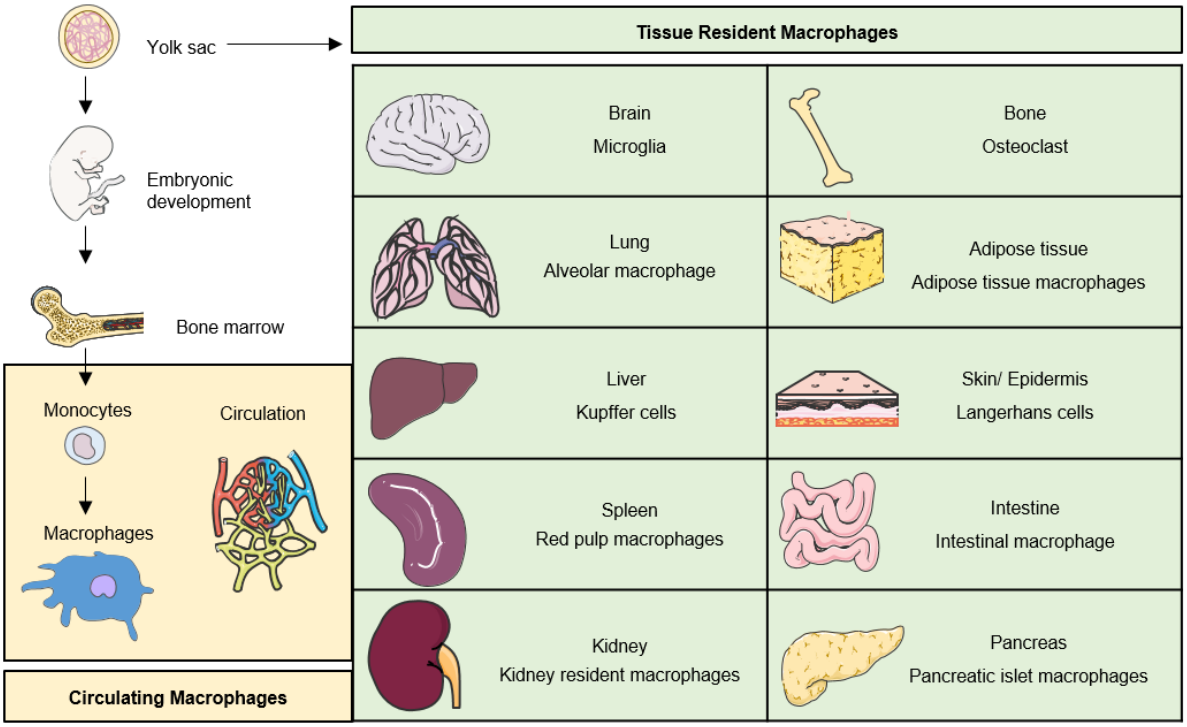

Figure 1. Macrophage development.

Macrophages are categorised as monocyte-derived macrophages (yellow box) or tissue resident macrophages (green box). A pool of replenishing macrophages arises from precursor monocytes generated from human bone marrows. During embryonic development, a pool of progenitor cells in tissues and organs have committed into macrophage development and become tissue resident.

Although microglia are a particular example to indicate the importance of tissue-resident macrophages as the blood-brain barrier protects against acute inflammation and leukocyte infiltration, other tissue resident macrophages also acquired specific characteristics during evolution in the tissue environment. The skin macrophage Langerhans cell (LC) forms a “web of immunity” across the epidermis of the skin and connects the lymph nodes. Their functions include but are not limited to the surveillance and defence against pathogen invasions, immediate recruitment of immune cells, priming and differentiation of lymphocytes at the lymph nodes, and most importantly antigen uptake via LC migration between keratinocytes and the lymph node has been described [14–16]. Furthermore, the most abundant tissue-resident macrophage Kupffer cells in the liver sinusoids are highly responsive to release proinflammatory factors against infections in the digestive tract and have acquired a unique role in liver regeneration and scavenging malformed haemoglobin [17]. Other tissue-resident macrophages such as Osteoclasts in the bone and alveolar macrophages have additional functions in bone remodelling and surfactant clearance, respectively [18, 19]. Contributed by these resident macrophages, our tissues and organs can respond to danger signals rapidly and appropriately in physiological conditions.

Apart from the well-portrayed tissue-resident macrophages, there are the type of “replenishing” macrophages which act in need and throughout human body. These macrophages are originated from the bone marrow –derived precursor monocytes in the blood circulation, which were differentiated into macrophages near the site of infection or injury. Human monocyte subsets are classified by their variation of CD14 and CD16 expressions, as the classical type is CD14 positive CD16 negative (CD14++CD16-), intermediate is CD14++CD16+, and non-classical is CD14dimCD16++ [20]. In mouse, monocyte subpopulations are divided upon the expression of Ly6C (Lymphocyte antigen 6C) and CD43 (leukosialin), equivalent to the human markers CD14 and CD16 [21]. The population orthologues are the classical LyC6++CD43-, the intermediate LyC6+CD43++, and the non-classical LyC6+CD43++. Although all these monocytes can be differentiated into macrophages, the classical monocytes, comprise the large majority of total population (87%), are mainly responsible for replenishing macrophages in rapid response to inflammation and injury

[22–25], while the intermediate monocytes facilitate later inflammatory responses, and the CD16-high nonclassical monocytes aid immune surveillance [26].

Whilst monocyte/macrophage development is affected by a mixture of stimulating factors, this transition predominantly relies on the presence of macrophage colony-stimulating factor (M-CSF, also known as CSF-1) that is secreted by the blood/tissue stromal cells [27]. In contrast to the alternative method of GM-CSF macrophage differentiation which renders cells ability to activate the inflammasome complex and release interleukins and other proinflammatory cytokines [28], M-CSF differentiation method is widely applied *in vitro* for its advantage of yielding a consistent population of resting macrophages that uniformly express type I interferons to viral challenges [29]. Upon M-CSF -induced cell fate commitment, a negative feedback loop is initiated to reduce CSF receptor expression and the consequent cell proliferation [30–32]. However, macrophage proliferation is not completely abolished and its aberrancy is often associate with pathologies. A typical example of this is the chronic inflammatory disease atherosclerosis, where monocyte-derived macrophages (MDM) recruited to the damaged endothelial site continue to proliferate, uptake oxidised lipids and become foam cells in the atherosclerotic plagues [33–35].

Similar to human cells, mouse macrophages maintain the two lineages. While the tissue-resident macrophages arise during embryonic development, the circulating macrophages are differentiated from bone marrow -released monocyte-macrophage progenitor cells upon exposure to murine M-CSF. The Fibroblast L929 cells are a widely-applied model to produce M-CSF –containing medium for bone marrow-macrophage differentiation in the laboratory [36].

1.2.2 Macrophage Phenotypes

Independent of monocyte differentiation, macrophages also display pleiotropic functions during their activities in tissue homeostasis and are thus further categorised into physiological subsets or phenotypes. In a broader classification method, macrophages are either a cytotoxic/killing character (M1) or a repairing/growth character (M2) [37]. This “Fight or Fix” switch is achieved predominantly by metabolic modulation of arginine, where the inducible nitric oxide synthase (iNOS) is more active in M1 phenotype and arginase is more active in M2 (at least in murine models), therefore promoting the respective Th1 and Th2 inflammatory response [38]. While the metabolic pathway of M1/M2 transition discussed in reviews helps to identify the nature of macrophage [38–41], it is the associated gene expression profile that is most critical to our study of pathology.

In the Th1 or “Fight” response, M1 macrophages respond to interferon-gamma (IFN-γ), lipopolysaccharide (LPS), tumour necrotic factor-α (TNF), viral nucleic acids, and promote iNOS-dependent NO production and proinflammatory activation [42]. Establishment of M1 phenotype is indicated by the enhanced expression of cell surface receptors CD86, CD80, CD68, major histocompatibility complex II (MHC II), TLR2 and TLR4 [43]. In addition to these stimulants, M1 phenotype is mostly induced by microbial infections and aberrant cell death as a defence mechanism for biological threats. A wide spectrum of pattern-recognition receptors expressed by macrophages detect pathogen or danger –associated molecular patterns named PAMPs or DAMPs. Cellular dysfunction may give rise to DAMP signals by releasing intracellular molecules such as ATP and DNA which are detected by purinergic receptors on macrophage surface [44], or are internalised and recognised by cytoplasmic receptors such us Stimulator for Interferon Genes (STING) [45]. In terms of pathogens, a variety of macrophage PRRs detects pathogenic proteins, lipoproteins, nucleic acids, as well as antibody/complement-labelled or opsonised bacteria to intercept infections. From the literature, M1 macrophages are significantly affected and activated by the well-known microbial infections including *Mycobacterium tuberculosis*, *Listeria monocytogenes*, *Salmonella typhimurium*, *Staphylococcus aureus*, Influenza virus,

Herpes simplex virus and Dengue virus [46–52], and their functions have recently been addressed in Zika virus pandemic [53, 54].

Alternatively, the Th2 or “Fix” phenotype of M2 macrophages is responsible for repairing tissue damage and resolution of inflammation. Despite the debate on M2 sub-classifications based on their functional statues, there are 4 agreed subtypes of M2 as group according to their gene expression profiles. M2a is stimulated by interleukin-4 (IL-4) and IL-13 (M2a), M2b is induced by IL-1 receptor ligands, immune complex and LPS, M2c is induced by glucocorticoids, IL-10 and transforming growth factor-β (TGF-β), and M2d is induced by IL-6 and adenosine [42, 55, 56]. These reviews have summarised the current findings on M2 phenotypes and the associated regulatory and anti-inflammatory mediators and responses, amongst which IL-10, TGF-β and mannose receptor CD206 are ubiquitously expressed.

The current classification of macrophage phenotypes by protein marker expression is still incomplete. An advanced approach is by RNA-seq (RNA sequencing) analysis of transcriptomic signatures of polarised macrophages to identify significantly induce or repressed genes. At this resolution, phenotypes can be associated with additional gene regulation mechanisms such as promoter activities, alternate transcription splicing, and untranslated region (UTR) regulation [57, 58]. To note, gene profiles of different phenotypes are constantly changing according to the microenvironment. For instance, while the classic M1 and M2 macrophages maintain their specific gene expression profiles, in atherosclerotic plaques, a rich signal of oxidised phospholipids is added to these cells which can induce additional transcription of antioxidant enzymes that helps limiting lipid accumulation [59]. Transcriptomic analysis of macrophage phenotypes more accurately reflects the change of environmental adaptations of different sub-populations, and it is an advanced tool with considerable clinical potential to diagnose and predict macrophage-associated pathologies [60].

Although it has been a general understanding that the naïve macrophages can switch between the major M1 and M2 phenotypes based on signalling transduction, and such

M1/M2 counteraction is a safety mechanism to prevent chronic inflammation and immunosuppression exhibited by each phenotype. However, the complexity of macrophage phenotypes has been built up throughout research, with the addition of numerous sub-phenotypes. The interplay between signalling pathways gives macrophages the plasticity to readily alter between phenotypes, and this certainly reflects the flexibility and broadness of macrophage response to modulate host immunity [61, 62]. Therefore, phenotypes may not be the most accurate method to describe the role of macrophages, their responses to the immune challenge are more essential to determine the phenotype in a specific condition.

1.2.3 Macrophage Functions

Macrophages exhibit two critical immune functions: phagocytosis and antigen presentation. Phagocytosis is a process employed by macrophages to scavenge “biological waste or stimuli”. By recognition of targets via cell surface Fc receptors, complement receptors, mannose receptors, scavenger receptors and lectin receptors, targets including apoptotic and necrotic cell debris, excessive proteins and lipids and incoming microorganisms which are vesicle-enwrapped and engulfed by macrophages [63–66]. Although most pathogens are digested by the acidic and enzymatic environment of phago-lysosomes, this antimicrobial exercise can sometimes be resisted. These evasion mechanisms are exemplified by internalised *Mycobacteria* which have evolved an anti-digestive cell wall and the ability to inhibit the vacuolar proton-ATPases to protect against phagolysosomal breakdown, so that it can persist until a chance for escape [67–69]. While phagocytosis is beneficial to restoring host physiology, it also contributes to pathogenesis when an excessive amount of waste is scavenged. One example is the generation of atherosclerotic plaques where macrophages are recruited to the site of lipid accumulation in the wall of blood vessels and later become the proinflammatory and pro-atherogenic “Foam cells” when their scavenging limits are exceeded [34, 35]. This process can be viewed as a double-edged sword, protecting the host from infections and biological wastes but becoming pathogenic once their functions are overwhelmed by stimuli. Thus, precise control of macrophage function is critical and is achieved via a tight regulation of intracellular inflammatory signalling networks.

Macrophages also act as professional antigen presenting cells (APC) together with dendritic cells and B cells [70]. Macrophages process the engulfed pathogens or cellular breakdown products to antigens which are complex with surface expressed major histocompatibility complex class II molecules (MHC II) to be presented to T cells. This helps to activate naïve T cells to become either CD8 positive cytotoxic T cells or CD4 positive helper T cells. Macrophages requires IFN-γ signal from memory T lymphocytes to express MHC II molecules [71]. MHC II complex were not expressed on the plasma membrane at abundance until immune challenge occurs. In Listeria monocytogenes-infected macrophages, they were initially found in lysosomes and were rapidly induced to the surface with bacterial antigens [72] where T cell receptors

can recognise and respond. The crosstalk between macrophages and the adaptive immunity critically underlies a sustained and secondary inflammatory response that secures the elimination of pathogens.

To orchestrate macrophage functions, a number of inflammatory proteins and signalling pathways have been studied to enable such precise actions at the appropriate time and duration.

1.3 Inflammatory signalling

Macrophages and dendritic cells are the critical players in host innate immunity while other immune cells support and compensate their functions at different stages and in different immune environments. Innate immunity predominantly contributes to the acute inflammatory response against physiological disturbances, during which cells frequently communicate via molecular signals named cytokines [73]. Post cellular interaction and PRR recognition, a complex network of signalling cascades is activated to facilitate the generation of correct and corresponding cytokine response downstream of PRRs. While the canonical PRRs such as TLRs, C-type Lectin receptors (CLRs), NLRs and the Retinoic acid-inducible gene (RIG)-I-like receptors (RLRs) have been well studied in the past [74], a number of novel inflammatory regulators have been characterised in the recent years and have demonstrated indispensable roles in regulating host immunity.

1.3.1 Canonical inflammatory regulators

TLR family receptors form the most well-established PRR system in innate immunity. Similar to the plasma membrane receptors of the CLR family including Dectin, MINCLE and mannose receptors [75], most TLRs are exposed on plasma membranes yet some are also present in endo-lysosomal structures [76]. For a wide spectrum of antigen recognition, each TLR detects a specific ligand and their signalling pathways crosstalk to respond to infections. The cell surface receptor TLR2 recognises microbial lipoproteins and TLR4 recognises bacteria endotoxin LPS, endosomal receptor TLR3 recognises viral double-stranded (ds)RNA and TLR7 recognise single-stranded (ss)RNA from microorganisms [77]. Activation of TLRs ignites the signalling transduction from the major adaptor proteins MyD88 and its accessory facilitators TRAM, TIRAP, Mal, and finally induces the proinflammatory pathways via mitogen-activated protein kinase (MAPK) / activator protein-1 (AP-1) and IKK (IκB kinase) / nuclear factor kappa-light-chain-enhancer of B cells (NF-κB). These two transcription factors coordinate the secretion of proinflammatory cytokines and chemokines such as IL-1, IL-6, IL-8, CCL3 and TNF-α [74, 78]. Alternatively, endosomal receptor TLR3 and the “late signalling” events of internalised TLR4 induce the TRIF/TRAM mediated response and activates interferon regulatory factor 3 (IRF3) [74, 79]. IRF3-dependent action elicits the type I interferon response which is antiviral, immune regulatory, pro-haematopoietic regeneration, and pro-apoptotic for infected and damaged cells [80, 81]. Dysregulation of type I interferons is associated with chronic inflammation and autoimmune diseases. Amongst all PRR ligands, LPS is capable of activating multiple inflammatory pathways and thus is a model immune stimulus for exploring novel inflammatory mediators involved in both the direct and late-signalling activation (Figure 2).

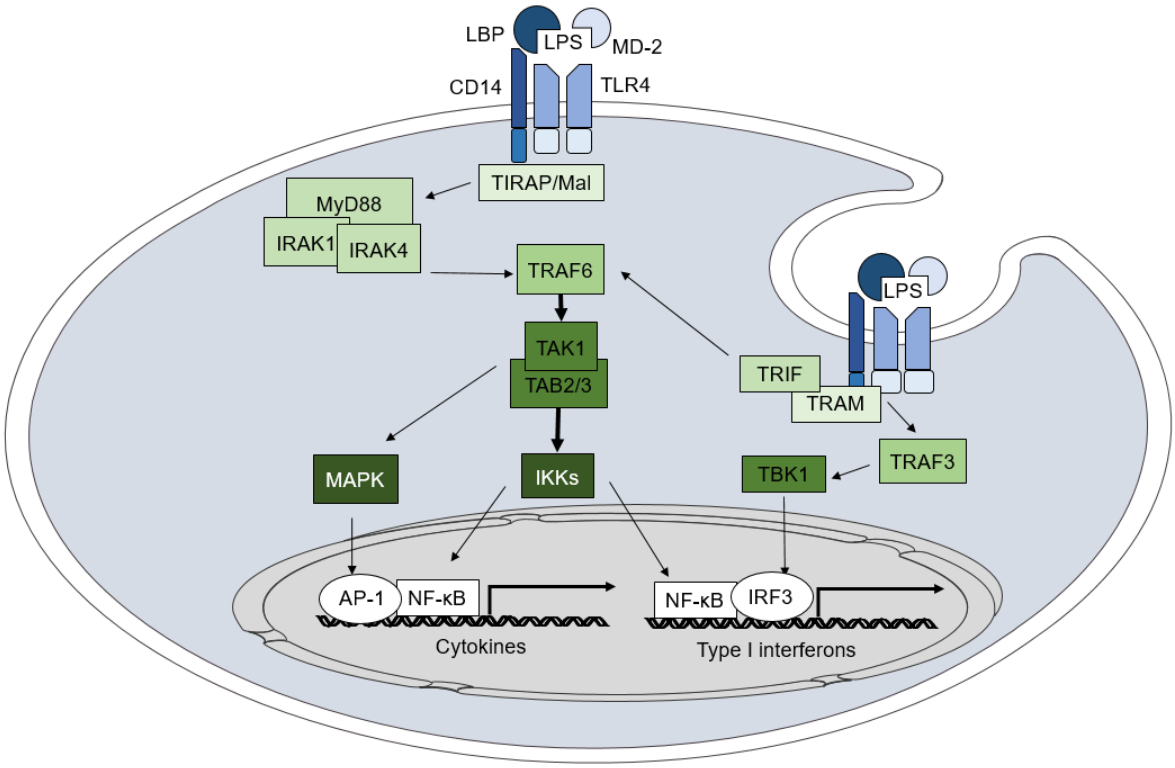

Figure 2. Overview of LPS activated TLR4 pathways.

Bacterial endotoxin LPS is recognised by TLR4 and the co-receptors CD14, LBP and MD-2 at the plasma membrane surface. TLR4 receptor couples to TIRAP and Mal and induces MyD88-dependent signalling through the IRAK-TRAF6-TAK axis, which then signals to IKKs and MAPK for activation of transcription factors NF-κB and AP-1, respectively. This results in the expression of classical proinflammatory cytokines. Alternatively, “late signalling” events cause LPS-bound TLR4 internalisation and activate TRAM/TRIF –dependent induction of TRAF3 and TBK1, which finally induces the transcription factor IRF3. TRAM/TRIF activation additionally induces the common signalling through TRAF6-TAK, and together with the product NF-κB, IRF3 upregulation of type I interferon expression. Abbreviations: LPS= lipopolysaccharide; TLR4= Toll-like receptor; LBP= LPS binding protein; TIRAP= Toll/interleukin-1 receptor domain-containing adaptor protein; Mal= MyD88 associated protein; MyD88= myeloid differentiation primary response 88; IRAK= interleukin-1 receptor-associated kinase 1; TRAF= tumour necrosis factor (TNF) receptor-associated factor; TAK1= transforming growth factor (TGF) beta-activated kinase 1; TAB= TGF-beta activated kinase; MAPK= mitogen-activated protein kinase; AP-1= activator protein 1; IKKs= IκB kinase; TRIF= TIR-domain-containing adaptor-inducing interferon-β; TRAM= translocating chain-associated membrane protein 2; TBK1= Tank-binding kinase; IRF3= interferon regulatory factor 3.

Pathogen induced proinflammatory cytokine production also instigates a positive feedback loop which leads to further cytokine amplification. For instance, NF-κB mediated cytokine expression can be enhanced by TNF and its receptor through a TRAF2-containing adaptor cascade [82]. Particularly, IL-1 secretion induced by the TLR4 recognition of LPS promotes further inflammation through a signalling cascade that highly resembles LPS-TLR4 signalling. Upon induction, IL-1 precursors are post-translationally processed by proteases (mostly calpain and granzyme B) or caspase-1 to release the mature IL-1α and IL-1β, respectively. The activation of receptor dimer by IL-1 proteins assembles intracellular adaptors including MyD88 and IRAK4, and these in turn initiate the IRAK1/TRAF6-dependent signalling to both NF-κB and AP-1 transcription factors which enhance proinflammatory cytokine production [Reviewed in [83]]. These feedback mechanisms can be beneficial to sustain inflammatory response throughout infections and immune regulations; however, it can also be associated with chronic inflammation and autoimmune diseases. Rheumatoid arthritis (RA) is a typical autoimmune disease resulted from chronic release of IL-1 and TNF-α (amongst other proinflammatory cytokines such as IL-17, IL-18 and RANKL) in an unresolved joint inflammation [84, 85]. Not only that chronic inflammation affects the local region, in recently identified cases of RA, patients were also found with cognitive impairment which was likely caused by the reduced life quality associated with disease management (use of glucocorticoid, income, mobility and other social aspects) [86]. Therefore, the feedback mechanism must also be exhibited in a tightly controlled manner to prevent adverse effects on immune resolution.

A limitation for the functioning of cell membrane-embedded receptors is the lack of surveillance in the cytoplasm. Molecules such as nucleic acids and proteins originating from microorganisms and cellular stress can bypass membrane PRR recognition, and thus necessitate the additional defence provided by the cytoplasmic PRR families NLRs and RLRs. NLR-mediated activities involve inflammasome formation and caspase activation and recruitment domain (CARD)-dependent activation of caspase-1 and IL-1β/ IL-18 processing [87, 88]. The well-studied members of NLR family NOD-1 and NOD-2 respond to peptidoglycan in the cytosol as a result of microbial breakdown or division [89]. As a result of cytosolic detection, NLR pathways commonly

crosstalk with other PRR families such as TLR and RLR, such as the TLR4 / NF-κB activation priming NLRP3 inflammasome assembly [90].

It is well appreciated that RNA and DNA molecules are potent immune stimulants. In addition to the NLR, another family of cytoplasmic receptors RLRs are responsible for detecting virus-released RNA [91]. These receptors were identified when the loss of TLR3, -7, -8 and -9 was unable to abolish type I interferon response upon certain viral infections [92–94]. RLRs receptors include the RNA helicases RIG-I and melanoma differentiation associated factor 5 (MDA5), which recognise 5’ triphosphate-tagged ssRNA and dsRNA molecules released by viruses such as Rotavirus, West Nile viruses and Dengue virus [95–98]. A third RLR member named laboratory of genetics and physiology 2 (LGP2) lacks the RLR signature CARD domain yet it still recognises dsRNA termini, and has regulatory functions for RIG-I and MDA5 –dependent antiviral activities [99–102]. RIG-I and MDA5 signal through the intracellular adaptor mitochondrial antiviral signalling protein (MAVS) which induces NF-κB and IRF3-dependent type I interferon response [98, 103].

1.3.2 Non-canonical inflammatory regulators

Further to these categorised PRRs, several non-canonical immune sensing pathways have been described. Pathogen-derived nucleic acids are detected by additional cytosolic proteins including RNA sensors RNase L, protein kinase R (PKR) and oligoadenylate synthase (OAS) family proteins [104–106]. Although these sensors lead to type I interferon response upon encountering cytoplasmic RNA, their interferon-inducing events are independent of TRIF and MAVS. For instance, RNase L and OAS are nucleases that inhibit infections by cleaving ssRNA and dsRNA, respectively, into smaller products which subsequently induce RIG-I/MDA5/MAVS axis for interferon augmentation [106, 107]. Type I interferon signalling also induce further inflammatory gene expression including OAS as a positive feedback mechanism to maximise antiviral response. Distinct from these nucleases, PKR is a dsRNA-recognising kinase that phosphorylates and inactivates translation factor eIF2α when it has been hijacked for microbial protein expression [105, 108, 109]. PKR is also involved in the regulation of IFN-α/-β mRNA integrity, where the loss of PKR functionality did not impair type I interferon expression but caused the absence of terminal polyadenylation of mRNA which prevents transcription degradation [110, 111].

Additionally, absence in melanoma 2 (AIM2), DEAD-Box helicase 41 (DDX41), cyclic di-GMP-AMP synthase (cGAS), interferon (IFN)-gamma inducible protein 16 (IFI16) [112–115] and the endonucleases such as TREX1 and MUS81 act as DNA sensors in the cytoplasm [116, 117]. DNA molecules are confined in the host nucleus and mitochondria unless cellular stress induces DNA leakage or pathogens introduce their genes into the cytoplasm. Therefore, cytoplasmic dsDNA are potent immune activators. Despite that AIM2 is activated by dsDNA to induce caspase-1 inflammasome assembly [112], all the other described DNA nucleases and sensors signal though an endoplasmic reticulum (ER) adapter protein Stimulator of Interferon Genes (STING), which has been reviewed by Barber [118] and later in Chapter 1.5 [119]. STING signalling not only forms a cytosolic DNA defence mechanism, its dysregulation is highly associated with autoimmune diseases [120–122], and its value as antiviral and anti-tumour adjuvant is a prominent focus in clinical laboratories [123–127].

1.3.3 Summary of inflammatory regulators

Immune cells, most importantly macrophages, exhibit inflammatory stimuli through the activation of the innate immune receptors PRRs which recognise PAMP and DAMP derived from pathogens and cell/tissue stress. The major PRR families TLRs, CLRs, NLRs and RLRs have adopted their specific recognition characteristics into a system for inflammatory signalling of cytokines, chemokines and type I interferons. These well-studied receptors are known as the canonical inflammatory regulators. Additionally, some of the un-categorised immune receptors are found to complement the canonical PRR activities, most of which are sensors for intracellular nucleic acids. Although these sensors differ in the nature of detection mechanisms, most of the RNA-induced signalling events are mediated by MAVS in the mitochondria and the DNA sensing pathways act through STING in the ER. Nucleic acid detection leads to adaptor activation which subsequently recruit interferon regulatory factors to induce type I interferon response, which is indispensable for antiviral immunity.

1.4 TMEM203 – a novel proinflammatory mediator

Our knowledge of pattern recognition receptors and components of the innate immune sensing pathways is continuously evolving. MAVS and STING were discovered only in the last 15 years, yet research has expanded rapidly in their role in antiviral, anti-tumour and autoimmune responses. Their significance in supporting inflammation and its regulatory mechanisms have become the focus for therapeutic targeting for their potential. To link nucleic acid sensing pathways to the previously identified immune regulators or to identify novel regulators are priorities to identify potential drug candidates.

Macrophages are central cellular regulators of inflammation, exhibiting potent anti-microbial effects, linking the innate and adaptive immunity, and coordinating cellular/tissue inflammatory dynamics. To identify novel inflammatory mediators, we activated murine macrophages RAW 264.7 cell line with LPS, a bacterial endotoxin that induces both classical inflammatory pathways and type I interferon response [128, 129]. In the functional screen of cDNA library of LPS-activated macrophages, 34 novel proinflammatory genes were identified [130, 131]. Amongst these, a protein named Tmem203 (transmembrane protein 203, TMEM203 in human) was shown to be upregulated Cxcl2 chemokine promoter activities upon LPS challenge. Preliminary studies on Tmem203 showed that the LPS-induced *Cxcl2* promoter activity in RAW 264.7 cells was enhanced by *Tmem203* overexpression and it is impaired by *Tmem203* knockdown (Chapter 2, Fig. 1D-E). However, Tmem203 overexpression-induced *Cxcl2* promoter activation was not reduced by the expression of dominant negative forms of the canonical LPS signalling components, such as MyD88 and TRIF (Chapter 2, Fig. F-G). Thus, we tested that whether TMEM203 could signal through an alternative immune regulator. Expression of Tmem203-mCherry showed a localisation pattern in punctate membrane structures (Chapter 2, Fig. 3A) and LPS stimulation causes Tmem203 translocation to LAMP1 positive endosomal membranes (Chapter 2, Fig. 3B). In 2015, Shambharkar *et al*., reported that TMEM203 predominantly expressed on the ER membranes and it is essential in modulating calcium homeostasis by co-regulation and interaction with IP3R (inositol 1, 4, 5-triphosphate receptor), SERCA (sarcoplasmic/endoplasmic reticulum calcium ATPase) and the calcium sensor STIM1 (stromal interaction molecule 1) [132]. To search for

potential candidate co-regulators for TMEM203, we considered the two intracellular signalling adaptors MAVS and STING. Considering its ER localisation, TMEM203 is likely to coordinate signalling events via nearby immune regulators, and a logical candidate would be the ER resident antiviral adaptor STING [132, 133]. STING is ubiquitously expressed in the ER and responds to DNA sensors and microbial secreted cyclic dinucleotides. It signals through the TBK1-IRF3 axis which specifies type I interferon activation and later an amplified interferon-stimulated response, including the expression of proinflammatory chemokines. Due to the close localisation in the ER, TMEM203 and STING are likely to interact directly and complex in a number of signalling activities. Thus, we tested the potential of TMEM203 signalling through STING. Knockdown of *Sting* and its signalling effectors *Tbk1* and *Irf3* can strongly suppress Cxcl2 promoter activation caused by *Tmem203* overexpression (Chapter 2, Fig. 1H). Not only that co-expression of STING-GFP and TMEM203-mCherry showed strong colocalisation pattern in HeLa cells (Chapter 2, Fig. 2D), these two proteins form a stable complex in co-immunoprecipitation (Chapter 2, Fig. 2E). From these evidences, the novel inflammatory mediator TMEM203 is of significant interest for the characterisation of immune functions and it is likely to associate with STING signalling components.

1.5 Regulating STING in health and disease

Paper 1, Review – STING regulation in Health and Disease

Authors: **Yang Li,** Heather L Wilson & Endre Kiss-Toth.

Affiliation: Department of Infection, Immunity and Cardiovascular Disease, University of Sheffield, Beech Hill Road, Sheffield, S10 2RX, UK

Journal: Journal of Inflammation (London), 14:11. eCollection 2017.

Status: Published, 2017 Jun 7

DOI: 10.1186/s12950-017-0159-2

Authors' Contributions:

I wrote the manuscript with further suggestions from my supervisor Dr Heather L Wilson and Professor Endre Kiss-Toth who also edited and critically reviewed the draft.

Regulating STING in Health and Disease

Yang Li[1], Heather L. Wilson[2] and Endre Kiss-Toth[3]*

Department of Infection, Immunity and Cardiovascular Disease, University of Sheffield, Beech Hill Road, Sheffield, S10 2RX, United Kingdom

Authors' information: *Corresponding author

Email addresses:

1. yli171@sheffield.ac.uk
2. h.l.wilson@sheffield.ac.uk
3. e.kiss-toth@sheffield.ac.uk*

Abstract

The presence of cytosolic double-stranded DNA molecules can trigger multiple innate immune signalling pathways which converge on the activation of an ER-resident innate immune adaptor named “STimulator of INterferon Genes (STING)”. STING has been found to mediate type I interferon response downstream of cyclic dinucleotides and a number of DNA and RNA inducing signalling pathway. In addition to its physiological function, a rapidly increasing body of literature highlights the role for STING in human disease where variants of the STING proteins, as well as dysregulated STING signalling, have been implicated in a number of inflammatory diseases. This review will summarise the recent structural and functional findings of STING, and discuss how STING research has promoted the development of novel therapeutic approaches and experimental tools to improve treatment of tumour and autoimmune diseases.

Keywords: Stimulator of Interferon Genes (STING), double-stranded DNA sensor, cyclic dinucleotide, cGAS

Background

Cellular stresses or infections lead to the release of DNA molecules into the cytoplasm which may threaten the stability of the host genome [1]. The intracellular appearance of naked DNA molecules triggers a double-stranded (ds)DNA sensing mechanism which consequently induces innate immune responses including the production and release of type I interferons (IFN-I). This response is central to the resolution of DNA-induced cellular stress [2–4] and prevents the emergence of autoimmunity [4, 5]. A recently described protein named STING (Stimulator of Interferon Genes, also known as TMEM173, ERIS, MITA and MPYS) is a critical regulator of these innate immune responses [6–9].

STING is an endoplasmic reticulum (ER)-resident transmembrane protein and was first recognised as part of the ER translocon system [6, 10]. Suppression of components of the translocon-associated protein (TRAP) complex such as TRAP-β and Sec61 β have been found to impair DNA-induced type I interferon (IFN-I) signals downstream of STING [11]. The TRAP complex has been shown to be involved in two of the ER's major responses: protein N-glycosylation [12] and endoplasmic reticulum-associated degradation (ERAD) [13]. Although the functional relevance of STING in the ER translocon system has not yet been fully elucidated, it has been proposed that STING can interact with TRAP component Ssr2/TRAPβ to enable its migration from the ER to perinuclear membranes, a process key to IFN-β promoter activation [6, 14].

Recent reports have demonstrated that cytoplasmic DNA released by microbes and viruses can trigger dsDNA-sensing pathways which activate STING [6, 15–17]. STING then signals to the TANK binding kinase 1 (TBK1) / interferon regulatory factor-3 (IRF3) axis to upregulate type I interferon production [11, 18]. As an IKK (IκB kinase) –related kinase, TBK1 can also interact with IκB kinases to induce phosphorylation and thus degradation of IκB, thereby liberating NF-κB (nuclear factor kappa B) subunits allowing their nuclear translocation resulting in upregulation of type I interferon and other pro-inflammatory cytokines such as IL-6 (interleukin-6), CXCL10 (C-X-C motif chemokine 10), CCL5 (C-C motif chemokine ligand 5) and

CCL2 [19]. Table 1 summarises the pathogens that have been shown to activate STING [6, 20–37]. Of note, STING knockout mice generated by Ishikawa and Barber were highly susceptible to infection by the single stranded RNA viruses vesicular stomatitis virus (VSV) and Sendai virus [6], suggesting STING activation pathways may overlap with RNA sensing mechanisms or reverse transcription of viral RNA [6, 24, 38].

Table 1. STING is activated by a range of pathogens.

The type I interferon signal adaptor protein STING is responsible for mediating double-stranded DNA sensing responses and the detection of bacterial cyclic dinucleotides c-di-AMP, c-di-GMP, and 3'-3' cGAMP. Many DNA viruses, RNA viruses and bacteria have been implicated in the activation of STING. Abbreviations: dsDNA = double-stranded DNA; ssRNA = single-stranded RNA.

Name	Type of Pathogen	Mechanism of STING activation	References
Adenovirus	Non-enveloped linear dsDNA virus	dsDNA activates cGAS-STING pathway (cytoplasmic)	[20]
Kaposi's sarcoma-associated herpesvirus	Enveloped dsDNA virus	dsDNA activates cGAS-STING pathway (cytoplasmic) and IFI16-STING pathway (nuclear)	[21]
Herpes simplex virus	Enveloped dsDNA virus	dsDNA activates cGAS-STING pathway (cytoplasmic) and IFI16-STING pathway (nuclear)	[22] [23]
Epstein-Barr virus	dsDNA virus	dsDNA activates IFI16-STING pathway (nuclear)	[24]
Human cytomegalovirus	dsDNA virus	dsDNA activates cGAS-STING pathway (cytoplasmic), DAI-STING (cytoplasmic), and IFI16-STING pathway (nuclear)	[25] [26] [27]
Sendai virus	Negative strand ssRNA virus	Possibly via RIG-I –dependent RNA detection which may in turn induce STING	[6]
Vesicular stomatitis virus	Negative strand ssRNA virus	Unknown	[6]
Human immunodeficiency virus	Negative strand ssRNA virus	dsDNA reverse transcribed from viral RNA induces cGAS-STING pathway	[28]
Influenza A virus	Negative strand ssRNA virus	Possibly via membrane fusion or unknown mechanism independent of DNA recognition	[29]
Mycobacteria tuberculosis	Bacteria producing c-di-GMP	c-di-GMP	[30] [31]
Streptococcus pneumoniae	Bacteria dsDNA	Bacterial dsDNA	[32]
Streptococcus pyrogenes	Bacteria dsDNA	Bacterial dsDNA	[33]
Staphylococcus aureus	Bacteria producing c-di-AMP	c-di-AMP	[34]
Listeria monocytogenes	Bacteria producing c-di-AMP	c-di-AMP	[35]
Vibrio cholera	Bacteria producing 3'-3' cGAMP	3'-3' cGAMP	[36] [37]

Whilst the STING-mediated dsDNA-sensing mechanism is critical for successful cellular protection against infections and disease progression, dysregulated STING activity leads to the excessive production of inflammatory mediators with potentially detrimental effects on surrounding cells and tissues. Recent studies revealed some important functions for STING in autoinflammatory diseases [39–41], cancer [41–44] and lipid regulations [45, 46], highlighting the importance of this protein in health and disease. Here we review the recent insights into STING function in human pathologies and discuss the potential of STING-targeted therapies which are of considerable scientific and clinical interest.

Main text

STING Mediated Signalling

Canonical STING Activators

Whilst STING acts as an adaptor protein in the dsDNA sensing pathway, it is not activated directly by DNA molecules. Instead, STING responds to DNA sensing proteins and molecules known as cyclic dinucleotides (CDNs) [35, 47–49] (**Figure 1**). CDNs are derived from infectious agents exogenously, or are produced by the mammalian dsDNA sensor cGAS (cyclic guanosine monophosphate – adenosine monophosphate synthase; cyclic GMP-AMP synthase). The canonical CDNs, or microbial secretory CDNs, are molecules made of 3'-5' phosphodiester bonds joining two adenosines (A) – cyclic di-AMP [35, 50], two guanosines (G) – cyclic di-GMP [47] or one of each – cyclic GMP-AMP [37]. One of the STING-activating universally expressed DNA sensors, cGAS, is capable of catalysing a unique form of CDN endogenously upon DNA recognition [51]. This molecule is comprised of one 3'-5' phosphodiester bond and a non-canonical 2'-5' linkage between adenosine and guanosine, and is thus named 2'-3' cGAMP to distinguish from the secretory cyclic dinucleotide cGAMP (3'-3' cGAMP) which contains two 3'-5' bonds [37]. Previous literature [52–54] has suggested that 2'-3' cGAMP is ten- to a thousand-fold more potent than 3'-3' cGAMP in activating STING. A number of studies reported that the change of phosphodiester linkage in 2'-3' cGAMP results in a higher binding affinity to STING and thus leads to an augmented type I interferon response [55, 56]. It is

also possible that hydrophilic secretory cyclic dinucleotides are excluded by the selectively permeable plasma membrane [57], and thus cannot be recognised by STING.

Alternative STING activators

In addition to being activated by cyclic dinucleotides, STING also mediates antiviral responses downstream of DNA sensors including DNA-dependent activator of IFN-regulatory factor (DAI) [17], IFNγ-inducible protein 16 (IFI16) [15], DEAD-Box Helicase 41 (DDX41) [16], and components of the RNA-sensing pathways [23, 38] (**Figure 1**). The Z-form DNA sensor DAI was the first identified activator for STING, whose expression is highly cell-type and tissue-specific and therefore could not fully account for the widespread IFN-I induction during viral infection [17, 58]. Further research identified that the DNA sensor DDX41 could interact with bacterial cyclic dinucleotides, in addition to DNA molecules [16], prior to activating STING signalling [59].

Figure 1. STING activation pathways.

The endoplasmic reticulum (ER) adaptor STING is activated via recognition of bacteria-secreted 3'-5' bond cyclic dinucleotides or DNA sensor cGAS-catalyzed 2'-5' cGAMP. Cytoplasmic DNA, released from DNA viruses or reverse transcribed from the RNA viral genome, can induce direct interaction between STING and DNA sensors (in red) such as DDX41, IFI16, and DAI. Alternatively, RNA viruses also induce the RIG-I dependent MAVS activation which alters mitochondrial dynamics and indirectly induce STING activation. Mitochondrial stress can result in the release of mitochondrial DNA (mtDNA) which also induces DNA sensor activation (not shown) and STING-mediated signalling. RNA polymerase III (RNA Pol III) can convert dsDNA into dsRNA which activates RIG-I/ MAVS axis which has been shown to induce STING activation.

Figure 1.

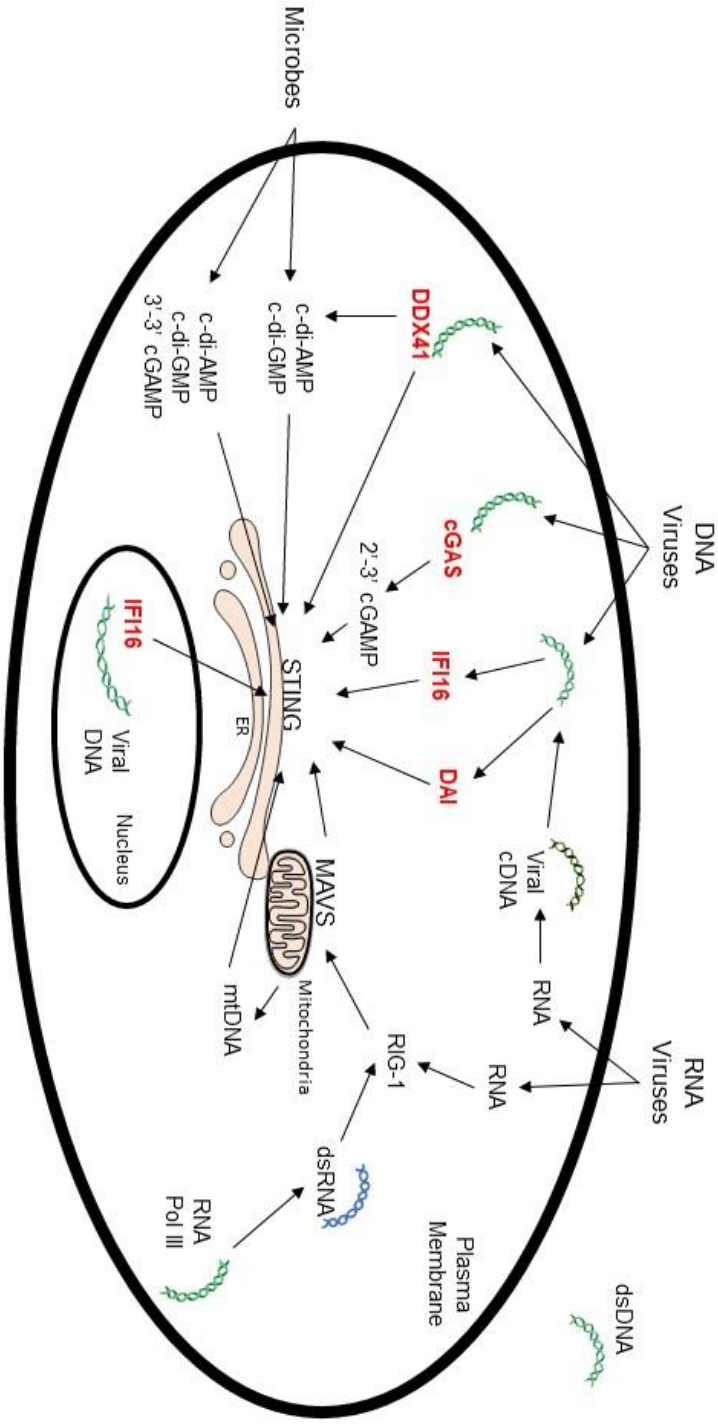
Microbes
c-di-AMP
c-di-GMP
3'-3' cGAMP
c-di-AMP
c-di-GMP
DDX41
cGAS
2'-3' cGAMP
IFI16
DAI
STING
ER
IFI16
Viral DNA
Nucleus
MAVS
Mitochondria
mtDNA
DNA Viruses
Viral cDNA
RNA
RNA Viruses
RNA
RIG-1
dsRNA
RNA Pol III
Plasma Membrane
dsDNA

Another interferon-inducible DNA sensor IFI61 is a pyrin-containing protein which also induces STING activation downstream of DNA detection. IFI16, as well as its mouse orthologue p204, is a universally expressed DNA sensor, which forms multimers prior to STING activation in response to HSV viral infections [15, 60]. Evidence shows that IFI16 is responsible for detecting foreign DNA both in the cytoplasm and in the nucleus and therefore it is capable of combating nuclear-replicating viruses such as Kaposi's Sarcoma associated herpesvirus [61, 62] and human cytomegalovirus (HCMV) [27, 63], implying an ability to discriminate between "self" and "non-self" DNA molecules. A recent report by Diner and colleagues showed dynamic regulation of IFI16 oligomers at different cellular compartments in response to altered viral infections [64]. Throughout HCMV infection, IFI16 oligomers are densely gathered nuclear "punctate" structures, whereas in Herpes simplex virus-1 (HSV-1) infection these "puncta" become gradually dispersed across the whole nucleoplasm and are eventually degraded. In contrast to previous studies, Diner *et al*. also found that IFI16 knockout cells do not impede TBK1 activation upon immune stimulation, whereas both STING and cGAS knockout cells will strongly suppress TBK1 activity, suggesting that nuclear DNA detection mediated by IFI16 is independent of the STING/TBK-1/IRF3 axis. Other studies indicate that antiviral cytokine production occurs in the absence of IFI16 via an unknown mechanism [64].

Recent reports have revealed an interesting relationship between IFI16 and cGAS during DNA detection. It was shown that HSV infection can induce both DNA sensors in various cell types, and that cGAS is partially nuclear, thus is able to regulate the stability of nuclear IFI16 oligomers during detection of viral DNA [65]. This provides a molecular mechanism by which cGAS regulates nuclear DNA sensing. Further evidence also suggests a DNA dose-dependent interaction between IFI16 and cGAS in keratinocytes [66]. Although this interaction does not affect cGAS's ability to generate cyclic dinucleotides, evidence indicates that IFI16 can facilitate the detection of these ligands by STING, and the loss of IFI16 can significantly impair downstream type I interferon and pro-inflammatory signalling [66]. Therefore, IFI16 and cGAS are not redundant during DNA infections, but instead cooperate and regulate each other's activities.

RNA-induced STING activation

Interestingly, several RNA viruses such as human immunodeficiency virus (HIV) [28, 67], influenza A virus [29], Sendai virus and vesicular stomatitis virus [6] have been found to activate STING signalling, via mechanisms both dependent and independent of DNA detection. Complementary DNA (cDNA) produced from reverse transcription of negative-stranded RNA in retroviruses such as HIV, murine leukemia virus (MLV) and Simian immunodeficiency virus (SIV) can induce a cGAS-dependent DNA sensing pathway and STING activation [28, 68] (**Figure 1**). However, HIV, in particular, is capable of inhibiting transcription of immediate anti-retroviral factors [69] and exploits the host STING blocker NOD-like receptor NLRX1 to aid the establishment of virus latency [67, 69]. It was also reported that cationic liposomes and nucleic acid-free herpesvirus-derived virus-like particles can directly induce STING/TBK1 relocation regardless of DNA sensing pathways, suggesting that the membrane fusion mechanism may be an alternative route for enveloped DNA and RNA viruses to activate STING. Enveloped RNA virus Influenza A virus has been shown to release haemagglutinin fusion peptide which induces STING but not cGAS activation [29], thus indicating another STING activation mechanism independent of cyclic dinucleotide recognition. It remains unclear whether the fusion particles alone are direct STING ligands or if activity requires facilitation by unidentified co-regulator(s).

The RNA-inducing adaptor MAVS (mitochondrial antiviral signalling protein; also known as VISA, Cardif, IPS-1) can also interact with and activate STING [6, 8] (**Figure 1**). The mitochondria-resident adaptor MAVS is the major molecular platform through which the RLR-dependent RNA sensing pathway elicits the type I interferon response. MAVS responds to the cytoplasmic RNA sensors RIG-I (the retinoic acid-inducible gene I) and MDA5 (melanoma differentiation-associated protein 5) [70], and in turn induces proinflammatory transcription factors NF-κB (nuclear factor kappa-light-chain-enhancer of activated B cells), IRF1, IRF3, IRF5 and IRF7 [70–73]. Castenier and colleagues [74] found that RIG-I induced MAVS activation can modulate mitochondrial dynamic changes promoting signalling to STING at MAMs, “mitochondria-associated membranes”, where mitochondria and ER are closely

associated [75]. This adaptor interaction was found to be dependent on a mitochondrial fusion mechanism which induces mitochondrial elongation towards the ER, and hence MAM formation. Virus-induced mitochondria fragmentation disrupts membrane association and hence abolishes MAVS activation and secondary STING signalling [74]. Another report also suggests that RNA virus-induced release of stress-associated mitochondrial (mt)DNA activates the STING-dependent dsDNA sensing pathway [76]. This process, which is also likely to involve mitochondrial stress-induced apoptosis, may provide an effective means to remove damaged cells for infection control.

Ablasser [77] and Chiu [78] noted that the STING inducer and a B-form dsDNA sensor RNA polymerase III (Pol III) activate the RIG-I –dependent RNA sensing pathways (**Figure 1**). RNA Pol III reversely transcribes dsDNA into dsRNA molecules that are activators of RIG-I. However, it is unclear how STING is involved in this process.

Post activation trafficking of STING

Activation of STING induces adaptor dimerization [7] and subsequent migration from ER membranes to punctate membranes of the Golgi by mechanisms similar to autophagy [11]. It remained difficult to identify the role of STING in autophagy regulation as little evidence was found to link STING with the recycling process during cell starvation. Yet many autophagy-related proteins such as autophagy-related gene (Atg) 9a and Vps34 are key to STING inter-organelle trafficking [79], and that the loss of early autophagy marker LC3 II can significantly impair the STING-dependent innate response to viral and bacterial infections [79–81]. This autophagy-like behaviour could also be related to the ER-originated pre-autophagosome formation, where STING is located [41].

Signalling Downstream of STING

The STING-dependent cellular responses are mainly dependent on two transcription factors, IRF3 and NF-κB (**Figure 2**). STING activation first induces adaptor dimerisation [82] and TRIM56-dependent ubiquitination to enable TBK1 docking [83]. Together, STING and TBK1 migrate to the perinuclear membranes of the Golgi via autophagy-like processes [6, 18, 79]. The association between STING-TBK1 leads to auto-phosphorylation of TBK1 at S172, a residue known to induce TBK1 activation [84, 85]. This further allows TBK1 to phosphorylate STING at S358 and S366 (S357 and S365, respectively, in mouse STING). Phosphorylated S366, together with L374, are important for the recruitment of IRF3 in close proximity to TBK1 at the C-terminus of STING, thereby enabling TBK1 to phosphorylate and activate IRF3 by exposing its nuclear localisation signal [18]. Activated IRF3 then translocates into the nucleus and promotes expression of type I interferons. Via a rapid feedback mechanism, IFN-I is released and binds to cell surface interferon receptors (IFNαRs), which then induces the expression of interferon-stimulated genes (ISGs) via Tyk2/JAK1 [86–88] and STAT1-STAT2 dimers [89, 90].

Figure 2. STING activated signalling pathways.

STING activation leads to translocation from ER membranes to the perinuclear vesicles where it induces the signalling of two major pathways: the NF-κB -dependent proinflammatory response and the IRF3-dependent type I interferon response. The activation of mitochondrial antiviral adaptor MAVS also results in the activation of STING and recruitment of TBK1, which upregulates the transcription of antiviral chemokines via STAT6.

Figure 2.

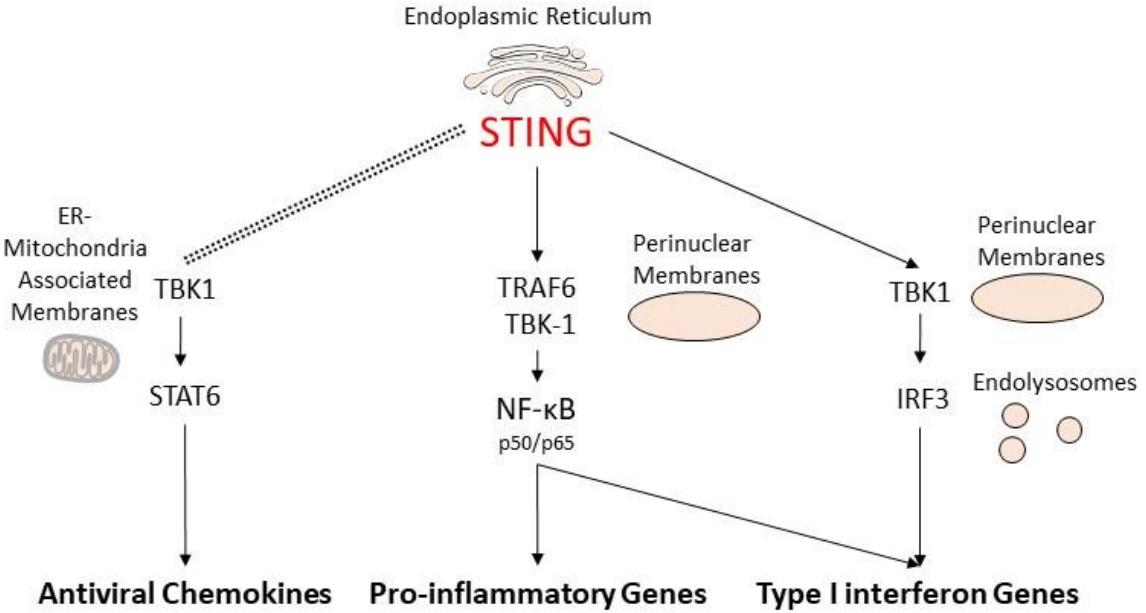
Endoplasmic Reticulum
STING
ER-
Mitochondria
Associated
Membranes
TBK1
STAT6
TRAF6
TBK-1
NF-κB
p50/p65
Perinuclear
Membranes
TBK1
IRF3
Perinuclear
Membranes
Endolysosomes
Antiviral Chemokines
Pro-inflammatory Genes
Type I interferon Genes

STING ligands have also been shown to activate the canonical NF-κB pathway (**Figure 2**), leading to the production of pro-inflammatory cytokines including IL-1α, TNF-α (tumour necrosis factor-α), IL-6, and numerous chemokines such as CXCL10 and CCL-2 [9][19]. The mechanism of this was found to be dependent on STING-TBK1 activation, which in turn regulates the activation loop of IKKα/β releasing p65 to form active dimers with p50. Hence, the functional NF-κB complex can translocate into the nucleus and promote transcription of pro-inflammatory genes. Abe and Barber also suggested that TRAF6 may be involved upstream of TBK1, which likely facilitates NF-kB activation [19]. However, the IFI16-dependent STING pathway can only induce IRF3 but not NF-κB activation, which would serve to preserve the survival activities regardless of the antiviral response during infection [91].

Regulatory Motifs of STING Activity

The sequence and topology of STING has been studied in parallel to its function. It is known that STING is a 379 amino acid long ER transmembrane protein encoded by the human *TMEM173* gene **(Accession NP_938023, XP_291127)** and homologous genes in other mammalian species. The STING structure is highly conserved between mammalian species, with the N-terminal forming a putative multi membrane-spanning region, a middle CDN-recognition domain, and a cytoplasmic tail (**Figure 3**).

Figure 3. The domain structure of human STING protein.

Human STING is a 379 amino-acid long ER-resident protein. The N-terminal contains 5 membrane-embedded domains (dark blue) including 4 transmembrane domains and Helix α1 responsible for ligand sensing and protein dimerisation. The C-terminal is mainly cytoplasmic (pale blue). It contains the cyclic dinucleotide (CDN) binding domain and interaction sites for TBK1 and IRF3 at the tail. Numbers above STING sequence indicate the amino acids comprising the functional domain.

Figure 3.

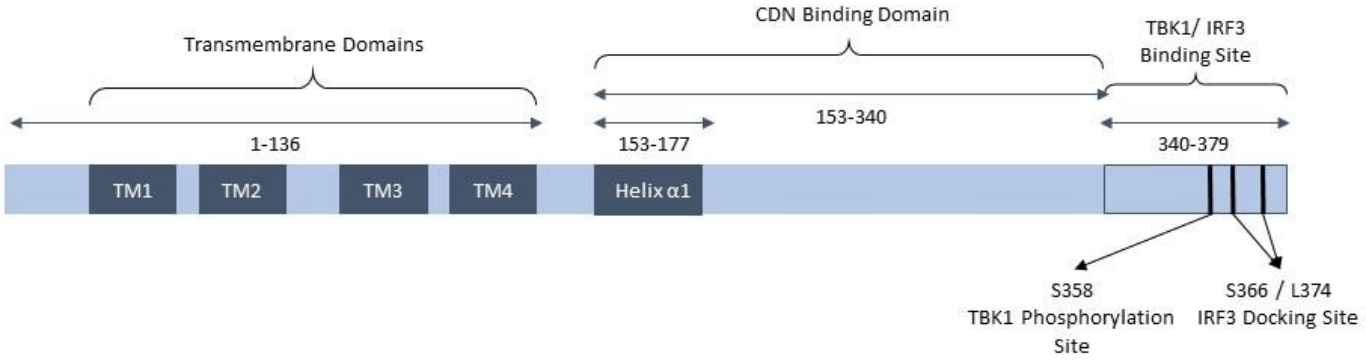
Transmembrane Domains
CDN Binding Domain
TBK1/ IRF3
Binding Site
153-340
1-136
153-177
340-379
TM1
TM2
TM3
TM4
Helix α1
S358
TBK1 Phosphorylation
Site
S366 / L374
IRF3 Docking Site

It is understood that the N-terminal 130 amino acids of STING form four transmembrane helices [92, 93] that are mainly responsible for membrane anchorage and inter-organelle trafficking [94] (**Figure 3**). An additional helix, named helix α1, was previously considered as the fifth transmembrane domain [6, 8, 95, 96] but has more recently been proposed to form a distinct domain with different functions [97]. Helix α1 is formed between residues 153-177 and has been reported to play an essential role in protein folding and dimerisation. Compromising the integrity of helix α1 causes STING precipitation in the cytoplasm and abolishes the homo-dimeric structure due to the loss of abundant hydrophobic interactions between dimers [97]. Ouyang's group reported that helix α1 also supports strong hydrogen force between STING dimers and cyclic di-GMP, suggesting its importance in multiple STING functions [98].

In addition to helix α1, the rest of the cytoplasmic tail also contributes to STING dimerisation [7], cyclic dinucleotide recognition [99], and TBK1 and IRF3 recruitment [18, 100] (**Figure 3**). In the absence of ligands, STING dimers show an open structure susceptible to cyclic dinucleotides [98]. Upon recognition of cyclic di-GMP, residues 139-344 are rearranged to expose a docking site for TBK1 [98], enabling TBK1 to phosphorylate STING at serine 358 [8]. This phosphorylation in turn enhances TBK1-STING attachment. Tanaka's group found that a 39-residue fragment at the carboxyl end of the STING protein was sufficient to activate IRF3 signalling in response to DNA challenge [18], and the loss of this tail region, encoded by exon 7, creates a dominant negative STING isoform for TBK1-IRF3 signalling [101]. Further truncation of the STING C-terminal fragment revealed that S366 and L374 are the key residues for IRF3 recruitment and activation [18]. Therefore, TBK1 and IRF3 are recruited to STING in a 20 amino acid –spanning region to facilitate their interaction by close proximity.

Crystallisation of the STING protein has revealed that key residue substitutions or segment deletions significantly alter its structure, resulting in a dysfunctional protein [6, 7, 53, 97, 98, 102]. Mutations of single or multiple amino acids of STING have been found to influence its dimerisation capability [39, 103–105], ligand binding

capacity [39, 104–106], or the ability to be post-translational modified by regulatory proteins [102, 107]. Some of these mutations occur naturally in humans to cause lethal autoinflammatory diseases [39, 105, 108], and some were generated experimentally in order to understand the structure-function relationship of STING [53, 96, 97, 102].

STING Variants

STING variations exist between mammalian species; the amino acid sequences of human and mouse STING are 68% identical and 81% similar [54]. Whilst this may not lead to dramatic differences in their three-dimensional structures, the structural differences at certain amino acid residues may be responsible for species-specific immune responses to some viral infections. For instance, Dengue virus (DENV) can inhibit STING signalling in human but not in mouse [107, 109]. DENV encodes for the protease NS2B3 that cleaves human STING at a highly-conserved putative cysteine motif (C88XXC91) to disable the adaptor. The equivalent cleavage target in mouse STING (mSTING) harbours a mutation that prevents NS2B3 cleavage, thus mouse STING can avoid DENV evasion. Mutant mouse embryonic fibroblasts transfected with hSTING re-constructed with a mouse NS2B3 cleavage site sequence blocks the type I interferon response against DENV. Specifically, a substitution of S135A in hSTING sequence results in inhibition of NS2B3 cleavage, suggesting that protecting STING at this residue may provide the basis for a novel anti-Dengue treatment [107].

In humans, single nucleotide polymorphisms (SNP) of STING were found to result in different levels of IFN-I signalling modulation (**Table 2**). Substitution at R284M can greatly stabilize the STING dimer, indicating its strong potential to cause chronic STING-dependent autoimmunity [103]. Substitution at R293Q can strongly reduce the c-di-GMP –induced IFN-I signals and completely abolishes the signals induced by other 3’-5’ bond cyclic dinucleotides [104]. Other single residue polymorphisms such as R232H and G230A may affect the ligand binding pocket of STING, thereby reducing its response to bacterial ligands [104]. In particular, a loss-of-function triple

STING mutant, R71**H**-G230**A**-R293**Q** (named HAQ), abolishes almost 90% of the interferon response to all cyclic dinucleotides [110]. The HAQ mutant occurs in one-fifth of the population from a thousand genome screen [104]. Homologous HAQ mutant knock-in mice have demonstrated that a variety of immune cells, including lymphocytes and Ly6C^{hi} monocytes, express significantly less STING protein compared to the wildtype, and the mutant animals completely failed to respond to CDN challenge [106]. This suggested that the HAQ mutant may be a *de facto* null allele of STING, thereby reducing the availability of the STING protein to mediate a dsDNA sensing response.

Table 2. Mammalian STING variants and mutants.

Single nucleotide polymorphisms of STING have been discovered in human and mouse which are implicated in dysregulation of type I interferon signalling and the proinflammatory innate immune response. STING mutations highlighted in green manifest as loss-of-function characteristics, mutations highlighted in red manifest as gain-of-function characteristics, and mutation in black lacks any gain-of-function or loss-of-function characteristic of STING. Gain-of-function mutations of V155M, N154S and V147L have been identified in human autoinflammatory disease called STING-associated vasculopathy with onset in infancy (SAVI), and substitution of G160E is the major cause of another human autoimmune disease known as familiar chilblain lupus (FCL). The most predominant loss-of-function STING mutant named HAQ is considered to compromise host innate response against infection, yet no clinical evidence is available for further discussion. Others STING mutations are experimentally created to study type I interferon signalling pathways, but they are potentially pathological.

Mutation	Motif	Functional effect/ Disease association	Occurrence	References
S162A	ligand binding site	Reduce c-di-GMP binding Increase hSTING sensitivity to DMXAA	N/A	[53]
G230A	ligand binding site	Impair C-terminal binding to c-di-GMP	N/A	[104]
G230A-R293Q	ligand binding site	Double mutant Partially reduced IFN-β response to bacterial ligands	5.2% / 1000 human genome	[104]
R293Q	ligand binding site	Significantly reduced IFN-β response to bacterial ligands	1.5%/ 1000 human genome	[104]
R232H	ligand binding site	Partially reduced IFN-β response to c-di-GMP and complete loss of IFN response to other bacterial ligands	13.7% / 1000 human genome	[104]
R71H-G230A-R293Q (HAQ)	Recessive Null allele	Triple mutant Low intrinsic IFN-β/NF-κB promoter activity Homologous significant decrease STING expression and abolish IFN-I response to all STING ligands	20.4% / 1000 human genome	[104] [106] [110]
V155M	Hydrophobic core, ligand binding site	SAVI, constitutive activation	Very rare	[39] [108]
N154S	Hydrophobic core, ligand binding site	SAVI, constitutive activation	Very rare	[39]
V147L	Hydrophobic core, ligand binding site	SAVI, constitutive activation	Very rare	[39]
I200N	Interior STING promoter	Complete abolish STING activity, equivalent to I199N mSTING missense mutation, Goldenticket strain	N/A	[111]
G160E	Dimerisation domain	FCL, constitutive activation	Very rare	[105]
S366A (loss) or S366D (gain)	Ulk1/2 target phosphorylation site	Both loss-of-function (S366A) & gain-of-function (S366D) mutations block IRF3 binding	N/A	[102]

The function of several STING residues has been characterised using experimental point mutations (**Table 2**), some of which were also found to occur naturally in mammals. A C57BL/6 –derived, Goldenticket (Gt) mouse strain harbouring a single I199N mutation in STING leads to the complete abolishment of IFN-I activity to *Listeria monocytogenes* infection or stimulation of cyclic di-GMP and cyclic di-AMP [111]. The human equivalent mutation I200N was also considered to have the same effects, but no such spontaneous mutant has been discovered. Only a few gain-of-function hSTING mutants have been identified clinically [39, 105] (**Table 2**). Patients with these STING mutations showed early on-set of severe systemic inflammation in blood vessels and various organs, displaying chronic inflammatory symptoms that are highly similar to pathologies of SLE (systemic lupus erythematous) and AGS (Aicardi-Goutières Syndrome) [39, 105]. All of these STING mutants have shown considerable structural resemblance to the active conformation, presumably leading to constitutive adaptor dimerization and signalling to type I interferon production. Both Liu and König's groups suggested that inhibition of the interferon signalling adaptor JAK could significantly dampen IFN-I over-expression as measured in biopsy samples from these patients, indicating that JAK inhibitors could be a promising avenue to therapeutically control disease progression.

As evidenced by the above studies, STING variants are likely to be associated with increased susceptibility to certain infections and autoimmune diseases, emphasising the value of genetic analysis of individual mutations to reveal novel targets for developing personalised therapy and immunisations.

STING Regulations

As a critical coordinator of the innate immunity, STING is tightly regulated by a variety of signalling molecules. Except that STING is post-translationally modified to enable dimerisation and activation, some regulators are essential for the prevention of constitutive type I interferon signalling which have been shown to cause autoimmunity both in animal models [6, 112] and in human [39, 108]. Negative

regulation of STING signalling is necessary for the resolution of inflammatory responses post infection (**Figure 4**).

Figure 4. Negative regulation of STING-mediated response.

STING-mediated signalling can be negatively regulated via multiple mechanisms, including E3 ubiquitin ligase TRIM30α- and TRIM21- mediated degradation of STING and its upstream DNA sensor DDX41, respectively. Certain phosphodiesterases (PDEs) also specifically hydrolyse bacterial cyclic dinucleotides to prevent them being sensed by STING. Akt kinase is also capable of inhibiting cGAS detection of cytoplasmic DNA. Activated cGAS produces 2'-3' cGAMP to release AMPK-mediated inhibition of ULK1, which in turn blocks IRF3 recruitment downstream of STING activation. 2'-3' cGAMP produced by cGAS can also activate Beclin-1 which can sequester cGAS as well as induce degradation of dsDNA. In a negative feedback loop, the product of the IRF3-dependent antiviral response, microRNA-576-3P (miR-576-3P), can prevent further STING activation. Some viruses can encode proteases or protein inhibitors to interfere in STING signalling, while others may enhance the activity of inflammasome complexes NLRC3 and NLRX1 to block STING/ TBK1 interaction.

Figure 4.

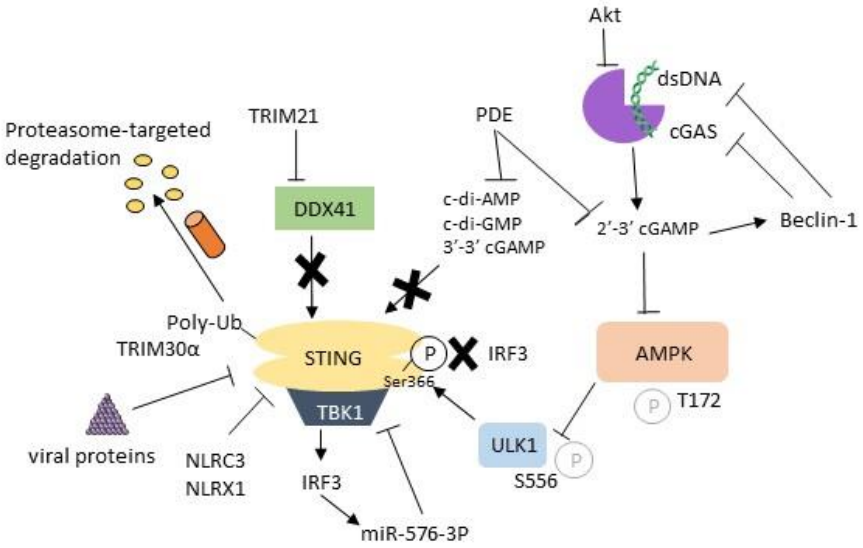
Akt
dsDNA
cGAS
TRIM21
PDE
Proteasome-targeted degradation
DDX41
c-di-AMP
c-di-GMP
3′-3′ cGAMP
2′-3′ cGAMP
Beclin-1
Poly-Ub
TRIM30α
STING
P
IRF3
Ser366
AMPK
TBK1
T172
ULK1
P
S556
viral proteins
NLRC3
NLRX1
IRF3
miR-576-3P

Post-translational regulators

Post-translational modifications contribute to the spatio-temporal regulation of STING signalling. STING is commonly modified by ubiquitination and phosphorylation. Upon ligand binding, the E3 ubiquitin ligase TRIM56 is recruited to initiate K-63 linked ubiquitination on STING, a prerequisite for STING dimerisation and activation [83]. Another E3 ligase AMFR (Autocrine motility factor receptor), together with its interacting partner INSIG1 (insulin-induced gene 1), catalyses K-27 linked poly-ubiquitination, which is critical for TBK1 recruitment [113]. In contrast, TRIM30α-dependent K275 ubiquitination [112] and RNF5 (RING finger protein 5) -dependent K150 ubiquitination [114] degrade STING dimers and negatively regulate antiviral signalling (**Figure 4**). This process is likely to involve the antiviral adaptor protein MAVS on mitochondria at the MAMs where the closely associated ER and mitochondrial membranes bring STING and MAVS in close proximity [115, 116]. Since ubiquitination is critical to STING regulation, some viruses can secrete proteases to specifically disrupt this process to suppress innate immune recognition, as summarised below (**Table 3**).

Table 3: STING-mediated evasion of antiviral immunity.

A number of DNA and RNA viruses have been found to encode and secrete STING-targeted proteases or inhibitors to prevent innate immune detection to help establish the of latent phase of infection. Viruses of the same family tend to adopt similar strategies/mechanisms to block STING activation. Some viruses also express multiple inhibitors to target both DNA sensors and STING, or release viral oncogenes in parallel to further compromise immunity, which consequently increases their chance of survival in the host.

Pathogen	Mechanism of Action	References
Yellow fever virus Dengue virus	NS4B interrupts STING activation	[11]
Hepatitis C virus	NS3/4A, NS4B proteases interrupt STING activation	[137] [138]
Herpes simplex virus-1	Release ICP0 E3 ubiquitin ligase to degrade IFI16 Viral protein ICP27 binds to STING-TBK1 complex to prevent IRF3 signalling	[139][140] [147]
Coronaviruses SARS and NL63	Disrupt K63-linked ubiquitin-mediated STING dimerisation	[140]
Human papillomavirus	E2 protein inhibits STING transcription E7 oncogene blocks cGAS/STING signalling	[141] [142]
Adenovirus	E1A oncogene blocks cGAS/STING signalling	[142]
Hepatitis B virus	Disrupts K63-linked ubiquitin-mediated STING dimerisation	[143]
Kaposi's sarcoma-associated herpesvirus	ORF52 proteins bind to and inhibit cGAS Targets IFI16 degradation during lytic reactivation	[62]
Epstein-Barr virus, Murine gammaherpesvirus 68, Rhesus monkey rhadinovirus	ORF52 proteins bind to and inhibit cGAS	[144] [145]
Human immunodeficiency virus	Enhance STING suppressor NLRX1 Enhance TREX1 to degrade excessive cDNA Viral Capsids prevent innate sensing of cDNA	[67] [65][68] [146][148]
Human cytomegalovirus	Tegument protein pUL83 disrupts IFI16 oligomerization and activation	[63]

Some STING activities are also critically dependent on its phosphorylation. One such example is the phosphorylation of S366 on the C-terminal domain to provide docking sites for IRF3 prior to its phosphorylation by TBK1 [6, 100, 117]. ULK1-dependent phosphorylation on S366 post Golgi trafficking blocks IRF3 binding to STING and thus prevents chronic STING activation [102] (**Figure 4**). ULK1 acts upon release from its repressor AMPK (adenosine monophosphate activated protein kinase) which is induced by production of 2'-3' cGAMP from cGAS. Interestingly, both loss-of-function (S366A) and gain-of-function (S366D) mutations can abrogate IRF3 signalling [18], suggesting that either the phosphorylation of S366 is temporally and spatially regulating IRF3 docking, or that alternative post-translational modifications are responsible for this functional regulation. In particular, S366-dependent inhibition of IRF3 does not impair the NF-κB pathway, indicating that these two pathways act independently of each other, which has likely evolved to prevent dysregulated antiviral responses from affecting survival activities [102].

STING can be negatively regulated by the NLR family inflammasome components NLRC3 [118] and NLRX1 [67] (**Figure 4**). Both of these have been shown to sequester STING to prevent TBK1 recruitment; in particular the latter is strongly enhanced in HIV infection to suppress STING-dependent recognition of reverse-transcribed dsDNA [67]. Depletion of NLRX1 not only impedes nuclear transportation of viral DNA, but also restores the STING-mediated interferon response to stall progression of infection. This suggests that pharmacological suppression of intrinsic STING inhibitors could potentially support the re-establishment of STING-mediated innate immunity against RNA viruses, and thus may offer promising adjuvant therapy to combat retrovirus infection. However, Guo and colleagues also noted that such suppression must be finely controlled to avoid excessive inflammatory responses that may lead to autoimmunity [67].

Post-transcriptional regulation

A primate specific microRNA (miR)-576-3p has been identified as a novel STING regulator that promotes virus replication [119] (**Figure 4**). Over expression of this

microRNA promotes the spread of vesicular stomatitis virus, whereas its inhibition protects against virus growth. Further studies show that miR-576-3p is an IRF3-induced gene that can target multiple genes of interferon-stimulators, including STING, MAVS, TRAF3 and STAT6, thereby reducing their levels [119]. Since IRF3 is a downstream signalling molecule in the STING-TBK1 axis, upregulation of miR-576-3p serves as a negative feedback loop to prevent sustained inflammatory response during and post infections.

Alternative mechanism of STING downregulation

A recent discovery suggests that certain phosphodiesterases (PDEs) may specifically degrade bacterial cyclic dinucleotides to halt excessive STING activation [120–123] (**Figure 4**). The pathogen *Mycobacterium tuberculosis* secretes phosphodiesterases MtbPDE (Rv3586), cnpB and CdnP to remove cytosolic CDN, thus avoiding STING mediated detection [124–126]. Although this may appear to undermine bacterial virulence and growth signals that are critical to infection [124], it can also significantly reduce early type I interferon induction. In particular, the enzyme CdnP can degrade both bacterial-derived and host-derived cyclic dinucleotides, critically promoting survival of *M. tuberculosis* at early stages of infection [125].

In addition to the above regulatory mechanisms, Akt kinase (or protein kinase B, PKB) has been shown to phosphorylate cGAS at residues S291 or S305 to stall signalling via STING [127], while the E3 ubiquitin ligase TRIM21 can specifically target the DNA sensor DDX41 at residues K9 and K115 for proteasome degradation and hence prevent recognition of DNA and STING-dependent type I interferon expression [128] (**Figure 4**). The autophagy protein Beclin-1 may also terminate STING-dependent immunity by sequestering cGAS and promoting autophagy-dependent digestion of dsDNA [129] (**Figure 4**). This is thought to prevent prolonged DNA recognition, which could lead to autoimmunity.

STING in parasitic infection

Immune responses to malaria infection are highly strain specific; the lack of understanding linked to these strain specific responses makes the disease clinically difficult to manage [130–132]. Recent studies on host-parasite interaction have revealed distinct roles for STING-dependent type I interferon responses during crosstalk with other pro-inflammatory pathways. CD40 receptors expressed on antigen-presenting cells are understood to initiate the cellular and humoral response of the adaptive immunity, specifically enhancing the generation of immunoglobulins against pathogens [133, 134]. Mice infected with *Plasmodium yoelii nigeriensis,* infected red blood cells, TLR ligands or parasitic DNA/RNA upregulate both CD40 and type I interferon expression, whereas the loss of CD40 can reduce the level of STING further impairing the early type I interferon response in macrophages and dendritic cells [135]. Although CD40-induced STING upregulation leads to reduced CD40 levels and thus downstream NF-κB signalling, type I interferon immunity has been suggested to be highly inducible in certain strains of parasitic infection [135].

The establishment of malaria infection in the host is critically dependent on early innate immune mechanisms. Yu *et al.* suggested that depletion of plasmacytoid dendritic cells, rather than canonical dendritic cells and macrophages, can significantly impair type I interferon signalling at 24 h post *Plasmodium yoelii* infection [136]. The ubiquitous STING-cGAS pathway has been shown to enhance type I interferon production, and also potently induces SOCS1 to inhibit the MyD88 / IRF7-dependent type I interferon production which specifically acts on pDCs to protect against early malaria infection. The loss of STING and cGAS in mice augments the immediate type I interferon response from pDCs following malaria infection, and therefore protects the animal against early mortality [136]. Therefore, STING’s activity and its crosstalk with other proinflammatory pathways may be variable in complex diseases such as malaria, and thus the manipulation of STING signalling axis for therapeutic benefits may be difficult to achieve.

Viral Evasion of STING

It is evident that many viruses can evade STING signalling to establish a biological niche in mammalian cells, and that those within the same family tend to adopt similar evasive strategies [11, 62, 63, 65, 67, 68, 137–148] (**Table 3**). For instance, several members of the *Gammaherpesviridae* family were found to express ORF52 protein homologs to disrupt cGAS activities, preventing subsequent production of 2'-3' cGAMP [48]. Species of the *Flaviviridae* and *Coronaviviridae* families tend to secrete proteases that directly cleave or block STING [140]; typical examples include the NS2B/3 and NS4B proteases released by *flaviviridae* Dengue virus and hepatitis C virus, respectively, which can both degrade hSTING. In particular, NS4B protease shows strong homology to the ER-embedded N-terminal domains of STING, leading to colocalisation and direct protein-protein interactions with STING [11]. It has also been suggested that tumour associated viruses such as human papillomavirus and adenovirus could potentially release oncogenic proteins to block cGAS/STING interactions with tumour suppressors, hence compromising innate immunity and supporting cancer progression [142].

The impairment or absence of interferon responses often seen in HIV infection has been proposed as one of the mechanisms by which this virus is capable of suppressing host immunity [148–151]. Recent research suggests that HIV-1 enhances the action of NLRX1 to dampen STING activity [67] and recruits host 3' exonuclease TREX1 to degrade excessively produced, reverse-transcribed, viral DNA thereby avoiding detection by the cGAS/STING pathway [68, 152]. The capsid of HIV also regulates its association with host protein cyclin A, which controls the masking of viral cDNA from cGAS recognition in the cytoplasm and its exposure in the nucleus to facilitate genome integration [146]. Mutations in the HIV-1 capsid sequence enhance its binding to cyclin A prematurely in the cytoplasm enabling DC sensing of double-stranded DNA and a potent innate immune response against viral infection [146].

STING Related Autoimmunity

Type I interferons are key cytokines induced by antimicrobial and antiviral immunity. This family of cytokines consists of the predominantly produced interferon-α and interferon-β, and the less abundantly expressed subtypes such as IFN-ε, -κ, -τ, and –ζ [153]. Type I interferons are ubiquitously expressed by a variety of cells including macrophages, lymphocytes, dendritic cells, fibroblasts and haematopoietic plasmacytoid dendric cells, with a widespread role in cellular biology [153, 154].

"Basal" expression of type I interferons is regulated via an autocrine mechanism [155], whereas the activation of interferon-inducing regulators such as STING can significantly boost their expression by activating the transcription factor IRF3. Type I interferons are released extracellularly for detection by self or nearby interferon receptors, IFNαRs, which are coupled to JAK1 (Janus kinase 1) and TyK2 (tyrosine kinase 2) [86, 87]. This activation further promotes the formation of STAT1-STAT2 heterodimers [23, 89, 90] and the subsequent recruitment of IRF9 to assemble the transcription complex ISGF3 to upregulates the expression of a series of interferon-stimulated genes (ISGs) [154]. A broad range of ISGs have been found to control chemotaxis, cell migration, apoptosis, cell proliferation, and to regulate immune detection and defence against infection; many of which have been thoroughly reviewed previously [156–160] (**Table 4**). Thus, dysregulation of type I interferon signalling can cause an excessive production of ISGs, in turn over-activating the immune system.

Table 4. Summary of interferon-stimulated genes (ISGs).

Expression of ISGs are induced by type I interferon via the JAK-STAT signalling pathway. ISGs are involved in a wide spectrum of cellular activities including apoptosis, immune modulation, cell migration and adhesion, and antiviral responses. Some ISGs have multiple roles in immune regulation but are not repeatedly indicated in the table.

Apoptosis	Immune Modultion	Cell Attraction & Adhesion	Antiviral & Pathogen Detection
CASP4	MxA	VEGF	OAS1
CASP8	MxB	FGF	Protein Kinase R
BAK1	ICAM1	VRP	Viperin
Fas/ CD95	SELL	PDGFRL	Tetherin
PLSCR1	CD47	ECGF1	IFI6
XAF-1	ALCAM	EREG	IFITM2
DAP kinase	IRF1-5 & 7	CTGF	IFITM3
RID	LGALS3B	MHC I&II	IRF1
	IFN-γ		IRF7
	IL-12		MHC I&II
	TNF-α		Ribonuclease L
	SOCS		GTPase Mx1
	USP18		ISG15
			ISG20
			ADAR1
			APOBEC

The persistent or excessive presence of cytoplasmic DNA is one of the major causes for chronic inflammation and autoimmune diseases. Chronic production of type I interferons, termed “type I interferonopathy”, is a key indication of immune dysregulation predominantly associated with DNA-induced autoimmunity. The overactive IFN-I response alerts cytotoxic immune cells systemically via ISG production. This in turn promotes sustained release of proinflammatory cytokines including IL-1α/β, IL-12, and TNF-α, causing excessive inflammation and tissue damage [161–163]. Autoimmunity also induces aberrant cell death, which releases cellular components to T and B lymphocytes and leads to the production of self-reacting antibodies that congest in capillaries [164]. Unresolved B cell activation predisposes individuals to the development of systemic lupus erythematosus (SLE) that is clinically challenging to treat [152, 165, 166].

Systemic lupus erythematosus is a systemic chronic autoimmune disease. [152, 165, 166] (**Figure 5**). SLE is often diagnosed by the accumulation of serological antinuclear antibodies (ANA) against nucleic acids released from dead cells, which cause multiple tissue and organ damage [167]. Chronic activation of DNA and RNA sensing pathways triggered by infection and cell death can contribute to the type I interferonopathy that predisposes individuals to SLE [166]. Mutations in nucleic acid sensors (such as endosomal Toll-like receptors [168], RIG-I [169], and DAI [170]), interferon regulatory factors [171] and DNases [172, 173] can also increase SLE susceptibility. Recently, Ding and colleagues proposed that the cGAS-STING axis could be another pathway potentially exacerbating SLE, via the upregulation of type I interferon production downstream of cytoplasmic DNA sensing cascades [174]. However, STING deficiency in macrophages in fact renders hyper-responsiveness to endosomal TLR ligands, and STING knockout mice have shown accelerated lymphocyte accumulation and expansion of an IFN-α -responding cell population [175]. This therefore suggests inhibitory roles for STING in SLE development. Sharma *et al*. also showed that STING suppression can restrict the expression of regulatory T cell activation factor IDO-1 and TLR negative regulators such as A20, SOCS1 and SOCS3, contributing to uncontrolled systemic inflammation [175]. Since

this effect is not seen in cells lacking IRF3, the transcription factor mediating most of DNA sensing responses downstream of the STING-TBK1 axis, it is possible that STING is immunosuppressive in inflammatory pathways independent of cytoplasmic DNA recognition. Therefore, autoimmune therapies targeting the STING pathway should be considered with caution and an awareness of the resultant STING down-regulation, which may have opposing effects in certain diseases.

Figure 5. Cells and cytokines involved in STING-associated autoimmune diseases.

Unresolved accumulation of cytoplasmic DNA can potentially trigger chronic inflammatory responses which result in autoimmune diseases, including (A) systemic lupus erythematosus (SLE) and (B) Aicardi-Goutières Syndrome (AGS). Both diseases are strongly associated with persistently enhanced type I interferon upregulation named type I interferonopathy and subsequent B and T lymphocyte activation that potentiates systemic tissue and organ damage. Though STING dysregulation has been suggested to play an essential role in the development of these diseases, current treatment of SLE and AGS still relies heavily on anti-inflammatory therapies and DNA resolving methods to ameliorate symptoms. Gain of function mutations of STING can cause two autoimmune diseases named (C) STING-associated vasculopathy with on-set in infancy (SAVI) and (D) familial chilblain lupus (FCL). Both diseases show similar manifestations to SLE and AGS and are much less responsive to STING ligands than other immune stimuli. Treatments for SAVI and FCL are limited but JAK inhibitors have been shown to ameliorate symptoms in patients with these two diseases.

Figure 5.

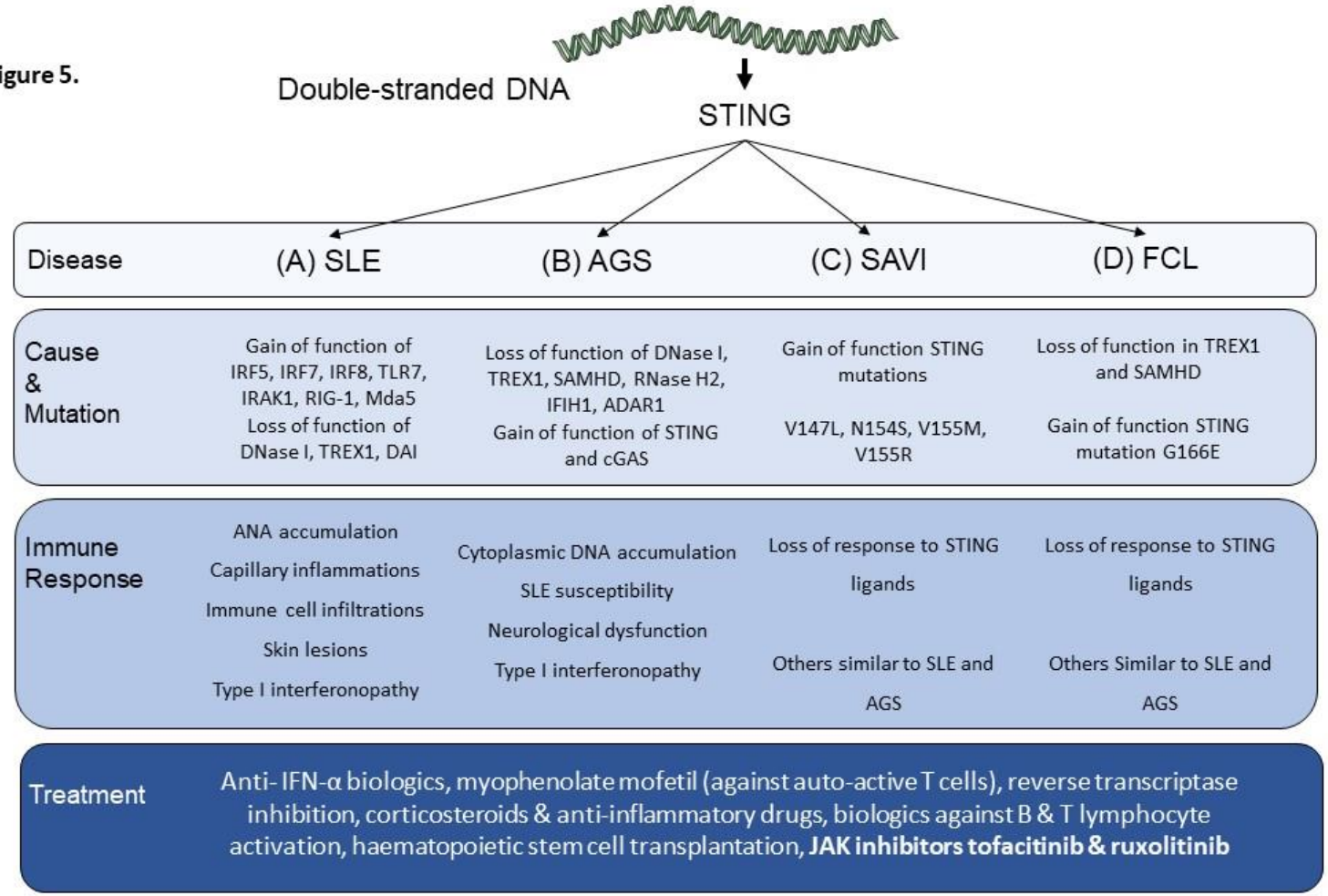
Double-stranded DNA
STING
Disease
(A) SLE
(B) AGS
(C) SAVI
(D) FCL
Cause & Mutation
Gain of function of IRF5, IRF7, IRF8, TLR7, IRAK1, RIG-1, Mda5
Loss of function of DNase I, TREX1, DAI
Loss of function of DNase I, TREX1, SAMHD, RNase H2, IFIH1, ADAR1
Gain of function of STING and cGAS
Gain of function STING mutations
V147L, N154S, V155M, V155R
Loss of function in TREX1 and SAMHD
Gain of function STING mutation G166E
Immune Response
ANA accumulation
Capillary inflammations
Immune cell infiltrations
Skin lesions
Type I interferonopathy
Cytoplasmic DNA accumulation
SLE susceptibility
Neurological dysfunction
Type I interferonopathy
Loss of response to STING ligands
Others similar to SLE and AGS
Loss of response to STING ligands
Others Similar to SLE and AGS
Treatment
Anti- IFN-α biologics, myophenolate mofetil (against auto-active T cells), reverse transcriptase inhibition, corticosteroids & anti-inflammatory drugs, biologics against B & T lymphocyte activation, haematopoietic stem cell transplantation, JAK inhibitors tofacitinib & ruxolitinib

AGS (Aicardi-Goutières Syndrome) is another genetically-based autoimmune disease, characterised by DNA-triggered type I interferonopathy [176] (**Figure 5**). Patients with AGS often carry mutations in DNA restriction factors including the 3' exonuclease TREX1 [177, 178], dNTP restriction factor SAMHD (SAM domain and HD domain) [179, 180], RNase H2 (ribonuclease H2) [181, 182], dsRNA sensor IFIH1 (IFN-induced helicase C domain containing protein 1) [183, 184], and the dsRNA-specific adenosine deaminase ADAR1 [185]. These regulators maintain a balance between the production and degradation of nucleic acids, providing intrinsic protection against immune activation due to "self-recognition". Mutations of DNA or RNA restricting factors cause nucleic acids to accumulate in the cytoplasm leading to SLE and AGS. Recent studies show that the type I interferonopathy associated with SLE and AGS is potentially cGAS-STING dependent, and that the aberrant IFN-I response can be suppressed by the loss of DNA sensor or STING in cells or animals expressing mutated *Trex1* or *Samhd* [180, 186].

Gain-of-function mutations in *STING* have been identified in infants who suffer from severe and chronic vasculopathy and pulmonary inflammation, a condition known as STING-associated vasculopathy with onset in infancy (SAVI) [39] (**Figure 5**). Mutations of STING V147L, N154S, V155M, and V155R were found to direct it to an active conformation enhancing dimerisation and inducing TBK1-IRF3 signalling (**Table 2**). This results in an excessive IFN-I response in fibroblasts, keratinocytes and immune cells to attract and amass proinflammatory cells and regulators in capillaries and tissues, ultimately causing lesions in these regions. Sustained IFN-I signals activate interferon receptors and promote expression of interferon-stimulated genes via JAK1-Tyk2 signalling and STAT1-STAT2 dimers. *In vitro* experiments and pioneering clinical studies suggest that JAK adaptor inhibition effectively dampens STING-mediated IFN-I over-activity. For instance, the elevated IFN-I levels in biopsy samples from SAVI patients can be restored close to that of the normal controls with treatment using the JAK inhibitor, tofacitinib [39]. Further investigation is required to examine the potential adverse effects of interferon suppression, which is likely to increase host susceptibility to infection.

Gain-of-function mutations of STING (**Table 2**) have also been linked to the autoimmune disease familial chilblain lupus (FCL) [105, 108], a rare hereditary form of SLE commonly associated with cytoplasmic DNA accumulation in monogenic mutations of exonucleases TREX1 [187, 188] or SAMHD [189] (**Figure 5**). A recent discovery reports FLC in five members of a four-generation family sharing the same *TMEM173* (STING) variant that encodes a single polymorphism of G166E. Structural analysis of mutated STING dimers reveals strong hydrogen attractions between E166 on one monomer and two threonine residues on the associating monomer, hence leading to enhanced adaptor dimerization and constitutive IFN-I -activated signalling [105]. Although limited treatment data is currently available for FCL, the authors showed that continuous administration of the JAK inhibitor tofacitinib can markedly ameliorate type I interferonopathy and associated symptoms in two patients. A similar therapeutic strategy was previously proposed by Liu and colleagues for treatment of STING-associated vasculopathy with onset in infancy (SAVI) [39]. Therefore, this therapeutic approach, based on mechanistic data, could be adapted to treat type I interferonopathy found in various diseases.

STING Regulates Lipid Metabolism

A new insight into STING research was recently provided by York and colleagues who suggested that this protein is a crucial element of cholesterol metabolism [45]. Previous studies indicate that high cholesterol levels in the plasma membrane correlate with viral loads and host susceptibility to infections [190, 191]. Virus and microbial infections have been shown to modulate lipid metabolism in the plasma membrane to facilitate infectivity. For instance, influenza virus encodes fusion protein haemagglutinin that is specialised in manipulating membrane lipid to permit penetration into the cytoplasm, a central step to viral infectivity and survival [192]. In addition, membrane lipids can also form signalling microdomain named lipid rafts which are frequently hijacked by HIV for attachment, signalling and budding to further promote infection [193, 194]. The antiviral type I interferon response reduces cholesterol availability in membranes to prevent viral infection; however the underlying mechanism remains largely unknown [195–197]. York's group recently identified that STING/TBK1 signalling is critical to the production of type I interferons to reprogram lipid biosynthesis in pathogenic infection [45]. They demonstrated that

the shift from lipid biosynthesis to lipid uptake not only affects the plasma membrane but also ER membranes, a cue to activate STING, bypassing the dsDNA sensing pathway. However, since STING is not the only adaptor for innate immunity against pathogenic DNA in the cytoplasm, it is conceivable that additional DNA sensors may further enhance STING actions to modulate cholesterol metabolism and promote antiviral processes. In light of the membrane fusion theory that potentially mediates STING activation [198], virus-host lipid regulation at the plasma membrane offers a promising and novel future research direction.

Therapeutic Targeting of the STING Pathway

Studies on STING regulatory pathways provide novel insights into antiviral and anti-inflammatory therapies. Activating STING-dependent pathways has been developed therapeutically for antiviral and, more recently, anti-tumour benefit. The predominant approach taken has been to introduce STING ligand cyclic dinucleotides to promote the IFN-I response, to combat infection or to prevent tumour progression. In contrast, type I interferonopathy associated with STING over-activity represents another set of pathologies underlying autoimmunity. Counteracting these disease processes requires potent suppression of STING signalling; attenuation of the interferon receptor adaptor JAK is used as a current target, whilst inhibiting immune cell activation may also help ameliorate symptoms.

Anti-tumour Immunotherapies

Certain types of cancer cells express molecular structures specifically recognised by CD8α+ dendritic cells (DCs), which subsequently interact with cytotoxic T cells to induce cancer cell death. This event, known as T cell priming, is a prerequisite for anti-tumour adaptive immunity relying on activation of CD8α+ dendritic cells to promote IFN-I signaling in immature T cells [199]. However, cancer cells also boost anti-inflammatory immune cells and regulatory T cells (Treg) to restrict CD8α+ DC activity thereby attenuating the activation of tumour-suppressive T cells [200, 201]. Therefore, a potent and long-acting adjuvant that can promote CD8α+ DC activities is highly desirable to enhance T cell priming and subsequent anti-tumour immunity.

It has been reported that the IFN-I response critical to T cell priming during tumourigenesis is dependent on the cGAS / STING pathway [42, 43]. Loss of STING in dendritic cells abolishes antigen cross-presentation from CD8α+ DC to T cells, whereas neither MyD88 nor TRIF knockouts can significantly affect DC IFN-I signalling, suggesting that STING may be the only adaptor central to this process [43]. In both immunogenic and irradiation-induced tumour models, tumour-derived DNA was engulfed and recognised by the universal DNA sensor cGAS prior to STING activation [42, 43]. However, direct stimulation with STING ligands also enhanced DC production of type I interferons, suggesting that STING-inducing therapies may offer potential as anti-tumour adjuvants.

Preclinical studies published recently suggest that DMXAA-derived cyclic dinucleotides have been successfully applied in established mouse models of malignant tumours achieving sustained tumour regression [202]. In malignant tumour B cells, STING also induces an ER stress response through the IRE-1 / XBP-1 (X-Box binding protein 1) pathway [203]. In the presence of 3'-3' cGAMP STING dimers are phosphorylated and aggregate, rather than undergoing degradation. This consequently enables prolonged STING signalling to induce apoptosis of tumour cells. Similarly, Tang *et al*. showed administration of 3'-3' cGAMP induces rejection of chronic lymphatic leukemia in mouse models [203]. Another promising vaccine candidate is the recently developed STINGVAX which combines granulocyte-macrophage colony-stimulating factor (GM-CSF) and formulated 2'-5' – 3'-5' linked cyclic dinucleotide [204]. In various established *in vivo* tumour models, STINGVAX has shown notable positive effects on dendritic cell activation and in promoting tumour-infiltrating T cells. Interestingly, activated cytotoxic T cells also upregulate the expression of PD-L1 (programmed death ligand 1), which enhances the therapeutic action of pro-apoptotic ligand PD-1 to promote tumour cell death. Although these STING-based vaccines have recently been developed and have been tested in mouse models, the synergistic effect of the combined STING agonist and immune promoting therapy represents a novel strategy to combat tumours by reinforcing both adaptive immunity and anti-tumour targets.

Inhibition of STING signalling can be achieved by targeting interferon receptors. As previously mentioned, gain-of-function mutations in *TMEM173* (the gene encoding STING) underlie type I interferonopathies that manifest in the autoimmune diseases, SAVI [39] and FCL [105]. Constitutive STING signalling was detected in both of these diseases resulting in dysregulated IFN-I signalling via interferon receptors and the adaptors JAK and Tyk. This leads to the accumulation of activated STAT1/2 dimers in the nucleus, promoting transcription of interferon-stimulated genes. Both Liu and König's groups demonstrated that treatment with the JAK1/3 inhibitor tofacitinib in patient biopsy samples suppresses STAT activation and restores the STING response to immune stimuli similar to healthy control cells [39, 105] (**Figure 5**).

Following the work of Liu and colleagues, Fremond's group conducted an 18-month clinical investigation on three patients expressing STING-mutations to assess the efficacy of the JAK1/2 inhibitor ruxolitinib [205] (**Figure 5**), which was previously found to partially inhibit STAT activation in *in vitro* studies of STING mutants [39]. Marked amelioration of systemic inflammation and reduction of interferon-stimulated gene expression was consistently observed in all three patients and in the subsequently recruited additional four patients with *STING* gain-of-function mutations. However, suspension of JAK inhibition in one patient resulted in a dramatic inflammatory relapse, though rescued by re-introducing ruxolitinib, demonstrating that this approach may be unsustainable and requires continuous monitoring [205–207]. Nonetheless, it is arguable that the partial inhibition of JAK-STAT pathway has the advantage of preserving STING-dependent immune protection against infection in these patients, since no excessive infection incidents were observed during these clinical trials [205]. Thus, it is timely to determine whether such JAK inhibitors can be modified and adapted for future treatment of type I interferonopathy.

Anti-inflammatory Biologics

Anti-inflammatory biologics represent a further opportunity to suppress interferon responses in order to control type I interferonopathy in autoimmune diseases, including but not limited to SLE, a major manifestation linked to STING over-activity. For instance, the anti-IFN-α drug sifalimumab is effective in controlling cutaneous and joint pain in SLE patients [208] (**Figure 5**).

Another approach to control SLE in STING gain-of-function mutations is to deplete or inhibit B-cell responses to prevent the over-production of auto-antibodies. The effective anti-SLE biologics, belimumab, targets the BLyS protein of B lymphocytes, preventing B cell activation and expansion critical to the production of autoantibodies and downstream activation of T lymphocytes [209, 210] (**Figure 5**). A series of stage II and stage III clinical trials have shown effective B-cell inhibition and significant improvement of clinical symptoms in combination with traditional care therapy of SLE in the treatment group compared to placebo control, whilst drug tolerance and immunosuppression-induced infection susceptibility were not markedly increased [210–212]. This suggests an effective drug efficacy and safety of belimumab over another B-cell depleting drug rituximab, which failed to ameliorate SLE symptoms in phase II and III trails [213]. Unlike JAK inhibitors and anti-IFN biologics, B-cell targeted therapies are much less effective in controling type I interferonopathy that consequently cause complex inflammatory responses in *STING* mutant patients. However, they are still commonly used to treat the SLE-related consequences of STING over-activation to stall symptom deterioration, while they have also been considered suitable adjuvant candidates for STING-targeted therapeutics.

Delivery of STING ligands

Accumulating evidence link STING-mediated IFN-I signaling to anti-tumour activity, and thus STING ligands have been proposed to offer promising immune-enhancing therapies to defend against DNA infections and tumourigenesis [41, 214]. However, targeting intracellular proteins such as STING remains challenging as the plasma membrane is a highly hydrophobic and size-selective barrier that resists passive entry of chemicals [57]. In contrast to the *de novo* STING ligand 2’-3’ cGAMP [48],

other cyclic dinucleotides are produced exogenously by pathogens and introduced into the cytoplasm by active transport or particle fusion [47, 50, 215]. Since the hydrophilic phosphate groups in dinucleotide compounds are strongly repelled by membrane lipid bilayers, designing an effective delivery system for cyclic dinucleotides would provide a significant step forward in the development of STING-specific therapeutics.

Under *in vitro* studies, transfection of microbial cyclic dinucleotides is aided by digitonin [35, 39, 50, 104] or liposomal-based systems such as Lipofectamine® [47, 102] (**Figure 6**). The former method, first described by Woodward's group [35], aims to achieve reversible permeabilisation of cellular membranes to increase uptake of chemicals [216–218], but is limited to *in vitro* studies due to high toxicity *in vivo*. In contrast, the liposomal-based delivery system is based upon the principle of encapsulating drugs in artificial double-layered liposomes for cytoplasmic delivery via liposomal fusion. The system is highly adapted for a variety chemicals and has been used in both laboratory studies and clinical practice [219].

Figure 6. *In vitro* and *in vivo* delivery of STING agonists.

The plasma membrane is a selectively permeable barrier that prevents cytoplasmic entry of large or hydrophilic molecules, including naked cyclic dinucleotides (CDNs) (1). *In vitro* (blue background) delivery of dinucleotide compounds could be achieved by the liposomal delivery system (2), or via reversible permeabilisation of plasma membrane to allow diffusion of naked CDNs into the cytoplasm (3). Recently designed YSK05-containing liposomes (4) could carry c-di-GMP across plasma membranes to induce DDX41-mediated STING activation as well as enhance the expression of MHC class I molecules and T cell co-stimulatory receptors (not demonstrated), and thus it is considered to be a potential adjuvant for cancer immunotherapy. In addition, the polyethyleneimine/ hyaluronic acid (LH) hydrogel-based vesicles use phagocytosis to deliver both STING ligands and antibody-stimulating agents such as ovalbumin (dark triangles) to cells (5), and enhance both STING-dependent innate immunity and MHC class II-activated adaptive immunity to suppress cancer growth. Both YSK05 particles and LH hydrogel-based particles have been tested *in vivo* (green background) to stall tumour progression in mice (6).

Figure 6.

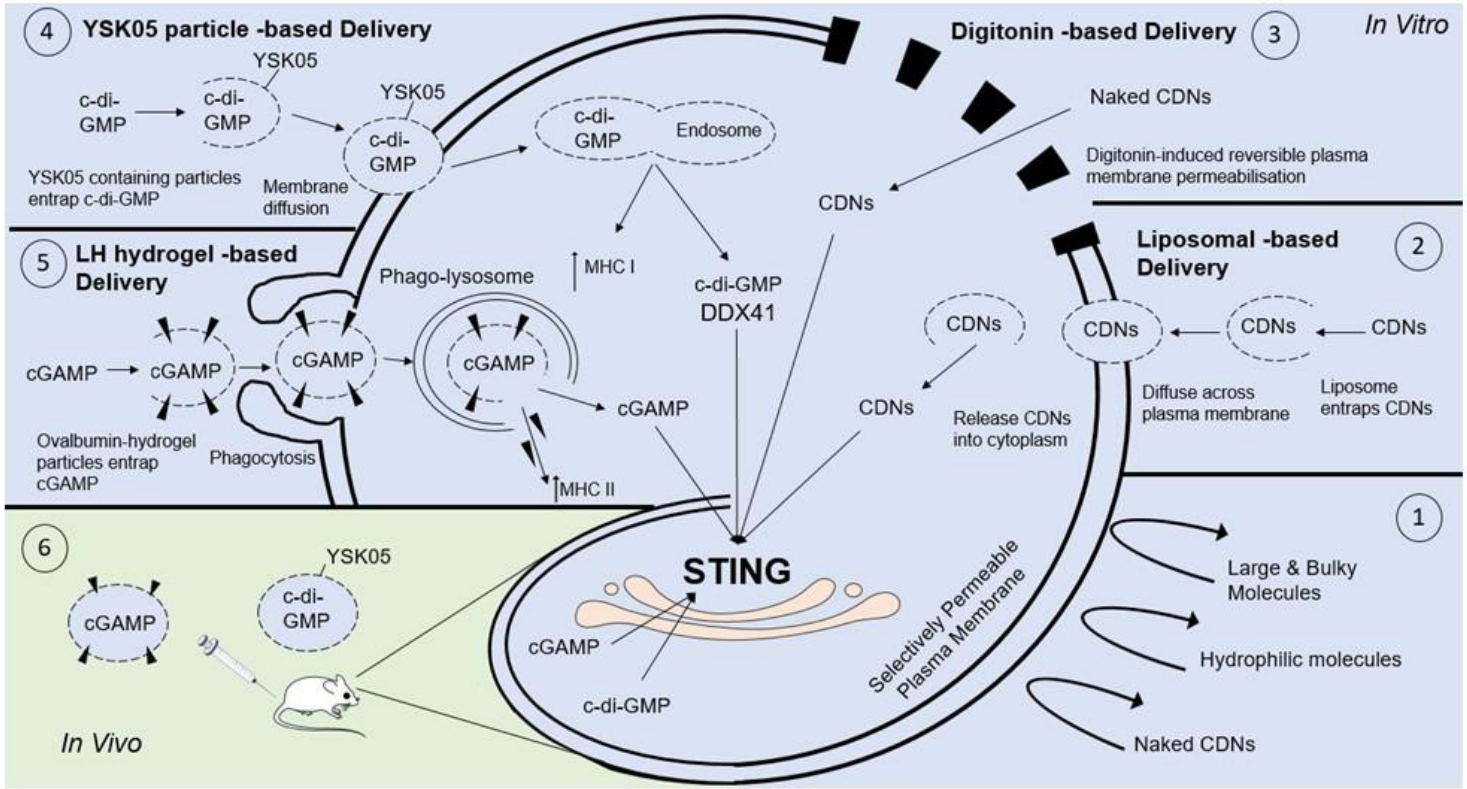
4
YSK05 particle -based Delivery
YSK05
c-di-GMP
c-di-GMP
YSK05
c-di-GMP
YSK05 containing particles entrap c-di-GMP
Membrane diffusion
c-di-GMP
Endosome
Digitonin -based Delivery
3
In Vitro
Naked CDNs
Digitonin-induced reversible plasma membrane permeabilisation
CDNs
5
LH hydrogel -based Delivery
Phago-lysosome
MHC I
c-di-GMP
DDX41
Liposomal -based Delivery
2
CDNs
CDNs
CDNs
CDNs
cGAMP
cGAMP
cGAMP
cGAMP
cGAMP
CDNs
Release CDNs into cytoplasm
Diffuse across plasma membrane
Liposome entraps CDNs
Ovalbumin-hydrogel particles entrap cGAMP
Phagocytosis
MHC II
1
6
YSK05
c-di-GMP
cGAMP
STING
cGAMP
c-di-GMP
Selectively Permeable Plasma Membrane
Large & Bulky Molecules
Hydrophilic molecules
Naked CDNs
In Vivo

In light of the liposome-based designs, Miyabe's group has reported that the YSK05-based lipid particles were able to entrap and deliver cyclic di-GMP into the RAW 264.7 macrophage cell line [220] (**Figure 6**). These particles induced cellular expression of type I interferon genes which were effectively blocked by the TBK1 inhibitor BX795, suggesting that the interferon response was specifically induced via the STING/TBK1 pathway. Furthermore, the YSK05-based particles also express high levels of the antigen-presenting molecule MHC class I and T cell co-stimulating molecules CD80 and CD86 that are a prerequisite of T lymphocyte activation; all of these characteristics suggest they offer potential as adjuvants in anti-tumour therapies. Preliminary tests carried out by Miyabe and colleagues showed that mice immunized with cyclic di-GMP containing YSK05-liposomes reject tumour implantation compared to matched controls [220]. Subsequently, Nakamura's group demonstrated that *in vivo* injection of these particles greatly enhances the expression of IFN-I and MHC class I molecules in tumourigenic mice, resulting in augmented NK cell activation and potent innate immune protection against lung melanoma metastasis [221]. Therefore, the YSK05 liposomes offer a potential vehicle to assist delivery of STING ligands and to develop STING-based adjuvants for cancer immunotherapy.

As an alternative approach, a nanoparticle-based delivery system developed by Lee and colleagues also enables *in vitro* delivery of cyclic dinucleotides to target STING pathways for anti-tumour effects [222] (**Figure 6**). This method employs polyethyleneimine / hyaluronic acid (LH) -based hydrogels to enclose dinucleotide drugs into micron size spheres, which are selectively taken up by phagocytic cells such as RAW 264.7 macrophages, L929 fibroblasts and bone marrow-derived macrophages (BMDMs), but not by non-phagocytic fibroblasts. Thus, the micron-sized particles appear to target phagocytosis specifically to gain entry into the cytoplasm. Furthermore, Lee *et al*. showed that LH-cGAMP hydrogel can induce IFN-I spikes in RAW264.7 macrophages, which were more than twice the magnitude of that induced by lipofectamine-delivered cGAMP at the same dose [222]. Administration of ovalbumin-containing LH-cGAMP particles in mice activates both the type I interferon response and humoral production of IgG to protect against ovalbumin challenge. Taken together, Miyabe and Lee's work indicates that the

modified liposome-based delivery systems can markedly enhance *in vitro* and *in vivo* delivery of cyclic dinucleotide to cytoplasmic STING, and this success will promote the development of novel cancer vaccination and immunotherapies dependent on STING signalling.

Conclusions

Cytoplasmic DNA has been implicated in many human pathologies, many associated with chronic inflammation. Research has revealed that the ER transmembrane protein STING is a crucial player in dsDNA pathogen -sensing pathways whose dysregulation contributes to the development of several diseases. By responding to DNA sensors and cyclic dinucleotides, STING induces IRF3- and NF-κB –dependent pathways to elicit proinflammatory responses against infection and cancer progression. STING also directly cross talks with several other regulators to modulate critical biological processes including autophagy and cholesterol biosynthesis. It is evident that activating STING results in the type I interferon response to protect against infection and tumour formation, while dysregulated gain-of-function STING mutations lead to detrimental consequences of autoimmunity. Understanding the molecular signalling mechanisms of STING activation has provided new insights to advance therapeutic strategies in treating infection, cancer and autoimmune diseases. It has also prompted the development of intracellular delivery systems to administer STING agonists. Despite the fact that STING has only been studied for a decade, this adaptor protein will continue to attract attention in immunology research and clinical practice into the future.

List of Abbreviations:

STING: STimulator of INterferon Genes

ER: Endoplasmic reticulum

DNA: deoxyribonucleic acid

RNA: ribonucleic acid

dsDNA: double-stranded DNA

ssRNA: single-stranded RNA

cDNA: complementary DNA

mtDNA: mitochondrial DNA

TRAP: Translocon-associated protein

ERAD: Endoplasmic Reticulum-associated degradation

Type I interferon/ interferon: IFN-I/ IFN

TBK1: TANK binding kinase 1

IRF: Interferon regulatory factor

VSV: Vesicular stomatitis virus

CDN: cyclic dinucleotide

cGAS: cyclic guanosine monophosphate – adenosine monophosphate synthase; cyclic GMP-AMP synthase

cGAMP: cyclic guanosine monophosphate – adenosine monophosphate; cyclic GMP-AMP

DAI: DNA-dependent activator of IFN-regulatory factor

IFI61: IFNγ-inducible protein 16

DDX41: DEAD-Box Helicase 41

HCMV: Human cytomegalovirus

HSV: Herpes simplex virus

HIV: Human immunodeficiency virus

MLV: Murine leukemia virus

SIV: Simian immunodeficiency virus

NLR: NOD-like receptor; nucleotide-binding oligomerization domain-like receptor

MAVS: Mitochondrial antiviral signalling protein

RLR: RIG-I like receptor; retinoic acid-inducible gene I –like receptor

MDA5: Melanoma differentiation-associated protein 5

NF-κB: Nuclear factor kappa-light-chain-enhancer of activated B cells

MAMs: Mitochondria-associated membranes

Pol III: RNA polymerase III

Atg: Autophagy-related gene

ISG: Interferon-stimulated gene

Tyk: Tyrosine kinase

JAK: Janus kinase

STAT: Signal transducer and activator of transcription 1

IL-1α: Interleukin-1α

TNF-α: Tumour necrotic factor-α

IKKα/β: IκB kinase α/β subunits

DENV: Dengue virus

hSTING / mSTING: human STING / mouse STING

SNP: single nucleotide polymorphism

HAQ mutant: R71**H**-G230**A**-R293**Q** mutant

SLE: Systemic Lupus Erythematous

AGS: Aicardi-Goutières Syndrome

TRIM56: Tripartite motif containing 56

AMFR: Autocrine motility factor receptor

INSIG1: Insulin-induced gene 1

RNF5: RING finger protein 5

AMPK: Adenosine monophosphate activated protein kinase

microRNA: miR

PDE: phosphodiesterase

TREX1: 3' repair exonuclease 1

ISGF3: Interferon-stimulated gene factor 3

ANA: Antinuclear antibody

SAMHD: SAM domain and HD domain

RNase: Ribonuclease

IFIH1: IFN-induced helicase C domain containing protein 1

ADAR1: Adenosine deaminase acting on RNA 1

FCL: Familial Chilblain Lupus

SAVI: STING-associated vasculopathy with onset in infancy

DC: Dendritic cell

Treg: Regulatory T cells

XBP-1: X-Box binding protein 1

GM-CSF: Granulocyte-macrophage colony-stimulating factor

PD-L1: Programmed death ligand 1

MHC class I: Major histocompatibility complex class I

LH: Polyethyleneimine / Hyaluronic acid

BMDM: Bone marrow-derived macrophage

Declarations:

- Ethics approval and consent to participate: N/A
- Consent for publication: N/A
- Availability of data and material: N/A

- Competing interests:
  The authors declare that they have no competing interests

- Funding: HLW was supported by funds from the Biotechnology and Biological Sciences Research Council (grant number BB/L000830/1) and the British Heart Foundation (grant number PG/13/80/30443). EKT was supported by funds from the British Heart Foundation (grant number PG/16/44/32146).

- Authors' contributions:
  All authors were involved in drafting and editing, they all read and approved the final manuscript.

- Acknowledgements: N/A

References:

1. Holm CK, Paludan SR, Fitzgerald KA. DNA recognition in immunity and disease. Current Opinion in Immunology. 2013;25:13–8.

2. Zheng M, Zheng M, Xie L, Xie L, Liang Y, Wu S, et al. Recognition of cytosolic DNA attenuates glucose metabolism and induces AMPK mediated energy stress response. Int J Biol Sci. 2015;11:587–94.

3. Fiszer-Kierzkowska A, Vydra N, Wysocka-Wycisk A, Kronekova Z, Jarząb M, Lisowska KM, et al. Liposome-based DNA carriers may induce cellular stress response and change gene expression pattern in transfected cells. BMC Mol Biol. 2011;12:27. doi:10.1186/1471-2199-12-27.

4. Atianand MK, Fitzgerald KA. Long non-coding RNAs and control of gene expression in the immune system. Trends in Molecular Medicine. 2014;20:623–31.

5. Hornung V, Latz E. Intracellular DNA recognition. Nat Rev Immunol. 2010;10:123–30. doi:nri2690 [pii]\r10.1038/nri2690 [doi].

6. Ishikawa H, Barber GN. STING is an endoplasmic reticulum adaptor that facilitates innate immune signalling. Nature. 2008;455:674–8. doi:10.1038/nature07317.

7. Sun W, Li Y, Chen L, Chen H, You F, Zhou X, et al. ERIS, an endoplasmic reticulum IFN stimulator, activates innate immune signaling through dimerization. Proc Natl Acad Sci U S A. 2009;106:8653–8. doi:0900850106 [pii]\r10.1073/pnas.0900850106.

8. Zhong B, Yang Y, Li S, Wang YY, Li Y, Diao F, et al. The Adaptor Protein MITA Links Virus-Sensing Receptors to IRF3 Transcription Factor Activation. Immunity. 2008;29:538–50.

9. Jin L, Getahun A, Knowles HM, Mogan J, Akerlund LJ, Packard T a, et al. STING/MPYS mediates host defense against Listeria monocytogenes infection by regulating Ly6C(hi) monocyte migration. J Immunol. 2013;190:2835–43. doi:10.4049/jimmunol.1201788.

10. Abe T, Harashima A, Xia T, Konno H, Konno K, Morales A, et al. STING Recognition of Cytoplasmic DNA Instigates Cellular Defense. Mol Cell. 2013;50:5–15.

11. Ishikawa H, Ma Z, Barber GN. STING regulates intracellular DNA-mediated, type I interferon-dependent innate immunity. Nature. 2009;461:788–92. doi:10.1038/nature08476.

12. Lakkaraju AK, Abrami L, Lemmin T, Blaskovic S, Kunz B, Kihara A, et al. Palmitoylated calnexin is a key component of the ribosome–translocon complex. EMBO J. 2012;31:1823–35.

13. Nagasawa K, Higashi T, Hosokawa N, Kaufman RJ, Nagata K. Simultaneous induction of the four subunits of the TRAP complex by ER stress accelerates ER degradation. EMBO Rep. 2007;8:483–9.

14. Ishikawa H, Barber GN. The STING pathway and regulation of innate immune signaling in response to DNA pathogens. Cellular and Molecular Life Sciences. 2011;68:1157–65.

15. Unterholzner L, Keating SE, Baran M, Horan KA, Jensen SB, Sharma S, et al. IFI16 is an innate immune sensor for intracellular DNA. Nat Immunol. 2010;11:997–1004. doi:10.1038/ni.1932.

16. Zhang Z, Yuan B, Bao M, Lu N, Kim T, Liu Y-J. The helicase DDX41 senses intracellular DNA mediated by the adaptor STING in dendritic cells. Nat Immunol. 2011;12:959–65. doi:10.1038/ni.2091.

17. Takaoka A, Wang Z, Choi MK, Yanai H, Negishi H, Ban T, et al. DAI (DLM-1/ZBP1) is a cytosolic DNA sensor and an activator of innate immune response. Nature. 2007;448:501–5. doi:10.1038/nature06013.

18. Tanaka Y, Chen ZJ. STING specifies IRF3 phosphorylation by TBK1 in the cytosolic DNA signaling pathway. Sci Signal. 2012;5:ra20.

19. Abe T, Barber GN. Cytosolic-DNA-Mediated, STING-Dependent Proinflammatory Gene Induction Necessitates Canonical NF-κB Activation through TBK1. Journal of virology. 2014;88:5328–41. doi:10.1128/JVI.00037-14.

20. Lam E, Stein S, Falck-Pedersen E. Adenovirus detection by the cGAS/STING/TBK1 DNA sensing cascade. J Virol. 2014;88:974–81. doi:10.1128/JVI.02702-13.

21. Ma Z, Jacobs SR, West JA, Stopford C, Zhang Z, Davis Z, et al. Modulation of the cGAS-STING DNA sensing pathway by gammaherpesviruses. Proc Natl Acad Sci U S A. 2015;112:E4306-15. doi:10.1073/pnas.1503831112.

22. Kalamvoki M, Roizman B. HSV-1 degrades, stabilizes, requires, or is stung by STING depending on ICP0, the US3 protein kinase, and cell derivation. Proc Natl Acad Sci U S A. 2014;111:E611-7. doi:10.1073/pnas.1323414111.

23. Liu Y, Goulet M-L, Sze A, Bel Hadj S, Belgnaoui SM, Lababidi RR, et al. RIG-I Mediated STING Up-Regulation Restricts HSV-1 Infection. J Virol. 2016;:JVI.00748-16. doi:10.1128/JVI.00748-16.

24. Kai Chan Y, Gack MU. Viral evasion of intracellular DNA and RNA sensing. Nat Publ Gr. 2016;14:360–73. doi:10.1038/nrmicro.2016.45.

25. DeFilippis VR, Alvarado D, Sali T, Rothenburg S, Früh K. Human cytomegalovirus induces the interferon response via the DNA sensor ZBP1. J Virol. 2010;84:585–98. doi:10.1128/JVI.01748-09.

26. Paijo J, D??ring M, Spanier J, Grabski E, Nooruzzaman M, Schmidt T, et al. cGAS Senses Human Cytomegalovirus and Induces Type I Interferon Responses in Human Monocyte-Derived Cells. PLoS Pathog. 2016;12.

27. Dell'Oste V, Gatti D, Gugliesi F, De Andrea M, Bawadekar M, Lo Cigno I, et al. Innate nuclear sensor IFI16 translocates into the cytoplasm during the early stage of in vitro human cytomegalovirus infection and is entrapped in the egressing virions during the late stage. J Virol. 2014;88:6970–82. doi:10.1128/JVI.00384-14.

28. Yan N, Regalado-Magdos AD, Stiggelbout B, Lee-Kirsch MA, Lieberman J. The cytosolic exonuclease TREX1 inhibits the innate immune response to human immunodeficiency virus type 1. Nat Immunol. 2010;11:1005–13. doi:10.1038/ni.1941.

29. Holm CK, Rahbek SH, Gad HH, Bak RO, Jakobsen MR, Jiang Z, et al. Influenza A virus targets a cGAS-independent STING pathway that controls enveloped RNA viruses. Nat Commun. 2016;7:10680. doi:10.1038/ncomms10680.

30. Collins AC, Cai H, Li T, Franco LH, Li XD, Nair VR, et al. Cyclic GMP-AMP Synthase Is an Innate Immune DNA Sensor for Mycobacterium tuberculosis. Cell Host Microbe. 2015;17:820–8. doi:10.1016/j.chom.2015.05.005.

31. Watson RO, Bell SL, MacDuff DA, Kimmey JM, Diner EJ, Olivas J, et al. The Cytosolic Sensor cGAS Detects Mycobacterium tuberculosis DNA to Induce Type I Interferons and Activate Autophagy. Cell Host Microbe. 2015;17:811–9. doi:10.1016/j.chom.2015.05.004.

32. Koppe U, Högner K, Doehn J-M, Müller HC, Witzenrath M, Gutbier B, et al. Streptococcus pneumoniae stimulates a STING- and IFN regulatory factor 3-dependent type I IFN production in macrophages, which regulates RANTES production in macrophages, cocultured alveolar epithelial cells, and mouse lungs. J Immunol. 2012;188:811–7. doi:10.4049/jimmunol.1004143.

33. Gratz N, Hartweger H, Matt U, Kratochvill F, Janos M, Sigel S, et al. Type I Interferon Production Induced By Streptococcus Pyogenes-Derived Nucleic Acids is Required for Host Protection. PLoS Pathog. 2011;7:1–16.

34. Gries CM, Bruger EL, Moormeier DE, Scherr TD, Waters CM, Kielian T. Cyclic di-AMP released from *Staphylococcus aureus* biofilm induces a macrophage type I interferon response. Infect Immun. 2016; October:IAI.00447-16. doi:10.1128/IAI.00447-16.

35. Woodward JJ, Iavarone AT, Portnoy DA. c-di-AMP secreted by intracellular Listeria monocytogenes activates a host type I interferon response. Science. 2010;328:1703–5. doi:10.1126/science.1189801.

36. Zhu D, Wang L, Shang G, Liu X, Zhu J, Lu D, et al. Structural Biochemistry of a Vibrio cholerae Dinucleotide Cyclase Reveals Cyclase Activity Regulation by Folates. Mol Cell. 2014;55:931–7. doi:10.1016/j.molcel.2014.08.001.

37. Davies BW, Bogard RW, Young TS, Mekalanos JJ. Coordinated regulation of accessory genetic elements produces cyclic di-nucleotides for V. cholerae virulence. Cell. 2012;149:358–70.

38. Nazmi A, Mukhopadhyay R, Dutta K, Basu A. STING Mediates Neuronal Innate Immune Response Following Japanese Encephalitis Virus Infection. Sci Rep. 2012;2:1–10.

39. Liu Y, Jesus AA, Marrero B, Yang D, Ramsey SE, Montealegre Sanchez GA, et al. Activated STING in a vascular and pulmonary syndrome. N Engl J Med. 2014;371:507–18. doi:10.1056/NEJMoa1312625.

40. Ahn J, Gutman D, Saijo S, Barber GN. STING manifests self DNA-dependent inflammatory disease. Proc Natl Acad Sci U S A. 2012;109:19386–91. doi:10.1073/pnas.1215006109.

41. Barber GN. STING: infection, inflammation and cancer. Nat Rev Immunol. 2015;15:760–70. doi:10.1038/nri3921.

42. Woo SR, Fuertes MB, Corrales L, Spranger S, Furdyna MJ, Leung MYK, et al. STING-dependent cytosolic DNA sensing mediates innate immune recognition of immunogenic tumors. Immunity. 2014;41:830–42.

43. Deng L, Liang H, Xu M, Yang X, Burnette B, Arina A, et al. STING-dependent cytosolic DNA sensing promotes radiation-induced type I interferon-dependent antitumor immunity in immunogenic tumors. Immunity. 2014;41:543–852.

44. Klarquist J, Hennies CM, Lehn MA, Reboulet RA, Feau S, Janssen EM. STING-Mediated DNA Sensing Promotes Antitumor and Autoimmune Responses to Dying Cells. J Immunol. 2014;193:6124–34. doi:10.4049/jimmunol.1401869.

45. York AG, Williams KJ, Argus JP, Zhou QD, Brar G, Vergnes L, et al. Limiting Cholesterol Biosynthetic Flux Spontaneously Engages Type I IFN Signaling. Cell. 2015;163:1716–29.

46. O'Neill LAJ. How Low Cholesterol Is Good for Anti-viral Immunity. Cell. 2015;163:1572–4.

47. Burdette DL, Monroe KM, Sotelo-Troha K, Iwig JS, Eckert B, Hyodo M, et al. STING is a direct innate immune sensor of cyclic di-GMP. Nature. 2011;478:515–8.

48. Wu J, Sun L, Chen X, Du F, Shi H, Chen C, et al. Cyclic GMP-AMP is an endogenous second messenger in innate immune signaling by cytosolic DNA. Science. 2013;339:826–30. doi:10.1126/science.1229963.

49. Collins AC, Cai H, Li T, Franco LH, Li XD, Nair VR, et al. Cyclic GMP-AMP Synthase Is an Innate Immune DNA Sensor for Mycobacterium tuberculosis. Cell Host and Microbe. 2014.

50. Barker JR, Koestler BJ, Carpenter VK, Burdette DL, Waters CM, Vance RE, et al. STING-dependent recognition of cyclic di-AMP mediates type I interferon responses during Chlamydia trachomatis infection. MBio. 2013;4.

51. Sun L, Wu J, Du F, Chen X, Chen ZJ, O'Neill LA, et al. Cyclic GMP-AMP synthase is a cytosolic DNA sensor that activates the type I interferon pathway. Science. 2013;339:786–91. doi:10.1126/science.1232458.

52. Lolicato M, Bucchi A, Arrigoni C, Zucca S, Nardini M, Schroeder I, et al. Cyclic dinucleotides bind the C-linker of HCN4 to control channel cAMP responsiveness. Nat Chem Biol. 2014;10:457–62. doi:10.1038/nchembio.1521.

53. Gao P, Ascano M, Zillinger T, Wang W, Dai P, Serganov AA, et al. Structure-function analysis of STING activation by c[G(2',5') pA(3',5')p] and targeting by antiviral DMXAA. Cell. 2013;154:748–62.

54. Diner EJ, Burdette DL, Wilson SC, Monroe KM, Kellenberger CA, Hyodo M, et al. The Innate Immune DNA Sensor cGAS Produces a Noncanonical Cyclic Dinucleotide that Activates Human STING. Cell Rep. 2013;3:1355–61.

55. Zhang X, Shi H, Wu J, Zhang X, Sun L, Chen C, et al. Cyclic GMP-AMP containing mixed Phosphodiester linkages is an endogenous high-affinity ligand for STING. Mol Cell. 2013;51:226–35.

56. Li L, Yin Q, Kuss P, Maliga Z, Millán JL, Wu H, et al. Hydrolysis of 2'3'-cGAMP by ENPP1 and design of nonhydrolyzable analogs. Nat Chem Biol. 2014;10:1043–8. doi:10.1038/nchembio.1661.

57. Torchilin VP. Recent approaches to intracellular delivery of drugs and dna and organelle targeting. Annu Rev Biomed Eng. 2006;8:343–75. doi:10.1146/annurev.bioeng.8.061505.095735.

58. Lippmann J, Rothenburg S, Deigendesch N, Eitel J, Meixenberger K, Van Laak V, et al. IFN?? responses induced by intracellular bacteria or cytosolic DNA in different human cells do not require ZBP1 (DLM-1/DAI). Cell Microbiol. 2008;10:2579–88.

59. Lee KG, Kim SSY, Kui L, Voon DCC, Mauduit M, Bist P, et al. Bruton's Tyrosine Kinase Phosphorylates DDX41 and Activates Its Binding of dsDNA and STING to Initiate Type 1 Interferon Response. Cell Rep. 2015;10:1055–65.

60. Jakobsen MR, Bak RO, Andersen A, Berg RK, Jensen SB, Tengchuan J, et al. IFI16 senses DNA forms of the lentiviral replication cycle and controls HIV-1 replication. Proc Natl Acad Sci U S A. 2013;110:E4571-80. doi:10.1073/pnas.1311669110.

61. Kerur N, Veettil MV, Sharma-Walia N, Bottero V, Sadagopan S, Otageri P, et al. IFI16 acts as a nuclear pathogen sensor to induce the inflammasome in response to Kaposi Sarcoma-associated herpesvirus infection. Cell Host Microbe. 2011;9:363–75.

62. Roy A, Dutta D, Iqbal J, Pisano G, Gjyshi O, Ansari MA, et al. Nuclear Innate Immune DNA Sensor IFI16 is Degraded During Lytic Reactivation of Kaposi's Sarcoma-Associated Herpesvirus (KSHV): Role of IFI16 in Maintenance of KSHV Latency. J Virol. 2016; July:JVI.01003-16. doi:10.1128/JVI.01003-16.

63. Li T, Chen J, Cristea IM. Human cytomegalovirus tegument protein pUL83 inhibits IFI16-mediated DNA sensing for immune evasion. Cell Host Microbe. 2013;14:591–9.

64. Diner BA, Lum KK, Toettcher JE, Cristea IM. Viral DNA Sensors IFI16 and Cyclic GMP-AMP Synthase Possess Distinct Functions in Regulating Viral Gene Expression , Immune Defenses , and Apoptotic Responses during Herpesvirus Infection. MBio. 2016;7:1–15.

65. Orzalli MH, Broekema NM, Diner B a., Hancks DC, Elde NC, Cristea IM, et al. cGAS-mediated stabilization of IFI16 promotes innate signaling during herpes simplex virus infection. Proc Natl Acad Sci. 2015;:201424637. doi:10.1073/pnas.1424637112.

66. Almine JF, Hare CAJO, Dunphy G, Haga IR, Naik RJ, Atrih A, et al. STING during DNA sensing in human keratinocytes. Nat Commun. 2017;8.

67. Guo H, König R, Deng M, Riess M, Mo J, Zhang L, et al. NLRX1 Sequesters STING to Negatively Regulate the Interferon Response, Thereby Facilitating the Replication of HIV-1 and DNA Viruses. Cell Host Microbe. 2016;19:515–28.

68. Gao D, Wu J, Wu Y-T, Du F, Aroh C, Yan N, et al. Cyclic GMP-AMP synthase is an innate immune sensor of HIV and other retroviruses. Science. 2013;341:903–6.

69. Barouch DH, Ghneim K, Bosche WJ, Li Y, Berkemeier B, Hull M, et al. Rapid Inflammasome Activation following Mucosal SIV Infection of Rhesus Monkeys. Cell. 2016;165:656–67.

70. Kawai T, Takahashi K, Sato S, Coban C, Kumar H, Kato H, et al. IPS-1, an adaptor triggering RIG-I- and Mda5-mediated type I interferon induction. Nat Immunol. 2005;6:981–8. doi:10.1038/ni1243.

71. Xu L-G, Wang Y-Y, Han K-J, Li L-Y, Zhai Z, Shu H-B. VISA is an adapter protein required for virus-triggered IFN-beta signaling. Mol Cell. 2005;19:727–40.

72. Meylan E, Curran J, Hofmann K, Moradpour D, Binder M, Bartenschlager R, et al. Cardif is an adaptor protein in the RIG-I antiviral pathway and is targeted by hepatitis C virus. Nature. 2005;437:1167–72.

73. Seth RB, Sun L, Ea CK, Chen ZJ. Identification and characterization of MAVS, a mitochondrial antiviral signaling protein that activates NF-kB and IRF3. Cell. 2005;122:669–82.

74. Castanier C, Garcin D, Vazquez A, Arnoult D, Ablasser A, Bauernfeind F, et al. Mitochondrial dynamics regulate the RIG-I-like receptor antiviral pathway. EMBO Rep. 2010;11:133–8. doi:10.1038/embor.2009.258.

75. Vance JE. MAM (mitochondria-associated membranes) in mammalian cells: Lipids and beyond. Biochimica et Biophysica Acta - Molecular and Cell Biology of Lipids. 2014;1841:595–609.

76. West AP, Khoury-Hanold W, Staron M, Tal MC, Pineda CM, Lang SM, et al. Mitochondrial DNA stress primes the antiviral innate immune response. Nature. 2015;520:553–7. doi:10.1038/nature14156.

77. Ablasser A, Bauernfeind F, Hartmann G, Latz E, Fitzgerald KA, Hornung V. RIG-I-dependent sensing of poly(dA:dT) through the induction of an RNA polymerase III-transcribed RNA intermediate. Nat Immunol. 2009;10:1065–72.

78. Chiu YH, MacMillan JB, Chen ZJ. RNA Polymerase III Detects Cytosolic DNA and Induces Type I Interferons through the RIG-I Pathway. Cell. 2009;138:576–91.

79. Saitoh T, Fujita N, Hayashi T, Takahara K, Satoh T, Lee H, et al. Atg9a controls dsDNA-driven dynamic translocation of STING and the innate immune response. Proc Natl Acad Sci U S A. 2009;106:20842–6. doi:10.1073/pnas.0911267106\r0911267106 [pii].

80. Rasmussen SB, Horan K a, Holm CK, Stranks AJ, Mettenleiter TC, Simon a K, et al. Activation of autophagy by α-herpesviruses in myeloid cells is mediated by cytoplasmic viral DNA through a mechanism dependent on stimulator of IFN genes. J Immunol. 2011;187:5268–76. doi:10.4049/jimmunol.1100949.

81. Watson RO, Manzanillo PS, Cox JS. Extracellular M. tuberculosis DNA targets bacteria for autophagy by activating the host DNA-sensing pathway. Cell. 2012;150:803–15.

82. Shu C, Yi G, Watts T, Kao CC, Li P. Structure of STING bound to cyclic di-GMP reveals the mechanism of cyclic dinucleotide recognition by the immune system. Nat Struct Mol Biol. 2012;19:722–4. doi:10.1038/nsmb.2331.

83. Tsuchida T, Zou J, Saitoh T, Kumar H, Abe T, Matsuura Y, et al. The ubiquitin ligase TRIM56 regulates innate immune responses to intracellular double-stranded DNA. Immunity. 2010;33:765–76.

84. Clark K, Plater L, Peggie M, Cohen P. Use of the Pharmacological Inhibitor BX795 to Study the Regulation and Physiological Roles of TBK1 and IκB Kinase ε. 2009;284:14136–46.

85. Kishore N, Huynh QK, Mathialagan S, Hall T, Rouw S, Creely D, Lange G, Caroll J, Reitz B, Donnelly A, Boddupalli H, Combs RG, Kretzmer K TC. IKK-i and TBK-1 are enzymatically distinct from the homologous enzyme IKK-2: comparative analysis of recombinant human IKK-i, TBK-1, and IKK-2. J Biol Chem. 2002;277:13840–7.

86. Uzé G, Schreiber G, Piehler J, Pellegrini S. The receptor of the type I interferon family. Current Topics in Microbiology and Immunology. 2007;316:71–95.

87. Gauzzi MC, Velazquez L, McKendry R, Mogensen KE, Fellous M, Pellegrini S. Interferon-??-dependent activation of Tyk2 requires phosphorylation of positive regulatory tyrosines by another kinase. J Biol Chem. 1996;271:20494–500.

88. Prchal-Murphy M, Semper C, Lassnig C, Wallner B, Gausterer C, Teppner-Klymiuk I, et al. TYK2 kinase activity is required for functional type I interferon responses in Vivo. PLoS One. 2012;7.

89. Li X, Leung S, Qureshi S, Darnell JE, Stark GR. Formation of STAT1-STAT2 heterodimers and their role in the activation of IRF-1 gene transcription by interferon-?? J Biol Chem. 1996;271:5790–4.

90. Au-Yeung N, Mandhana R, Horvath CM. Transcriptional regulation by STAT1 and STAT2 in the interferon JAK-STAT pathway. Jak-Stat. 2013;2:e23931. doi:10.4161/jkst.23931.

91. Thompson MR, Sharma S, Atianand M, Jensen SB, Carpenter S, Knipe DM, et al. Interferon γ-inducible protein (IFI) 16 transcriptionally regulates type I interferons and other interferon-stimulated genes and controls the interferon response to both DNA and RNA viruses. J Biol Chem. 2014;289:23568–81.

92. Burdette DL, Vance RE. STING and the innate immune response to nucleic acids in the cytosol. Nat Immunol. 2013;14:19–26. doi:10.1038/ni.2491.

93. Jin L, Waterman PM, Jonscher KR, Short CM, Reisdorph N a, Cambier JC. MPYS, a novel membrane tetraspanner, is associated with major histocompatibility complex class II and mediates transduction of apoptotic signals. Mol Cell Biol. 2008;28:5014–26.

94. Surpris G, Chan J, Thompson M, Ilyukha V, Liu BC, Atianand M, et al. Cutting Edge: Novel Tmem173 Allele Reveals Importance of STING N Terminus in Trafficking and Type I IFN Production. J Immunol. 2015;196:547–52. doi:10.4049/jimmunol.1501415.

95. Yin Q, Tian Y, Kabaleeswaran V, Jiang X, Tu D, Eck MJ, et al. Cyclic di-GMP Sensing via the Innate Immune Signaling Protein STING. Mol Cell. 2012;46:735–45. doi:10.1016/j.molcel.2012.05.029.

96. Ouyang S, Song X, Wang Y, Ru H, Shaw N, Jiang Y, et al. Structural Analysis of the STING Adaptor Protein Reveals a Hydrophobic Dimer Interface and Mode of Cyclic di-GMP Binding. Immunity. 2012;36:1073–86. doi:10.1016/j.immuni.2012.03.019.

97. Huang Y-H, Liu X-Y, Du X-X, Jiang Z-F, Su X-D. The structural basis for the sensing and binding of cyclic di-GMP by STING. Nat Struct Mol Biol. 2012;19:728–30. doi:10.1038/nsmb.2333.

98. Ouyang S, Song X, Wang Y, Ru H, Shaw N, Jiang Y, et al. Structural Analysis of the STING Adaptor Protein Reveals a Hydrophobic Dimer Interface and Mode of Cyclic di-GMP Binding. Immunity. 2012;36:1073–86. doi:10.1016/j.immuni.2012.03.019.

99. Lou YC, Kao YF, Chin KH, Chen JK, Tu J Le, Chen C, et al. Backbone resonance assignments of the 54??kDa dimeric C-terminal domain of murine STING in complex with DMXAA. Biomol NMR Assign. 2014;9:271–4.

100. Tsuchiya Y, Jounai N, Takeshita F, Ishii KJ, Mizuguchi K. Ligand-induced Ordering of the C-terminal Tail Primes STING for Phosphorylation by TBK1. EBioMedicine. 2016.

101. Chen H, Pei R, Zhu W, Zeng R, Wang YY, Wang YY, et al. An Alternative Splicing Isoform of MITA Antagonizes MITA-Mediated Induction of Type I IFNs. J Immunol. 2014;192:1162–70. doi:10.4049/jimmunol.1300798.

102. Konno H, Konno K, Barber GN. XCyclic dinucleotides trigger ULK1 (ATG1) phosphorylation of STING to prevent sustained innate immune signaling. Cell. 2013;155.

103. Tang ED, Wang CY. Single amino acid change in STING leads to constitutive active signaling. PLoS One. 2015;10.

104. Yi G, Brendel VP, Shu C, Li P, Palanathan S, Cheng Kao C. Single Nucleotide Polymorphisms of Human STING Can Affect Innate Immune Response to Cyclic Dinucleotides. PLoS One. 2013;8.

105. König N, Fiehn C, Wolf C, Schuster M, Costa EC, Tüngler V, et al. Familial chilblain lupus due to a gain-of-function mutation in STING. Ann Rheum Dis. 2016;:annrheumdis-2016-209841. doi:10.1136/annrheumdis-2016-209841.

106. Patel S, Blaauboer SM, Tucker HR, Mansouri S, Ruiz-Moreno JS, Hamann L, et al. The Common R71H-G230A-R293Q Human *TMEM173* Is a Null Allele. J Immunol. 2016;:1601585. doi:10.4049/jimmunol.1601585.

107. Aguirre S, Maestre AM, Pagni S, Patel JR, Savage T, Gutman D, et al. DENV Inhibits Type I IFN Production in Infected Cells by Cleaving Human STING. PLoS Pathog. 2012;8.

108. Jeremiah N, Neven B, Gentili M, Callebaut I, Maschalidi S, Stolzenberg MC, et al. Inherited STING-activating mutation underlies a familial inflammatory syndrome with lupus-like manifestations. J Clin Invest. 2014;124:5516–20.

109. Yu CY, Chang TH, Liang JJ, Chiang RL, Lee YL, Liao CL, et al. Dengue virus targets the adaptor protein MITA to subvert host innate immunity. PLoS Pathog. 2012;8.

110. Jin L, Xu L-G, Yang I V, Davidson EJ, Schwartz DA, Wurfel MM, et al. Identification and characterization of a loss-of-function human MPYS variant. Genes Immun. 2011;12:263–9. doi:10.1038/gene.2010.75.

111. Sauer JD, Sotelo-Troha K, Von Moltke J, Monroe KM, Rae CS, Brubaker SW, et al. The N-ethyl-N-nitrosourea-induced Goldenticket mouse mutant reveals an essential function of sting in the in vivo interferon response to Listeria monocytogenes and cyclic dinucleotides. Infect Immun. 2011;79:688–94.

112. Wang Y, Lian Q, Yang B, Yan S, Zhou H, He L, et al. TRIM30α Is a Negative-Feedback Regulator of the Intracellular DNA and DNA Virus-Triggered Response by Targeting STING. PLoS Pathog. 2015;11.

113. Wang Q, Liu X, Cui Y, Tang Y, Chen W, Li S, et al. The E3 Ubiquitin ligase AMFR and INSIG1 bridge the activation of TBK1 kinase by modifying the adaptor STING. Immunity. 2014;41:919–33.

114. Zhong B, Zhang L, Lei C, Li Y, Mao AP, Yang Y, et al. The Ubiquitin Ligase RNF5 Regulates Antiviral Responses by Mediating Degradation of the Adaptor Protein MITA. Immunity. 2009;30:397–407.

115. Marchi S, Patergnani S, Pinton P. The endoplasmic reticulum-mitochondria connection: One touch, multiple functions. Biochimica et Biophysica Acta - Bioenergetics. 2014;1837:461–9.

116. Chen H, Sun H, You F, Sun W, Zhou X, Chen L, et al. Activation of STAT6 by STING is critical for antiviral innate immunity. Cell. 2011;147:436–46.

117. Liu S, Cai X, Wu J, Cong Q, Chen X, Li T, et al. Phosphorylation of innate immune adaptor proteins MAVS, STING, and TRIF induces IRF3 activation. Science (80-). 2015;347:aaa2630. doi:10.1126/science.aaa2630.

118. Zhang L, Mo J, Swanson K V., Wen H, Petrucelli A, Gregory SM, et al. NLRC3, a member of the NLR family of proteins, is a negative regulator of innate immune signaling induced by the DNA sensor STING. Immunity. 2014;40:329–41.

119. Yarbrough ML, Zhang K, Sakthivel R, Forst C V, Posner B a, Barber GN, et al. Primate-specific miR-576-3p sets host defense signalling threshold. Nat Commun. 2014;5 May:4963. doi:10.1038/ncomms5963.

120. Bai Y, Yang J, Zarrella TM, Zhang Y, Metzger DW, Bai G. Cyclic Di-AMP impairs potassium uptake mediated by a cyclic Di-AMP binding protein in streptococcus Pneumoniae. J Bacteriol. 2014;196:614–23.

121. Christen M, Christen B, Folcher M, Schauerte A, Jenal U. Identification and characterization of a cyclic di-GMP-specific phosphodiesterase and its allosteric control by GTP. J Biol Chem. 2005;280:30829–37.

122. Schmidt AJ, Ryjenkov DA, Gomelsky M. The ubiquitous protein domain EAL is a cyclic diguanylate-specific phosphodiesterase: Enzymatically active and inactive EAL domains. J Bacteriol. 2005;187:4774–81.

123. Gao P, Patel DJ. V-cGAPs: attenuators of 3′3′-cGAMP signaling. Cell Res. 2015;25:529–30. doi:10.1038/cr.2015.48.

124. Ruchi Jain Dey, Bappaditya Dey, Yue Zheng, Laurene S Cheung, Jie Zhou, David Sayre, Pankaj Kumar, Haidan Guo, Gyanu Lamichhane HOS& WRB. Deletion of the cyclic di-AMP phosphodiesterase gene (cnpB) in Mycobacterium tuberculosis leads to reduced virulence in a mouse model of infection. Mol Microbiol. 2014;93:65–79.

125. Dey RJ, Dey B, Zheng Y, Cheung LS, Zhou J, Sayre D, et al. Inhibition of innate immune cytosolic surveillance by an M . tuberculosis phosphodiesterase. Nat Publ Gr. 2016;13 December. doi:10.1038/nchembio.2254.

126. Manikandan K, Sabareesh V, Singh N, Saigal K, Mechold U, Sinha KM. Two-step synthesis and hydrolysis of cyclic di-AMP in Mycobacterium tuberculosis. PLoS One. 2014;9.

127. Seo GJ, Yang A, Tan B, Kim S, Liang Q, Choi Y, et al. Akt Kinase-Mediated Checkpoint of cGAS DNA Sensing Pathway. Cell Rep. 2015;13:440–9.

128. Zhang Z, Bao M, Lu N, Weng L, Yuan B, Liu YJ. The E3 ubiquitin ligase TRIM21 negatively regulates the innate immune response to intracellular double-stranded DNA. Nat Immunol. 2013;14:172–8. doi:10.1038/ni.2492.

129. Liang Q, Seo GJ, Choi YJ, Kwak MJ, Ge J, Rodgers MA, et al. Crosstalk between the cGAS DNA sensor and beclin-1 autophagy protein shapes innate antimicrobial immune responses. Cell Host Microbe. 2014;15:228–38.

130. Wu J, Tian L, Yu X, Pattaradilokrat S, Li J, Wang M, et al. Strain-specific innate immune signaling pathways determine malaria parasitemia dynamics and host mortality. Proc Natl Acad Sci U S A. 2014;111:E511-20. doi:10.1073/pnas.1316467111.

131. Flück C, Smith T, Beck HP, Irion A, Betuela I, Alpers MP, et al. Strain-specific humoral response to a polymorphic malaria vaccine. Infect Immun. 2004;72:6300–5.

132. Langhorne J, Ndungu FMM, Sponaas A-M, Marsh K. Immunity to malaria: more questions than answers. Nat Immunol. 2008;9:725–32. doi:10.1038/ni.f.205.

133. van Kooten C, Banchereau J. CD40-CD40 ligand. J Leukoc Biol. 2000;67:2–17.

134. Benveniste EN, Nguyen VT, Wesemann DR. Molecular regulation of CD40 gene expression in macrophages and microglia. Brain, Behavior, and Immunity. 2004;18:7–12.

135. Yao X, Wu J, Lin M, Sun W, He X, Gowda C, et al. Increased CD40 Expression Enhances Early STING-Mediated Type I Interferon Response and Host Survival in a Rodent Malaria Model. PLoS Pathog. 2016;12.

136. Yu X, Cai B, Wang M, Tan P, Ding X, Wu J, et al. Cross-Regulation of Two Type I Interferon Signaling Pathways in Plasmacytoid Dendritic Cells Controls Anti-malaria Immunity and Host Mortality. Immunity. 2016;45:1093–107. doi:10.1016/j.immuni.2016.10.001.

137. Yi G, Wen Y, Shu C, Han Q, Konan K V, Li P, et al. The Hepatitis C Virus NS4B Can Suppress STING Accumulation to Evade Innate Immune Responses. J Virol. 2015; October:JVI.01720--15. doi:10.1128/JVI.01720-15.

138. Nitta S, Sakamoto N, Nakagawa M, Kakinuma S, Mishima K, Kusano-Kitazume A, et al. Hepatitis C virus NS4B protein targets STING and abrogates RIG-I-mediated type I interferon-dependent innate immunity. Hepatology. 2013;57:46–58.

139. Cuchet-Lourenco D, Vanni E, Glass M, Orr a., Everett RD. Herpes Simplex Virus 1 Ubiquitin Ligase ICP0 Interacts with PML Isoform I and Induces Its SUMO-Independent Degradation. J Virol. 2012;86:11209–22.

140. Maringer K, Fernandez-Sesma A. Message in a bottle: Lessons learned from antagonism of STING signalling during RNA virus infection. Cytokine and Growth Factor Reviews. 2014;25:669–79.

141. Sunthamala N, Thierry F, Teissier S, Pientong C, Kongyingyoes B, Tangsiriwatthana T, et al. E2 proteins of high risk human papillomaviruses down-modulate STING and IFN-?? transcription in keratinocytes. PLoS One. 2014;9.

142. Lau L, Gray EE, Brunette RL, Stetson DB. DNA tumor virus oncogenes antagonize the cGAS-STING DNA-sensing pathway. Science (80-). 2015;350:568–71. doi:10.1126/science.aab3291.

143. Liu Y, Li J, Chen J, Li Y, Wang W, Du X, et al. Hepatitis B Virus Polymerase Disrupts K63-Linked Ubiquitination of STING To Block Innate Cytosolic DNA-Sensing Pathways. J Virol. 2015;89:2287–300.

144. Christensen MH, Paludan SR. Viral evasion of DNA-stimulated innate immune responses. Cell Mol Immunol. 2016; October 2015:1–10. doi:10.1038/cmi.2016.06.

145. Wu JJ, Li W, Shao Y, Avey D, Fu B, Gillen J, et al. Inhibition of cGAS DNA Sensing by a Herpesvirus Virion Protein. Cell Host Microbe. 2015;18:333–44.

146. Lahaye X, Satoh T, Gentili M, Cerboni S, Conrad C, Hurbain I, et al. The Capsids of HIV-1 and HIV-2 Determine Immune Detection of the Viral cDNA by the Innate Sensor cGAS in Dendritic Cells. Immunity. 2013;39:1132–42.

147. Christensen MH, Jensen SB, Miettinen JJ, Luecke S, Prabakaran T, Reinert LS, et al. HSV-1 ICP27 targets the TBK1 -activated STING signalsome to inhibit virus-induced type I IFN expression. EMBO J. 2016;35:1385–99.

148. Kamga I, Kahi S, Develioglu L, Lichtner M, Marañón C, Deveau C, et al. Type I interferon production is profoundly and transiently impaired in primary HIV-1 infection. J Infect Dis. 2005;192:303–10. doi:10.1086/430931.

149. Harman AN, Lai J, Turville S, Samarajiwa S, Gray L, Marsden V, et al. HIV infection of dendritic cells subverts the IFN induction pathway via IRF-1 and inhibits type 1 IFN production. Blood. 2011;118:298–308.

150. Ranganath N, Sandstrom TS, Fadel S, Côté SC, Angel JB, Chun TW, et al. Type I interferon responses are impaired in latently HIV infected cells. Retrovirology. 2016;13:66. doi:10.1186/s12977-016-0302-9.

151. Doyle T, Goujon C, Malim MH. HIV-1 and interferons: who's interfering with whom? Nat Rev Microbiol. 2015;13:403–13.

152. Crow MK. Type I interferon in the pathogenesis of lupus. J Immunol. 2014;192:5459–68. doi:10.4049/jimmunol.1002795.

153. Trinchieri G. Type I interferon: friend or foe? J Exp Med. 2010;207:2053–63. doi:10.1084/jem.20101664.

154. Ivashkiv LB, Donlin LT. Regulation of type I interferon responses. Nat Rev Immunol. 2013;14:36–49. doi:10.1038/nri3581.

155. Gough DJ, Messina NL, Clarke CJP, Johnstone RW, Levy DE. Constitutive Type I Interferon Modulates Homeostatic Balance through Tonic Signaling. Immunity. 2012;36:166–74.

156. Schoggins JW, Rice CM. Interferon-stimulated genes and their antiviral effector functions. Curr Opin Virol. 2011;1:519–25.

157. de Veer MJ, Holko M, Frevel M, Walker E, Der S, Paranjape JM, et al. Functional classification of interferon-stimulated genes identified using microarrays. J Leukoc Biol. 2001;69:912–20.

158. Schneider WM, Chevillotte MD, Rice CM. Interferon-stimulated genes: a complex web of host defenses. Annu Rev Immunol. 2014;32:513–45. doi:10.1146/annurev-immunol-032713-120231.

159. Sadler AJ, Williams BRG. Interferon-inducible antiviral effectors. Nat Rev Immunol. 2008;8:559–68.

160. Chawla-Sarkar M, Lindner DJ, Liu YF, Williams BR, Sen GC, Silverman RH, et al. Apoptosis and interferons: Role of interferon-stimulated genes as mediators of apoptosis. Apoptosis. 2003;8:237–49.

161. Saukkonen K, Sande S, Cioffe C, Wolpe S, Sherry B, Cerami A, et al. The role of cytokines in the generation of inflammation and tissue damage in experimental gram-positive meningitis. J Exp Med. 1990;171:439–48. http://www.pubmedcentral.nih.gov/articlerender.fcgi?artid=2187712&tool=pmcentrez&rendertype=abstract.

162. Hommes DW, van Deventer SJ. Anti- and proinflammatory cytokines in the pathogenesis of tissue damage in Crohn's disease. Curr Opin Clin Nutr Metab Care. 2000;3:191–5. doi:10.1097/00075197-200005000-00005.

163. Goverman J. Autoimmune T cell responses in the central nervous system. Nat Rev Immunol. 2009;9:393–407. doi:10.1038/nri2550.

164. Eguchi K. Apoptosis in autoimmune diseases. Intern Med. 2001;40:275–84. doi:10.2169/internalmedicine.40.275.

165. Su KY, Pisetsky DS. The role of extracellular DNA in autoimmunity in SLE. Scandinavian Journal of Immunology. 2009;70:175–83.

166. Niewold TB, Clark DN, Salloum R, Poole BD. Interferon alpha in systemic lupus erythematosus. J Biomed Biotechnol. 2010;2010:948364. doi:10.1155/2010/948364.

167. Arbuckle MR, McClain MT, Rubertone M V, Scofield RH, Dennis GJ, James J a, et al. Development of autoantibodies before the clinical onset of systemic lupus erythematosus. N Engl J Med. 2003;349:1526–33. doi:10.1056/NEJMoa021933.

168. Rahman AH, Eisenberg RA. The role of toll-like receptors in systemic lupus erythematosus. Springer Seminars in Immunopathology. 2006;28:131–43.

169. Enevold C, Kjær L, Nielsen CH, Voss A, Jacobsen RS, Hermansen MLF, et al. Genetic polymorphisms of dsRNA ligating pattern recognition receptors TLR3, MDA5, and RIG-I. Association with systemic lupus erythematosus and clinical phenotypes. Rheumatol Int. 2014;34:1401–8.

170. Zhang W, Zhou Q, Xu W, Cai Y, Yin Z, Gao X, et al. DNA-dependent activator of interferon-regulatory factors (DAI) promotes lupus nephritis by activating the calcium pathway. J Biol Chem. 2013;288:13534–50.

171. Salloum R, Niewold TB. Interferon regulatory factors in human lupus pathogenesis. Transl Res. 2011;157:326–31. doi:10.1016/j.trsl.2011.01.006.

172. de Vries B, Steup-Beekman GM, Haan J, Bollen EL, Luyendijk J, Frants RR, et al. TREX1 gene variant in neuropsychiatric systemic lupus erythematosus. Ann Rheum Dis. 2010;69:1886–7.

173. Martínez Valle F, Balada E, Ordi-Ros J, Vilardell-Tarres M. DNase 1 and systemic lupus erythematosus. Autoimmunity Reviews. 2008;7:359–63.

174. Ding L, Dong G, Zhang D, Ni Y, Hou Y. The regional function of cGAS/STING signal in multiple organs: One of culprit behind systemic lupus erythematosus? Med Hypotheses. 2015;85:846–9.

175. Sharma S, Campbell AM, Chan J, Schattgen SA, Orlowski GM, Nayar R, et al. Suppression of systemic autoimmunity by the innate immune adaptor STING. Proc Natl Acad Sci. 2015;112:E710-7. doi:10.1073/pnas.1420217112.

176. Crow YJ, Manel N. Aicardi-Goutières syndrome and the type I interferonopathies. Nat Rev Immunol. 2015;15:429–40. doi:10.1038/nri3850.

177. Wolf C, Rapp A, Berndt N, Staroske W, Schuster M, Dobrick-Mattheuer M, et al. RPA and Rad51 constitute a cell intrinsic mechanism to protect the cytosol from self DNA. Nat Commun. 2016;7 May:11752. doi:10.1038/ncomms11752.

178. Gao D, Li T, Li X-D, Chen X, Li Q-Z, Wight-Carter M, et al. Activation of cyclic GMP-AMP synthase by self-DNA causes autoimmune diseases. Proc Natl Acad Sci U S A. 2015;112:E5699-705. doi:10.1073/pnas.1516465112.

179. Rice GI, Bond J, Asipu A, Brunette RL, Manfield IW, Carr IM, et al. Mutations involved in Aicardi-Goutières syndrome implicate SAMHD1 as regulator of the innate immune response. Nat Genet. 2009;41:829–32. doi:10.1038/ng.373.

180. Maelfait J, Bridgeman A, Benlahrech A, Cursi C, Rehwinkel J. Restriction by SAMHD1 Limits cGAS/STING-Dependent Innate and Adaptive Immune Responses to HIV-1. Cell Reports. 2016.

181. Mackenzie KJ, Carroll P, Lettice L, Revuelta A, Abbondati E, Rigby RE, et al. Ribonuclease H2 mutations induce a cGAS / STING- dependent innate immune response. EMBO J. 2016;35:1–14.

182. Pokatayev V, Hasin N, Chon H, Cerritelli SM, Sakhuja K, Ward JM, et al. RNase H2 catalytic core Aicardi-Goutieres syndrome-related mutant invokes cGAS-STING innate immune-sensing pathway in mice. J Exp Med. 2016;213:329–36.

183. Oda H, Nakagawa K, Abe J, Awaya T, Funabiki M, Hijikata A, et al. Aicardi-goutières syndrome is caused by IFIH1 mutations. Am J Hum Genet. 2014;95:121–5.

184. Diamond J. Autosomal dominant IFIH1 gain-of-function mutations cause Aicardi-Goutieres syndrome. Clin Genet. 2014;86:473–4. doi:10.1111/cge.12471.

185. Rice GI, Kasher PR, Forte GMA, Mannion NM, Greenwood SM, Szynkiewicz M, et al. Mutations in ADAR1 cause Aicardi-Goutières syndrome associated with a type I interferon signature. Nat Genet. 2012;44:1243–8. doi:10.1038/ng.2414.

186. Gray EE, Treuting PM, Woodward JJ, Stetson DB. Cutting Edge: cGAS Is Required for Lethal Autoimmune Disease in the Trex1-Deficient Mouse Model of Aicardi-Goutières Syndrome. J Immunol. 2015;195:1939–43. doi:10.4049/jimmunol.1500969.

187. Günther C, Berndt N, Wolf C, Lee-Kirsch MA. Familial Chilblain Lupus Due to a Novel Mutation in the Exonuclease III Domain of 3′ Repair Exonuclease 1 (TREX1). JAMA Dermatology. 2014;:1–6. doi:10.1001/jamadermatol.2014.3438.

188. Günther C, Meurer M, Stein A, Viehweg A, Lee-Kirsch MA. Familial chilblain lupus - A monogenic form of cutaneous lupus erythematosus due to a heterozygous mutation in TREX1. Dermatology. 2009;219:162–6.

189. Ravenscroft JC, Suri M, Rice GI, Szynkiewicz M, Crow YJ. Autosomal dominant inheritance of a heterozygous mutation in SAMHD1 causing familial chilblain lupus. Am J Med Genet Part A. 2011;155:235–7.

190. Moore NF, Patzer EJ, Shaw JM, Thompson TE, Wagner RR. Interaction of vesicular stomatitis virus with lipid vesicles : depletion of cholesterol and effect on virion Membrane Fluidity and Infectivity. J Virol. 1978;27:320–9. http://jvi.asm.org/content/27/2/320.short.

191. Barman S, Nayak DP. Lipid raft disruption by cholesterol depletion enhances influenza A virus budding from MDCK cells. J Virol. 2007;81:12169–78. doi:10.1128/JVI.00835-07.

192. Chizmadzhev YA. The mechanisms of lipid-protein rearrangements during viral infection. In: Bioelectrochemistry. 2004. p. 129–36.

193. Nguyen DH, Hildreth JEK. Evidence for Budding of Human Immunodeficiency Virus Type 1 Selectively from Glycolipid-Enriched Membrane Lipid Rafts. J Virol. 2000;74:3264–72. doi:10.1128/JVI.74.7.3264-3272.2000.

194. Liao Z, Cimakasky LM, Hampton R, Nguyen DH, Hildreth JE. Lipid rafts and HIV pathogenesis: host membrane cholesterol is required for infection by HIV type 1. AIDS Res Hum Retroviruses. 2001;17:1009–19.

195. Blanc M, Hsieh WY, Robertson KA, Kropp KA, Forster T, Shui G, et al. The Transcription Factor STAT-1 Couples Macrophage Synthesis of 25-Hydroxycholesterol to the Interferon Antiviral Response. Immunity. 2013;38:106–18.

196. Bansal D, Bhatti HS, Sehgal R. Role of cholesterol in parasitic infections. Lipids Health Dis. 2005;4:10. doi:10.1186/1476-511X-4-10.

197. Ravnskov U. High cholesterol may protect against infections and atherosclerosis. QJM - Mon J Assoc Physicians. 2003;96:927–34.

198. Holm CK, Jensen SB, Jakobsen MR, Cheshenko N, Horan KA, Moeller HB, et al. Virus-cell fusion as a trigger of innate immunity dependent on the adaptor STING. Nat Immunol. 2012;13:737–43. doi:10.1038/ni.2350.

199. Diamond MS, Kinder M, Matsushita H, Mashayekhi M, Dunn GP, Archambault JM, et al. Type I interferon is selectively required by dendritic cells for immune rejection of tumors. J Exp Med. 2011;208:1989–2003. doi:10.1084/jem.20101158.

200. Palucka K, Ueno H, Fay J, Banchereau J. Dendritic cells and immunity against cancer. In: Journal of Internal Medicine. 2011. p. 64–73.

201. Tran Janco JM, Lamichhane P, Karyampudi L, Knutson KL. Tumor-Infiltrating Dendritic Cells in Cancer Pathogenesis. J Immunol. 2015;194:2985–91. doi:10.4049/jimmunol.1403134.

202. Corrales L, Glickman LH, McWhirter SM, Kanne DB, Sivick KE, Katibah GE, et al. Direct Activation of STING in the Tumor Microenvironment Leads to Potent and Systemic Tumor Regression and Immunity. Cell Rep. 2015;11:1018–30.

203. Tang CHA, Zundell JA, Ranatunga S, Lin C, Nefedova Y, Del Valle JR, et al. Agonist-mediated activation of STING induces apoptosis in malignant B cells. Cancer Res. 2016;76:2137–52.

204. Fu J, Kanne DB, Leong M, Glickman LH, McWhirter SM, Lemmens E, et al. STING agonist formulated cancer vaccines can cure established tumors resistant to PD-1 blockade. Sci Transl Med. 2015;7:283ra52. doi:10.1126/scitranslmed.aaa4306.

205. Frémond M-L, Rodero MP, Jeremiah N, Belot A, Jeziorski E, Duffy D, et al. Efficacy of the Janus Kinase 1/2 Inhibitor Ruxolitinib in the Treatment of Vasculopathy Associated with TMEM173-Activating Mutations in three children. J Allergy Clin Immunol. 2016;1:1–4.

206. König N, Fiehn C, Wolf C, Schuster M, Costa EC, Tüngler V, et al. Familial chilblain lupus due to a gain-of-function mutation in STING. Ann Rheum Dis. 2016;:annrheumdis--2016--209841. doi:10.1136/annrheumdis-2016-209841.

207. Rodero MP, Frémond M-L, Rice GI, Neven B, Crow YJ. JAK inhibition in STING-associated interferonopathy. Ann Rheum Dis. 2016;75:e75–e75. doi:10.1136/annrheumdis-2016-210504.

208. Khamashta M, Merrill JT, Werth VP, Furie R, Kalunian K, Illei GG, et al. Sifalimumab, an anti-interferon-α monoclonal antibody, in moderate to severe systemic lupus erythematosus: a randomised, double-blind, placebo-controlled study. Ann Rheum Dis. 2016;:1–8. doi:10.1136/annrheumdis-2015-208562.

209. Borba HHL, Wiens A, De Souza TT, Correr CJ, Pontarolo R. Efficacy and safety of biologic therapies for systemic lupus erythematosus treatment: Systematic review and meta-analysis. BioDrugs. 2014;28:211–28.

210. Boyce EG, Fusco BE. Belimumab: Review of Use in Systemic Lupus Erythematosus. Clinical Therapeutics. 2012;34:1006–22.

211. Wallace DJ, Stohl W, Furie RA, Lisse JR, McKay JD, Merrill JT, et al. A phase II, randomized, double-blind, placebo-controlled, dose-ranging study of belimumab in patients with active systemic lupus erythematosus. Arthritis Rheum. 2009;61:1168–78. doi:10.1002/art.24699.

212. Furie R, Petri M, Zamani O, Cervera R, Wallace DJ, Tegzová D, et al. A phase III, randomized, placebo-controlled study of belimumab, a monoclonal antibody that inhibits B lymphocyte stimulator, in patients with systemic lupus erythematosus. Arthritis Rheum. 2011;63:3918–30.

213. Merrill JT, Neuwelt CM, Wallace DJ, Shanahan JC, Latinis KM, Oates JC, et al. Efficacy and safety of rituximab in moderately-to-severely active systemic lupus erythematosus: The randomized, double-blind, phase II/III systemic lupus erythematosus evaluation of rituximab trial. Arthritis Rheum. 2010;62:222–33.

214. Woo SR, Corrales L, Gajewski TF. The STING pathway and the T cell-inflamed tumor microenvironment. Trends in Immunology. 2015;36:250–6.

215. Jin L, Hill KK, Filak H, Mogan J, Knowles H, Zhang B, et al. MPYS Is Required for IFN Response Factor 3 Activation and Type I IFN Production in the Response of Cultured Phagocytes to Bacterial Second Messengers Cyclic-di-AMP and Cyclic-di-GMP. J Immunol. 2011;187:2595–601.

216. Hagstrom JE, Ludtke JJ, Bassik MC, Sebestyén MG, Adam S a, Wolff J a. Nuclear import of DNA in digitonin-permeabilized cells. J Cell Sci. 1997;110 (Pt 1:2323–31.

217. Moore MS, Schwoebel ED. Nuclear import in digitonin-permeabilized cells. Curr Protoc Cell Biol. 2001;Chapter 11:Unit 11.7.

218. Miyamoto K, Yamashita T, Tsukiyama T, Kitamura N, Minami N, Yamada M, et al. Reversible membrane permeabilization of mammalian cells treated with digitonin and its use for inducing nuclear reprogramming by Xenopus egg extracts. Cloning Stem Cells. 2008;10:535–42. doi:10.1089/clo.2008.0020.

219. Allen TM, Cullis PR. Liposomal drug delivery systems: From concept to clinical applications. Advanced Drug Delivery Reviews. 2013;65:36–48.

220. Miyabe H, Hyodo M, Nakamura T, Sato Y, Hayakawa Y, Harashima H. A new adjuvant delivery system “cyclic di-GMP/YSK05 liposome” for cancer immunotherapy. J Control Release. 2014;184:20–7.

221. Nakamura T, Miyabe H, Hyodo M, Sato Y, Hayakawa Y, Harashima H. Liposomes loaded with a STING pathway ligand, cyclic di-GMP, enhance cancer immunotherapy against metastatic melanoma. J Control Release. 2015;216:149–57.

222. Lee E, Jang HE, Kang YY, Kim J, Ahn JH, Mok H. Submicron-sized hydrogels incorporating cyclic dinucleotides for selective delivery and elevated cytokine release in macrophages. Acta Biomater. 2016;29:271–81.

1.6 Interferon signalling

STING is an indispensable regulator of type I interferon signalling as initially described by Ishikawa and Barber. In the next section, I summarise the interferon signalling and the importance of type I interferon in immune regulation and pathogenesis.

1.6.1 Interferons

The term “interferon” was first proposed by Isaaca and Lindenmann to describe a type of secretory protein produced in chick embryonic culture (chorio-allantoic membrane) that could interfere influenza virus infection in other cells [134]. After 60 years of research on these proteins, our knowledge of interferons has expanded with regard to their classifications, actions, and the physiological changes that are associated with either their activation or dysregulation. Interferon release is central to the activation of cellular and molecular responses against infections, tumourigenesis, and neurological disorders [135]. They are ubiquitously produced by many tissues and cells including monocytes, macrophage, dendritic cells, lymphocytes, leukocytes, fibroblasts, and natural killer cells to regulate immune and proliferative functions and to enhance further immune activations [128, 135–138].

Interferons (IFN) belong to the super family of class II α-helical cytokines which are further categorised into three subtypes, I, II and III (IFN-I, IFN-II and IFN-III) [139]. Interferon signalling is initiated by cytokines binding to heterodimeric interferon receptors on the plasma membrane to trigger the intracellular Janus kinase - signal transduces and activators of transcription (JAK – STAT) pathways, leading to the phosphorylation and assembly of STAT dimers [140]. This complex recruits IRF9 to form a trimeric transcriptional complex ISGF3 (STAT1-STAT2-IRF9) which migrates to the nucleus and promote the expression of interferon-stimulated genes. Although interferons engage distinct sets of receptors and activate specific DNA promoter regions, their signalling process is highly conserved, facilitating a rapid antiviral and immune regulatory response.

1.6.2 Type II and Type III interferon signalling

The type II and the type III interferon families consist of fewer members in comparison to the type I interferons. The IFN-γ is encoded by multiple genes and is largely released by T lymphocytes and natural killer cells. It binds to a distinct receptor complex the interferon-γ receptor (IFNGR or IFN-γR) which promotes MHC II - dependent pathogen eradicating mechanisms [141–143]. A crucial function of IFN-γ is to program macrophage proinflammatory polarisation (Th1 or M1 activation) [42, 144] which has been discussed in Chapter 1.2.2.2. Whilst IFN-γ has similar, albeit less significant function in direct host microbial/stress defence, it strongly promotes adaptive immune activation and potentiates antigen-specific immune response and cytotoxic cytokine secretion [144–148]. IFNGR activation induces JAK1/2 - TyK2 (Tyrosine kinase 2) which assembles STAT1 homodimers [149]. STAT1 promotes nuclear accumulation of gamma-interferon activating factor (GAF) and binding to interferon-γ -specific promoter site (GAS), which controls the expression of interferon-stimulated genes (ISG) [150, 151].

IFN-III is a family of IL-10 related proteins consist of IFN-λ1, -2, -3 (also known as IL-29, IL-28A and IL-28B, respectively), and a recently identified and poorly characterised IFN-λ4 [152–154]. These cytokines signal through the heterodimeric interferon-λ receptors (IFNLR) complex made up of interferon-lambda receptor 1 (IFN-λR1 or CRF2-12) and IL-10 receptor 2 (or CRF2-4). In addition to the STAT1 dimer-GAS axis, IFN-λ signalling also assembles STAT1-STAT2 heterodimer which further recruits IRF9 to form ISGF3. This complex recognises the DNA promoter interferon-stimulated response element (ISRE) to induce expression of interferon-stimulated genes (ISG) [155–157]. IFN-λ has also been shown to activate STAT3, STAT4 and STAT5 in a cell specific manner [158]. Since type I and type III interferons activate the same kinase cascades and both GAS and ISRE promoted gene expression, their biological activities are largely similar. Viruses including vesicular stomatitis virus, Dengue virus, Sindbis virus, encephalomyocarditis virus and rotavirus can activate both IFN-I and IFNIII [145,151]. IFN-λ is preferentially induced over type I interferons by certain viruses such as influenza A virus and respiratory syncytial virus as an mechanism of immune redundancy, potentially to protect local cell/tissue environment [160–162].

1.6.3 Type I interferon signalling

The IFN-I family includes the abundantly expressed IFN-α and IFN-β and numerous less-widely expressed cytokines such as IFN-ε, -κ, -τ, and –ζ [139]. In humans, IFN-α is transcribed by 12 different genes whereas IFN-β is encoded by a single transcript [163]. The type I interferons are stimulated in macrophages, myeloid and plasmacytoid dendritic cells amongst a wide spectrum of infected cells. The type I interferon response is triggered in response to RNA and DNA sensing by TLRs, RLRs and cytosolic DNA sensors. These PRR receptors mediate signal transduction through adaptor proteins TRIF, MAVS and STING, where their activities converge at the induction of TANK-binding kinase 1 (TBK1) and IκB kinase (IKK), which further recruit and activate IRF3 and NF-κB [164–167]. These transcription factors then accumulate into the nucleus and initiate the expression of type I interferons [Reviewed in [81]]. IRF3, NF-κB and other IRFs (IRF1, IRF4, IRF5, IRF7 and IRF8) bind to different sets of the positive regulatory domains (PRD) of interferon promoters [168–171]. TNF also weakly activates type I interferons due to its induction of IRF1 rather than IRF3 and IRF7 [172, 173]. All transcription factors other than IRF3 and IRF7 have lower and different affinities for interferon promoters and hence these two IRFs are the most critical regulators of interferon expression [81]. The type I interferon response not only provides early defence against infection and immune dysfunction, it also induces a secondary and higher amplitude of interferon-stimulated response. A schematic summary of type I interferon / ISG signalling cascade is shown in Figure 3.

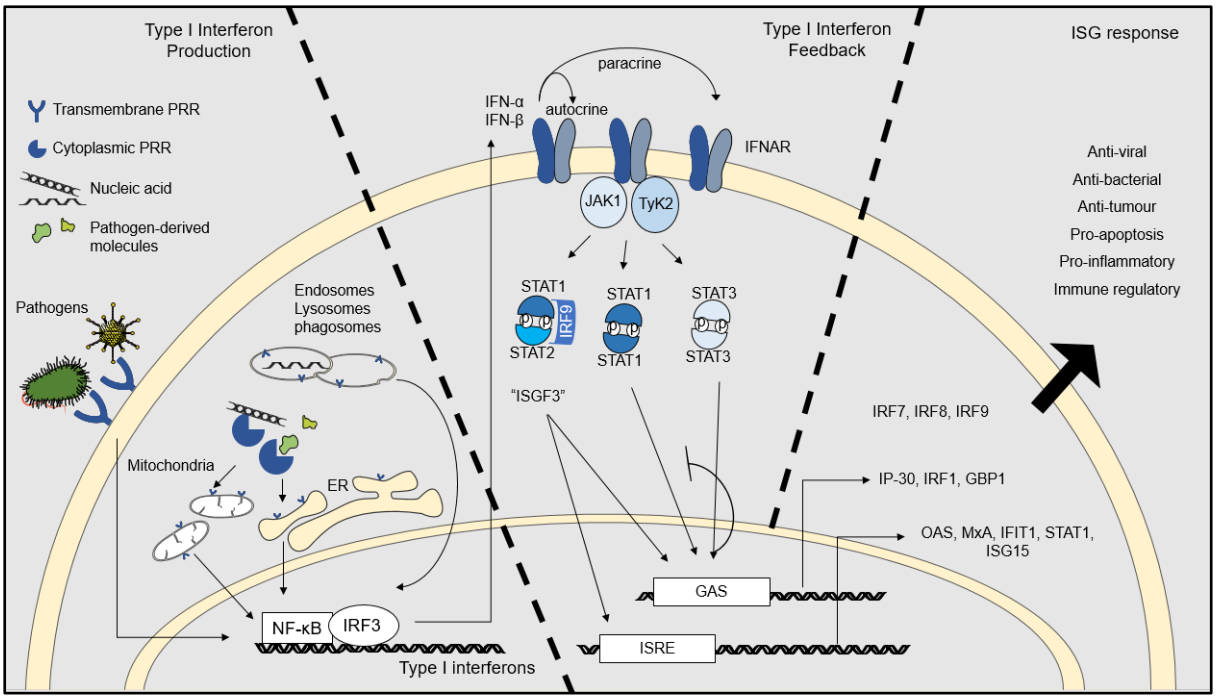

Figure 3. Schematic summary of Type I interferon signalling/ ISG feedback pathway. Pathogen-derived molecules and nucleic acids are recognised by transmembrane and cytoplasmic pattern-recognition receptors (PPRs) and induce signalling activation of NF-κB and IRF3 –dependent transcription of type I interferons (predominantly IFN-α and IFN-β). These cytokines are released to the extracellular interferon receptors IFNARs and respond in both autocrine and paracrine manners. These receptors couple to the adaptor protein Tyk2 and JAK1 which activates three transcriptional complexes: ISGF3 (consists of STAT1-STAT2-IRF9), STAT1 homodimer, and STAT3 homodimer. These factors bind to and activate GAS or ISRE promoter-containing interferon-stimulated genes (ISGs), including the ones indicated in the figure. STAT3-dependent ISG production negatively feeds back to STAT1 activation and hence suppresses further ISG response. ISGs are responsible for various cellular response against microbial infections and immune regulatory activities. Figure summarised from [174–177]. Abbreviations: ER= endoplasmic reticulum, JAK1= Janus kinase 1, IFNAR= Interferon-alpha/beta receptor, TyK2= Tyrosine kinase 2, STAT= signal transducer and activator of transcription 1, GAS= gamma-interferon-activation site, ISRE= interferon-stimulated response element, IP-30= gamma-interferon-inducible protein 30, GBP1= guanylate-binding protein 1, OAS= 2'-5'-oligoadenylate synthase, MxA= Myxovirus resistance protein 1, IFIT1= interferon-induced protein with tetratricopeptide repeats 1, ISG15= interferon-stimulated gene 15.

IFN-I signals through the heterodimeric IFNAR1/IFNAR2 receptor complex named IFNAR (interferon-α/ β receptor) [156]. The receptor complex shows little architectural change when binding to cytokines; however, the receptor affinity to IFN-β was ten to twenty-fold higher than that to IFN-α, and the former is reflectively more capable of activating downstream signalling effects [178]. Following IFNAR activation, kinases JAK1/2-TyK2 are activated and in turn induce ISGF3 formation (STAT1-STAT2-IRF9) [140, 179] which promotes ISRE-regulated gene transcription [155–157]. Unlike IFN-γ which recruits STAT1 homodimers, IFN-I activates both GAS and ISRE promoters via STAT1 homodimers or ISGF3 [Reviewed in [174]], exhibiting an overlapping but much broader antiviral response compared to IFN-γ. IFN-I/IFNAR also recruit STAT3 homodimer to antagonise STAT1 dimer assembly but it supports ISGF3-dependent antiviral ISG expression [180, 181]. The competition between STAT1 and STAT3 controls an appropriate cellular response.

Gene CHIP (chromatin immunoprecipitation) analysis of type I (α and β) and type II (γ) interferon-activated human fibrosarcoma cells revealed that STAT1 and gamma-interferon inducible GTPase guanylate-binding protein (GBP) are universally induced by all three interferons, whereas IRF1 and gamma-interferon-inducible protein (IP-30) are preferentially stimulated by IFN-γ [182]. Furthermore, IFI16, STAT1 and GBP-2 are preferentially induced by IFN-β over IFN-α. This selective ISG induction is likely regulated by STAT1 C-terminal transcriptional activation domains (TAD, or transactivation domain) where multiple serines are available for targeting by JAK, TyK, and other kinases (p38, CaMKII, PKCδ and others) [183–187].

1.6.4 Interferon-stimulated genes (ISG)

More than a hundred ISGs have been found to control cellular processes including but not limited to chemotaxis, apoptosis, cell proliferation, infection detection and defence, and some ISGs obtain redundant functions to others [188]. Some ISGs have been characterised with specific functions, such as the RNA sensors OAS1 and PKR, whereas others are multifunctional, such as the pro-apoptotic factors of the caspase family. One of the most important ISG is IRF7. This interferon-activating transcription factor has high affinity for interferon promoters yet it is only expressed at high levels during ISG production to exhibit and sustain further antiviral response [81, 189, 190]. Chapter 1.5 (Table 4) summarises some of the ISGs involved in apoptosis, immune modulation, cell adhesion and motility, and antiviral responses, although many more ISGs are being identified to have physiological importance in enhancing innate immunity [176, 191, 192].

1.6.5 Mechanisms of activating type I Interferons

Despite the similarity between type I and type III interferons, the antiviral response is a lot potent in the former [193]. IFN-α and IFN-β are the most highly expressed cytokines of the interferon superfamily. Rapid release of type I interferons underpins the success of anti-pathogenic defence. Apart from the TRIF-dependent signalling, other intracellular TLRs also contribute to interferon release through MyD88 and the transcription factors IRF1, IRF3 and IRF7 [164, 194]. The depletion of RNA-recognising TLR3, TLR7, and TLR8 in combination has not fully abolish the IFN-I release, nor did the depletion of the CpG motif-containing DNA sensor TLR9 impair the recognition of DNA challenge. This evidence highlights the necessity and importance of TLR receptor redundancy in nucleic acid sensing mechanism.

As previously mentioned (Chapter 1.3), the mitochondrial adaptor protein MAVS and the ER adaptor STING are the two TLR-independent platforms downstream of nucleic acid sensing mechanisms [Reviewed by [118, 195]]. These two adaptors are central in complementing the canonical PRR recognition paradigms, where MAVS facilitates RNA activated RLR receptors and RNA sensor such as OAS and RNAse L, and STING regulates DNA-activated sensor dynamics. Signalling though these two proteins results in distinct IFN-I induction mechanisms. Upon interacting with RNA sensors via the N-terminal CARD domain, MAVS polymer transforms into prion-like filaments and complexes with multiple TRAFs (tumour necrotic factor (TNF) receptor-associated factors) to activate the TBK1 – IRF3 axis [165, 196–198]. TBK1 and IKK trigger IRF3 and NF-κB - dependent signalling events respectively, and together they upregulate type I interferon gene expression. MAVS has been found on both peroxisomal and mitochondrial membranes, especially at mitochondria-associated membranes (MAM) [103, 199].

The discovery of DNA sensing adaptor protein STING by Ishikawa and Barber led to a new paradigm of understanding virus infection and autoimmunity [133]. As mentioned in Chapter 1.3.2 and reviewed in the Chapter 1.5 [119], STING responds to a number of DNA sensors and signalling messengers named cyclic dinucleotides (CDN) [119]. CDNs consist a chemical made of two purine nucleotides GMP

(guanosine monophosphate) and AMP (adenosine monophosphate). These molecules are either directly released into the cytoplasm by bacteria such as *Listeria monocytogenes*, *Vibrio cholerae*, *Streptococcus pyrogenes* and *Staphylococcus aureus* [200–202] or endogenously produced from ATP and GTP by the DNA sensor cyclic-GMP-AMP synthase (cGAS) [114, 203, 204]. Bacteria-secreted STING ligands c-di-AMP, c-di-GMP and c-GMP-AMP (cGAMP or 3'-3' cGAMP) are joint by two 3'-5' phosphodiester bonds between the nucleotides whereas the endogenous cGAMP contains a combination of canonical 3'-5' bonds and a unique 2'-5' link between GMP and AMP, giving its name 2'-3' cGAMP (cyclic[G(2'-5')pA(3'-5')p]). Ligand recognition activates STING dimers which signal though the TBK1-IRF3/NF-κB –dependent interferon signalling cascade [165–167]; a pathway that is common to both MAVS and intracellular TLRs.

Both MAVS and STING protect the host by recognising viral and bacterial genomes or their products. RIG-I/MAVS and cGAS/STING pathways not only converge at the induction of IRF3-mediated interferon response, they also directly collaborate in antimicrobial defence. RIG-I -engaged MAVS at the MAM of mitochondrial and ER membranes can transduce activation signal via STING, displaying an amplification antiviral response to ssRNA viruses, such as Japanese encephalitis virus, Sendai virus, Hepatitis C virus and vesicular stomatitis virus [133, 205, 206]. The DNA virus herpes simplex virus-1 (HSV-1) can directly activate both STING and MAVS by either the DNA-sensing mechanism and Pol III –catalysed DNA breakdown to generated ssRNA for RIG-I/MAVS recognition [207, 208]. In contrast, single-stranded retrovirus HIV can be detected by RIG-I while its cDNA, produced by reverse transcription, can be processed and recognised by DNA sensors TREX1 and cGAS which activate STING [116, 209–211]. MAVS, STING and nucleic acid sensing redundancy not only broadens detection spectrum but also prevents viral antagonism of interferon response, providing alternative sources for antiviral defence.

1.6.6 Mechanisms of type I interferon inhibition

Type I interferons are regulated at various levels, from the detection of pathogens to the production of interferon-inhibitory ISG. The need for downregulating type I interferon signalling is mainly to restricting the amount and duration of proinflammatory response [174]. Intercepting IFN-I signalling can be achieved by E3 ubiquitin ligase SCF(HOS) (Skp1-Cullin1-HOS-Roc1)-dependent degradation of IFNAR or via clathrin-dependent receptor endocytosis [212, 213]. Furthermore, IFNAR activity is also regulated by Jak and TyK through USP18 (Ubiquitin specific protease 18) and SOCS (suppressor of cytokine signalling) proteins via IFN-I promoted negative feedback loops. USP18 competitively associates with IFNAR and hence dissociating Jak1 from the receptor as well as blocking the recognition site for IFN-α2 [214, 215]. Similarly, SOCS1 indirectly reduces the level of active IFNAR by phosphorylating and associating with TyK2, hence blocking its activation capacity [216]. Persistent infection also induces interferon-inhibitory ISG release, such as ISG56, which is induced by VSV (vesicular stomatitis virus) that disrupts STING - TBK1 communication and consequent in a reduced IRF3-mediated ISG production [217]. The regulation of IFN-I signal protects against chronic inflammation and yet can be hijacked by viruses to evade antiviral response.

1.6.7 Virus inhibition of STING-dependent type I interferons

Type I interferon responses are readily induced by viral and bacterial infections and therefore numerous PRRs are limited by microbial evasion techniques as reviewed in the literature [218–220]. The two intracellular antiviral adaptors STING and MAVS are heavily suppressed in favour of establishing infection. As these central adaptors mediate the majority of intracellular pathogen detection, antagonising them in addition to the upstream sensors would be an effective approach to intercept interferon activation. As reviewed in Chapter 1.5 [119], several viruses are known to specifically degrade DNA sensors and STING by secreting protease complexes, and members of the family *Flaviviridae* are the most renowned culprits [221].

Flavivirus has the most abundant members compared to the other three genera of the family (*Hepacivirus*, *Pegivirus*, and *Pestivirus*). This genus is comprised of arthropod-borne viruses (arboviruses) that encode the positive-sense single stranded (ss)RNA genome with a 5' G7 cap [221]. This group contains Dengue virus (DENV), Yellow Fever virus (YFV), West Nile virus (WNV), Japanese encephalitis virus (JEV), and Zika virus (ZIKV). These pathogens are known to cause severe diseases including haemorrhagic, fever, and various neurological disorders such as encephalitis (brain inflammation) and microcephaly (a birth defect associated with a reduced head circumference) [222, 223]. Through insect vectors, these viruses penetrate mammalian cells and introduce their RNA molecules, containing a single, 9.5 to 12.5 kb long open reading frame, into the host cytoplasm where they hijack the *de novo* molecular machineries to translate a single polyprotein. The protein is processed by viral and cellular enzymes and released as three structural (S) and seven non-structural (NS) proteins [224]. The structural proteins capsids (C), pre-membrane proteins (prM) and envelop glycoproteins (E) support the virion structure [225], and the non-structural proteins form the RNA polymerases, helicases, proteases, and nucleoside phosphatases and together functions as the replicative complex [224]. Compared to the other five non-structural proteins (NS1, NS2a, NS2b, NS4a and NS4b), the functions of NS3 helicase and NS5 RNA polymerase are pivotal for viral replication [226, 227]. Due to these features, anti-replication drugs often target NS3 activation and binding to co-factor NS2B or NS5-dependent RNA-capping methyltransferase activity and RNA polymerisation [228, 229]. Furthermore, the

structural C and E proteins are also common targets to block attachment, folding and spreading of flaviviruses. Examples are C protein inhibitor ST-148 and E protein inhibitors NITD-448 and Compound 6 [230, 231].

Chapter 1.5 (Viral Evasion of STING, Page 73) [119] has reviewed the key strategies used by flaviviruses to inhibit and evade STING activation. However, Dengue virus amongst other flaviviruses can inhibit only human but not mouse STING [232, 233]. The principle of inhibition lies at residue 78R/79G within the third transmembrane domain which is a cleavage target for dengue-secreted NS2B/3 protease complex specifically present in human and closely related species [234]. STING in Rodents and several primates contains different sequences in the Dengue cleavage site and are thus remain immune responsive to dengue infection.

Studies of STING-targeted type I interferon inhibition are also considered critical for characterising novel flaviviruses, one of which is Zika virus. ZIKV is emerging as an important pathogen around the globe [235–237]. ZIKV and DENV are closely related species and can induce similar and cross-reactive serological responses in human, suggesting similarity between their envelope protein structures [238, 239]. This characteristic is likely to impact on their pathogenesis in human and animals and thus it is of intense interest whether these two viruses adopt the same STING blocking strategies. ZIKV is most devastating in mother-to-child transmission and causing microcephaly and other neurological defects in the new born [240, 241]. In human, this transmission is highly dependent on the placental macrophages which substantially facilitate ZIKV replication and spread [54]. Although type I interferon signalling was detected in these cells, limited viral restriction and cell death was observed. It has been established that early ZIKV invasion in murine placenta can induce type I interferons which lead to tissue remodelling and fetal resorption [242]. Furthermore, ZIKV also expresses NS5 protease to intercept interferon-activated STAT1 and STAT2 in human cells [243, 244], a strategy also observed by DENV-secreted NS5 [245, 246]. I therefore wanted to test whether the ZIKV-secreted NS2B/3 protease homolog is capable of degrading STING, and whether macrophages are essential regulators of ZIKV infection. Addressing these questions will help us reveal novel

functions of STING and to compare and contrast the physiological regulation of key immune mediators that can distinguish flaviviruses. Understanding virus-mediated interferon inhibitory mechanism is critical to innovate antiviral therapeutic development.

1.6.8 Type I interferon -associated pathologies

Dysregulation of type I interferons and the stimulated ISG response is implicated in a variety of pathologies, ranging from immunodeficiency to autoimmunity.

Signalling in both autocrine and paracrine manners, type I interferons form one of the broadest acting signalling networks across the host system, involving almost every cell type and tissue, and exhibiting their pivotal role in early pathogen defence. The role for IFN-I in bacterial and viral infections has been extensively reviewed [175, 247, 248]. Deficient IFNAR expression in mice reduces early viral interference as observed by an elevated and extended vaccinia virus accumulation in the liver and spleen compared to wildtype (WT) mice [249]. Also, both the individual and combined knockout of IRF3 and IRF7 can significantly enhance infection susceptibility to HSV-1 [250]. Additionally, RIG-I deficient variants render higher severity of influenza virus infection in patients [251] and loss-of-function STING allele HAQ (R71H-G230A-R293Q) leads to a defective type I interferon response and an enhanced *Streptococcus pneumoniae* and *Legionella pneumophila* infection [252, 253]. Furthermore, cytotoxicity and antigen presentation on CD8+ T cells, macrophages and CD8α+ dendritic cells also rely on the appropriate IFN-I signature, and it potentiates B cell-associated humoral immunity [254–256]. Breast cancer, melanoma and gastrointestinal cancer patients also displayed downregulated IFN-I (IFN-α) immunity in peripheral blood lymphocytes, suggesting an possible role for type I interferon signal in cancer progression and immunotherapies [257].

Excessive IFN-I production, termed type I interferonopathy, also drives pathological processes. Non-resolving inflammatory activation is a major cause of disease. In chronic infection, viruses can persist in the host system and continuously stimulate type I interferon that damage the infected tissues and organs. Human immunodeficiency virus (HIV), Hepatitis C virus (HCV) and the mouse chronic infection model lymphocytic choriomeningitis virus (LCMV) have been shown to induce and exacerbate chronic IFN-I release, leading to a dysregulated and prolonged immune response that stimulates cell apoptosis [258, 259]. Although IFN-I is often suppressed by viruses to establish a stable niche in the host, during the pathogenic stage of

infection, type I interferons are highly active and they can induce aberrant proliferation and activations of CD4+ T cells and antibody-producing B cells. Although IFN-I initially promotes viral clearance and cellular activations, a prolonged presence of IFN-I signal drives immune exhaustion, and a proportion of patients with established chronic infection show IFN-α unresponsiveness potentially due to immunosuppression via an IFN-I blocking negative feedback loop [Reviewed in [260, 261]]. IFN-I signalling can then become a double-edged sword in specific viral infections. For instance, LCMV takes advantage of the negative feedback mechanism that suppresses B cell-mediated humoral response and CD4+ T-cell replenishment, enabling their survival in a dampened immune environment [262]. Similarly, CD4+ T-cell depletion was seen in HIV-1 –induced IFN-I hyperactivation, which can be rescued by administrating an IFNAR blocker [263].

Over-activated type I interferon response is one of the critical factors contributing to and amplifying autoimmunity. Autoimmune diseases arise when type I interferon responses overcome the limit of immune tolerance directed by B cells and T cells [264, 265]. This can be caused by chronic infections, injuries and natural mutants that constitutive activate IFN-I inducing pathway. This may result in an excessive leukocyte infiltration and cytotoxicity which cause aberrant cell apoptosis and necrosis, processes that break down cells and expose the intracellular contents. The DNA molecule is one of the most potent stimulant of immune response and the extracellular release will induce B cells to produce autoantibodies [266]. Additionally, autoantigens activate a number of additional PRRs which further augment IFN-I signalling [267, 268]. A growing literature reports that type I interferonopathy is observed in patients with type I diabetes, multiple sclerosis, myositis, rheumatoid arthritis, and the prototypical systemic disease SLE [269, 270]. The “IFN signature”, an overexpression of type I interferon transcripts (normally IFN-α and IFN-β) in the circulating peripheral blood and multiple organs, reflects disease severity and the level of anti-dsDNA autoantibodies amongst other disease parameters [271, 272]. In particular, IFN-α therapies administered to HCV infected patients sometimes leads them to develop spontaneous and *de novo* lupus-like symptoms, indicating the complexity of IFN-I regulation at different stages of infection-immunity balance [273, 274].

1.7 Background summary

Macrophages are a potent defender of pathogenic infection and a critical regulator of tissue homeostasis. Macrophages exhibit their immune functions via signalling networks coordinated by numerous pattern recognition receptors. In addition to the canonical inflammatory receptors TLRs, CLRs, NLRs and RLRs, a non-canonical inflammatory signalling network makes a substantial contribution to innate immunity. To reveal novel inflammatory mediators, a functional cDNA screen was undertaken in murine macrophage RAW 264.7 cell line. One of the “hits” from this screen was a protein with unknown biological properties. This gene, Tmem203, encodes a transmembrane protein TMEM203, known to maintain ER calcium store homeostasis yet with unknown functions in immunity. Based on some unpublished pilot data (2014) from our group, we speculate that TMEM203 is a potential co-regulator for the antiviral adaptor protein Stimulator of Interferon Genes (STING). STING is ubiquitously expressed in the ER and responds to DNA sensors and microbial secreted cyclic dinucleotides. It signals through the TBK1-IRF3 axis which specifies type I interferon activation and later an amplified interferon-stimulated response. Due to the close localisation in the ER, TMEM203 and STING are likely to interact directly and complex in a number of signalling activities. To facilitate our research, we reviewed the recent findings for STING and type I interferon signalling to explore the potential areas that can relate to TMEM203 characterisation [119]. Type I interferon signals through the JAK-STAT axis and mediates ISG feedbacks. Both Type I interferons and ISGs are indispensable for antiviral and antibacterial response in human. Viruses often adopt evasive strategies to inhibit type I interferon activation and STING is a critical target for such inhibition. The *Flaviviridae* family is particularly renowned for blocking STING-interferon signalling, and the two close-related members Dengue virus and Zika virus have shown similarity in the mechanism of STING antagonism. Due to the profound influence of STING research that identified its value in anti-tumour, anti-microbial, and auto-inflammation regimes, novel studies on STING regulation will be innovative to scientific and clinical advancement.

1.8 Hypotheses

1.8.1 Chapter 2 (Paper 2): TMEM203 is a novel binding partner and regulator of STING mediated inflammatory signalling in macrophages.

Hypothesis: TMEM203 interacts directly with STING to regulates its type I interferon response in macrophages.

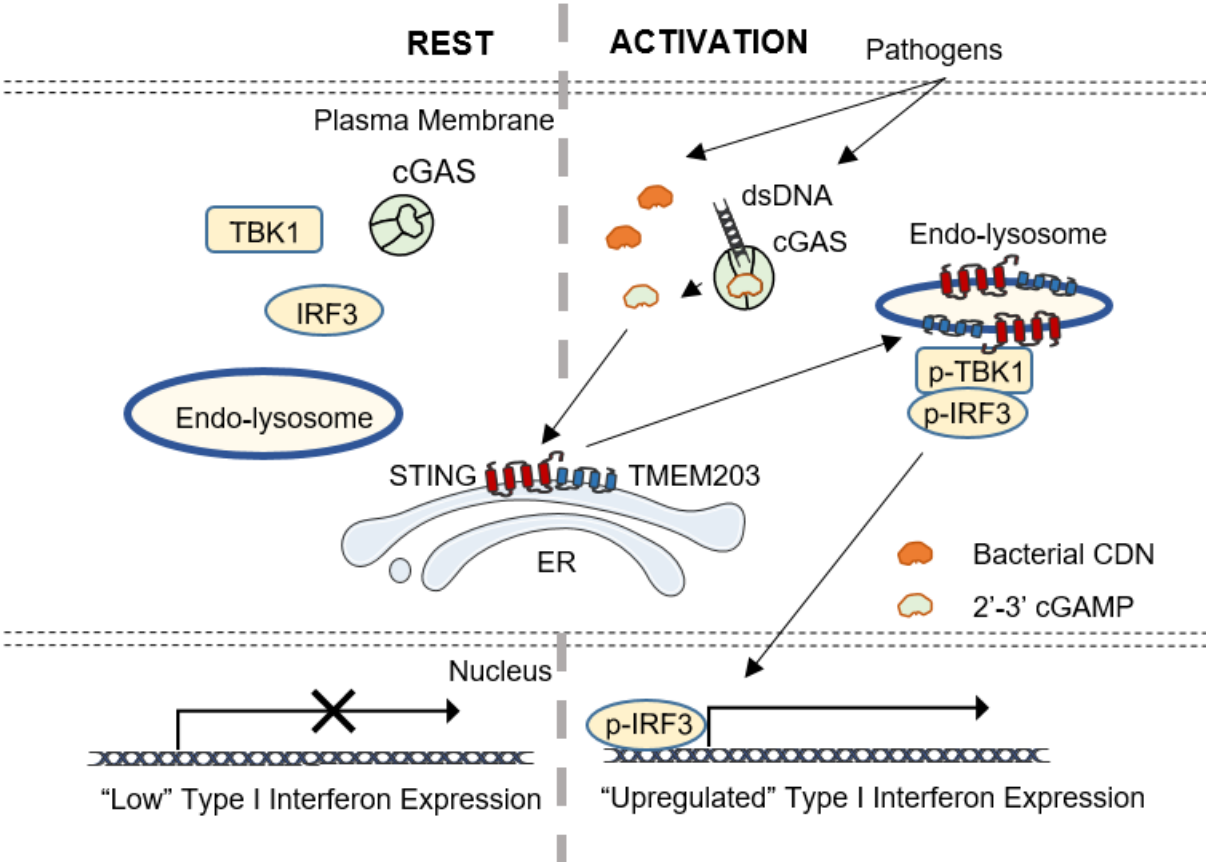

Figure 4. Hypothesis for paper 2.

A schematic describing the hypothesis of this research. The novel proinflammatory protein TMEM203 regulates the STING-mediated immune detection of bacterial cyclic dinucleotides (CDN) and the DNA sensor cGAS-catalysed 2'-3' cGAMP. STING and TMEM203 interact and together they promote TBK1-IRF3 axis which upregulates type I interferon expression. STING exists as a dimer yet a monomeric structure is shown here for simplicity.

1.8.2 Chapter 4 (Paper 3): STING mediates responses to Zika virus and Dengue virus infection in human primary monocyte-derived macrophages.

Hypothesis: STING regulates type I interferon stimulated gene expression upon infection of Zika virus (ZIKV) and Dengue virus (DENV) in human monocyte-derived macrophages.

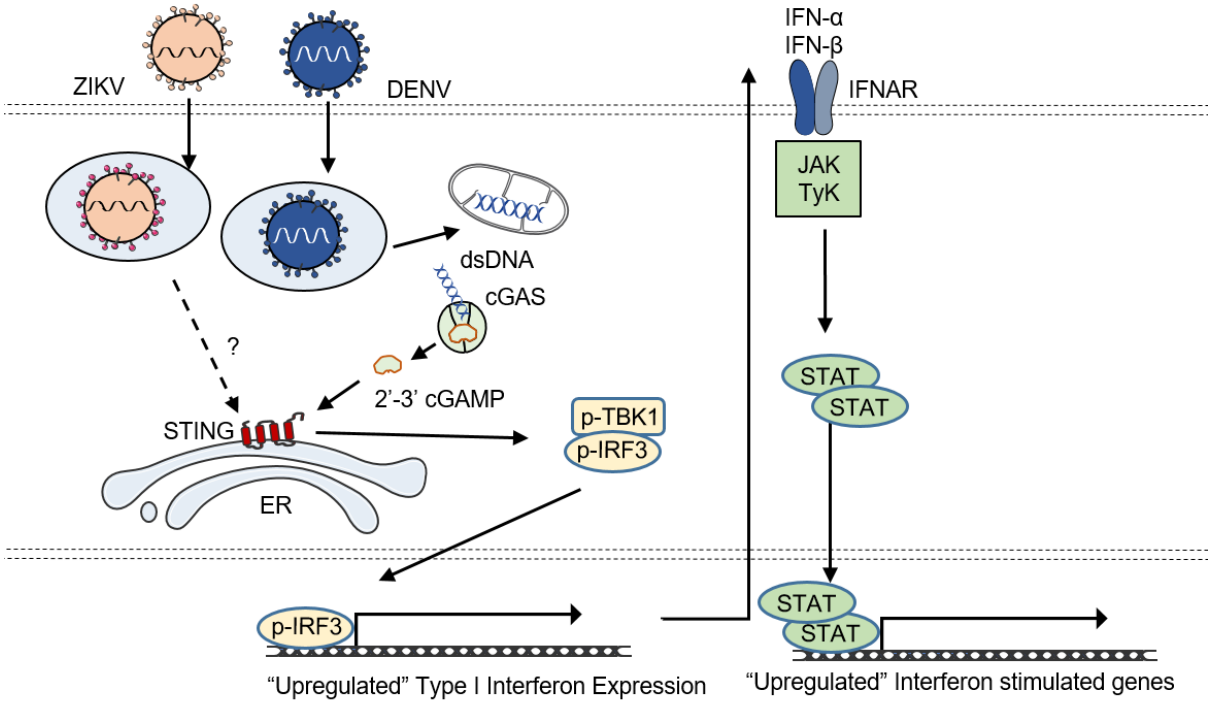

Figure 5. Hypothesis for paper 3.

ZIKV and DENV attach to, enter and replicate in human macrophages. Accumulation of ZIKV activates STING via unknown mechanism whereas DENV induces mitochondrial dsDNA leakage which is recognised by DNA sensor cGAS. This enables the production of 2'-3' cGAMP and activation of the STING-dependent TBK1-IRF3 axis, which in turn upregulates type I interferon expression. The type I interferons can then activate IFNAR receptors and induce the JAK/TyK-STAT pathway and express interferon-stimulated genes.

1.9 Aims and objectives:

Chapter 2 (Paper 2) contains the PhD research work addressing the hypothesis stated in Chapter 1.8.1. My experiments, determined in Authors' Contributions, aim to investigate the following points:

1. To understand if TMEM203 is critical to STING-activated type I interferon expression in macrophages.
2. To identify if a direct interaction exists between TMEM203 and STING.
3. To identify the immunological challenge that alters TMEM203-STING interaction.
4. To identify the molecular determinant of TMEM203-STING interaction.

Chapter 4 (Paper 3) resulted from the EMBO-funded collaborative work between our lab and Dr Marlene Dreux's lab. This report addresses the hypothesis stated in Chapter 1.8.2 and aims to elucidate the following points:

1. To investigate how Zika virus (ZIKV) and Dengue virus (DENV) infection in M-CSF differentiated primary monocyte-derived macrophages.
2. To compare and contrast the dose and time-dependent ISG response caused by ZIKV/DENV infections.
3. To investigate whether STING is regulated by or regulating the infection of ZIKV/DENV in primary macrophages.

Chapter 2 (Paper 2): TMEM203 is a novel binding partner and regulator of STING mediated inflammatory signalling in macrophages

Authors: Yang Li[1], Sharmy J. James[4,5], David H. Wyllie[3], Claire Wynne[2], Agnes Czibula[6], Katherine Pye[1], Seri Musfirah Bte Mustafah[4,5], Roberta Fajka-Boja[1,6], Adrienn Angyal[1], Zoltan Hegedus[6,9], Laszlo Kovacs[7], Adrian V.S. Hill[3], Caroline A. Jefferies[8], Heather L. Wilson[1], Zhang Yongliang[4,5], Endre Kiss-Toth[1]

Affiliations:

1: Department of Cardiovascular Science, University of Sheffield, Beech Hill road, Sheffield, S10 2RX, United Kingdom

2: School of Biological Sciences, Dublin Institute of Technology, Kevin St, Dublin 8, Ireland

3: Jenner Institute, Old Road Campus Research Building, Oxford University, Roosevelt Drive, Oxford, OX3 9DU, United Kingdom

4: Department of Microbiology and Immunology, Yong Loo Lin School of Medicine, National, University of Singapore, 117545, Singapore

5. Immunology Programme, the Life Science Institute, National University of Singapore, 117597, Singapore

6: Biological Research Centre of the Hungarian Academy of Sciences, Temesvari krt 62, Szeged, H-6726, Hungary

7: Department of Rheumatology and Immunology, University of Szeged, Faculty of Medicine, Albert Szent-Gyorgyi Health Centre, Kalvaria sgt 57, Szeged, H-6725, Hungary

8: Cedars-Sinai Medical Center, 8700 Beverly Blvd, Los Angeles, CA 90048, USA

9: Department of Biochemistry and Medical Chemistry, University of Pecs, Hungary

Status: Submitted to Molecular Cell, Dec 2018.

Authors' Contributions:

This work was the result of collaboration between Zhang's lab at Singapore and Kiss-Toth lab at Sheffield. I conducted experiments presented in Figure 2 G-I, Figure 3 C-E, all of Figure 4, all of Figure 6 except for C-E, and all of Figure 7. I supervised my Master student Katherine Pye for experiment in Figure 6C. I also contributed to the experiments and result analysis of Supplementary Figure S2 A-E and G and all of S4. I wrote the manuscript with my supervisor Dr Heather Wilson and Prof. Endre Kiss-Toth, and it was reviewed, edited and approved by all authors. Please refer to PNAS (2019) for the revised manuscript version.

Further experiments that facilitated the production of this paper is presented in Appendix 1.

1) Relative mRNA expression level of TMEM203, STING and MAVS in human MDMs.
2) siRNA transfection does not activate IFN-β and IL-8 mRNA upregulation in MDMs.
3) Optimising siRNA-directed knockdown in human MDMs
4) Site-directed mutagenesis for the generation of Sting truncation mutants
5) Optimising organelle staining and co-transfection of protein complementation fluorescence for confocal imaging

Detailed materials and methods regarding my contributions to this paper and additional data listed above are presented in Appendix 2 and 3.

TMEM203 is a novel binding partner and regulator of STING mediated inflammatory signalling in macrophages

Yang Li[1*], Sharmy J. James[4,5], David H. Wyllie[3], Claire Wynne[2], Agnes Czibula[6], Katherine Pye[1], Seri Musfirah Bte Mustafah[4,5], Roberta Fajka-Boja[1,6], Adrienn Angyal[1], Zoltan Hegedus[6,9], Laszlo Kovacs[7], Adrian V.S. Hill[3], Caroline A. Jefferies[8], Heather L. Wilson[1], Zhang Yongliang[4,5], Endre Kiss-Toth[1]

Affiliations:

1: Department of Cardiovascular Science, University of Sheffield, Beech Hill road, Sheffield, S10 2RX, United Kingdom

2: School of Biological Sciences, Dublin Institute of Technology, Kevin St, Dublin 8, Ireland

3: Jenner Institute, Old Road Campus Research Building, Oxford University, Roosevelt Drive, Oxford, OX3 9DU, United Kingdom

4: Department of Microbiology and Immunology, Yong Loo Lin School of Medicine, National University of Singapore, Singapore 117545;

5. Immunology Programme, the Life Science Institute, National University of Singapore, Singapore 117597.

6: Biological Research Centre of the Hungarian Academy of Sciences, Temesvari krt 62, Szeged, H-6726, Hungary

7: Department of Rheumatology and Immunology, University of Szeged, Faculty of Medicine, Albert Szent-Györgyi Health Centre, Kálvária sgt 57, Szeged, H-6725, Hungary

8: Cedars-Sinai Medical Center, 8700 Beverly Blvd, Los Angeles, CA 90048, USA

9: Department of Biochemistry and Medical Chemistry, University of Pécs, Hungary

Summary:

Regulation of interferon signalling is critical in host recognition and response to pathogens, whilst its dysregulation underlies the pathogenesis of several chronic diseases. STimulator of INterferon Genes (STING) has been identified as a critical mediator of Interferon inducing innate immune pathways, but little is known about direct co-regulators of this protein. We report here that TMEM203, a conserved putative transmembrane protein, is a novel intracellular regulator of STING-mediated signalling. We show that TMEM203 binds to, co-migrates to the lysosome and functionally cooperates with STING following cell stimulation, which in turn controls the activation of TBK1, IRF3 and the induction of target genes in macrophages, including interferon-β. Using *Tmem203* knockout bone marrow-derived macrophages and transient knockdown of TMEM203 in human monocyte-derived macrophages, we show that this protein is required for cGAMP induced STING activation. Unlike *STING*, *TMEM203* mRNA levels are elevated in T cells from patients with SLE, a disease characterised by the overexpression of type I interferons. Moreover, *TMEM203* mRNA levels are associated with disease activity, as measured by C3 serum levels. Identification of TMEM203 sheds new light into the control of STING mediated innate immune responses, providing a potential novel mechanism for therapeutic interventions in STING associated inflammatory diseases.

Keywords:

TMEM203, STING, cGAMP, type I interferon

Introduction:

Innate immune sensing of microbial infections involves pathogen pattern recognition receptors (PPRs), such as Toll-like receptors (TLRs). Many TLR-dependent and –independent innate signalling systems, including NOD-like receptors and systems recognising intracellular DNA (1, 2) activate the TBK1/IRF3 axis, a pathway of fundamental importance in immune defence in both bacterial and viral diseases (3). Activation of this pathway, which is of great phylogenetic antiquity (4), results in the production of interferon-β, a cytokine critical for host defence against both viruses and bacteria. As increasing evidence links the PPR/TBK1/IRF3 axis to autoimmune disease (including SLE) (5, 6), vaccine responses (7) and the development of malignancy (8–10), the identification of regulators of this pathway may reveal novel therapeutic targets.

One important component mediating the activation of the TBK1/IRF3 pathway is the endosomal multi-transmembrane protein, STimulator of INterferon Genes (STING) (2, 11). STING is activated by the double-stranded DNA (dsDNA) sensor IFI16, or by direct binding to bacteria-secreted cyclic dinucleotide c-di-AMP, c-di-GMP and 3'3'-cGAMP, as well as cGAS-catalysed (12, 13) mammalian ligand 2'3'-cGAMP. Its critical role is proven both by the lack of interferon induction following viral, bacterial or synthetic DNA stimulation in STING deficient cells (2, 14), and by the increased sensitivity of STING deficient mice to DNA viruses such as HSV-1 (2). Constitutively-activated STING variants have been found in patients diagnosed with severe symptoms of type I interferonopathy and leading to diseases such as STING-associated vasculopathy with onset in infancy (SAVI) (15), systemic lupus erythematosus (SLE) (5, 6, 16), and familial chilblain lupus (FCL) (17). The importance of STING activity in health and disease has also been the subject of several recent reviews (3, 18, 19).

Following STING activation, the serine/threonine kinase TBK1 is recruited to the cytosolic face of the endo-lysosome/endoplasmic reticulum (ER) (20). At these intracellular vesicles, STING is targeted for K27-linked ubiquitination by AMFR, triggering its activation and the subsequent phosphorylation of the transcription factor IRF3 (21). Once phosphorylated, IRF3 dimerises and translocates to the nucleus where it drives the expression of genes containing IRF binding sites in their promoter, predominantly the type I interferons IFN-α and IFN-β (20). Post-activation, STING is sorted to the endo-lysosomes where it is targeted by LC3 and autophagy-related protein 9a (Atg9a) to attenuate its functions (22, 23).

Whilst most studies have described STING as a critical component in cytosolic nucleic acid recognition, STING has also been shown to play a role in augmented IRF3 activation and type I interferon (IFN-I) induction upon concomitant ER stress and LPS stimulation (2, 24) via late-TLR4 signalling (25). Despite the fundamental importance of STING in both anti-bacterial and anti-viral immunity, its partners remain largely unknown, with many aspects of its mechanism of action still being poorly understood.

In previous functional screens discovering novel regulators of inflammation (26, 27), we reported the identification of TMEM203 as a previously unknown proinflammatory gene in mouse macrophages (26). Here we demonstrate that TMEM203, a protein that was recently shown to be endosomal and interacts with the pleiotropic inositol phosphate signalling pathway protein IP3R (28), is associated with SLE disease activity, forms a functional and ligand-dependent complex with STING and is a novel regulator of signalling pathways activated in response to diverse bacterial and viral stimuli, including cyclic dinucleotides.

Results:

TMEM203 is an evolutionarily conserved putative transmembrane protein, regulated by inflammatory stimuli

We have previously identified multiple regulators of inflammatory signalling in macrophages by genome-wide expression screening for genes which drove *Cxcl2* expression when transfected into RAW 264.7 cells (26); TMEM203 was one such protein. Multiple alignment of TMEM203 orthologues from a wide range of species demonstrated that TMEM203 is an evolutionally highly conserved gene (**Fig. 1A**) encoding a 136 amino acid protein, with the mouse and human orthologues being 98% identical. Interestingly, a survey of the GenBank database revealed that only a single copy of this gene is present in both invertebrate and vertebrate species; with TMPred (29) predicting four putative membrane-spanning helices (**Fig. 1A, TM1-4**). One distantly related homologue of TMEM203 has been described so far, the 133 amino acid protein TMEM60 with about 21% identity (30).

Dysregulated expression of key innate immune signalling molecules has previously been linked to the development of human pathologies, including systemic lupus erythematous (SLE), an inflammatory disease often characterised by the recruitment of immune cells, including T lymphocytes and their excessive type I interferon production in the affected tissues. Thus, we have analysed the mRNA levels of two well characterised intracellular signalling regulators, MAVS (mitochondrial antiviral signalling protein) and STING (Stimulator of Interferon Genes), as well as TMEM203 in T cells isolated from the blood of recently diagnosed, treatment naïve SLE patients. Both MAVS and STING have previously been implicated in driving interferon production in SLE (5, 31, 32). We found significantly reduced, almost abolished MAVS expression, with marked upregulation of TMEM203 (Mean 13.83 ± SD 6.52 fold induction, lower:upper interquartile = 8.59:18.84) (**Fig. 1B**). Further, TMEM203 mRNA levels inversely correlated with the plasma levels of complement factor C3, a clinically used marker of activated innate immunity. Taken together, this suggests that TMEM203 may play a role in the development of this disease (**Fig. 1C**) and that this activity might be coupled to excessive production of type I interferon.

A search in the transcriptome database thebiogps.org (33) indicated that TMEM203 is highly expressed in myeloid cells, including macrophages. Since our expression screen showed that TMEM203 may act as a signalling regulator in myeloid cells (26), we first tested how chemokine expression in murine macrophages is controlled by TMEM203. Compared to controls, *Cxcl2* promoter activity in LPS stimulated RAW 264.7 cells was enhanced by the overexpression of *Tmem203* (**Fig. 1D**), whilst being impaired by the siRNA-mediated

downregulation of *Tmem203* (**Fig. 1E**), suggesting that TMEM203 is likely to act downstream of Toll-like receptors (TLRs) and/or other innate immune sensors.

We next characterised the molecular pathways for *Tmem203* action, using *Cxcl2* promoter activity as a surrogate of the activation of canonical TLR pathways (34). Whilst LPS-induced activation of a *Cxcl2*-luciferase reporter in RAW 264.7 cells is blocked (**Fig. 1F**), the *Tmem203*-induced Cxcl2 activation is not inhibited by the expression of the dominant negative forms of *Irak1*, *Trif*, *MyD88*, *Tram*, *Mal* and *Traf6* (**Fig. 1G**). Similarly, pharmacological MAPK inhibitors impair LPS-, but not overexpressed (OE) *Tmem203*-induced *Cxcl2* promoter activities (**Fig. S1**). Therefore, we concluded that whilst *TMEM203* is a novel pro-inflammatory mediator/effector, it is likely to act independently from the canonical TLR and MAPK networks. We therefore explored whether TMEM203 acts on the non-canonical inflammatory pathway, since LPS also induces the TRIF-TRAM/TBK1/IRF3 pathway via endosomal “late signalling”, leading to activation of multiple inflammatory cytokines, including interferons (35–37). The TBK1/IRF3 axis is known to couple to the adaptor protein STING, a critical regulator of cytosolic double-stranded DNA detection mechanism (38–40), and whose activities are mostly independent of MAPK and canonical TLR mediators (20, 39, 41). Activation of STING induces TBK1 phosphorylation (20) which subsequently induces IRF3 or NF-κB to elicit the type I interferon response and a variety of pro-inflammatory genes including TNF, IL-6, and several chemokines (12, 20, 42).

Since Shambharkar *et al* (28) previously reported that TMEM203 is localised on ER membranes, and that our above data suggested that TMEM203 is closely related to chemokine expression and SLE disease indications, we hypothesised that TMEM203 may regulate STING-mediated signalling events. Therefore, a *Tmem203* overexpressing plasmid construct and siRNA against the individual STING signalling effectors were co-transfected into RAW 264.7 cells, followed by the measurement of *Cxcl2* promoter activities. As *Tmem203* overexpression resulted in elevated *Cxcl2* activity and the simultaneous suppression of *Sting* or its downstream regulators significantly reduced it (**Fig. 1H**), we concluded that TMEM203 potentially acts upstream or in parallel to a STING-dependent signalling pathway.

Figure 1: TMEM203 is an evolutionarily conserved, SLE associated signalling mediator.

1A. Alignment of TMEM203 orthologues: Vertebrate and invertebrate homologues of the mouse Tmem203 proteins were identified by BLAST search in the GenBank database. The collected sequences were aligned using the Clustal W algorithm. Four transmembrane regions (TM1-4) were predicted by TMpred (29). Abbreviations: H.h.: *Homo sapiens*, P.t.: *Pan trogloides*, M.m.: *Mus musculus*, G.g.: *Gallus gallus*, X.l.: *Xenopus laevis*, T.n.: *Tetraodon nigroviridis*, D.r.: *Danio rerio*, B.f.: *Branchiostoma floridae*, S.p.: *Strongylocentrotus purpuratus*, D.m.: *Drosophila melanogaster*, A.e.: *Aedes aegypti*, B. m.: *Bombyx mori*, C.c.: *Caligus clemensi*, L.s.: *Lepeophtheirus salmonis*, A.m.: *Apis mellifera*, C.f.: *Camponotus floridanus*, H.m.: *Hydra magnipapillata*, C.i.: *Cionia intestinalis*.

1B. C. TMEM203 level is elevated in a cohort of SLE patients. (B) MAVS, TMEM203 and STING mRNA levels in PHA-L -activated T cells were assessed by RT-qPCR from a cohort of treatment-naïve systemic erythematous lupus (SLE) patients in comparison to cells from healthy individuals. (C) Spearman correlation coefficient of C3 complement plasma level was assessed against fold TMEM203 mRNA induction in SLE patients (95% confidence interval: dash lines). Data is presented as mean ± SD, one dot per person.

1D. **Overexpression of Tmem203 augments LPS-induced Cxcl2 activation.** RAW 264.7 cells were transfected with the Cxcl2-pLuc and EF1-rLuc reporters, and with Tmem203 expression plasmid (dashed line) or empty control vector (solid line). Cells were stimulated with the stated concentration of LPS for 6 hours. Two-way ANOVA with Sidak correction was performed to ascertain the impact of Tmem203 overexpression on LPS induced cxcl2 activation (****: $p < 0.0001$). Data is presented as mean ± SEM, n=3.

1E. Knockdown of Tmem203 impairs LPS-induced Cxcl2 activation. RAW 264.7 cells were transfected with the Cxcl2-pLuc and EF1-rLuc reporters, and with siRNA against Tmem203 (dashed line) or non-targeting si-scrambled (solid line). Cells were stimulated with the stated concentration of LPS for 6 hours. Two-way ANOVA with Sidak correction was performed to ascertain the impact of siTmem203 treatment on LPS induced cxcl2 activation (**: $p<0.01$, ***: $p<0.001$). Data is presented as mean ± SEM, n=3.

1F. Dominant negative signalling molecules impair LPS-induced Cxcl2 promoter activity. RAW 264.7 cells were transfected with the Cxcl2-pLuc and EF1-rLuc reporters, and the indicated expression plasmids encoding for dominant negative (DN) mutants of known pro-inflammatory molecules (mouse Irak1, Trif, MyD88, Tram, Mal and Traf6, respectively). LPS (100 ng/ml, 6 hours) was used as a positive control to test for the inhibitory activity of the DN constructs. Data is presented as mean ± SD, n=2.

1G. Dominant negative signalling molecules fail to inhibit Tmem203 induced Cxcl2 promoter activity. RAW 264.7 cells were transfected as in F and the ability of the DN constructs to block overexpressed Tmem203 -induced Cxcl2 activation was tested. Data is presented as mean ± SD, n=2.

1H. Tmem203 induces Cxcl2 promoter via the Sting/Tbk1/Irf3 pathway. RAW 264.7 cells were transfected with the Cxcl2-pLuc, TK-rLuc reporters and Tmem203 expression plasmid, together with scrambled siRNA (siNC) or an siRNA against Irf3, Tbk1 or Sting. Data was analysed by one-way ANOVA ($p<0.05$: *, $p<0.01$: **, $p<0.001$: ***). Data is presented as mean ± SEM, n=3.

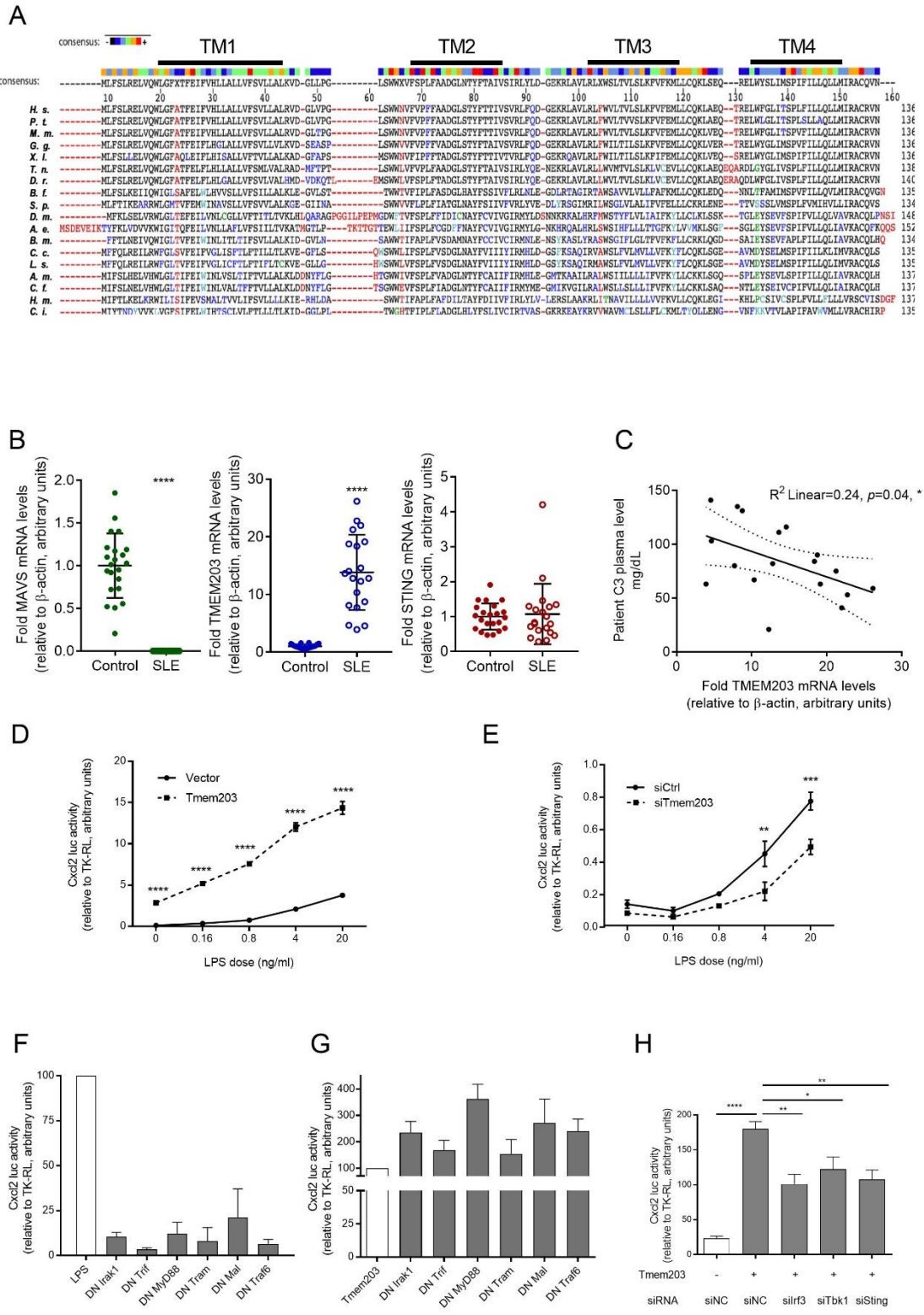
A
TM1
TM2
TM3
TM4
B
Fold MAVS mRNA levels (relative to β-actin, arbitrary units)
Fold TMEM203 mRNA levels (relative to β-actin, arbitrary units)
Fold STING mRNA levels (relative to β-actin, arbitrary units)
Control
SLE
C
R² Linear=0.24, p=0.04, *
Patient C3 plasma level mg/dL
Fold TMEM203 mRNA levels (relative to β-actin, arbitrary units)
D
Vector
Tmem203
Cxcl2 luc activity (relative to TK-RL, arbitrary units)
LPS dose (ng/ml)
E
siCtrl
siTmem203
Cxcl2 luc activity (relative to TK-RL, arbitrary units)
LPS dose (ng/ml)
F
Cxcl2 luc activity (relative to TK-RL, arbitrary units)
LPS
DN Irak1
DN Trif
DN MyD88
DN Tram
DN Mal
DN Traf6
G
Cxcl2 luc activity (relative to TK-RL, arbitrary units)
Tmem203
DN Irak1
DN Trif
DN MyD88
DN Tram
DN Mal
DN Traf6
H
Cxcl2 luc activity (relative to TK-RL, arbitrary units)
Tmem203
siRNA
siNC
siNC
siIrf3
siTbk1
siSting

TMEM203 co-localises and interacts with STING

To establish whether TMEM203 co-regulates STING, *Tmem203* expression levels were examined in mouse bone marrow-derived macrophages (isolated from C57/BL6 mice) after stimulation with LPS, endogenous STING ligand 2'3'-cGAMP (38) or microbial secreted STING ligand 3'3'-cGAMP (43). Each tested stimuli rapidly induced Tmem203 mRNA levels, albeit with different kinetics (**Fig. 2 A, B, C**).

Based on our observation that suppression of STING expression impaired TMEM203 induced *Cxcl2* activation (Fig. 1H) and that STING and TMEM203 are both localised in intracellular membranes (28, 44), we questioned whether STING and TMEM203 directly interact and co-regulate the activation of an inflammatory response. Co-localisation of STING and TMEM203 within punctate, intracellular structures was detected in HeLa cells co-transfected with GFP-Sting and mCherry-Tmem203, respectively (**Fig. 2D**). The observed interaction between TMEM203 and STING was further confirmed by co-immunoprecipitation of Myc-Sting and Flag-Tmem203 in HEK293T cells (**Fig. 2E**), indicating that a stable molecular complex is formed upon the contact of these two proteins.

To further validate the association of TMEM203 and STING, we used the Yellow Fluorescence Protein (YFP, Venus derivative) fragment complementation assay (PCA), which is based on expressing each putative binding partner in fusion with either the N-terminal (V1) or C-terminal (V2) portion of YFP (45–47) (**Fig. 2F**). When the two test proteins interact, the V1 and V2 parts of YFP fluorophore self-assembles in a cyclisation reaction which is essentially irreversible (48). This stable fluorescent signal can be detected by flow cytometry or fluorescence microscopy. We used this technique to ask whether TMEM203 and STING can interact intracellularly (**Fig. 2F**). As expected from the distribution of TMEM203 and STING alone, a punctate membrane / vesicular distribution of fluorescence was observed by confocal microscopy (**Fig. 2G**). Interestingly, a similar distribution of TMEM203 dimer (or oligomer) was also observed (**Fig. 2H**). As TMEM203 and STING are each predicted to contain four transmembrane domains, the positioning of the V1 or V2 PCA tags enabled us to map the relative orientation of the C- and N-termini of these proteins. In agreement with the proposed schematic model in **Fig. 2F**, TMEM203 and STING with either N-terminus and C-terminus tags were transfected into HEK293 cells and mean GFP signal was analysed by FACS. TMEM203 and STING can lead to the formation of a fluorescent complex (**Fig. 2I, 2nd & 3rd bar**), while a strong signal was also seen by TMEM203 dimerisation (**Fig. 2I, 4th bar**).

Figure 2. TMEM203 co-localises and interacts with STING.

2A. B. C. Tmem203 expression is transiently induced by inflammatory stimuli. Murine bone marrow-derived macrophages were stimulated with LPS (A), 2'3'-cGAMP (B) or 3'3'-cGAMP (C) for the time indicated. The expression of Tmem203 was determined by RT-qPCR. (Data is presented as mean ± SD for 2 independent experiments).

2D. Tmem203 co-localises with Sting. HeLa cells were co-transfected with Sting-GFP and mCherry-Tmem203 expression plasmids and their localisation was visualised by fluorescence microscopy under 63X magnification. n=15 images (total>30 cells) from 2 independent experiments were processed, a set of representative images is shown here.

2E. Tmem203 co-precipitates with Sting. HEK293 T cells were transfected with either empty vector, Flag-Tmem203 or Myc-Sting. Tmem203-containing complexes were immuno-precipitated (IP) using anti-Flag coated beads and blotted for Myc and Flag, as indicated. Lysates were also immunoblotted for Myc and Flag. Immunoblots (IB) shown are from a single experiment and are representative of two independent experiments.

2F. Illustration of Tmem203-Sting interaction by PCA. Tmem203 was tagged at its N terminus with the V1 fragment of Venus yellow fluorescent protein, whilst Sting was tagged at its N-terminus with the V2 Venus fragment to test for a molecular interaction between these proteins in live cells. Both Tmem203 and Sting proteins were predicted to encode for four transmembrane domains (28, 76). Thus, this arrangement was predicted to localise the V1 and V2 tags to the same side of the lipid membrane.

2G. H. Tmem203 and its complex with Sting is located in the cytoplasm, in perinuclear structures. HeLa cells were transfected with the above-described Venus fusion protein expression plasmids. The 'Venus' fluorescent signal, demonstrating TMEM203-STING interaction (G) or TMEM203 dimerisation (H) was visualised in live cells at 80X magnification, scale bar = 20 µm. Two experiments, 30 cells each.

2I. Tmem203 forms dimers and interacts with Sting in live cells. HEK293 T cells were co-transfected with the indicated fusion protein expression vectors; Venus fluorescence signal generated by Tmem203 and Sting interaction was detected by flow cytometry. Relative geometric mean fluorescence intensity was plotted compared to the control single transfection of V2 construct (V2_ZIP). Data is presented as mean ± SEM, n=4.

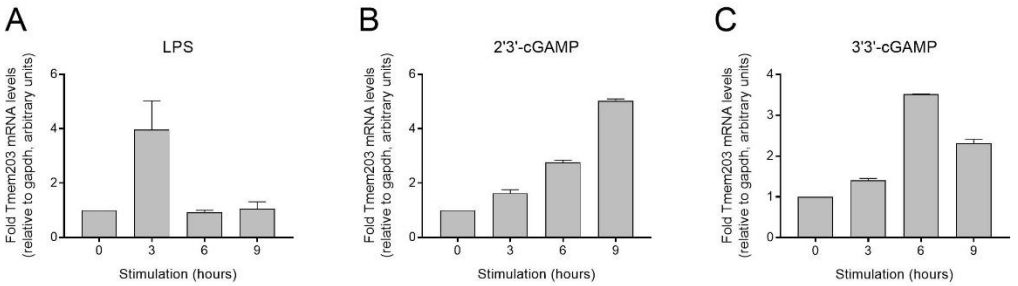
A
LPS
Fold Tmem203 mRNA levels (relative to gapdh, arbitrary units)
Stimulation (hours)
B
2'3'-cGAMP
Fold Tmem203 mRNA levels (relative to gapdh, arbitrary units)
Stimulation (hours)
C
3'3'-cGAMP
Fold Tmem203 mRNA levels (relative to gapdh, arbitrary units)
Stimulation (hours)

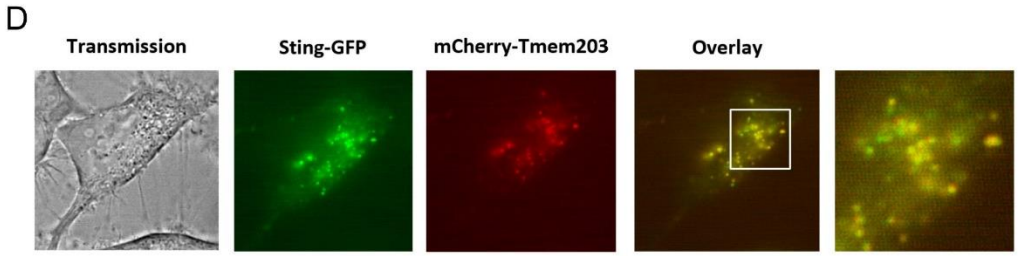
D
Transmission
Sting-GFP
mCherry-Tmem203
Overlay

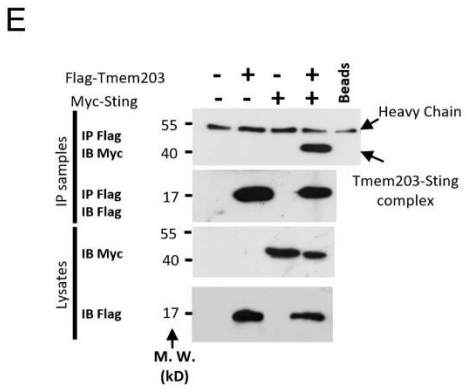
E
Flag-Tmem203
Myc-Sting
Beads
Heavy Chain
Tmem203-Sting complex
IP samples
IP Flag
IB Myc
IP Flag
IB Flag
Lysates
IB Myc
IB Flag
55
40
17
M. W. (kD)

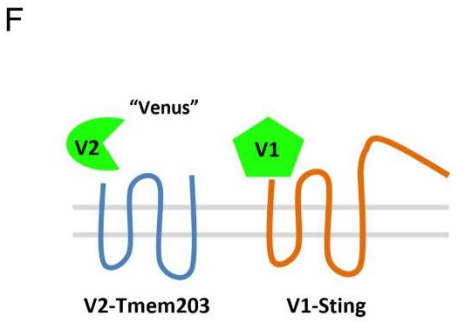
F
"Venus"
V2
V1
V2-Tmem203
V1-Sting

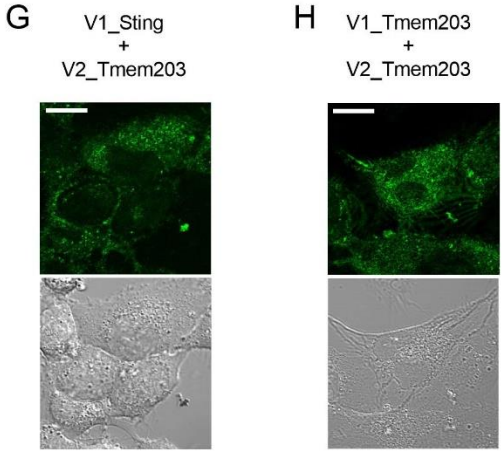
G
V1_Sting
+
V2_Tmem203
H
V1_Tmem203
+
V2_Tmem203

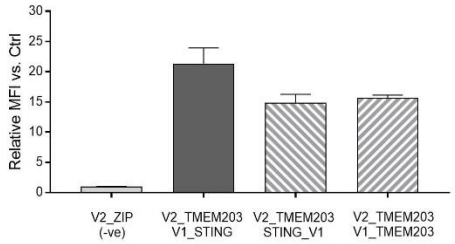
I
Relative MFI vs. Ctrl
V2_ZIP (-ve)
V2_TMEM203 V1_STING
V2_TMEM203 STING_V1
V2_TMEM203 V1_TMEM203

The TMEM203-STING complex is localised in the ER and lysosomes

To further study the localisation of TMEM203, HeLa cells were transiently transfected with mCherry-Tmem203. TMEM203 was predominantly found in perinuclear membrane structures in accordance with a previous report of ER localisation (**Fig. 3A**) (28)**.** Stimulation with LPS led to TMEM203 translocation to perinuclear, punctate membranes or vesicles (**Fig. 3A**). A more detailed analysis revealed a transient co-localisation between TMEM203 and the lysosomal marker LAMP1 at 30 mins stimulation with LPS in HeLa cells (**Fig. 3B**). This rapid ER-to-vesicle translocation of TMEM203 correlates with the kinetics of translocation seen for STING during activation (49). To study the localisation of the TMEM203-STING complex, we co-transfected the previously described Venus PCA constructs of these two proteins (**Fig. 2F**) into HeLa cells and co-stained with either cell permeable, lysosome- or ER- specific fluorescent dyes. The STING-TMEM203 complex was mainly expressed on lysosomal membranes rather than the ER (**Fig. 3C-E**), a distribution consistent with the previously described localisation pattern of activated STING (44). We therefore speculated that co-expression of TMEM203 and STING may pre-activate or sensitise the STING pathway, thus leading to a lysosomal translocation, even in the absence of ligands. In HeLa cells, which express lower levels of STING than the RAW 264.7 cells used in initial screening (26), overexpression of TMEM203 alone did not elevate proinflammatory activities, as measured by the activation of a previously described (50) luciferase reporter, but it augmented overexpressed STING-induced responses (**Fig. 3F)**. Constitutive overexpression of Tmem203 (**Fig 3 - S1**) in RAW 264.7 cells potentiated STING-ligand induced interferon activation **(Fig. 3G**). In summary, our data demonstrate that TMEM203 accompanies STING to transiently translocate to the lysosomes and that this co-expression sensitises cells to interferon and chemokine activation.

Figure 3. Inflammation induces TMEM203 trafficking and augments STING activity.

3A. LPS induced perinuclear translocation of Tmem203. HeLa cells were transfected with Tmem203-mCherry fusion protein expression plasmid and stimulated with 1 µg/ml LPS for the stated length of time. Two independent experiments, 20 cells each.

3B. Tmem203 transiently co-localises with LAMP1 in LPS induced cells. HeLa cells were transfected with Tmem203-mCherry fusion protein expression plasmid and stimulated with 1 µg/ml LPS for indicated time. LAMP1 localisation was visualised using Alexa Fluor® 488 conjugated anti-mouse secondary antibody. Images were taken under oil immersion at 63X magnification. Three independent experiments, 15 cells each.

3C-E. Co-expressed Sting – Tmem203 localises to lysosomes. HeLa cells were co-transfected with the V1_Sting WT and V2_Tmem203 WT prior to ER (C) or lysosome (D) staining; fluorescence signal was detected under confocal microscopy at 80X. Images are representative of two independent experiments. (E) Overlay of Tmem203-Sting signals and organelle signals were quantified with Fiji and co-localisation was calculated as the percentage of organelle with positive Tmem203-Sting detection. One dot per cell analysed from two independent experiments. Data is presented as mean ± SEM, scale bar = 20 µm.

3F. Tmem203 augments Sting induced IL-8 activation. HEK293 T cells were co-transfected with IFN-β reporter and plasmids expressing Sting, Tmem203, or controls. Data are expressed as fold change in reporter induction relative to the control plasmid, with (grey bars) or without (black bars) stimulation of DMXAA (100 µg/ml, 6 hrs). Data was analysed by 2-way ANOVA ($p<0.0001$: ****). Data is presented as mean ± SEM, n=3.

3G. Tmem203-overexpression augments Ifnb activation in RAW 264.7 cells. Vector or Tmem203 overexpression (OE Tmem203) transfected RAW 264.7 cells were stimulated with 3’3’-cGAMP for the time indicated. The expression of Tmem203 and Ifnb was determined by quantitative RT-qPCR. Data is presented as mean ± SD for 2 independent experiments.

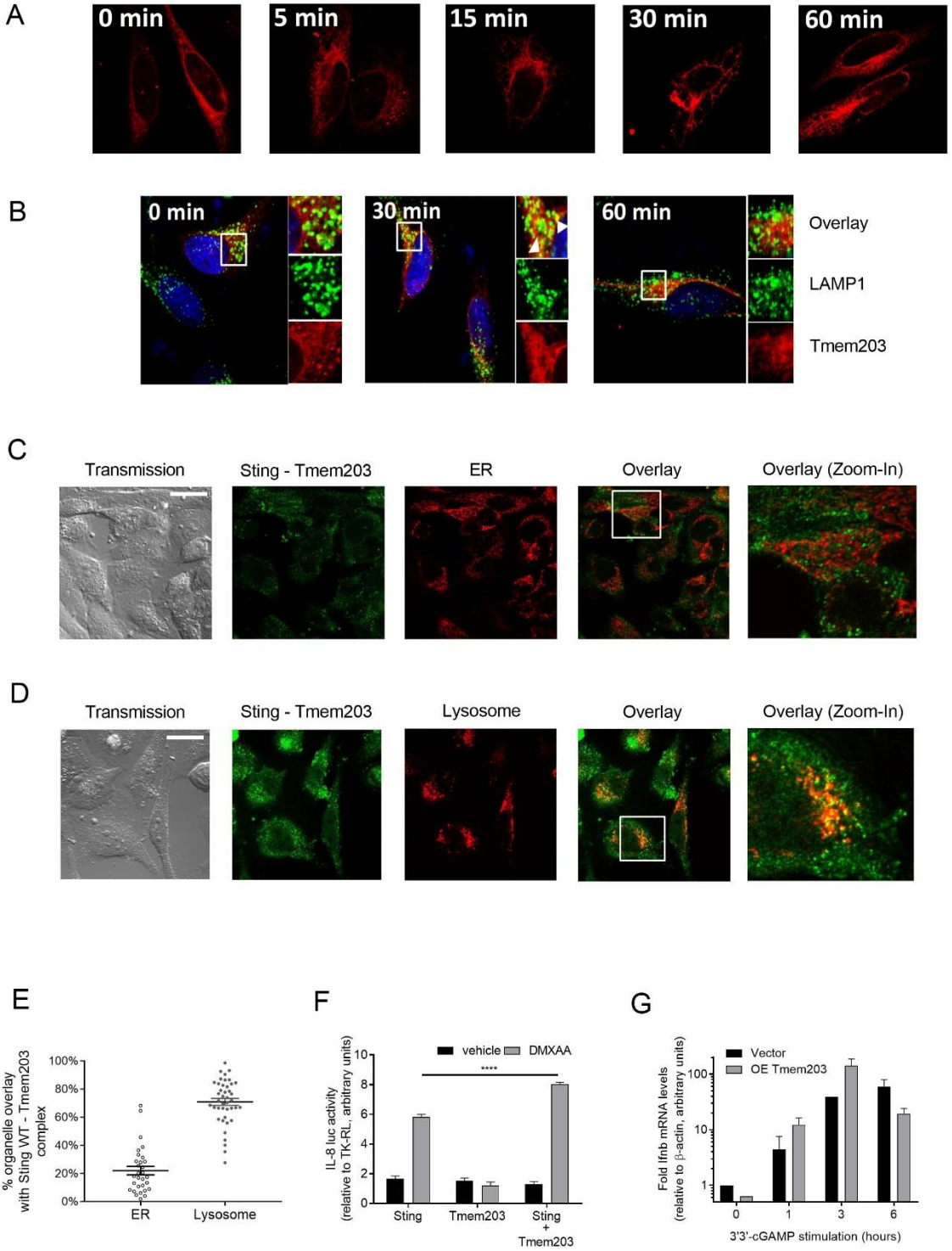
A
0 min
5 min
15 min
30 min
60 min
B
0 min
30 min
60 min
Overlay
LAMP1
Tmem203
C
Transmission
Sting - Tmem203
ER
Overlay
Overlay (Zoom-In)
D
Transmission
Sting - Tmem203
Lysosome
Overlay
Overlay (Zoom-In)
E
% organelle overlay with Sting WT - Tmem203 complex
100%
80%
60%
40%
20%
0%
ER
Lysosome
F
IL-8 luc activity (relative to TK-RL, arbitrary units)
vehicle
DMXAA
****
Sting
Tmem203
Sting + Tmem203
G
Fold Ifnb mRNA levels (relative to β-actin, arbitrary units)
Vector
OE Tmem203
3'3'-cGAMP stimulation (hours)

TMEM203 downregulation impairs cGAMP-induced STING-mediated type I interferon expression

STING predominantly mediates type I interferon activation in response to pathogen-associated cyclic-dinucleotide production in the cytoplasm (38–40, 51). Building on these findings, we investigated the importance of TMEM203 in mediating STING activation in human monocyte-derived macrophages (MDMs). CD14 positive human monocytes (**Fig. S2 A**) were isolated from whole blood and differentiated into MDMs (**Fig. S2 B**) by M-CSF. MDMs were transfected with control or TMEM203 targeting siRNA, followed by a 3-hour stimulation of these cells with 2'3'-cGAMP or 3'3'-cGAMP, 48 hours post-transfection. RT-qPCR analysis of TMEM203 mRNA levels confirmed a highly robust (>70%) knockdown in siTMEM203-targeted MDMs (**Fig. 4A & 4B**), which was accompanied by a significant inhibition of cGAMP-induced IFN-I expression in human MDM samples obtained from a cohort of healthy individuals (**Fig. 4C & 4D, IFN-β**). Whilst the amount of IFN-β mRNA produced in these samples showed donor-specific variation upon ligand stimulation (**Fig. S2 C&D**), siTMEM203 treatment in each case reduced 2'3'-cGAMP and 3'3'-cGAMP -induced IFN-β mRNA levels by approx. 50% (**Fig. 4C & 4D**). In contrast, *IL-8* mRNA was not induced under both stimulation conditions (0-3 fold, depending on the specific donor or MDM isolation, not shown); although its levels were also reduced by *TMEM203* suppression in response to 2'3'-cGAMP treatment (**Fig. 4C**).

To expand on the above findings from primary human macrophages, we investigated whether TMEM203 displays similar STING regulatory behaviour in mouse macrophages. siRNA knockdown of *Tmem203* or *Sting* was performed in immortalised bone marrow-derived macrophages (iBMDMs) followed by 3 h stimulation with the physiological STING ligand 2'3'-cGAMP or the synthetic ligand DMXAA (52, 53), that selectively targets the mouse but not the human protein. Efficient suppression of both *Tmem203* and *Sting* was confirmed by RT-qPCR analysis (**Fig. 4E-F**). Similarly to MDMs, 2'3'-cGAMP robustly induced IFN-I expression in iBMDMs (**Fig. S2 E**) and this was impaired by *Tmem203* or *Sting* knockdown (**Fig. 4G**). However, IFN-I induction by DMXAA was only reduced by the knockdown of *Sting* but not *Tmem203* (**Fig. 4G**), suggesting that *Tmem203* regulation of *Sting* may be ligand dependent. To further test this, we used primary bone marrow-derived macrophages (BMDMs) isolated from WT or CRISPR-Cas9 –targeted *Tmem203* knockout mice (**Fig. S2 F**) and stimulated them with DMXAA or 2'3'-cGAMP. In controls, both STING ligands induced a marked *Ifnb1* upregulation (**Fig. S2 G**), but only 2'3'-cGAMP and not DMXAA -mediated *Ifnb1* expression was reduced by *Tmem203* deficiency (**Fig. 4H**). From the above data we conclude that TMEM203 is a critical regulator of STING-induced type I interferon production and that its suppression impedes this process in response to specific STING ligands.

Figure 4. TMEM203 downregulation impairs cGAMP-induced STING-mediated type I interferon expression.

4A. B. Efficient TMEM203 knockdown in human monocyte derived macrophages (MDMs). MDMs were transiently transfected by scrambled control (siCtrl) or TMEM203 targeting siRNA. Post transfection, MDMs were left stimulated with +/- 4 µg/ml 2'3'-cGAMP (A) or 1 µg/ml 3'3'-cGAMP (B) for 3 hours. TMEM203 knockdown was quantified by RT-qPCR. Multiple Student's t-tests with Holm-Sidak corrections were performed to ascertain the impact of siTMEM203 treatment on TMEM203 mRNA levels ($p < 0.0001$: ****). Data is presented as mean ± SEM, n=10 (A) and n=4 (B).

4C. D. TMEM203 knockdown impairs 2'3'-cGAMP (C) and 3'3'-cGAMP (D) induced IFN-β production in MDMs. 2'3'-cGAMP (4 µg/ml) or 3'3'-cGAMP (1 µg/ml) –stimulated (3h) IFN-β production of siCtrl vs. siTMEM203 transfected MDMs from 4 donors was compared by normalizing IFN-β levels of siTMEM203 treated cells to the siCtrl treatment for each individual. Student's t-test was performed to ascertain the impact of siTMEM203 treatment ($p < 0.01$: **, $p < 0.001$: ***, $p < 0.0001$: ****). Data is presented as mean ± SEM, n=4.

4E. F. Efficient Tmem203 (E) and Sting (F) knockdown in immortalised mouse bone marrow-derived macrophages (iBMDMs). iBMDMs were transiently transfected by scrambled control (siCtrl), Tmem203, or Sting targeting siRNA. Post transfection, cells were left stimulated with +/- 25 µg/ml DMXAA or 20 µg/ml 2'3'-cGAMP for 3 hours. Tmem203 and Sting knockdown was quantified by RT-qPCR. Multiple Student's t-tests with Holm-Sidak corrections were performed to ascertain the impact of siTmem203 and siSting treatment on Tmem203 and Sting mRNA levels, respectively ($p < 0.01$: **, $p < 0.0001$: ****). Data is presented as mean ± SEM, n=4.

4G. 2'3'-cGAMP, but not DMXAA, -induced Ifnb1 expression is impaired by Tmem203 knockdown in iBMDMs. IFN-β induction by DMXAA (25 µg/ml) or 2'3'-cGAMP (20 µg/ml) stimulation (3h) in the siTmem203 or siSting transfected iBMDMs was compared to that in the siCtrl treated cells. One-way ANOVA test was performed to ascertain the impact of siTmem203 / siSting treatment on Ifnb1 mRNA levels compared to the siCtrl group ($p < 0.05$: *, $p < 0.001$: ***, $p < 0.0001$: ****). Data is presented as mean ± SEM, n=4.

4H. **2'3'-cGAMP, but not DMXAA, -induced Ifnb1 expression is impaired by Tmem203 knockout in bone marrow-derived macrophages (BMDMs).** BMDMs derived from WT or Tmem203 knockout C57BL/6 mice were stimulated with DMXAA (50 µg/ml) or 2'3'-cGAMP (10 µg/ml) for 3 h before Ifnb1 expression levels were analysed by RT-qPCR. Multiple Student's t-tests with Holm-Sidak corrections were performed to ascertain the impact of

Tmem203 knockout on IFN-β mRNA levels (p <0.05: *, one dot per mouse). Data is presented as mean ± SEM, n=6

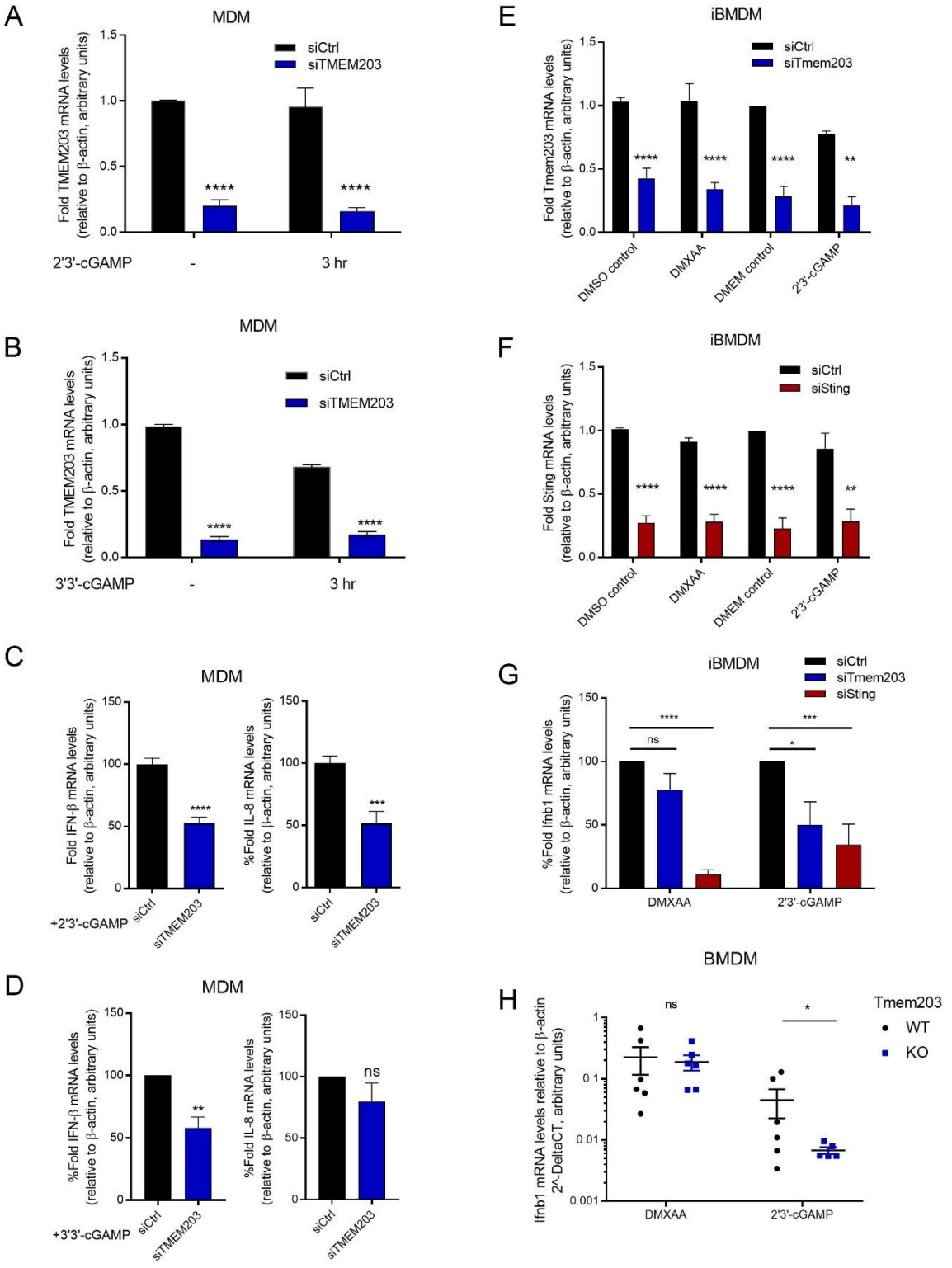

TMEM203 levels regulate TBK1/IRF3 activation downstream of STING

To further characterise the functional contribution of TMEM203 to cGAMP-induced STING signalling events, activation of TBK1 and IRF3 were compared between control and TMEM203-overexpressing or knockout RAW 264.7 cells. Each of these signalling molecules have previously been shown to be phosphorylated (and thus activated) in a STING-dependent manner, including responses to cytosolic dsDNA sensing (20, 54). Whilst CRISPR/Cas9-mediated *Tmem203* knockout in RAW 264.7 cells (**Fig. S3 A**) resulted in an impaired Tbk1/Irf3 phosphorylation (**Fig. 5A**), *Tmem203* overexpression (**Fig. S3 B**) augmented Tbk1/Irf3 activation after 3'3'-cGAMP stimulation (**Fig. 5B**). Similar TMEM203-dependent changes were seen in these cells after human simplex virus-1 (HSV-1) infection (**Fig. 5C**), a dsDNA virus known to activate the STING/TBK1/IRF3 signalling axis (55–58). Considering that the phosphorylation level of Tbk1 and Ifr3 only signatures the initiation of type I interferon expressions, we further quantify Sting activation by analysing Ifnb1 secretion level in the Tmem203 overexpressing and knockout cells. Consistently, HSV-1 stimulated Ifnb1 secretion is enhanced in *Tmem203* overexpressing cells (**Fig. 5D right**) while it is impaired in *Tmem203* knockout cells (**Fig. 5D left**), confirming the functional significance of Tmem203 in the regulation of STING-interferon signalling.

Finally, we analysed IRF3 activation downstream of STING by measuring the nuclear localisation of IRF3 in control and *Tmem203*-overexpressing macrophages. Activated STING induces TBK1-IRF3 activation leading to nuclear translocation of IRF3 that is critical for the initiation of transcription of the type I interferon genes (20). Elevated *Tmem203* expression in RAW 264.7 cells indeed led to an enhanced, 3'3'-cGAMP induced IRF3 nuclear localisation (**Fig. 5E & 5F**) in line with the timeframe observed for IRF phosphorylation (**Fig. 5B**).

Figure 5: TMEM203 level regulates TBK1/IRF3 activation downstream of STING.

5A. CRISPR/Cas9-mediated Tmem203 knockout resulted in reduced TBK1 and IRF3 phosphorylation upon STING stimulation. Vector or CRISPR/Cas9-mediated Tmem203 knockout (KO Tmem203) RAW 264.7 cells were stimulated with 3'3'-cGAMP (1 µg/ml) for the time indicated. Activation of Tbk1 and Irf3 was examined by western blot analysis. Membranes were blotted with anti-phospho-Tbk1 (-Tbk1), anti-total Tbk1 (tTbk1), anti-phospho-Irf3 (p-Irf3) and anti-total Irf3 (t-Irf3) as indicated (n=3).

5B. Increased TBK1-IRF3 activation in Tmem203-overexpressing RAW 264.7 cells in response to STING stimulation. Vector- or Tmem203-overexpressing (OE Tmem203) RAW 264.7 cells were stimulated with 3'3'-cGAMP (1 µg/ml) for the time indicated. Activation of Tbk1 and Irf3 was examined by western blot analysis. Membranes were blotted with anti-phospho-Tbk1 (-Tbk1), anti-total Tbk1 (tTbk1), anti-phospho-Irf3 (p-Irf3) and anti-total Irf3 (t-Irf3) as indicated (n=3).

5C. Increased TBK1-IRF3 activation in Tmem203-overexpressing RAW 264.7 cells in response to HSV infection. Vector- or Tmem203-overexpressing RAW 264.7 cells were infected with HSV-1 for the time indicated. Activation of Tbk1 and Irf3 was examined by western blot analysis. Membranes were blotted with anti-phospho-Tbk1 (-Tbk1), anti-total Tbk1 (tTbk1), anti-phospho-Irf3 (p-Irf3) and anti-total Irf3 (t-Irf3) as indicated (n=3). MOI=0.2.

5D. Ifnb cytokine secretion is impaired in Tmem203 knockout RAW 264.7 cells (left) and is enhanced in Tmem203-overexpressing cells (right) in response to HSV infection. CRISPR/Cas9-mediated Tmem203 knockout (or Vector) and Tmem203-overexpressing (or Vector) RAW 264.7 cells were infected with HSV-1 for 6 hours and Ifnb1 secretion was measured by ELISA. Data is presented as mean ± SEM, n=3.

5E & F. Tmem203 overexpression enhances IRF3 nuclear accumulation in macrophages in response to STING stimulation. Vector- and Tmem203-overexpressing RAW 264.7 cells were stimulated with 1 µg/ml 3'3'-cGAMP for 6 hours. Subcellular localization of Irf3 was determined by Irf3 intracellular staining, and confocal fluorescence images were captured (F). Scale bar is 10 µm. Average Irf3 nuclear fluorescence intensity of 50-200 cells was quantified using ImageJ (F). Data is presented as mean ± SEM.

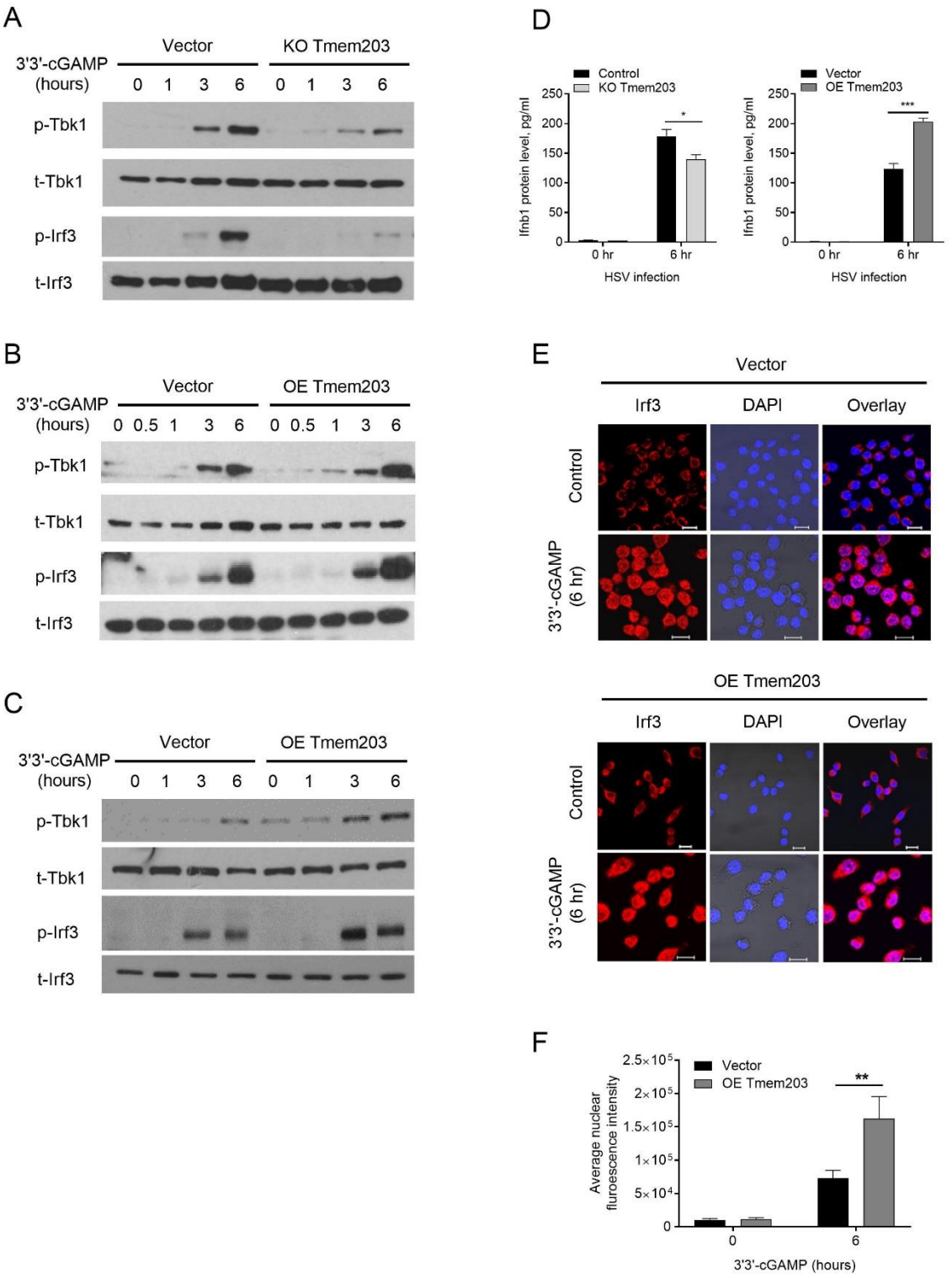
A
Vector
KO Tmem203
3'3'-cGAMP
(hours)
0 1 3 6 0 1 3 6
p-Tbk1
t-Tbk1
p-Irf3
t-Irf3
B
Vector
OE Tmem203
3'3'-cGAMP
(hours)
0 0.5 1 3 6 0 0.5 1 3 6
p-Tbk1
t-Tbk1
p-Irf3
t-Irf3
C
Vector
OE Tmem203
3'3'-cGAMP
(hours)
0 1 3 6 0 1 3 6
p-Tbk1
t-Tbk1
p-Irf3
t-Irf3
D
Control
KO Tmem203
Ifnb1 protein level, pg/ml
250
200
150
100
50
0
*
0 hr
6 hr
HSV infection
Vector
OE Tmem203
Ifnb1 protein level, pg/ml
250
200
150
100
50
0
***
0 hr
6 hr
HSV infection
E
Vector
Irf3
DAPI
Overlay
Control
3'3'-cGAMP
(6 hr)
OE Tmem203
Irf3
DAPI
Overlay
Control
3'3'-cGAMP
(6 hr)
F
Vector
OE Tmem203
**
Average nuclear
fluroescence intensity
2.5×10^5
2×10^5
1.5×10^5
1×10^5
5×10^4
0
0
6
3'3'-cGAMP (hours)

Transmembrane domains of STING are required for the formation of its complex with TMEM203

Having demonstrated the functional significance of TMEM203-mediated regulation of STING, we sought to further explore the mechanisms by which these two proteins interact and investigate the underlying mechanisms of selective TMEM203-mediated regulation of STING activation. Since TMEM203 regulates cGAMP-, but not DMXAA-induced STING activation in macrophages, we proposed that these ligands may differentially influence the physical contact between TMEM203 and STING. We established the Renilla fragment complementation assay (Renilla PCA), which is based on expressing Tmem203 or Sting in fusion with either the small part (1.1) or the large part (2.1) of an engineered Renilla luciferase, NanoBit (**Fig. 6A**). The association of TMEM203 and STING causes a reversible assembly of Renilla formation, which then catalyses the breakdown of a luciferase substrate. A robust interaction between TMEM203 and STING was observed upon co-transfecting the Renilla PCA fusion constructs, and their strong association was demonstrated by comparison to the Rel A-IκBa complex which has been reported to form a stable complex in resting cells (**Fig. 6B**). Next, we co-expressed 2.1 N Sting and 1.1 C Tmem203 in HEK293 T cells that were stimulated with either 2'3'-cGAMP or DMXAA. We detected a rapid, time-dependent reduction of the TMEM203-STING complex following cGAMP treatment, in contrast to an enhanced association of these proteins upon DMXAA treatment (**Fig. 6C**). This opposing effect of the two STING ligands on STING-TMEM203 association is likely to underlie the differential regulation of STING signalling by TMEM203 as demonstrated in BMDMs (**Fig. 4G & H**). The different association of TMEM203-STING by the two ligands may potentially affect the binding of STING's signalling effector TBK1 to this complex. However, further experiments are required to understand the mechanism of this opposite structural change and how it reflects on immune regulation of STING-TMEM203 complex.

TMEM203 is a 136 amino acid transmembrane protein with no obvious regulatory domains at the exposed short cytoplasmic regions. The protein sequence is highly conserved across vertebrates with only a three amino acid difference in the sequence between the human and the mouse genes (28) (**Fig. 1A**). Thus, we speculated that the interaction between STING and TMEM203 is likely to be coordinated by STING, which contains complex regulatory domains. Although human and mouse STING are only 81% similar in primary sequence and 68% similar in amino acid composition (13), functional domains in STING are nonetheless spatially and structurally conserved across the two species. Previous studies on the structure of STING have identified the C-terminal cytoplasmic domain as the site for protein-protein interactions and ligand binding, whereas the N-terminal transmembrane (TM) domains are mainly thought

to be responsible for membrane anchorage (59). The cytoplasmic region of STING (approximately amino acids 153-378 in mouse) comprises of three domains: the dimerization domain (DD) (or helices α-5/α-6) formed by amino acids ~155-180; the cyclic dinucleotide binding domain (CBD) formed by amino acids ~153-340; and the cytoplasmic-terminal tail domain (CTT) formed by amino acids ~340-378 (amino acids ~340-379 in human) (4, 60). The CTT is involved in TBK1 / IRF3 binding and activation and is essential for type I interferon induction (20). To identify the molecular domains of STING required for its interaction with TMEM203, we created mutant Sting constructs that contain deletions of TM, CBD, or the CTT domain (**Fig. 6D**). Co-immunoprecipitation of HA-tagged WT or mutant Sting with Flag-Tmem203 from HEK293 T lysates showed that the STING – TMEM203 complex is formed in the presence of STING's TM domains (**Fig. 6E, lines 1-3, 5)**, whereas the presence of CBD alone led to a very weak STING – TMEM203 interaction (**Fig. 6E, lines 4, 6**).

To substantiate these findings, 141A, 184L, 243V and 344A Sting truncations were created (**Fig. 6F**), expressing TM domains only (TM), TM and dimerisation domain (TM+DD), a disrupted cyclic dinucleotide binding domain (d-CBD), or CTT deleted STING (ΔCTT), respectively. Both the mutant and WT Sting were fused with the YFP expression plasmids and their expression was tested by Western blot. Compared to the WT Sting, TM and ΔCTT mutants (**Fig. 6G, line 3 & 6**) showed enhanced protein expression whereas the TM+DD and d-CBD mutants showed reduced expression (**Fig. 6G, line 4-5**). Next, we fused the mutants and WT Sting with V1 fragment of the previously described split YFP (**Fig. 2F**) which were co-transfected with the complementary V2-tagged Tmem203 expression plasmid into HEK293 T cells; fluorescent signal was quantified by flow cytometry (**Fig. 6H**). To ensure the overexpression of Tmem203 or Sting does not induce a non-specific ER stress response (61), the level of spliced XBP1 gene was assessed in HEK293 T cells, transfected with pcDNA3.1(control) or Tmem203 - Sting PCA constructs. No significant increase of XBP1 splicing was detected by RT-qPCR in Tmem203 and Sting expressing cells (**Fig. S4 A-C**). Compared to the WT Tmem203 – WT Sting interaction, a stronger protein interaction was observed between Tmem203 and Sting TM, TM+DD, and ΔCTT, respectively (**Fig. 6F**). However, d-CBD Sting showed an impaired interaction with Tmem203 due to reduced protein expression levels (**Fig. 6F & 6G, d-CBD**), potentially caused by degradation of dysfunctional Sting protein. Of note, while the enhanced interaction between Tmem203 and Sting TM mutant was paralleled with high expression of this truncated Sting protein, the TM+DD mutant exhibited similar association at a much lower Sting protein expression level (**Fig. 6F & 6G, TM+DD**). Furthermore, the Tmem203 – Sting TM complex showed a more equal localisation between the ER and lysosomes (**Fig. 7 A-C**), compared to the Tmem203 – WT Sting complex (**Fig. 3 C-E**), likely due to the loss of STING's regulatory site for post-translational modification

required to direct its trafficking. This also suggests that TMEM203 may rely on STING to relocate from the ER to other intracellular structures. Therefore, we conclude that interaction with TMEM203 is dependent on the N-terminal transmembrane domain of STING and its dimerisation domain is potentially a significant regulator of their interaction.

Figure 6: Molecular determinants of Tmem203-Sting complex formation.

6A. Detection of Tmem203-Sting interaction by Renilla PCA. Tmem203 was tagged at its C terminus with the 1.1 (small) fragment of Renilla luciferase reporter, whilst Sting was tagged at its N-terminus with the 2.1 (large) Renilla fragment to test for a molecular interaction between these proteins in live cells.

6B. Tmem203 and Sting interact in live cells. HEK293 T cells were co-transfected with the indicated fusion protein expression vectors; Renilla luciferase signal was detected by Nano-Glo live cell luciferase assay. Relative luminescence intensity was plotted compared to the negative control transfection of Nano-BIT construct. Data is presented as mean ± SEM, n=3.

6C. Tmem203-Sting interaction is differentially regulated by DMXAA and 2'3'-cGAMP. TMEM203 and STING were tagged at its N terminus with the 1.1 and 2.1 fragment of Renilla luciferase, respectively, to test for a molecular interaction between these proteins in live cells (upper). Tmem203 and Sting were transfected into HEK293 T cells for 24 h and were then stimulated with DMXAA (50 µg/ml) and 2'3'-cGAMP (10 µg/ml) for the indicated time. Relative luciferase activity was assessed according to Hoechst (cell numbers) and calculated relative to early 2.5 stimulation time point. Data is presented as mean ± SEM, n=4.

6D. E. Tmem203 co-precipitates with Sting N terminal transmembrane region. (D) WT and five mutant Sting constructs were created as indicated and fused with HA tags. WT Sting, aa 1-378; TM = transmembrane domain, aa 1-153; ΔCTT = Sting without cytoplasmic tail, aa 1-340; ΔTM = Sting without transmembrane domain, aa 147-378; ΔCBD = Sting without cyclic-dinucleotide binding domain (CBD), aa 1-153 & 340-378; CBD = CBD domain of Sting, aa 147-340. (E) HEK293 T cells were transfected with either empty vector, Flag-Tmem203 or HA-Sting (WT / mutants). Tmem203-containing complexes were immuno-precipitated (IP) using anti-Flag coated beads and blotted for Flag and HA, as indicated. Lysates were also immunoblotted (IB) for Flag and HA. Immunoblots shown are from a single experiment and are representative of two independent experiments.

6F. Sting truncation mutants. 4 serial truncation mutants were individually created on the WT Sting after the N-terminal transmembrane domains (TM), after the dimerisation domain (TM+DD), inside the cyclic dinucleotide binding domain (d-CBD), and before the C-terminal cytoplasmic terminal tail (ΔCTT).

6G. C-terminal truncations alter Sting protein expression. HEK293 T cells were transfected with the YFP fusion vectors expressing Sting WT and mutants as indicated. YFP-Sting protein levels were examined by western blot analysis. Membranes were blotted with

anti-GFP and anti-PDHX (housekeeper) as indicated. Relative expressions of mutant Sting were compared to the WT expression. Data is presented as mean ± SEM, n=5.

6H. Tmem203-Sting association is not eliminated by C-terminal truncations of Sting. HEK293 T cells were co-transfected with the Tmem203 and Sting WT/mutants cloned into the Venus vector system as described in Figure 2F; Venus fluorescence signal was detected by flow cytometry. Relative mean fluorescence intensity was plotted compared to the control Sting WT – Tmem203 interaction. Data is presented as mean ± SEM, n=4-7.

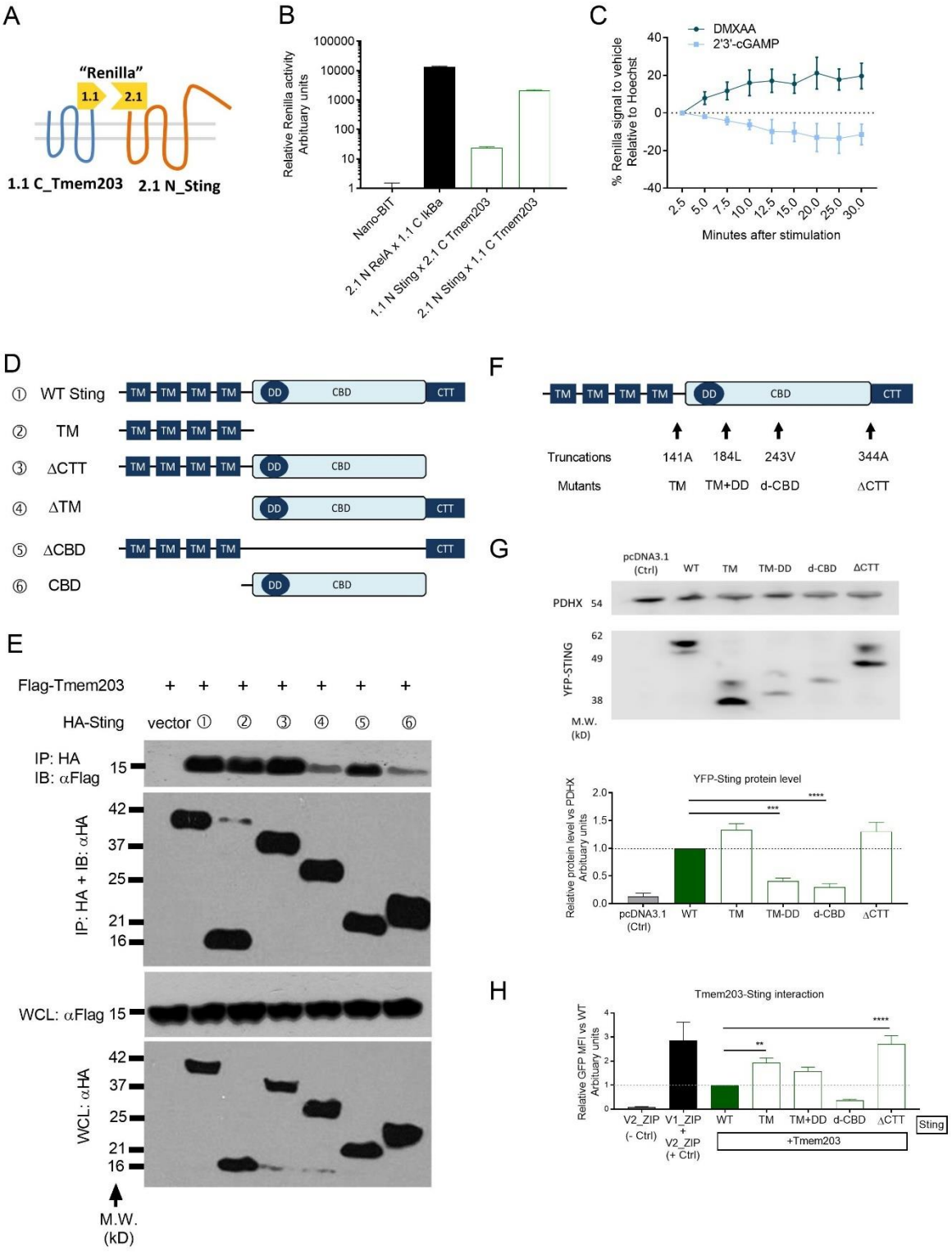
A
"Renilla"
1.1
2.1
1.1 C_Tmem203
2.1 N_Sting
B
Relative Renilla activity
Arbituary units
100000
10000
1000
100
10
1
Nano-BIT
2.1 N RelA x 1.1 C IkBa
1.1 N Sting x 2.1 C Tmem203
2.1 N Sting x 1.1 C Tmem203
C
DMXAA
2'3'-cGAMP
% Renilla signal to vehicle
Relative to Hoechst
40
20
0
-20
-40
2.5
5.0
7.5
10.0
12.5
15.0
20.0
25.0
30.0
Minutes after stimulation
D
① WT Sting
② TM
③ ΔCTT
④ ΔTM
⑤ ΔCBD
⑥ CBD
TM
DD
CBD
CTT
F
Truncations
141A
184L
243V
344A
Mutants
TM
TM+DD
d-CBD
ΔCTT
E
Flag-Tmem203
HA-Sting
vector
IP: HA
IB: αFlag
IP: HA + IB: αHA
WCL: αFlag
WCL: αHA
M.W.
(kD)
G
pcDNA3.1
(Ctrl)
WT
TM
TM-DD
d-CBD
ΔCTT
PDHX
YFP-STING
M.W.
(kD)
YFP-Sting protein level
Relative protein level vs PDHX
Arbituary units
H
Tmem203-Sting interaction
Relative GFP MFI vs WT
Arbituary units
V2_ZIP
(- Ctrl)
V1_ZIP
+
V2_ZIP
(+ Ctrl)
Sting
+Tmem203

Figure 7: C-terminal region of STING is required for preferential localisation of the STING-TMEM203 complex to the lysosome.

7A-C. Localisation of TM Sting – WT Tmem203. HeLa cells were co-transfected with the V1_TM Sting and V2_WT Tmem203 prior to ER (A) or lysosome (B) staining; fluorescence signal was detected under confocal microscopy at 80X. Images are representative of two independent experiments. (C) Overlay of Tmem203-Sting signals and organelle signals were quantified with Fiji and co-localisation was calculated as the percentage of organelle with positive Tmem203-Sting detection. One dot per cell analysed from two independent experiments. Data is presented as mean ± SEM, scale bar = 20 µm.

7D: Proposed molecular model for TMEM203 action. In the absence of immune stimuli, the type I interferon promoter has no transcriptional activity. Pathogen-released 3'3'-cGAMP or cGAS-produced 2'3'-cGAMP can induce the canonical STING pathway, resulting in TBK1-IRF3 interaction and subsequent type I interferon expression. Internalised LPS-bound TLR4 activates the "late signalling" events which induce TMEM203-STING interaction in the ER, leading to STING-TBK1-IRF3 activation and type I interferon expression. CDN = cyclic dinucleotide; cGAMP = cyclic GMP-AMP; cGAS = cyclic GMP-AMP synthase; ER = endoplasmic reticulum; IRF3 = interferon regulatory factor 3; LPS = lipopolysaccharide; STING = Stimulator of Interferon Genes; TLR4 = Toll-like receptor 4; TBK1 = TANK binding kinase; TMEM203 = transmembrane protein 203.

A

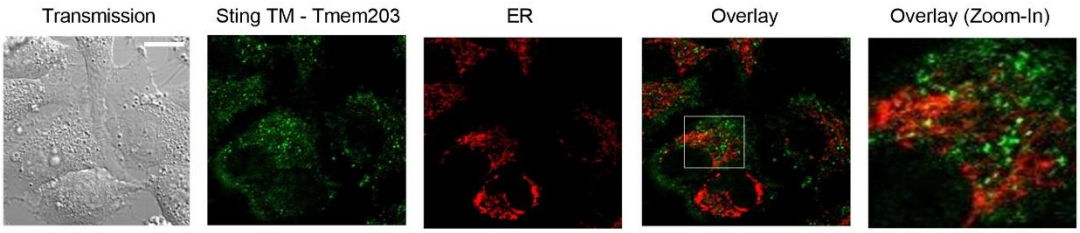
Transmission
Sting TM - Tmem203
ER
Overlay
Overlay (Zoom-In)

B

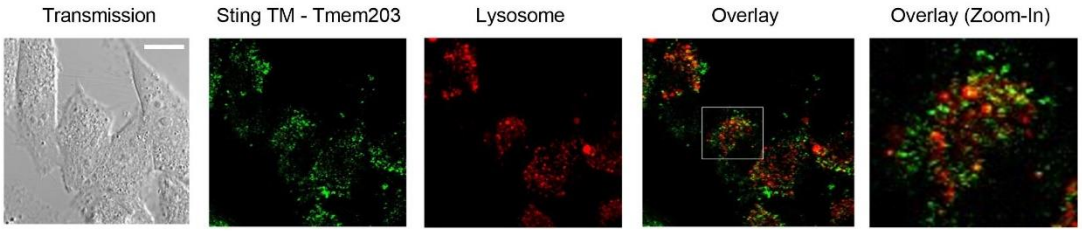
Transmission
Sting TM - Tmem203
Lysosome
Overlay
Overlay (Zoom-In)

C

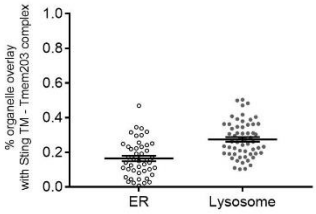
% organelle overlay
with Sting TM - Tmem203 complex
1.0
0.8
0.6
0.4
0.2
0.0
ER
Lysosome

D

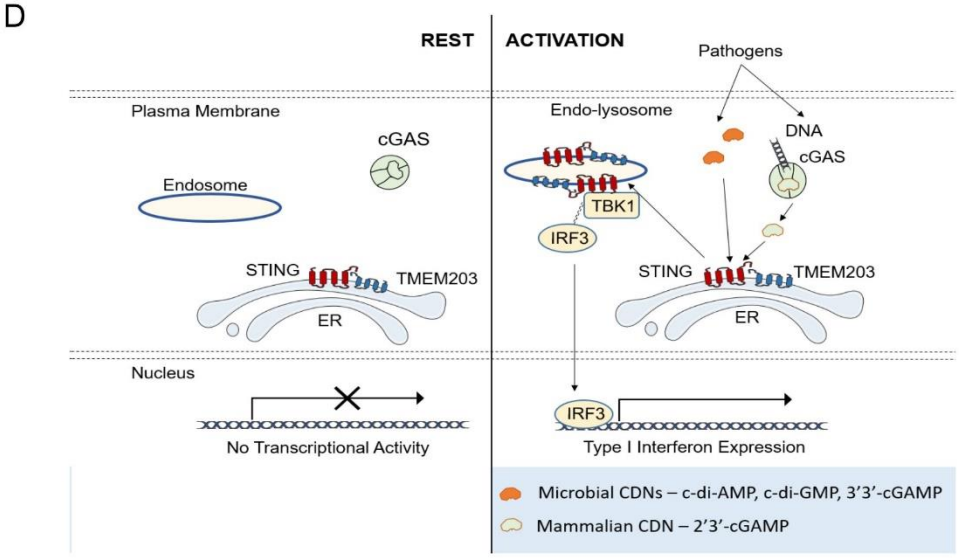
REST
ACTIVATION
Pathogens
Plasma Membrane
Endo-lysosome
DNA
cGAS
cGAS
Endosome
TBK1
IRF3
STING
TMEM203
STING
TMEM203
ER
ER
Nucleus
IRF3
No Transcriptional Activity
Type I Interferon Expression
Microbial CDNs – c-di-AMP, c-di-GMP, 3'3'-cGAMP
Mammalian CDN – 2'3'-cGAMP

Discussion:

In this study, we show that a novel inflammatory regulator, TMEM203 forms part of a functional signalling complex with STING, thus regulating the activity of the effector kinase TBK1 and the transcription factor IRF3, leading to activation of type I interferon expression. TMEM203 acts independently of the canonical PRR systems and the STING/TMEM203 complex localises in cytoplasmic punctate membranes. Our experiments aiming to further dissect the underlying molecular mechanisms in human and mouse macrophages revealed that TMEM203 regulates STING in a ligand-dependent manner. Upon STING activation by cyclic dinucleotides and HSV-1 but not by DMXAA, TMEM203 promotes the activation of TBK1 and IRF3. Finally, our data on different truncated forms of STING reveal that its N-terminal transmembrane domain itself is sufficient to form a complex with TMEM203 and that this interaction is regulated by the α-helix / dimerisation domain on STING. Supported by the mechanistic studies presented here, we propose a model (**Fig. 7D**) by which TMEM203-STING acts and promotes the TBK1-IRF3-interferon activation.

Whilst detailed structural studies will be required to shed light on the exact molecular mechanisms by which TMEM203 regulates STING activity, our data demonstrates the first time the important role for TMEM203 in ligand-dependent STING activation. In three primary and established macrophage systems, immuno-stimulation by cGAMP was impeded by the reduction/loss of TMEM203, whilst DMXAA induced IFN-β expression only changed in parallel to Sting but not Tmem203 RNA levels. The mouse-specific ligand DMXAA binds to STING via mechanisms similar to cGAMP but different amino acids are involved. Point mutations of hSTING S162A and E260I render it sensitive to DMXAA (64, 65). Upon ligand binding, STING dimer switches from an open-inactive to a close-active conformation, the binding pocket being much tighter in the presence of 2’3’-cGAMP versus DMXAA (64). This model is further supported by our finding that DMXAA strengthens TMEM203-STING association while cGAMP weakens it.

Our data also highlights the role for TMEM203 in directing STING between intracellular compartments. Whilst TMEM203 overexpression alone did not strongly enhance type I interferon expression in the mechanistic studies presented here, it has nevertheless promoted vesicular translocation of STING and its downstream IFN-β transcriptional activities. Recent literature suggests that the N-terminal of STING is indispensable for its translocation from the ER to other membranes during stimulation (59). Thus, the association of this domain with TMEM203 may provide a mechanistic explanation for the importance of this STING domain.

Host innate immunity is governed by a complex network of proteins cooperating in response to a variety of pathogens and autoimmune stimuli. Apart from the four well-established PRR systems controlled by TLR, C-type lectin receptors, NOD-like receptors and RIG-I-like receptors, innate immune signalling also utilises a range of accessory/adaptor proteins to maintain the homeostasis of inflammation. STING is one of the major intracellular sensors of cytoplasmic double-stranded DNA and is a critical switch to initiate type I interferon production. Recent work in mouse models of SLE have demonstrated that STING is required for homeostatic expression of negative regulators of immune activation (6); whilst analysis of human monocytes from SLE patients revealed a hyperactive STING signalling that is regulated by the interferon induced gene, IFIT3 (31). Analysis of T cells (a critical source of Type I interferon in this disease (62, 63)) from a cohort of SLE positive, treatment naïve patients revealed unaltered STING and an elevated level of TMEM203 with a concurrent suppression of MAVS RNA levels, suggesting that TMEM203 may be an important, novel player in the pathology of SLE.

The physiological significance of STING has been demonstrated during HSV, adenovirus (ADV), human papillomavirus (HPV) and negative-stranded RNA viruses such as vesicular stomatitis virus (VSV) infections (2, 44, 66). Gain-of-function STING variants lead to auto-immune, inflammatory diseases such as SAVI and FCL, manifesting symptoms of type I interferonopathy (15, 17). STING mediated signalling is known to involve TBK1/IRF3 and NF-κB; targeting STING activity for therapeutic purposes nonetheless thus far focussed on inhibiting downstream interferon receptors, and JAK/STAT (15, 17, 67). Several cancer adjuvants showed promising anti-tumour effects in early clinical trials but none has yet progressed to the clinic (68, 69). Therefore, revealing TMEM203 as a novel STING-centred signalling regulator is of significant interest to both basic research to the understanding of diseases of interferon dysregulation, and to the development of therapeutics and adjuvants modifying interferon induction.

Acknowledgement:

This work was funded by a grant from the Foundation for the National Institutes of Health through the Grand Challenges in Global Health Initiative of the Gates Foundation, by the Singapore National Medical Research Council (NMRC/OFIRG/0059/2017) and by the National Research Foundation, Prime Minister's Office, Singapore under its Campus of Research Excellence and Technological Enterprise (CREATE) programme. RFB was supported by an EMBO short-term fellowship, ASTF 299-2012. We acknowledge MRC Harwell, Oxford, for generating the WT and Tmem203 knockout mice and kindly providing bone marrow for our experiments. The immortalised BMDMs were a kind gift from Dr David Brough, University of Manchester.

Author Contributions:

DHW, AVSH, CAJ, HLW, ZY and EKT designed the experiments. YL, SJJ, DHW, CW, AC, KP, SMBM, RFB and AA carried out the experimental work; ZH performed the bioinformatics analysis; LK obtained samples from SLE patients. All authors were involved in the analysis and interpretation of the results. YL, DHW, CW, HLW, ZY, CAJ, HLW and EKT wrote and edited the manuscript.

Declaration of Interest:

Authors declare no conflict of interest.

References:

1. Unterholzner, L, Keating, SE, Baran, M, Horan, KA, Jensen, SB, Sharma, S, Sirois, CM, Jin, T, Latz, E, Xiao, TS, Fitzgerald, KA, Paludan, SR, Bowie, AG. IFI16 is an innate immune sensor for intracellular DNA. *Nat Immunol*. 2010;11(11):997–1004.

2. Ishikawa, H, Ma, Z, Barber, GN. STING regulates intracellular DNA-mediated, type I interferon-dependent innate immunity. *Nature*. 2009;461(7265):788–792.

3. Barber, GN. STING: infection, inflammation and cancer. *Nat Rev Immunol*. 2015;15(12):760–770.

4. Wu, X, Wu, FH, Wang, X, Wang, L, Siedow, JN, Zhang, W, Pei, ZM. Molecular evolutionary and structural analysis of the cytosolic DNA sensor cGAS and STING. *Nucleic Acids Res*. 2014;42(13):8243–8257.

5. Ding, L, Dong, G, Zhang, D, Ni, Y, Hou, Y. The regional function of cGAS/STING signal in multiple organs: One of culprit behind systemic lupus erythematosus. *Med Hypotheses*. 2015

6. Sharma, S, Campbell, AM, Chan, J, Schattgen, SA, Orlowski, GM, Nayar, R, Huyler, AH, Nündel, K, Mohan, C, Berg, LJ, Shlomchik, MJ, Marshak-Rothstein, A, Fitzgerald, KA. Suppression of systemic autoimmunity by the innate immune adaptor STING. *Proc Natl Acad Sci U S A*. 2015;112(7):E710–7.

7. Kennedy, RB, Ovsyannikova, IG, Pankratz, VS, Haralambieva, IH, Vierkant, RA, Jacobson, RM, Poland, GA. Genome-wide genetic associations with IFNγ response to smallpox vaccine. *Hum Genet*. 2012;131(9):1433–1451.

8. Li, T, Cheng, H, Yuan, H, Xu, Q, Shu, C, Zhang, Y, Xu, P, Tan, J, Rui, Y, Li, P, Tan, X. Antitumor Activity of cGAMP via Stimulation of cGAS-cGAMP-STING-IRF3 Mediated Innate Immune Response. *Sci Rep*. 2016;6:19049.

9. Gravekamp, C, Chandra, D. Targeting STING pathways for the treatment of cancer. *Oncoimmunology*. 2015;4(12):e988463.

10. Woo, SR, Fuertes, MB, Corrales, L, Spranger, S, Furdyna, MJ, Leung, MY, Duggan, R, Wang, Y, Barber, GN, Fitzgerald, KA, Alegre, ML, Gajewski, TF. STING-Dependent Cytosolic DNA Sensing Mediates Innate Immune Recognition of Immunogenic Tumors. *Immunity*. 2014;41(5):830–842.

11. Sun, W, Li, Y, Chen, L, Chen, H, You, F, Zhou, X, Zhou, Y, Zhai, Z, Chen, D, Jiang, Z. ERIS, an endoplasmic reticulum IFN stimulator, activates innate immune signaling through dimerization. *Proc Natl Acad Sci U S A*. 2009;106(21):8653–8658.

12. Abe, T, Harashima, A, Xia, T, Konno, H, Konno, K, Morales, A, Ahn, J, Gutman, D, Barber, GN. STING Recognition of Cytoplasmic DNA Instigates Cellular Defense. *Mol Cell*. 2013;50(1):5–15.

13. Burdette, DL, Vance, RE. STING and the innate immune response to nucleic acids in the cytosol. *Nat Immunol*. 2013;14(1):19–26.

14. Langereis, MA, Rabouw, HH, Holwerda, M, Visser, LJ, van Kuppeveld, FJ. Knockout of cGAS and STING Rescues Virus Infection of Plasmid DNA-Transfected Cells. *J Virol*. 2015;89(21):11169–11173.

15. Liu, Y, Jesus, AA, Marrero, B, Yang, D, Ramsey, SE, Sanchez, GAM, Tenbrock, K, Wittkowski, H, Jones, OY, Kuehn, HS, Lee, CR, DiMattia, MA, Cowen, EW, Gonzalez, B, Palmer, I, DiGiovanna, JJ, Biancotto, A, Kim, H, Tsai, WL, Trier, AM, Huang, Y, Stone, DL, Hill, S, Kim, HJ, St Hilaire, C, Gurprasad, S, Plass, N, Chapelle, D, Horkayne-Szakaly, I, Foell, D, Barysenka, A, Candotti, F, Holland, SM, Hughes, JD, Mehmet, H, Issekutz, AC, Raffeld, M, McElwee, J, Fontana, JR, Minniti, CP, Moir, S, Kastner, DL, Gadina, M, Steven, AC, Wingfield, PT, Brooks, SR, Rosenzweig, SD, Fleisher, TA, Deng, Z, Boehm, M, Paller, AS, Goldbach-Mansky, R. Activated STING in a vascular and pulmonary syndrome. *N Engl J Med*. 2014;371(6):507–518.

16. Sharma, S, Fitzgerald, KA, Cancro, MP, Marshak-Rothstein, A. Nucleic Acid-Sensing Receptors: Rheostats of Autoimmunity and Autoinflammation. *J Immunol*. 2015;195(8):3507–3512.

17. König, N, Fiehn, C, Wolf, C, Schuster, M, Cura Costa, E, Tüngler, V, Alvarez, HA, Chara, O, Engel, K, Goldbach-Mansky, R, Günther, C, Lee-Kirsch, MA. Familial chilblain lupus due to a gain-of-function mutation in STING. *Ann Rheum Dis*. 2017;76(2):468–472.

18. Patel, S, Jin, L. TMEM173 variants and potential importance to human biology and disease. *Genes Immun*. 2018

19. Li, Y, Wilson, HL, Kiss-Toth, E. Regulating STING in health and disease. *J Inflamm (Lond)*. 2017;14:11.

20. Tanaka, Y, Chen, ZJ. STING specifies IRF3 phosphorylation by TBK1 in the cytosolic DNA signaling pathway. *Sci Signal*. 2012;5(214):ra20.

21. Wang, Q, Liu, X, Cui, Y, Tang, Y, Chen, W, Li, S, Yu, H, Pan, Y, Wang, C. The E3 Ubiquitin Ligase AMFR and INSIG1 Bridge the Activation of TBK1 Kinase by Modifying the Adaptor STING. *Immunity*. 2014;41(6):919–933.

22. Gonugunta, VK, Sakai, T, Pokatayev, V, Yang, K, Wu, J, Dobbs, N, Yan, N. Trafficking-Mediated STING Degradation Requires Sorting to Acidified Endolysosomes and Can Be Targeted to Enhance Anti-tumor Response. *Cell Rep*. 2017;21(11):3234–3242.

23. Saitoh, T, Fujita, N, Hayashi, T, Takahara, K, Satoh, T, Lee, H, Matsunaga, K, Kageyama, S, Omori, H, Noda, T, Yamamoto, N, Kawai, T, Ishii, K, Takeuchi, O, Yoshimori, T, Akira, S. Atg9a controls dsDNA-driven dynamic translocation of STING and the innate immune response. *Proc Natl Acad Sci U S A*. 2009;106(49):20842–20846.

24. Liu, YP, Zeng, L, Tian, A, Bomkamp, A, Rivera, D, Gutman, D, Barber, GN, Olson, JK, Smith, JA. Endoplasmic reticulum stress regulates the innate immunity critical transcription factor IRF3. *J Immunol*. 2012;189(9):4630–4639.

25. Liu, S, Cai, X, Wu, J, Cong, Q, Chen, X, Li, T, Du, F, Ren, J, Wu, Y, Grishin, N, Chen, ZJ. Phosphorylation of innate immune adaptor proteins MAVS, STING, and TRIF induces IRF3 activation. *Science*. 2015

26. Wyllie, DH, Sogaard, KC, Holland, K, Yaobo, X, Bregu, M, Hill, AV, Kiss-Toth, E. Identification of 34 novel proinflammatory proteins in a genome-wide macrophage functional screen. *PLoS One*. 2012;7(7):e42388.

27. Kiss-Toth, E, Guesdon, FM, Wyllie, DH, Qwarnstrom, EE, Dower, SK. A novel mammalian expression screen exploiting green fluorescent protein-based transcription detection in single cells. *J Immunol Methods*. 2000;239(1-2):125–135.

28. Shambharkar, PB, Bittinger, M, Latario, B, Xiong, Z, Bandyopadhyay, S, Davis, V, Lin, V, Yang, Y, Valdez, R, Labow, MA. TMEM203 Is a Novel Regulator of Intracellular Calcium Homeostasis and Is Required for Spermatogenesis. *PLoS One*. 2015;10(5):e0127480.

29. Ikeda, M, Arai, M, Okuno, T, Shimizu, T. TMPDB: a database of experimentally-characterized transmembrane topologies. *Nucleic Acids Res*. 2003;31(1):406–409.

30. Attwood, MM, Krishnan, A, Pivotti, V, Yazdi, S, Almén, MS, Schiöth, HB. Topology based identification and comprehensive classification of four-transmembrane helix containing proteins (4TMs) in the human genome. *BMC Genomics*. 2016;17:268.

31. Wang, J, Dai, M, Cui, Y, Hou, G, Deng, J, Gao, X, Liao, Z, Liu, Y, Meng, Y, Wu, L, Yao, C, Wang, Y, Qian, J, Guo, Q, Ding, H, Qu, B, Shen, N. Elevated IFIT3 Contributes to Abnormal Overactive cGAS-STING Signaling in Human Systemic Lupus Erythematosus Monocytes. *Arthritis Rheumatol*. 2018

32. Shao, WH, Shu, DH, Zhen, Y, Hilliard, B, Priest, SO, Cesaroni, M, Ting, JP, Cohen, PL. Prion-like Aggregation of Mitochondrial Antiviral Signaling Protein in Lupus Patients Is Associated With Increased Levels of Type I Interferon. *Arthritis Rheumatol*. 2016;68(11):2697–2707.

33. Wu, C, Jin, X, Tsueng, G, Afrasiabi, C, Su, AI. BioGPS: building your own mash-up of gene annotations and expression profiles. *Nucleic Acids Res*. 2016;44(D1):D313–6.

34. Zhao, C, Pavicic, PG, Datta, S, Sun, D, Novotny, M, Hamilton, TA. Cellular stress amplifies TLR3/4-induced CXCL1/2 gene transcription in mononuclear phagocytes via RIPK1. *J Immunol*. 2014;193(2):879–888.

35. Petrasek, J, Iracheta-Vellve, A, Csak, T, Satishchandran, A, Kodys, K, Kurt-Jones, EA, Fitzgerald, KA, Szabo, G. STING-IRF3 pathway links endoplasmic reticulum stress with hepatocyte apoptosis in early alcoholic liver disease. *Proc Natl Acad Sci U S A*. 2013;110(41):16544–16549.

36. Piao, W, Song, C, Chen, H, Diaz, MA, Wahl, LM, Fitzgerald, KA, Li, L, Medvedev, AE. Endotoxin tolerance dysregulates MyD88- and Toll/IL-1R domain-containing adapter inducing IFN-beta-dependent pathways and increases expression of negative regulators of TLR signaling. *J Leukoc Biol*. 2009;86(4):863–875.

37. Reimer, T, Schweizer, M, Jungi, TW. Stimulation-specific contribution of p38 and JNK to IFN-beta gene expression in human macrophages. *J Interferon Cytokine Res*. 2007;27(9):751–755.

38. Sun, L, Wu, J, Du, F, Chen, X, Chen, ZJ. Cyclic GMP-AMP synthase is a cytosolic DNA sensor that activates the type I interferon pathway. *Science*. 2013;339(6121):786–791.

39. Burdette, DL, Monroe, KM, Sotelo-Troha, K, Iwig, JS, Eckert, B, Hyodo, M, Hayakawa, Y, Vance, RE. STING is a direct innate immune sensor of cyclic di-GMP. *Nature*. 2011;478(7370):515–518.

40. Woodward, JJ, Iavarone, AT, Portnoy, DA. c-di-AMP secreted by intracellular Listeria monocytogenes activates a host type I interferon response. *Science*. 2010;328(5986):1703–1705.

41. Wu, J, Sun, L, Chen, X, Du, F, Shi, H, Chen, C, Chen, ZJ. Cyclic GMP-AMP is an endogenous second messenger in innate immune signaling by cytosolic DNA. *Science*. 2013;339(6121):826–830.

42. Jin, L, Getahun, A, Knowles, HM, Mogan, J, Akerlund, LJ, Packard, TA, Perraud, AL, Cambier, JC. STING/MPYS mediates host defense against Listeria monocytogenes infection by regulating Ly6C(hi) monocyte migration. *J Immunol*. 2013;190(6):2835–2843.

43. Davies, BW, Bogard, RW, Young, TS, Mekalanos, JJ. Coordinated regulation of accessory genetic elements produces cyclic di-nucleotides for V. cholerae virulence. *Cell*. 2012;149(2):358–370.

44. Ishikawa, H, Barber, GN. STING is an endoplasmic reticulum adaptor that facilitates innate immune signalling. *Nature*. 2008;455(7213):674–678.

45. Guan, H, Dower, S, Kiss-Toth, E. Inflammation Immunomics. In: Falus, A, ed. *Clinical Applications of Immunomics*. Springer; 2008:

46. Remy, I, Michnick, SW. A cDNA library functional screening strategy based on fluorescent protein complementation assays to identify novel components of signaling pathways. *Methods*. 2004;32(4):381–388.

47. Remy, I, Michnick, SW. Dynamic visualization of expressed gene networks. *J Cell Physiol*. 2003;196(3):419–429.

48. Michnick, SW, Ear, PH, Landry, C, Malleshaiah, MK, Messier, V. A toolkit of protein-fragment complementation assays for studying and dissecting large-scale and dynamic protein-protein interactions in living cells. *Methods Enzymol*. 2010;470:335–368.

49. Barker, JR, Koestler, BJ, Carpenter, VK, Burdette, DL, Waters, CM, Vance, RE, Valdivia, RH. STING-dependent recognition of cyclic di-AMP mediates type I interferon responses during Chlamydia trachomatis infection. *MBio*. 2013;4(3):e00018–13.

50. Larsen, KC, Spencer, AJ, Goodman, AL, Gilchrist, A, Furze, J, Rollier, CS, Kiss-Toth, E, Gilbert, SC, Bregu, M, Soilleux, EJ, Hill, AV, Wyllie, DH. Expression of tak1 and tram induces synergistic pro-inflammatory signalling and adjuvants DNA vaccines. *Vaccine*. 2009;27:5589–5598.

51. Diner, EJ, Burdette, DL, Wilson, SC, Monroe, KM, Kellenberger, CA, Hyodo, M, Hayakawa, Y, Hammond, MC, Vance, RE. The Innate Immune DNA Sensor cGAS

Produces a Noncanonical Cyclic Dinucleotide that Activates Human STING. *Cell Rep*. 2013;3(5):1355–1361.

52. Conlon, J, Burdette, DL, Sharma, S, Bhat, N, Thompson, M, Jiang, Z, Rathinam, VA, Monks, B, Jin, T, Xiao, TS, Vogel, SN, Vance, RE, Fitzgerald, KA. Mouse, but not human STING, binds and signals in response to the vascular disrupting agent 5,6-dimethylxanthenone-4-acetic acid. *J Immunol*. 2013;190(10):5216–5225.

53. Shih, AY, Damm-Ganamet, KL, Mirzadegan, T. Dynamic Structural Differences between Human and Mouse STING Lead to Differing Sensitivity to DMXAA. *Biophys J*. 2018;114(1):32–39.

54. Abe, T, Barber, GN. Cytosolic DNA-Mediated, STING-Dependent Pro-Inflammatory Gene Induction Necessitates canonical NF-kappaB activation Through TBK1. *J Virol*. 2014

55. Jakobsen, MR, Bak, RO, Andersen, A, Berg, RK, Jensen, SB, Tengchuan, J, Laustsen, A, Hansen, K, Ostergaard, L, Fitzgerald, KA, Xiao, TS, Mikkelsen, JG, Mogensen, TH, Paludan, SR. IFI16 senses DNA forms of the lentiviral replication cycle and controls HIV-1 replication. *Proc Natl Acad Sci U S A*. 2013

56. Kalamvoki, M, Du, T, Roizman, B. Cells infected with herpes simplex virus 1 export to uninfected cells exosomes containing STING, viral mRNAs, and microRNAs. *Proc Natl Acad Sci U S A*. 2014

57. Orzalli, MH, Broekema, NM, Diner, BA, Hancks, DC, Elde, NC, Cristea, IM, Knipe, DM. cGAS-mediated stabilization of IFI16 promotes innate signaling during herpes simplex virus infection. *Proc Natl Acad Sci U S A*. 2015;112(14):E1773–81.

58. Diner, BA, Lum, KK, Toettcher, JE, Cristea, IM. Viral DNA Sensors IFI16 and Cyclic GMP-AMP Synthase Possess Distinct Functions in Regulating Viral Gene Expression, Immune Defenses, and Apoptotic Responses during Herpesvirus Infection. *MBio*. 2016;7(6)

59. Surpris, G, Chan, J, Thompson, M, Ilyukha, V, Liu, BC, Atianand, M, Sharma, S, Volkova, T, Smirnova, I, Fitzgerald, KA, Poltorak, A. Cutting Edge: Novel Tmem173 Allele Reveals Importance of STING N Terminus in Trafficking and Type I IFN Production. *J Immunol*. 2016;196(2):547–552.

60. Ouyang, S, Song, X, Wang, Y, Ru, H, Shaw, N, Jiang, Y, Niu, F, Zhu, Y, Qiu, W, Parvatiyar, K, Li, Y, Zhang, R, Cheng, G, Liu, ZJ. Structural analysis of the STING

adaptor protein reveals a hydrophobic dimer interface and mode of cyclic di-GMP binding. *Immunity*. 2012;36(6):1073–1086.

61. Ogen-Shtern, N, Ben David, T, Lederkremer, GZ. Protein aggregation and ER stress. *Brain Res*. 2016;1648(Pt B):658–666.

62. Kammer, GM, Perl, A, Richardson, BC, Tsokos, GC. Abnormal T cell signal transduction in systemic lupus erythematosus. *Arthritis Rheum*. 2002;46(5):1139–1154.

63. Comte, D, Karampetsou, MP, Tsokos, GC. T cells as a therapeutic target in SLE. *Lupus*. 2015;24(4-5):351–363.

64. Gao, P, Ascano, M, Zillinger, T, Wang, W, Dai, P, Serganov, AA, Gaffney, BL, Shuman, S, Jones, RA, Deng, L, Hartmann, G, Barchet, W, Tuschl, T, Patel, DJ. Structure-function analysis of STING activation by c[G(2',5')pA(3',5')p] and targeting by antiviral DMXAA. *Cell*. 2013;154(4):748–762.

65. Che, X, Du, XX, Cai, X, Zhang, J, Xie, WJ, Long, Z, Ye, ZY, Zhang, H, Yang, L, Su, XD, Gao, YQ. Single Mutations Reshape the Structural Correlation Network of the DMXAA-Human STING Complex. *J Phys Chem B*. 2017;121(9):2073–2082.

66. Lau, L, Gray, EE, Brunette, RL, Stetson, DB. DNA tumor virus oncogenes antagonize the cGAS-STING DNA-sensing pathway. *Science*. 2015;350(6260):568–571.

67. Frémond, ML, Rodero, MP, Jeremiah, N, Belot, A, Jeziorski, E, Duffy, D, Bessis, D, Cros, G, Rice, GI, Charbit, B, Hulin, A, Khoudour, N, Caballero, CM, Bodemer, C, Fabre, M, Berteloot, L, Le Bourgeois, M, Reix, P, Walzer, T, Moshous, D, Blanche, S, Fischer, A, Bader-Meunier, B, Rieux-Laucat, F, Crow, YJ, Neven, B. Efficacy of the Janus kinase 1/2 inhibitor ruxolitinib in the treatment of vasculopathy associated with TMEM173-activating mutations in 3 children. *J Allergy Clin Immunol*. 2016;138(6):1752–1755.

68. Fu, J, Kanne, DB, Leong, M, Glickman, LH, McWhirter, SM, Lemmens, E, Mechette, K, Leong, JJ, Lauer, P, Liu, W, Sivick, KE, Zeng, Q, Soares, KC, Zheng, L, Portnoy, DA, Woodward, JJ, Pardoll, DM, Dubensky, TW, Kim, Y. STING agonist formulated cancer vaccines can cure established tumors resistant to PD-1 blockade. *Sci Transl Med*. 2015;7(283):283ra52.

69. Mullard, A. Can you trust your cancer cell lines. *Nat Rev Drug Discov*. 2018;17(9):613.

70. Wyllie, DH, Kiss-Toth, E, Visintin, A, Smith, SC, Boussouf, S, Segal, DM, Duff, GW, Dower, SK. Evidence for an accessory protein function for Toll-like receptor 1 in anti-bacterial responses. *J Immunol*. 2000;165(12):7125–7132.

71. Mizushima, S, Nagata, S. pEF-BOS, a powerful mammalian expression vector. *Nucleic Acids Res*. 1990;18(17):5322.

72. Eder, K, Guan, H, Sung, HY, Ward, J, Angyal, A, Janas, M, Sarmay, G, Duda, E, Turner, M, Dower, SK, Francis, SE, Crossman, DC, Kiss-Toth, E. Tribbles-2 is a novel regulator of inflammatory activation of monocytes. *Int Immunol*. 2008;20(12):1543–1550.

73. Xiao, JH, Davidson, I, Matthes, H, Garnier, JM, Chambon, P. Cloning, expression, and transcriptional properties of the human enhancer factor TEF-1. *Cell*. 1991;65(4):551–568.

74. Hochberg, MC. Updating the American College of Rheumatology revised criteria for the classification of systemic lupus erythematosus. *Arthritis Rheum*. 1997;40(9):1725.

75. Hornung, V, Bauernfeind, F, Halle, A, Samstad, EO, Kono, H, Rock, KL, Fitzgerald, KA, Latz, E. Silica crystals and aluminum salts activate the NALP3 inflammasome through phagosomal destabilization. *Nat Immunol*. 2008;9(8):847–856.

76. Jin, L, Waterman, PM, Jonscher, KR, Short, CM, Reisdorph, NA, Cambier, JC. MPYS, a novel membrane tetraspanner, is associated with major histocompatibility complex class II and mediates transduction of apoptotic signals. *Mol Cell Biol*. 2008;28(16):5014–5026.

Methods:

Plasmids:

- Expression vectors

Tmem203 expression constructs were generated using standard molecular biological techniques. For details of other inserts used, see (50).

- Reporter vectors

pGL4.*cxcl2* reporter vector, which contain the mouse *cxcl2* promoter in pGL4 (Promega) have been previously described (50). Similarly, the IL8-luc has previously been reported (70). As an internal control, pGL4.EF1.rLuc was used; this was constructed by PCR amplification of the human EF1 promoter from pEF-BOS (71) and inserted into pGL4 at the Nhe I site. Sequences of all vectors used were confirmed by sequencing. Plasmid vectors for studies of the TMEM203/STING complex by EYFP-PCA have been reported previously (72). For Renilla-PCA, plasmids from the NonBIT-PPI (Promega) were used. Plasmids used in co-immunoprecipitation were cloned into pXJ40 vector (73) which contains CMV enhancer/ promoter. HA tag sequence is MVPYDVPDYAGS, Flag tag sequence is MDYKDDDDKG, Myc tag sequence is EQKLISEEDL. Sequences of all vectors used were confirmed by sequencing.

SLE cohort

A cohort of patients diagnosed with SLE on the basis of the 1997 updated criteria of the American College of Rheumatology (74) were examined in this study and patient samples were followed-up at the Department of Rheumatology and Immunology, University of Szeged, Hungary. Patients aged 18-80 years with clinical disease activity in at least one organ system were eligible for the study. Exclusion criteria included the presence of an overlapping connective tissue disease, an infectious or other inflammatory process, and corticosteroid treatment with a prednisolone dose higher than 10 mg/day. The most important demographic characteristics and disease activity parameters of the cohort are presented in Table S1. All subjects gave informed consent to donate blood for research purposes prior to starting treatment of SLE. SLEDAI2K, anti-DNA, C3 and C4 complement levels in the patient serum were measured as part of the assessment of disease activity during lupus flare. The study was approved by the Human Investigation Review Board of the University of Szeged, Albert Szent-Györgyi Health Centre (reference number 2833/2011).

Study Ethics

All human tissue samples were collected under protocols approved by the University of Szeged Review Board (Ref No 2833/2011) and conformed to the declaration of Helsinki (World Medical Association. 1964. Declaration of Helsinki). Human blood was taken and used

under protocols approved by the University of Sheffield Research Ethics Committee (UREC) (Ref. SMBRER310). All participants gave written informed consent.

Isolation of primary macrophages

Peripheral blood mononuclear cells (PBMCs) were isolated from total blood using standard Ficoll-Pague gradient (GE Healthcare). Monocytes were isolated by positive selection using CD14-targeting magnetic microbeads (Miltenyi Biotec) according to manufacturer's instructions. The purified cell population was found to contain over 90% CD14-positive monocytes. To differentiate human monocytes into human monocyte-derived macrophages (MDMs) 250,000 cells were seeded in a 12 well plate in 1.5 ml complete RPMI (1% PS, 1% L-G and 10% LE HI FBS) supplemented with 100 ng/ml human recombinant M-CSF (PeproTech). MDMs were fully differentiated at the seventh day of incubation (37 ℃ 5% CO_2) and used for further experimental purposes. At day 7 of M-CSF incubation, fresh complete RPMI medium was supplied before further treatment.

Mice hind limbs were a gift from MRC Harwell, Oxford. Bone marrow were eluted from mice bones are were cultured in DMEM (10% low endotoxin FCS (Biowest); 1% Penicillin-Streptomycin; 10% L929 conditioned medium) for 5 days to be differentiated into primary bone marrow-derived macrophages (BMDMs). Cells were seeded in 12 well plates for further experiments.

Isolation and analysis of T cells:

PBMCs were isolated from SLE and healthy donors using Ficoll (GE Healthcare) gradient centrifugation. PBMCs were stimulated with 1 µg/mL Phytohaemagglutinin (PHA-L, Sigma-Aldrich) and were cultured for 72 hours in RPMI-1640 medium (Gibco®) supplemented with 10% fetal bovine serum (FBS) (Gibco®), 2 mM L-glutamine (Gibco®) and penicillin-streptomycin (Sigma-Aldrich). Total RNA was extracted from activated T cells (1-3 × 10^6 cells) using PerfectPure RNA Cultured Cell kit (5 Prime) according to the manufacturer's instructions with on-column DNase digestion. For cDNA synthesis, 1 µg of total RNA / reaction was reverse transcribed using RevertAid Reverse Transcriptase (Thermo Fisher Scientific Inc.) in the presence of 1.66 µM of oligo(dT)18 and random hexamer primers, 0.5 mM dNTP, 10 U RiboLock RNase Inhibitor and 200 U RevertAid H Minus Reverse Transcriptase for 60 min at 42°C then heated for 10 min at 70°C. Quantitative PCR was carried out using TaqMan Universal mastermix II (Applied Biosystems®) in 10 µl reaction volumes in duplicates using Roto-Gene Q real-time PCR cycler (Qiagen). The following Taqman® Gene Expression

Assays (Applied Biosystems®) were used: (Hs01060665_g1 for ACTB, Hs01057884_s1 for TMEM203, Hs00736955_g1 for TMEM173, Hs00920075_m1 for MAVS with a Roto-Gene Q instrument (Qiagen). Quantitative real-time PCR data were analysed using the Rotor Gene software (v6.1 build 93).

Cell cultures, transient transfection

RAW 264.7 cells were purchased from ATCC (Cat. No: TIB-71). RAW 264.7 cells were plated overnight and the next day transfected using DharmaFECT transfection reagents (Dharmacon, GE Healthcare) according to the manufacturer's guidelines. Cells were further treated 24 h post plasmid transfection or 48 h post siRNA transfection. All transfections were performed in 96-well plates, unless stated otherwise.

Differentiated human monocyte-derived macrophages (MDMs) were transfected with On-target Plus siRNAs smartpool (Dharmacon, GE Healthcare) against human TMEM203 or non-targeting control siRNA using Viromer green transfection reagent (Lipocalyx) at a final concentration of 12.5 nM. Transfection lasts 48 h before cells are used for other purposes.

Immortalised bone marrow-derived macrophages (iBMDMs) cell line was generated by David Brough's lab (University of Manchester) using the method described by (75). Cells (75,000 in 0.5 ml) were seeded overnight to allow attachment and were transfected with siRNA pool (Dharmacon, GE Healthcare) against mouse Tmem203 or Sting or non-targeting control siRNA using the same Viromer green transfection method as described for MDMs. Cells were assayed 48 h post transfection.

HeLa cells (200,000) were plated in 35mm glass-bottom petri dish to attach overnight and the next day were transfected with Lipofectamine 3000 according to the manufacturer's protocol. Cells were used 18-24 h post plasmid transfection.

For Renilla and Venus protein complementary assay, HEK293 T cells were transfected using PolyFECT (Qiagen) according to manufacturer's guidelines. Equal quantities were used for co-transfecting plasmids. Transfection lasts 18-24 h before cells are used in further treatments.

RAW 264.7 and iBMDMs were maintained in Dulbecco's Modified Eagle's medium (DMEM) supplemented with 1% Penicillin-Streptomycin (PS) (Gibco), 1% L-glutamine (L-G) (Gibco) and 10% low-endotoxin heat-inactivated fetal bovine serum (LE HI FBS) (Biowest). Human MDMs were maintained in RPMI-1640 medium supplemented with 1% PS, 1% L-G and 10% LE HI FBS. HeLa cells were maintained in DMEM supplemented with 1% PS, 1% L-G, 1% non-essential amino acids and 10% HI FBS. HEK293 T cells were maintained in DMEM

supplemented with 1% PS, 1% L-G and 10% HI FBS. All cells were kept at 37 ℃ and 5% CO_2; all established cells were used at 30 or lower passages.

Generation of CRISPR/Cas9 Tmem203 Knockout RAW 264.7 cells

Four suitable sgRNA oligos were designed and used in the generation of pGL3-U6 sgRNA-Puromycin expression vectors. Vectors were transformed into *E*.coli DH5α and positive clones were screened on Ampicillin selection plates. Identified clones containing correct insertion of sgRNA oligos were further confirmed by sequencing using the primer: 5'-cgattagtgaacggatctcgacg-3'. Transfection of RAW 264.7 with pGL3-U6 sgRNA expression vectors was carried out using Lipofectamine 2000 according to the manufacturers' instructions. 6h post-transfection, media was replaced with RPMI complete medium. Antibiotic selection using Puromycin (2 µg/ml) and Blasticidin (10 µg/ml) was started at 24 hours (h) post-transfection and continued for a total of 72 h before passaging cells for downstream applications. Clonal isolation was performed, and successful clones that consistently showed 3-4 folds decrease in *Tmem203* expression determined by quantitative real-time PCR. These colonies were selected for establishment of a stable cell lines along with CRISPR-Cas 9 control group using selective medium containing Puromycin (2 µg/ml) and Blasticidin (10 µg/ml).

Generation of Tmem203 Stably Expressing RAW 264.7 cells

Mouse Tmem203 cDNA was cloned into the pcDNA 3.0 vector between the Hind III and BamHI restriction sites. The construct was then transfected into RAW 264.7 cells using Lipofectamine (Invitrogen) according to the manufacturer's instruction. 18-24h after the transfection, RPMI-1640 medium supplemented with 10% FCS, Penicillin/ Streptomycin and 500µg/ml G418 was added to initiate the selection of stably expressing Tmem203 cells. Clones were selected for further culture after two weeks of selection. qPCR was carried out to confirm the level of overexpression.

STING ligand stimulation:

RAW 264.7 cells were transfected with 1µg 3'3'-cGAMP using Lipofectamine LTX (Invitrogen) according to the manufacturer's instructions.

For MDM, immortalised BMDM (iBMDM) and BMDM stimulation, macrophages were stimulated with 2'3'-cGAMP, 3'3'-cGAMP or DMXAA at the indicated doses and time. 2'3'-cGAMP was delivered with fresh medium (control treated with fresh DMEM only); 3'3'-cGAMP was delivered with 20 mins incubation of reversible Digitonin permeabilisation method as described in by Woodward and colleagues (2010 *Science* 328(5986): 1703-5) (control treated with ligand free Digitonin buffer); DMXAA is reconstituted in DMSO and delivered to cells with fresh medium (control treated with DMSO only medium). All ligands were purchased from Invivogen.

HSV-1 infection

RAW264.7 cells (control and Tmem203-overexpression / CRISPR-Tmem203 knockout) were grown in RPMI 1640 medium (Hyclone) supplemented with 10%(v/v) FBS (Sigma) and seeded to 50% confluency in 6 well plates and allowed to rest overnight. Cultures were then replaced with antibiotic free media before infection with HSV-1 virus at MOI of 0.2. Cell lysates were obtained at 0, 1, 3 and 6 hr post infection for western analyses. Cells were harvested at 0 and 6hr post infection for RNA extraction and cell culture supernatants were subjected to ELISA.

Enzyme-linked immunosorbent assay (ELISA)

IFN-β ELISA kit (PBL Interferon Source) were used for the measurement of IFN-β concentrations according to the manufacturer's protocol. The concentration was determined by reading the absorbance at 450 nm using the BioTek® Microplate Reader.

Standard and quantitative real-time PCR

Following experiments, RAW 264.7 cells were lysed using Isol (5 prime) and then chloroform extracted prior to RNA isolation on RNeasy Mini columns, including DNase digestion (Qiagen). cDNA was made from total RNA with Maxima First Strand cDNA Synthesis Kit for RT-qPCR (Thermo scientific) according to the manufacturer's protocol. Quantitative real-time PCR (qPCR) was performed with the PerfeCTa qPCR FastMix (Quanta Biosciences) in 20 µl reaction volumes in duplicate wells and cycled in a StepOnePlus™ Real-Time PCR cycler. The following TaqMan® Gene Expression Assays (Applied Biosystems®) were used: IFN-β (Hs01077958_s1), TNF (Hs00174128_m1).

For analysis of mRNA levels in MDM, BMDMs, iBMDMs, and ER stress response in HEK293 T cell: Following treatment, cells were washed with PBS and harvested for total RNA extraction on ReliaPrep Cell Isolation columns (Promega) following the manufacturer's instructions. Complementary DNA was made from 500 ng total RNA (Biorad iScript cDNA synthetic kit) for gene expression analysis. Real-time quantitative PCR was performed using Primerdesign SYBR green mastermix in 10µl reaction volume in triplicate wells and quantified in Biorad CFX384 Touch™ real-time PCR cycler. Primers for amplification of human genes were as follows (Forward and Reverse):

Human:

IFN-β: 5'-AAGCAGCAATTTTCAGTGTCAGA–3' and 5'-CCTCAGGGATGTCAAAGTTCA–3'; IL-8: 5'-TGCCAAGGAGTGCTAAAG–3' and 5'-CTCCACAACCCTCTGCAC–3'; TMEM203 5'-GTCTTCGAGATGCTGTTGTGC–3' and 5'-ACGTAATGAGGCCGAACCAG–3'; Total XBP1 5'-TGGCCGGGTCTGCTGAGTCCG–3' and 5'-ATCCATGGGGAGATGTTCTGG–3'; Spliced XBP1 5'-CTGAGTCCGAATCAGGTGCAG–3' and 5'-ATCCATGGGGAGATGTTCTGG–3'; Non-spliced XBP1 5'-CAGCACTCAGACTACGTGCA–3' and 5'-ATCCATGGGGAGATGTTCTGG–3'; β-actin 5'-GGATGACAGAAGGAGATCACTG–3' and 5'-CGATCCACACGGAGTACTTG–3'.

Mouse:

Sting: 5'- GCTGGCATCAAGAATCGGGT–3' and 5'- TACTCCAGGATACAGACGCC–3'; Tmem203: 5'- CCCTGTTGGTGTTCTCCGTA–3' and 5'- GCACAAAGACGTTCCACCAG–3'; Ifnb1: 5'- TGTCCTCAACTGCTCTCCAC–3' and 5'- CATCCAGGCGTAGCTGTTGT–3'; Cxcl2: 5'- ATCCAGAGCTTGAGTGTGACG–3' and 5'- TTTGACCGCCCTTGAGAGTG–3'; β-actin: 5'-GGGACCTGACAGACTACCTCATG–3' and 5'-GTCACGCACGATTTCCCTCTCAGC–3';

Site-directed Mutagenesis and molecular cloning

Single-amino acid mutation was performed using Agilent QuikChange Mutagenesis kit following the manufacturer's protocol. Forward and reverse primers were designed to substitute the target tri-nucleotide with a stop codon to generate truncation mutations in Sting coding region (ENSMUSG00000024349; NP_082537.1, Q3TBT3). Reverse primers are complementary to the forward primers. Primers were purchased from Sigma Aldrich. Sting mutants used in co-immunoprecipitation were generated by standard PCR with respective primers using AccuPrime™ Taq DNA Polymerase system from Thermo Scientific following manufacturer's instructions. EcorV site was introduced to facilitate ligation between internal deletion sites. Fidelity of the constructs were confirmed by Sanger sequencing.

Mutations and primers are described below:

Sting mutants for co-immunoprecipitation:

Gene	Mutation	Mutagenesis Primer Sequences
Sting WT	WT aa 1-379	Forward: 5'-AAAAAGCTTATGCCATACTCCAACCTGCATCCAGCCATCCCACGGC-3' Reverse: 5'AAACTCGAGTCAGATGAGGTCAGTGCGGAGTGGGAGAGGCTGA-3'
TM	TM1 – TM4 aa 1-146	Forward: 5'-AAAAAGCTTATGCCATACTCCAACCTGCATCCAGCCATCCCACGGC-3' Reverse: 5'-AAACTCGAGTCAGACTGCAGAGACTTCCGCTGG-3'
ΔCTT	TM1 – CBD aa 1-338	Forward: 5'-AAAAAGCTTATGCCATACTCCAACCTGCATCCAGCCATCCCACGGC-3' Reverse: 5'-AAACTCGAGTCACTCCTTTTCTTCCTGACGAATGTGCC-3'
ΔTM	CBD – CTT Aa 147-379	Forward: 5'-GGGAAGCTTATGTGTGAAGAAAAGAAGTTAAATGTTGCCCACGG-3' Reverse: 5'-AAACTCGAGTCAGATGAGGTCAGTGCGGAGTGGGAGAGGCTGA-3'
ΔCBD	Internal deletion of CBD Aa 1-146, 340-379	Forward: 5'-AAGATATCGAGGTTACCATGAATGCCCCCATGACCTCAGTGGCA-3' Reverse: 5'-AAGATATCGACTGCAGAGACTTCCGCTGGAGTCAAGCTCTGAAGG-3'
CBD	CBD only Aa 147-379	Forward: 5'-GGGAAGCTTATGTGTGAAGAAAAGAAGTTAAATGTTGCCCACGG-3' Reverse: 5'-AAACTCGAGTCACTCCTTTTCTTCCTGACGAATGTGCC-3'

Sting truncation mutants used in protein complementation assays and Western blotting were generated using QuikChange II Site-Directed Mutagenesis kit following the manufacturer's guidelines. Gateway Entry clones were used in mutagenesis reaction to induce point mutations and the correct gene-encoding sequence were fused into desired EYFP-PCA (as described above) or EYFP expression clones to express the gene of interests. Plasmids were transformed into NEB® 5-alpha Competent *E*. coli (high efficiency) cells and selected by 50 µg/ml Kanamycin (Entry clones) or 100 µg/ml Ampicillin (Destination clones) during amplification. Plasmid were isolated from bacteria cultures on GenElute plasmid DNA midiprep kit (Sigma Aldrich) according to the manufacturer's protocol. Mutagenesis were confirmed by Sanger sequencing (Source Bioscience, Birmingham).

Sting truncation mutants:

Gene	Mutation	Mutagenesis Primer Sequences
141A	GCG->TGA A -> STOP	Forward 5' CAGAGCTTGACTCCATGAGAAGTCTCTGCAGTC 3' Reverse 5' GACTGCAGAGACTTCTCATGGAGTCAAGCTCTG 3'
184L	CTA->TGA L -> STOP	Forward 5' CGAATGTTCAATCAGTGACATAACAACATGCTC 3' Reverse 5' GAGCATGTTGTTATGTCACTGATTGAACATTCG 3'
243V	GTC->TGA V -> STOP	Forward 5' GTTTATTCCAACAGCTGATACGAGATTCTGGAG 3' Reverse 5' CTCCAGAATCTCGTATCAGCTGTTGGAATAAAC 3'
344A	GCC->TGA A -> STOP	Forward 5' GAGGTTACCATGAATTGACCCATGACCTCAGTG 3' Reverse 5' CACTGAGGTCATGGGTCAATTCATGGTAACCTC 3'

Protein complementary assay

To determine protein interaction using split Venus protein complementary assay (PCA), 125,000 HEK293 T cells were seeded in 24 well plates and transfected with 500 ng total plasmid per well. Post transfection, cells were harvested in FACS buffer (5% (v/v) FBS-PBS) and assessed by flow cytometry (BD Bioscience LSRII). Cell viability was determined by TO-PRO-3 (0.002 nM, Thermo Fisher) negativity. Geometric means of GFP determined in the alive cells were compared to the selected control samples.

For split Renilla PCA, 25,000 HEK293 T cells were seeded in 96 well plates and transfected with 100 ng total plasmid per well. Post transfection, Renilla signal was analysed using Nano-Glo® Luciferase Assay System (Promega). Cells were stimulated with STING ligands for indicated time when Renilla activities were measured accordingly. Cells were also stained with Hoechst33324 (0.002 nM, ThermoFisher) to indicate cell number for normalisation. Cells were maintained at 37℃ throughout the experiment.

Immunostaining and confocal microscopy:

HeLa cells were transiently transfected with 2 µg of Tmem203-mCherry for 48 hours using Metafectene™ (Biontex) according to the manufacturer's recommendations. HeLa cells were then seeded onto UV-irradiated coverslips in a 6-well plate (2ml at 2×10^5 per ml) and treated with 1µg/ml LPS for 30 and 60 minutes as indicated. Cells were fixed with methanol/acetone at a 1:1 ratio and stained with an anti-TBK1 (Alexis Biochemicals) antibody or an anti-IRF3 (C20, SC-15991, Santa Cruz) antibody as indicated. Localisation of TBK1 and IRF3 was visualised using Alexa Fluor 488 conjugated anti-mouse and anti-goat secondary antibodies respectively (Molecular Probes). LAMP1, (H5G11, SC-18821, Santa Cruz) localisation was visualised using Alexa Fluor 488 conjugated anti-mouse secondary antibody (Molecular Probes).

For live cell imaging of Tmem203-Sting organelle localisation, attached HeLa cells were transfected with 750 ng of each V2_Tmem203 and V1_Sting (WT or mutant) for 18-24 hours using Lipofectamine 3000 according to the manufacturer's guidelines. Post transfection, samples were washed three times with PBS and were stained for 10 mins with ER or lysosome Cytopainter staining kit (Abcam) at 1/5 and 1/3 of manufacturer's recommended concentrations, respectively. Cells were then washed three times with PBS and were maintained in colourless DMEM medium (1% PS and 10% HI FBS) until imaging. Images were acquired by confocal microscopy on a Zeiss LSM 510 META with 40X inverted water-lens (Molecular Probes). Images were analysed by Fiji. ROI was selected around the organelles to calculate the number of pixels of the organelle, Sting-Tmem203 fluorescence and co-localised signals. The percentage of localisation was calculated as the ratio of number of co-localised pixels to number of pixels occupied by the organelle.

RAW 264.7 macrophages stably expressing Tmem203 or empty vector were grown on coverslips and transfected with 1 µg 3'3'-cGAMP for 6h, along with controls. Cells were fixed with 3.7% (v/v) formaldehyde for 15 minutes (min) at 37°C. Fixed cells were washed twice with PBS, twice with 4mM NH_4Cl in PBS, twice with PBS and then permeabilised with 0.2% (v/v) Triton X-100 (BioRad) in PBS for 15 min at room temperature. Blocking was carried out with 2% (w/v) bovine serum albumin and 7% (w/v) FBS in PBS for 60 min at room temperature. Cells were incubated with rabbit anti-IRF3 antibody (Cell Signaling Technology) in blocking solution overnight. Samples were washed three times with 0.1% (v/v) Triton X-100-containing PBS before incubation with Alexa Fluor 546-conjugated donkey anti-rabbit IgG for 60 min, washed three times with 0.1% (v/v) Triton X-100-containing PBS and incubated with DAPI for 5 min, washed twice and mounted using Fluorsave. Confocal fluorescence images were captured on a Zeiss LSM510 META microscope.

Human MDMs were seeded in 8 well chamber slides (40,000) and were washed twice with PBS and fixed with 4% (v/v) formaldehyde for 30 min at 37°C. Fixed cells were washed 3 times with PBS and then permeabilised with 0.1% Triton X-100 – PBS for 15 mins. Cells were then washed 3 times with PBS and blocked with 2% bovine serum albumin (BSA)-PBS for 1 h at room temperature. Cells were washed with PBS and incubated with mouse anti-human CD68 (Dako) (1:100 in 1% BSA-PBS) at 4°C overnight. Cells were then washed 3 times with PBS and reacted with AlexaFluor 488-conjugated goat anti-mouse secondary antibodies. Nuclei were visualised with DAPI (1:1000 PBS) (ThermoFisher). Cells were imaged on a LEICA AFI6000 Time-Lapse microscope at 10X magnification.

Western-blotting and immunoprecipitation analysis

Post treatment, cells were washed twice with PBS and harvested in RIPA buffer (Sigma Aldrich) and phosphatase inhibitors (Roche). The samples were vortexed on ice and sonicated for 15 mins in ice cold water. Protein concentrations were determined by Pierce BCA assay (Thermo Fisher). 10 µg proteins were diluted with equal volume of 2x Laemmli reducing buffer (4% SDS (w/v), 10% (v/v) 2-mercaptoethanol, 20% (v/v) glycerol, 0.0004% (w/v) bromophenol blue, 0.125M Tris-HCl, pH 6.8) to separate on 4-12% NuPAGE gels (Life Technologies), then transferred on nitrocellulose or PVDF membrane.

TBK1 protein and its phosphorylated form were blocked with TBST (TBS + 0.05% (v/v) Tween-20) and 3% (w/v) cold fish gelatin (Sigma), then reacted with specific rabbit antibodies (Cell Signalling #3013 and #5483, respectively) followed by anti-rabbit Ig-HRP (DAKO). All antibodies were diluted in 1.5% (w/v) cold fish gelatin-TBST. The chemi-illuminescent signal of EZ-ECL (Biological Industries) was detected on ChemiDoc™ XRS imager (Bio-Rad), and the band densities were quantified using the Image Lab™ Software. The relative pTBK1 levels were calculated by dividing the intensity of pTBK1 form by the intensity of total TBK1 in each sample. Western blot analysis was carried out with anti-pIRF3 (Ser396) (Cell Signalling Technology) for IRF3 phosphorylation, or anti-pTBK1 for TBK1 phosphorylation respectively.

For detection of YFP-STING WT and mutants, membranes were blocked with TBST containing 10% (w/v) skimmed milk, then reacted with mouse monoclonal anti-GFP antibodies (Cusabio, CSB-MA000283) or mouse monoclonal anti-PDHX (housekeeper, Santz Cruz #Sc-377255), followed by anti-mouse IgG-HRP (DAKO). All antibodies were diluted in 5% (w/v) milk-TBST. The chemi-illuminescent signal of EZ-ECL (Biological Industries) was detected on a Li-COR c-digit blot scanner and protein bands were quantified using Image Studio Digit software Ver 5.0. Band intensities were normalised against PDHX in the same sample.

For immunoprecipitation experiments, HEK293 T cells were seeded at 5×10^5 per ml, in 10 ml, in 10 cm^2 dishes and transfected with a total of 2µg of plasmid for 18-24 hours. Cells were lysed on ice in radioimmunoprecipitation lysis buffer (1× PBS, 1% (v/v) Nonidet P-40, 0.5% (w/v) Na-deoxycholate, 0.1% (w/v) SDS, 1 mM KF, 1 mM Na_3VO_4, 10 µg/ml leupeptin, and 1 mM PMSF) followed by immunoprecipitation with anti-Flag (M2, F1804, Sigma) pre-coupled to protein-G Sepharose beads (Sigma). Both immunoprecipitate samples and lysates were immunoblotted for Flag and Myc (Ab18185, Abcam).

Supplementary figure/table titles and legends:

Figure S1 (relate to Figure 1): Tmem203 induced Cxcl2 activation is independent of MAPK pathways. The impact of MAPK inhibition on Tmem203 overexpression vs. LPS induced cxcl2 expression was investigated in RAW 264.7 cells transfected with the cxcl2-pLuc and EF1-rLuc reporters. LPS (100 ng/ml) was added for 3 hours and used to induce cxcl2 luciferase reporter. Data is presented as mean ± SEM, n=3.

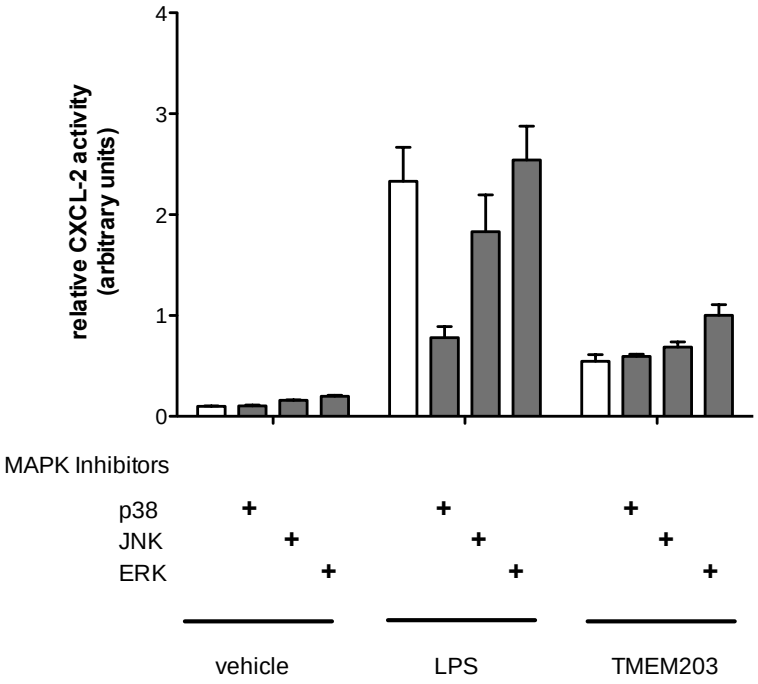

Figure S2 (relate to Figure 4): Interferon response in human and mouse macrophages.

A. Assessment of high purity primary human monocyte isolated from whole PBMC. Post monocyte isolation, monocytes, B cells and T cells were stained with fluorescence-conjugated CD14, CD19 and CD3 antibodies, respectively. Over 90% purity of CD14 positive human monocytes were assessed by flow cytometry.

B. Human monocyte-derived macrophages express CD68. CD14 positive monocytes were differentiated into macrophages with M-CSF incubation and purity was examined by blotting with anti-human CD68 and detected with Alexa Fluor® 488 conjugated goat anti-human. Scale bar = 100 µm.

C. & D. TMEM203 knockdown reduces 2'3'-cGAMP (C) and 3'3'-cGAMP (D) induced IFN-β expression in MDMs. IFN-β production of control vs. stimulated MDMs was compared in individual blood donor MDMs. Mean IFN-β mRNA levels (relative to β-actin) ±SEM are plotted from 3 biological replicates for each MDM culture.

E. DMXAA (dark) and 2'3'-cGAMP (light) induces potent IFN-β mRNA increase in iBMDMs. IFN-β production of control vs. stimulated iBMDMs was compared. Mean Ifnb1 mRNA levels (relative to b-actin) ± SEM are plotted from n=3.

G. Genotype of *Tmem203* gene in the WT and *Tmem203* knockout mice. CRISPR-Cas9 induced deletion mutation of 11 nucleotides of exon ENSMUSE00000665152 (WT *Tmem203*) to generate a knockout allele (H-Tmem203-DEL11-EM1-B6N) of C57BL/6 background mice. Genotyping information confirmed by Sanger sequencing, MRC Harwell Institute, Oxford.

H. IFN-β response in BMDM stimulated with STING ligands. BMDM isolated from WT mice were stimulated with DMXAA (50 µg/ml) (dark) or 2'3'-cGAMP (10 µg/ml) (light) for 3 h. Mean IFN-β mRNA levels (relative to unstimulated controls, not shown) ± SEM are plotted from 3 biological replicates for each BMDM culture.

A

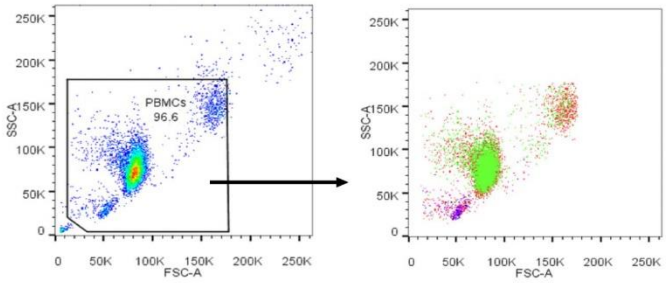

	Total	CD14	CD19	CD3
Subset	PBMCs	monocytes	B cells	T cells
Count	10735	9681	151	200
Freq. of Total (%)	96.6	91.7	1.43	1.90

B

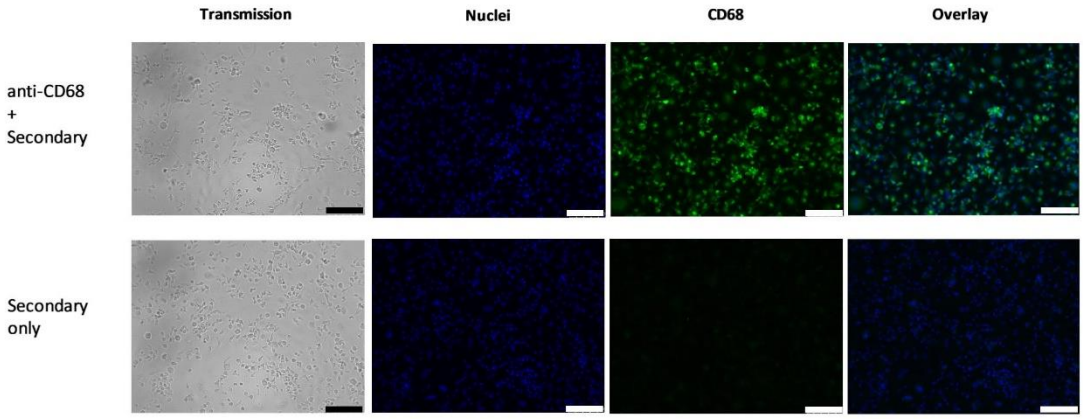

C

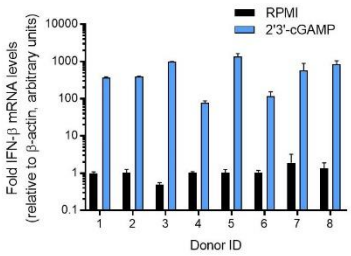

D

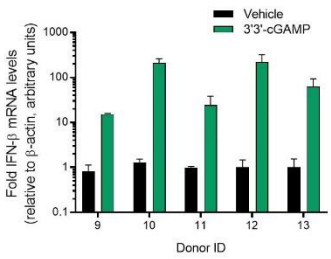

E

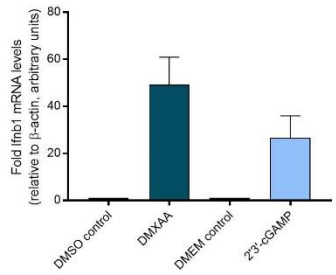

F

Tmem203 WT

ATGTTATTCTCGCTGCGGGAGCTGGTGCAGTGGCTGGGCTTCGCCACCTTTGAGATATTCGTGCACCTGCTGG
CCCTGTTGGTGTTCTCCGTACTGTTGGCACTGCGAGTGGATGGCTTGACTCCGGGCCTCTCCTGGTGGAACGT
CTTTGTGCCCTTTTTCGCCGCCGACGGGCTCAGTACCTACTTCACCACCATCGTTTCCGTTCGACTCTTCCAAGA
TGGGGAGAAGCGACTGGCTGTGCTGCGCCTCTTCTGGGTTCTCACCGTCCTTAGCCTCAAGTTTGTCTTTGAGA
TGTTGCTGTGCCAGAAGCTAGTGGAGCAGACTCGAGAGCTCTGGTTCGGCCTGATCACGTCTCCGGTCTTCAT
TCTCCTGCAGCTGCTCATGATCCGGGCTTGTCGCGTCAAC

H-Tmem203-DEL11-EM1-B6N

ATGTTATTCTCGCTGCGGGAGCTGGTGCAGTGGCTGGGCTTCGCCACCTTTG**[*11nt del*]**CACCTGCTGGCCCTGTTGGTGTTCTCCGTACTGTTGGCACTGCGAGTGGATGGCTTGACTCCGGGCCTCT
CCTGGTGGAACGTCTTTGTGCCCTTTTTCGCCGCCGACGGGCTCAGTACCTACTTCACCACCATCGTTTCCGTTC
GACTCTTCCAAGATGGGGAGAAGCGACTGGCTGTGCTGCGCCTCTTCTGGGTTCTCACCGTCCTTAGCCTCAA
GTTTGTCTTTGAGATGTTGCTGTGCCAGAAGCTAGTGGAGCAGACTCGAGAGCTCTGGTTCGGCCTGATCACG
TCTCCGGTCTTCATTCTCCTGCAGCTGCTCATGATCCGGGCTTGTCGCGTCAAC

G

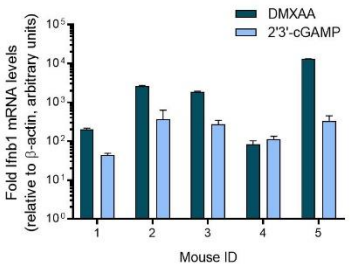

Figure S3 (relate to Figure 5) – Establishing Tmem203 knockout and Tmem203 overexpressing RAW 264.7 cell lines.

A. CRISPR/Cas9 TMEM203 Knockout RAW 264.7 cell line. CRISPR-Cas9 –directed Tmem203 knockout in RAW 264.7 cell line (KO Tmem203) showed a 3-4 -fold decrease in Tmem203 (against β-actin mRNA) expression determined by RT-qPCR and the cell line was established for further experiments.

B. Stable Tmem203 overexpression in RAW 264.7 cell line. Stable Tmem203 overexpression in RAW 264.7 cell line (OE Tmem203) showed a robust 8-fold increase in Tmem203 (against β-actin mRNA) expression determined by RT-qPCR and the cell line was established for further experiments.

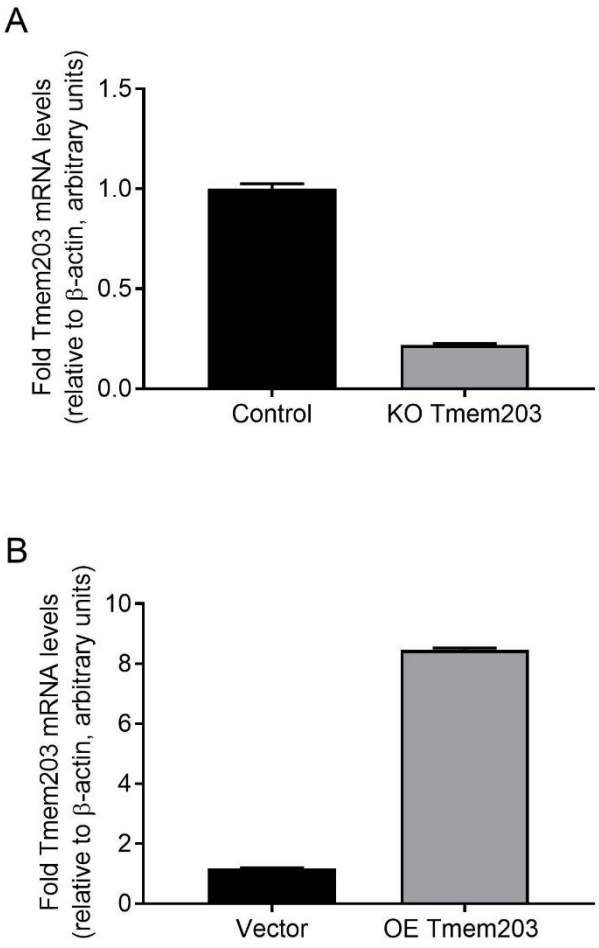
A
Fold Tmem203 mRNA levels
(relative to β-actin, arbitrary units)
1.5
1.0
0.5
0.0
Control
KO Tmem203
B
Fold Tmem203 mRNA levels
(relative to β-actin, arbitrary units)
10
8
6
4
2
0
Vector
OE Tmem203

Figure S4 (relate to Figure 6): Overexpression of Tmem203 and Sting does not induce ER stress.

S4. A-C. Venus PCA Tmem203 and Sting co-expression does not induce ER stress in HEK293 T cells. Co-transfection of Tmem203 (A) and Sting (B) Venus PCA constructs resulted in high expression of both genes but only little increase of XBP1 mRNA splicing (C).

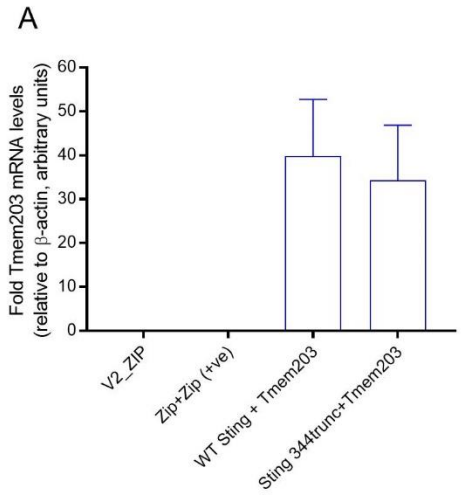
A
Fold Tmem203 mRNA levels
(relative to β-actin, arbitrary units)
60
50
40
30
20
10
0
V2_ZIP
Zip+Zip (+ve)
WT Sting + Tmem203
Sting 344trunc+Tmem203

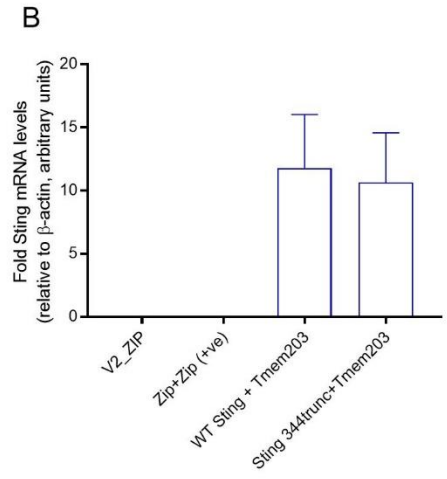
B
Fold Sting mRNA levels
(relative to β-actin, arbitrary units)
20
15
10
5
0
V2_ZIP
Zip+Zip (+ve)
WT Sting + Tmem203
Sting 344trunc+Tmem203

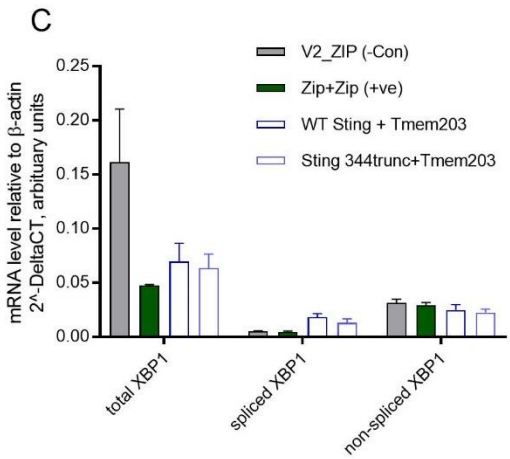
C
mRNA level relative to β-actin
2^-DeltaCT, arbitrary units
0.25
0.20
0.15
0.10
0.05
0.00
V2_ZIP (-Con)
Zip+Zip (+ve)
WT Sting + Tmem203
Sting 344trunc+Tmem203
total XBP1
spliced XBP1
non-spliced XBP1

Table S1 (relate to Figure 1): Clinical description of SLE patient cohort. A cohort of 20 patients were diagnosed with SLE and clinical data were acquired. Asterisks denote data being presented as Mean±SD (Lower:Upper interquartile range). Abbreviation: F=female; M=male; SLEDAI-2K=systemic lupus erythematosus disease activity index 2000; Anti-DNA=serum level of antibody to double-stranded DNA; C3=serum C3 complement level; C4=serum C4 complement level; NA=not available.

Age at Sampling (Years)	**Gender**	**SLEDAI-2K**	**Anti-DNA IU/ml**	**C3 mg/dL**	**C4 mg/dL**
18	F	9	151	82	10
42	F	23	151	84	11
25	F	18	220	63	7
46	F	12	12	141	29
20	F	9	45	103	7
63	F	NA	74	131	11
37	M	16	220	80	15
36	F	16	220	59	15
35	F	NA	13	111	18
49	M	16	18	135	23
56	F	30	200	75	10
54	F	15	200	53	11
35	F	30	200	21	3
31	F	18	NA	NA	NA
45	F	8	14	41	10
59	F	2	10	90	20
37	F	19	220	67	12
52	F	17	200	63	15
38	F	6	41	116	23
30	F	NA	NA	NA	NA
N=20	F:18 M:2	*15.53±7.62 (9:18)	*122.72±87.63 (29.5:200)	*84.17±32.39 (63:107)	*13.89±6.41 (10:16.5)
			Normal range: 0-20	Normal range: 90-180	Normal range: 10-40

Chapter 3: Discussion and future work for TMEM203

3.1 Discussion

Maintaining tissue homeostasis relies on the complex network of inflammatory signalling events which respond to a wide spectrum of stimuli. Since the description of Toll-like receptors a century ago [275], numerous proteins have been identified in immune regulation and thus completing our knowledge of human physiology. Novel inflammatory mediators are continuing to be discovered for their potential in therapeutic development and academic interest. Unlike the TLR-dependent pathways, other pattern recognition receptors are less well-characterised and yet of significant physiological importance. For instance, the intracellular nucleic acid sensing adaptors MAVS and STING have become the centre of research since their discovery in 2005 and 2008, respectively [276, 277]. These emerging inflammatory mediators have provided strong evidence supporting the endosomal TLRs and the cytosolic NLR-inflammasome independent sensor of cytoplasmic nucleic acids, while it also emphasises the role for mitochondria and the ER in immune regulation. This also refined the function of Golgi vesicles and lysosomes which are indispensable signalling platforms downstream of MAVS and STING in addition to the role as transport for protein and enzyme cargos [278–280].

The initial purpose of the cDNA functional screen in LPS-induced RAW 264.7 murine macrophages was to identify novel inflammatory proteins with unclear roles in controlling innate immune response, which may mediate distinct impacts of TLR activation [131]. From the screen, Tmem203 was identified as an activator of the *Cxcl2* chemokine. At the beginning of Chapter 2, our preliminary study aimed to link Tmem203 to the canonical MyD88 or TRIF dependent pathways downstream of TLR4 activation. However, our results suggested an alternative mechanism for Tmem203 action. Tmem203 is a small protein with 4 transmembrane domains and no obvious N-terminal and C-terminal cytoplasmic regions, and therefore generating a specific and high affinity antibody for immunofluorescence studies was a challenge. Despite this limitation, we constructed the mCherry-fusion protein for Tmem203 and visualised its localisation in the punctate membrane structures in HeLa cells. These structures

highly resemble the endoplasmic reticulum. As our research continued, a paper published by Shambharkar and colleagues has confirmed the ER residency of Tmem203, yet the roles for this protein was mainly discussed in the context of calcium signalling and implications for spermiogenesis [132]. Although the paper did not discuss the relevance to immune regulation, it confirmed our findings of Tmem203 ER-localisation, thus the potential to colocalise and interact with the nearby ER resident inflammatory mediators. We hypothesised that STING would demonstrate direct association with TMEM203. Although we considered MAVS as co-regulator for TMEM203, several publications have suggested that MAVS and STING crosstalk is not indispensable for their individual activation, suggesting that an interaction between mitochondria and the ER was not critical to MAVS's activation, and it was very limited at the mitochondria-associated membrane regions [206]. Even though TMEM203 could be part of signalling transduction between MAVS and STING, the role for TMEM203 in MAVS regulation could be minimal.

We have used human primary monocyte-derived macrophages as a comparable cell model to study STING activation in human. However, we were aware that donor-variation may exist in the expression level of *TMEM203*, *STING* and *MAVS* in primary cells isolated from different people. By analysing mRNA expression of these genes in MDMs from 9 individuals, a strong correlation was found between TMEM203 and STING but not with TMEM203-MAVS, although further studies of a large n>30 population is required to understand the expression relation between these genes (Appendix A1.1, page 268). Because of this donor-variation, we have also tested if siRNA transfection alone could induce immune response prior to further immune stimulations. For this, we have shown that non-specific siRNA transfection into MDMs does not induce potent type I interferon and IL-8 mRNA upregulation (Appendix A1.2, page 269), and the dose of siRNA transfection has been optimised in this primary cell type to ensure an even distribution of siRNA delivery in every cell (Appendix A1.3, page 270).

In addition to the macrophages, we have used a number of other cell models for various purposes. HeLa cells were used for all imaging STING and TMEM203

expression and colocalization for their advantage of flat morphology. We have also optimised the staining concentration of ER and lysosome and doses of V1_Sting/V2_Tmem203 co-transfection to obtain an optimal fluorescent signal and cell viability in microscopy (Appendix A1.5-1.7, page 272-274). HEK293 cells were used to study STING wildtype and mutant interaction with Tmem203 as this cell line is known to express extremely low level of STING and cGAS [281], and thus avoiding the trouble of overexpressing this gene. Although both HeLa cells and HEK293 cells were sufficient models to study protein interactions, neither of these cells were well-known to exhibit strong immune response as compared with immune cells, and therefore the studies involving STING-mediated immune response were conducted in macrophages.

Our research has repeatedly revealed that TMEM203 enhances type I interferon expression via STING but not directly. As demonstrated in Chapter 2, Fig. 3G, Fig. 5B-F, overexpression of Tmem203 only amplifies *Ifnb1* expression and TBK1/IRF3 activation in the presence of STING activation, and thus identified it as an enhancer but not an upstream activator for STING. The structure of TMEM203 does not possess functional domains to support ligand recognition and effector binding. Although data suggested that a multimeric TMEM203 structure exists, this does not rectify a lack of cytoplasmic region for functional interaction. This is also a potential reason that TMEM203 binds preferentially to the N-terminal transmembrane domains of STING, with STING acting as a signalling platform for TMEM203. However, TMEM203 overexpression primes STING trafficking to lysosomal vesicles, which is a signal for STING activation and post-activation processing [280, 282, 283]. Although it was previously reported that STING translocation can be achieved in the absence of TBK1 and IKK, a dsDNA stimulation was required to induce such dynamic [283]. Our evidence suggests a ligand-free, TBK-free translocation of STING-TMEM203 complex from the ER to lysosomal vesicles, being solely induced by the upregulation of TMEM203. It is unclear how an almost completely membrane-embedded protein is capable of directing the movement of protein complexes; the answer may relate to additional signalling cascades providing the trafficking machinery to facilitate their migration.

One possibility is related to calcium spikes which are strongly perturbed by TMEM203 overexpression [132]. A novel area was explored by Kim *et al.* demonstrating a role for STING in regulating calcium response [284]. The experiments identified a calcium spike upon DMXAA and 3'-3' cGAMP stimulations in RAW 264.7 cells. Whereas STING downregulation impairs calcium pulses induced by the ligands, the intracellular calcium chelator BAPTA-AM also inhibited DMXAA-induced STING activation. However, calcium mobilisation was not essential for cGAMP-induced STING activation, and distinct regulatory mechanisms between the two STING ligands was also indicated in our work (Chapter 2, Fig. 2G-H and Fig. 6C). Further to the authors' suggestions that cGAMP more likely activates calcium-independent STING signalling, TMEM203 obtains a high potential to link calcium transients to the type I interferon activation, opening an area to explore in relation to STING activation and trafficking in ligand-free conditions.

An alternative hypothesis for TMEM203-enhanced STING activation relates to with the confirmation change of the receptor. Several groups have reported the change of 3D structure of STING when in contact with different ligands [285–287]. STING conformation is switched between the "open-inactive" and a "close-active" forms. The contact of ligands with the dimeric ligand binding pocket alters the open structure to a closed conformation which enabled the rearrangement of C-terminal cytoplasmic tail to expose the docking sites for TBK1 and IRF3 [286, 288]. The "lid" region of STING aa 224 - 244 positions adjacent to the ligand binding site, and it was predominantly tightened by ligand recognition and highly affected by the different affinities of ligand binding [288]. This is why DMXAA can activate mouse but not human STING, and the mutation G230I renders hSTING sensitive to DMXAA binding [286]. However, ligand-independent activation of STING was observed in Sendai virus (a RNA virus) infection where activated RIG-I induce mitochondrial elongation which translates to the nearby ER membranes and promotes ER de-reticulation, a mechanism found to induce STING-mediated antiviral response [212]. The study of natural STING mutants revealed a further ligand-free activation mechanism through mutations in-between the transmembrane domains and the "lid" region. Four gain-of-function mutations, V147L,

N154S, V155M, and V155R, showed significantly enhanced ability to sustain the "close-active" conformation of STING dimer and they are constitutively phosphorylated by TBK1, promoting type I interferon signalling in the absence of ligand challenge [120]. Moreover, further cGAMP stimulation does not induce or alter the existing interferon signalling, suggesting that a conformational change is sufficient to activate STING. A prevalent loss-of-function STING variant was also identified in 20.4% human population [289]. This HAQ mutant, R71H-G230A-R293Q, showed a lower intrinsic NF-κB promoter activity and a reduced IFN-I response to bacterial cyclic dinucleotides. These three mutations individually lie within the transmembrane domain, "lid" region, and the ligand binding domain, was proposed to alter C-terminal conformation that clamps c-di-GMP, thus incurring the impaired interferon signalling functions. All the evidence supports the idea that conformation change critically regulates STING activation, and the specific STING ligands can induce such changes.

To address how TMEM203 may impact on this STING activation, our protein complementary assays and co-immunoprecipitation experiments shown in Chapter 2, Fig. 6E and 6H have demonstrated a strong association between TMEM203 and the N-terminal domain of STING. The addition of STING's dimerisation domains (DD) to its transmembrane domains (TM) enhanced its interaction with TMEM203 even though the protein level of STING is impaired. As described above, this region is involved in the reorganisation of the cytoplasmic domains and STING activation. It is speculated that our over-expansion of TMEM203 could be facilitating the "close-active" conformation of STING. Nonetheless overexpression of TMEM203 alone did not induce type I interferon activation (Chapter 2, Fig. 3G & 5D), we believe that it is more likely to help stabilise ligand-bound STING, and thus sustain and prolongate the downstream interferon activation. On the other hand, reduced TMEM203 level may affect STING structural stability which does not abolish the type I interferon expression but significantly impaired the amplitude (Chapter 2, Fig. 4), and potentially also incurs early signalling attenuation.

3.2 Future work

Our work has demonstrated that STING-dependent type I interferon expression is regulated by the novel proinflammatory mediator TMEM203. The function of TMEM203 was previous reported to relate to calcium signalling, while our data strongly support a previously unidentified immune regulatory role. As my project mainly investigated the role for TMEM203 and STING IFN-I induction, a number of areas could be explored regarding the additional functions of TMEM203.

One area to expand is the LPS-induced TMEM203 upregulation, initially discovered in the cDNA functional screen in RAW 264.7 cells. As the project evolved, STING became the priority area of research, but questions remain as to how TMEM203 expression is upregulated by LPS stimulation and whether TMEM203 acts as the intermediate platform for crosstalk between LPS/TLR and STING pathways. There is a lack of strong evidence for STING and TLR signalling communication, although an intact microbe presents multiple PAMPs that can be recognised by several PRRs. For example, the bacterium *Brucella abortus* is able to activate both TLR/MyD88 and RNA polymerase III/STING pathways [290]. Further experiments could explore the function of TMEM203 in the context of LPS-induced inflammation and address the mechanistic pathways of STING regulation. This area is of significant interest to link complex antimicrobial immune signalling between STING and TLR.

Commercial purified STING ligands (Invitrogen) were used throughout experiments as the focus was to identify and monitor the interaction between TMEM203 and STING, and thus the use of complex microorganism was not required. However, human physiology almost never encounters clean bacterial molecules, but rather as biologically active organisms that can change and interact with host system. It is yet unclear whether complex immune stimuli may induce alternative TMEM203 activation other than pathway via STING. The aspect of TMEM203-dependent chemokine upregulation by LPS challenge was under-addressed, and questions arise as whether TMEM203 can switch between signalling routes in response to different immune challenges. Furthermore, the mechanism underlying re-localisation of TMEM203 induced by LPS was unclear (Chapter 2, Fig. 3A-B). Whether LPS or other bacterial

ligands could promote TMEM203 translocation to lysosomes and thus potentiates STING activation will require further investigation.

In Chapter 2, we have extensively investigated the localisation and translocation of TMEM203 and TMEM203-STING complex to provide reason for their interaction in immune activation. However, limited by the little cytosolic exposed region in TMEM203, our investigation on TMEM203 relies solely on the expression of fusion plasmids which inevitably resulted in the overexpression of this gene. Overexpression of ER proteins has been implicated in unfolded protein stress response which disturbs the physiological condition of the organelle, creating an additional variable in the experiment system [291, 292]. To eliminate the possibility, we have measured the transcriptional splicing of XBP1 as an indicator of ER stress unfolded protein response (UPR), and little stress event was detected (Chapter 2, Fig. S4). Despite this, TMEM203 upregulation could possibly induce calcium perturbation and showed an intracellular localisation pattern of its post-activated state [132]. A specific anti-TMEM203 antibody will be required to solve this problem, as well as to quantify the protein levels in *TMEM203* knockdown experiments in human monocyte-derived macrophages (Chapter 2, Fig. 4A-B). More importantly, the time and spatial regulation of TMEM203 will be better characterised with antibody labelling which may reveal differential trafficking strategies to various immune challenges.

Protein complementation assay was frequently used in this project to investigate protein-protein interaction. This technique shown in Chapter 2 Fig. 6A-C has helped us to quantify molecular interaction in living cells. Although cells are monitored in a short 30-minute period under restricted CO_2-free condition, we were able to capture the association of proteins at 2.5 to 5-minute time points. Such assays can be developed into tools for *in vitro* drug screen [293, 294]. The advantage of this experiment was to compensate the unspecific false positive protein interactions reveal by a protein-only screen test, as live-cell drug screen ensures that proteins are available in the native cellular environment with all potential influence of natural inhibitors and scaffolding proteins, and it also assesses the permeability of drugs across the plasma membrane. Combining this live-cell assay with hi-throughput

analysis [294] can be both effective and accurate in validating pharmacological influence on protein association in a real physiological setting. Similar live-cell based PCA has already been used to screen protein interactions using the reporter of dihydrofolate reductase (DHFR) to reflect protein interactions by yeast growth under different chemical conditions [295]. In comparison, our system is superior in rapid detection of protein interactions via luciferase reporter, and hence it can precisely distinguish both the strength and duration of interaction.

Although the interaction and functional relevance between STING and TMEM203 has been established, we have to acknowledge that much is unknown about the activities of TMEM203 in regulating inflammation. It is still unclear whether TMEM203 is a stabiliser of STING dimerisation and functional conformation, whether TMEM203 also couples to additional receptors or ion channels (most likely calcium channels), and whether TMEM203-STING interaction is a promising therapeutic target for STING deficiency or over-activation. Although we have analysed the level of *TMEM203*, *STING* and *MAVS* in T cells isolated from a cohort of treatment naïve patients, it still remains unclear how these genes contribute to or affected by this pathology, or if there are other cell types that can better represent the roles of these interferon regulators. Particularly, patient-derived T cells were activated by PHA (phytohaemagglutinin) prior to TMEM203 and STING mRNA measurement, and its potentially impact to T cell characteristics and interferon response should be addressed in future. Although we have demonstrated the role for TMEM203 and STING in a variety of macrophage models, it is crucial to ascertain whether they have similar functions in other type I interferon-producing cells, particularly T cells which largely contribute to SLE [139]. Furthermore, a loss-of-function STING HAQ (R71H-G230A-R293Q) variant has been identified to show 90% reduction in the ability to activate IFN-β signal in response to *Legionella pneumophila* and bacterial STING ligands [296]. The series of mutations occurs in the transmembrane domain and ligand binding domain of STING which impairs but not completely abolishes STING's ability to become activated. Thus, the HAQ mutant would likely alter STING's ability to dimerise and interact with TMEM203. Questions also remain to the potential of single nucleotide polymorphisms (SNPs) in TMEM203 gene, nevertheless there was none discovered at present, this would be worth investigating in future.

Particularly, since STING overactivation can cause autoimmunity and its deficiency increases infection susceptibility, the challenge for targeting STING therapeutically is to identify the fine balance for its activation and inactivation. Based on our evidence, TMEM203 has the potential to be a surrogate for STING intervention because of its ability to alter but not complete abolish STING signalling. This can ideally prevent excessively immunodeficiency and renders the host certain ability to exhibit interferon response. Further studies on the human and mouse STING orthologues can also inform us how the TMEM203-dependent regulation in these two species will likely be comparable or distinct in antiviral response. In general, the discovery of TMEM203 has widened our knowledge on inflammatory signalling and has added a substantial piece of evidence to address the importance of STING-regulated immunity.

Chapter 4 (Paper 3): STING regulation in response to Zika virus and Dengue virus infection in primary human monocyte-derived macrophages.

Authors: **Yang Li**[1], Elodie Décembre[2], Endre Kiss-Toth[1] & Marlène Dreux[2].

Affiliations:

1: Department of Infection, Immunity and Cardiovascular Disease, University of Sheffield, Beech Hill Road, Sheffield, S10 2RX, UK

2: CIRI, Inserm, U1111, Université Claude Bernard Lyon 1, CNRS, UMR5308, École Normale Supérieure de Lyon, Univ Lyon, Lyon, France

Status: Submitted as EMBO short-term fellowship end report (STF_7459).

Authors' Contribution:

My supervisors Prof. Endre Kiss-Toth and Dr Marlene Dreux helped me designing the experiments. Elodie Décembre conducted all the virus infection work and infected-cell harvest with the help from Séverin Coléon and Vicent Grass in Dr Dreux's lab. I generated all the results for gene analysis and wrote the manuscript. All authors except for Elodie were involved in the analysis and interpretation of results, and the editing of the manuscript.

EMBO Short-term Fellowship End Report

Recipient: Ms Yang Li, PhD student.

[1]Home Institute: University of Sheffield, Department of Infection Immunity & Cardiovascular Disease. Prof. Endre Kiss-Toth & Dr Heather L Wilson.

[2]Visiting Institute: CIRI, INSERM U1111, ENS Lyon. Dr Marlene Dreux.

Fellowship ASTF reference: 7459.

Research Period: 15 January 2018 to 16 March 2018 (9 weeks)

STING regulation in response to Zika virus and Dengue virus infection in human primary monocyte-derived macrophages

Authors:

Yang Li[1], Elodie Décembre[2], Endre Kiss-Toth[1] and Marlene Dreux[2].

Keywords:

STING, Zika virus, Dengue virus, Type I interferon, Macrophage.

Abbreviations:

2'3'-cGAMP: Cyclic 2'3'-guanosine monophosphate–adenosine monophosphate

DENV: Dengue virus

GTC: guanidinium thiocyanate citrate

Hpi: Hour(s) post infection

IRF3: Interferon regulatory factor 3

ISG15: Interferon stimulated gene 15

M-CSF: macrophage-colony stimulating factor

MDM: (human) monocyte-derived macrophages

MOI: Multiplicity of Infection

MxA: MX Dynamin Like GTPase 1

NS2B/3: non-structural protein complex 2B/3

RIG-I/MAVS: Retinoid acid-inducible gene I/ Mitochondrial antiviral signalling protein

RT-qPCR: RealTime-quantitative polymerase chain reaction

STING: Stimulator of Interferon Genes

TBK1: TANK-binding kinase

ZIKV: Zika virus

Abstract:

Dengue virus (DENV) is a member of the family *Flaviviridae* which poses major health threats. The signalling by the DNA sensor cGAS and adaptor Stimulator of Interferon Genes (STING) is critical for the host antiviral response against DENV, notably via the production of type I interferon (IFN) and IFN stimulated genes (ISG). Nonetheless, this signalling is targeted by the viral proteases, leading to immune evasion. Zika virus (ZIKV) is an emerging flavivirus that causes neurological disorders in foetus and adults. As ZIKV and DENV are genetically closely related, ZIKV is predicted to share similarities with DENV for its interaction with host factors. ZIKV can infect placental tissue macrophages and this greatly contributes to *in utero* transmission and foetus disease. Thus, we investigated whether ZIKV and DENV infect human primary monocyte-derived macrophages and addressed the potential involvement of STING. Our results revealed that active viral replication of both viruses induces a potent type I IFN/ISG response and that the level of STING can impact the degree of virus-mediated ISG upregulation.

Introduction:

Members of the Flavivirus including Zika virus (ZIKV) and Dengue virus (DENV) cause human pathologies globally. These genetically closely related viruses belong to the *flavivirus* genus and are both transmitted by mosquito bites. In its severe form, DENV induces severe hemorrhagic fever and shock syndrome. In contrast, ZIKV infection was thought to be primarily asymptomatic; however, recent epidemics have led to foetal demise and detrimental neurological development, i.e., microcephaly in newborns and Guillain–Barré syndrome in adults (rapid-onset of muscle weakness caused by immunological damage on the peripheral nerve system) [1–3]. Seeking mechanisms of protection against these viral infections is of significant medical demand.

Type I interferons (IFNs) are potent antiviral host effectors against viral infections [4]. Stimulator of Interferon Genes (STING) and its downstream effectors TANK-binding kinase (TBK1) and interferon regulatory factor 3 (IRF3) form a key antiviral signalling cascade that notably regulates type I IFN response [5–7]. The upstream DNA sensor cyclic GMP-AMP synthase (cGAS) and STING mediate an immune response dependent on the recognition of mitochondrial DNA released in the cytosol upon DENV infection [8]. Nonetheless, DENV has evolved mechanisms to inhibit and evade this host response, including the proteolytic cleavage of STING and cGAS by the viral NS2B/3 protease complex, leading to blunted type I IFN induction [9, 10]. STING inactivation is critical to ensure viral replication in the host cells [9, 10] and might contribute to host species restriction [11]. Reversing or blocking STING inhibition could, therefore, offer a potential therapeutic approach to combat DENV and other related flavivirus infections.

Interestingly, the cGAS/STING pathway is known as a critical antiviral signalling mechanism in monocytes/macrophages [11–15]. Previous reports suggested that placental tissue macrophages contribute to ZIKV transmission from mother to foetus [12, 16]. Owing to the high level of sequence homology between DENV and ZIKV genome, their known interactions with host factors and the viral replication cycle also display high similarities [17–19]. Along this line, a recent report demonstrated that ZIKV cleaves STING in fibroblasts in a species-restricted manner [20]. This study has also pointed out the conservation between ZIKV and DENV in the cleavage target of human STING and the mechanism of action of their NS2B/3 protease complexes, suggested it was logical to compare ZIKV with DENV in virus research.

Abundant recent research on Dengue virus have focused on its infectivity and regulation in primary human T cells, dendritic cells (DC) and plasmacytoid DCs [21–23] whereas few has investigeted how human macrophages contribute to viral pathology. This is potentially due to that macrophages produce less interferons than the previously mentioned cell types [22]. Macrophages are also plastic cells that show heterogeneous response to stimuli when they are in different tissue environments. The most well described M1 and M2 phenotypes distinguish macrophage subsets into the “pro-inflammatory” or the “pro-resolution” states, respectively, which often impact differently on the cellular response to microbial infections [24, 25]. In contrast to various of macrophage differentiation techniques, macrophage colony-stimulating factor (M-CSF) is most well-known for its role in consistent monocyte-macrophage differentiation *in vitro* compared to that by granulocyte-macrophage colony-stimulating factor (GM-CSF) [26, 27]. Differentiation by these two cytokines does not clearly polarise the cells to a well-defined M1 or M2 phenotype. Whilst it has been discovered that both growth factors cause similar level of type I interferon secretion in DENV-infected cells, GM-CSF can additionally activate potent inflammasome-mediated interleukin-1 response [27, 28]. Although GM-CSF promotes macrophage sensitivity to Dengue virus, it also causes more complex immune crosstalk between macrophages and multiple cytokine-stimulating pathways are involved in the regulatory process. For an accurate characterisation of the role of type I interferon signalling in Dengue-infected human macrophages, M-CSF has the advantage of creating a simple cell model that best depicts this biological event.

Therefore, we here investigated the importance of ZIKV-induced host response in human monocyte-derived macrophages differentiated by M-CSF. We aim to define the potential interplay between ZIKV and the cGAS/STING-induced antiviral response that shapes viral replication in this cell model. We will also address the susceptibility of M-CSF -MDMs to DENV and ZIKV infection and to compare and contrast the infection-induced type I interferon stimulated response. These assessments will be used to understand the antiviral activation of cGAS/STING signalling against these viral infections.

Results:

ZIKV/DENV infection in human monocyte-derived macrophages (MDMs) induce a potent ISG response

Myeloid cells / monocytes are known to efficiently respond to different viruses and other stimuli via the cGAS/STING pathway [11–15, 33, 34] and they represent key cellular targets for ZIKV/DENV infection. We thus first aimed to validate a cell system for infection by ZIKV and DENV and for subsequent assessment of host responses (Fig. 1A). Human blood isolated monocytes were cultured *ex vivo* in the presence of M-CSF, which is known to induce their differentiation to macrophages (MDMs). These naïve macrophages do not exhibit clearly defined M1/M2 phenotypes in the absence of IFN-γ and IL-4 [35]; although literature shows that M-CSF derived macrophages become IFN promoting [36, 37] and display cGAS/STING activation upon human cytomegalovirus infection [38]. After 6 days of culture, cells were infected by ZIKV at different multiplicity of infections (MOIs). Our results demonstrate that ZIKV RNA levels increased over-time in MDMs, thus reflecting viral replication (Fig. 1B). The levels of ZIKV RNA amplification were in keeping with the MOI applied. Interestingly, ISG15 and MxA expression was potently induced upon ZIKV infection, as detected as early as 24 hpi and persisting at 72 hpi. (Fig. 1C-D).

Next, we compared the viral infectivity and the host response to ZIKV versus DENV infection (MOI of 1) and assessed the level of ISG expression in a 3 day-kinetic analysis post-infection. For this donor, ZIKV and DENV replication levels in MDMs were similar (Fig. 1E-F) with a peak of viral RNA detected at 24 hours and decreased at 72 hpi. However, the kinetics of viral replication in this donor (Fig. 1B-C) were different from that detected in the previous donor (Fig. 1E-F at MOI of 1), the difference was likely due to the variation of infection susceptibility between different primary macrophages. Nonetheless, marked ISG induction was consistently observed upon ZIKV and DENV infection in MDMs and maintained over time despite the decrease of viral RNA load observed at 72 hpi (Fig. 1G-H). M-CSF differentiated human macrophages have been reported to exhibit a potent interferon response to Dengue infection [39] whereas other macrophage cultures were less permissive for Dengue [9, 10]. Together our results suggest that this cell model is susceptible to ZIKV and DENV infections and constitute a stable human cell model to study type I interferon-mediated ISG induction in primary human macrophages due to these viral infections.

Figure 1: ZIKV/DENV infections in human monocyte-derived macrophages (MDMs) induce a strong ISG response.

A. Schematic representation of experiment timeline.

B. At day 6 post isolation from a healthy donor, MDMs were infected or not with ZIKV at multiplicity of infection (MOI) of 0.2, 1 and 2, and cells were assessed for ZIKV intracellular RNA levels by RT-qPCR at 2, 24 and 72 hours post infection (hpi).

C, D. Interferon-stimulated genes (ISG) ISG15 (B) and MxA (C) induction was assessed in MDMs upon ZIKV infection at the indicated MOIs and times post-infection. The mRNA expressions were compared to the uninfected control cells. Gene mRNA expression levels were assessed by RT-qPCR and presented as in A.

E, F. MDMs isolated from a healthy donor were mock infected or infected with ZIKV (E) or DENV (F) at MOI of 1 and viral RNA levels were assessed by RT-qPCR at 2, 24 and 72 hpi.

G, H. MDMs were infected as in Fig. 1E&F and ISG15 (G) and MxA (H) mRNA levels were assessed in ZIKV and DENV infected MDMs at 2, 24 and 72 hpi by RT-qPCR. ISGs mRNA expressions were compared to the uninfected control cells. Data is presented as Genome equivalent (GE) per µg of total RNA. All figures were plotted from n=1 donor, 2 technical repeats, mean±SD.

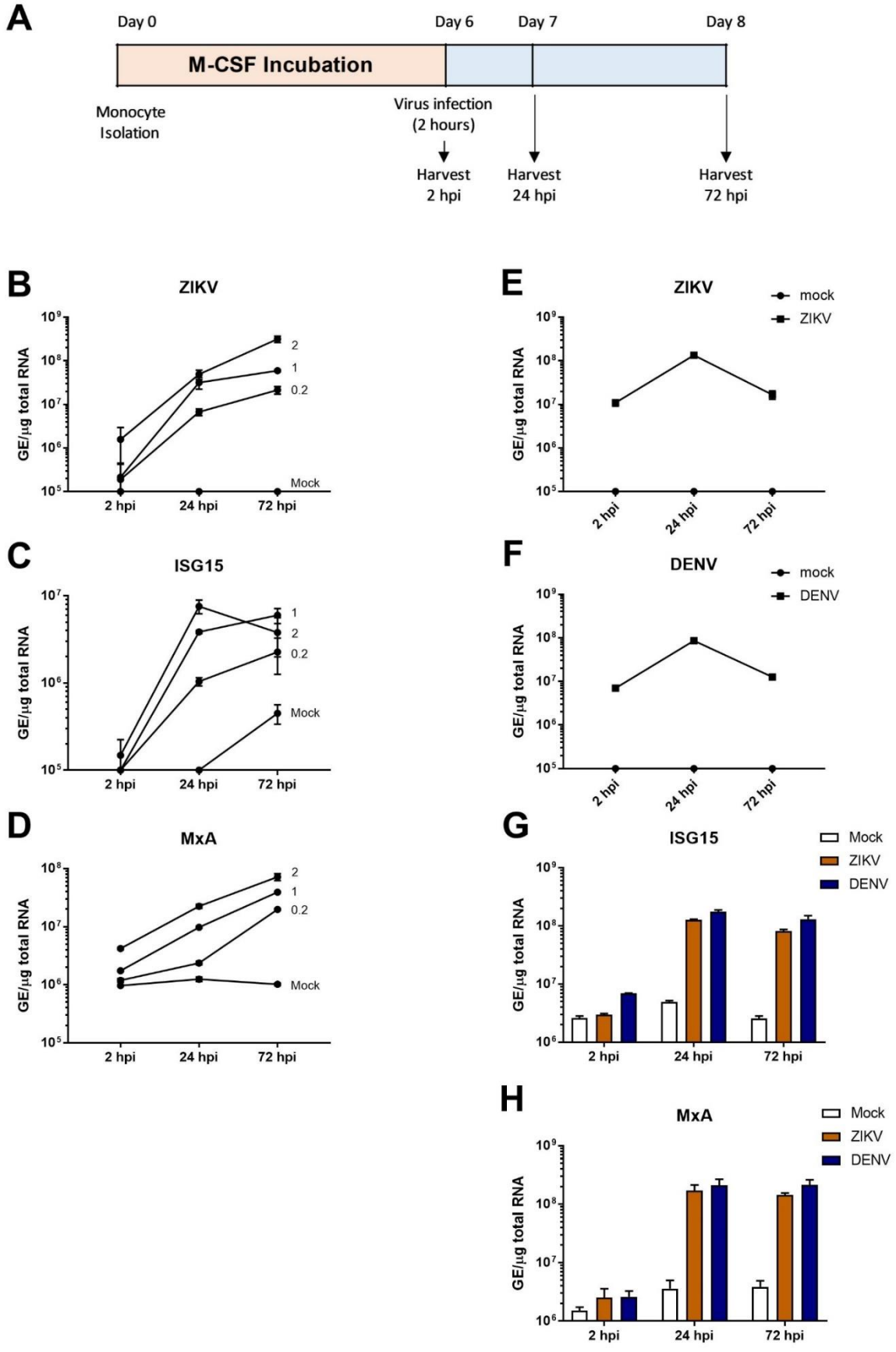
A
Day 0
Day 6
Day 7
Day 8
M-CSF Incubation
Monocyte Isolation
Virus infection (2 hours)
Harvest 2 hpi
Harvest 24 hpi
Harvest 72 hpi
B
ZIKV
GE/µg total RNA
2
1
0.2
Mock
2 hpi
24 hpi
72 hpi
C
ISG15
D
MxA
E
ZIKV
mock
ZIKV
F
DENV
mock
DENV
G
ISG15
Mock
ZIKV
DENV
H
MxA

ISG activation in MDMs is induced upon replication of ZIKV/DENV.

Since previous reports indicated that the cGAS/STING/JAK/STAT axis is induced upon modification of the mitochondria [8, 40], we next asked whether active viral replication is required to induce antiviral responses in MDMs. Human macrophages were infected with active or UV-inactivated ZIKV/DENV (Fig. 2A). UV radiation is widely used to abolish viral activities by permanently and chemically damage their genome [41]. As expected, UV-inactivated ZIKV and DENV viruses have demonstrated limited ability to replicate (Fig. 2 B-C) and were unable to induce ISG expressions in MDMs compared to the replication competent viruses (Fig. 2D-E). Therefore, this study reveals that the replication of ZIKV and DENV is required for the stimulation of type I interferon–mediated response in MDMs, in agreement with the proposed activation mechanism of cGAS/STING signalling.

Figure 2. The induction of ISG is dependent on viral replication.

A. Schematic representation of experiment timeline.

B, C. MDMs isolated from a healthy donor were infected with mock, UV-inactivated or replication-active ZIKV (B) and DENV (C) at MOI of 2 for 2 h and viral replication was assessed by RT-qPCR at 24 hpi.

D, E. MDMs were infected with ZIKV or DENV as above and the mRNA inductions was assessed for ISG15 (D) and MxA (E) by RT-qPCR at 24 hpi. Data is presented as Genome equivalent (GE) per µg of total RNA. All figures were plotted from n=1 donor, 2 technical repeats, mean±SD.

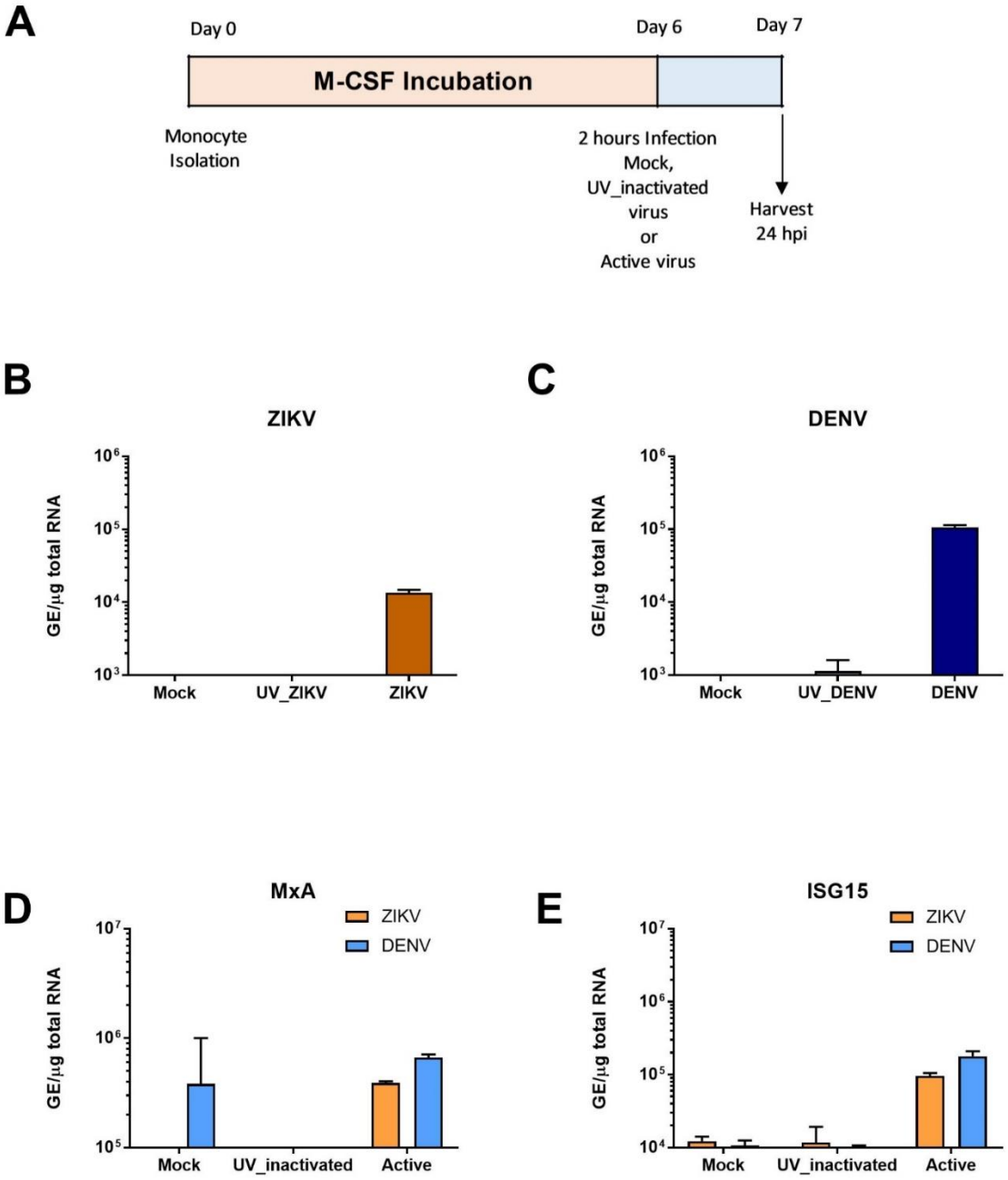
A
Day 0
Day 6
Day 7
M-CSF Incubation
Monocyte Isolation
2 hours Infection Mock, UV_inactivated virus or Active virus
Harvest 24 hpi
B
ZIKV
GE/µg total RNA
Mock
UV_ZIKV
ZIKV
C
DENV
GE/µg total RNA
Mock
UV_DENV
DENV
D
MxA
ZIKV
DENV
GE/µg total RNA
Mock
UV_inactivated
Active
E
ISG15
ZIKV
DENV
GE/µg total RNA
Mock
UV_inactivated
Active

ZIKV/DENV infection does not impair STING activation by cGAMP

Given the previous evidence indicating that the DENV-secreted NS2B/3 protease complex targets the STING-cGAS axis and thus type I interferon signalling [9, 10], we next addressed whether ZIKV, similar to DENV, inhibits STING-activated ISG expression in primary macrophages. We infected MDMs with ZIKV for 24 hours followed by 6 hours of STING stimulation with 2'3'-cGAMP (Fig. 3A), the level of viral replication and ISG induction were assessed by RT-qPCR. Upon ascertaining the replication of ZIKV (Fig. 3B), STING-dependent ISG expression was found not impaired by the prior ZIKV infection (Fig. 3C-D). Nonetheless, 2'3'-cGAMP was able to promote ISG expression to a seemingly saturated level, which could potentially cover/outcompete the underlying viral antagonism of the interferon response. This result was validated in MDMs isolated from a different donor to that of the DENV infection (Fig. 3E-J). After assessing the same parameters, we reached the same conclusion that the competent replication of both ZIKV/DENV (Fig. 3E&H) did not result in suppression of cGAMP-STING –mediated ISG expression (Fig. 3F-G & I-J). We therefore suggest that STING activation in M-CSF-treated macrophages was unaffected by pre-infection of ZIKV and DENV, at this time point post-infection. Possibly, the absence of virus-mediated STING antagonism could be due to an insufficient infection establishing period, and/or a restricted number of infected cells in the total MDM population or alternatively due to an alternative ISG signalling mechanism being activated by 2'3'-cGAMP.

Figure 3: The activation of ISG expression by cGAMP was not inhibited by ZIKV and DENV infection.

A. Schematic representation of experiment timeline.

B. MDMs isolated from a healthy donor were mock infected or infected with ZIKV at MOI of 2 for 24 h and further treated with 4 µg/ml 2'3'-cGAMP for 6 h before being assessed for ZIKV replication by RT-qPCR at 30 hpi.

C, D. MDMs were treated as in Fig. 3A and ISG15 (B) and MxA (C) mRNA levels were assessed by RT-qPCR post treatment.

E-G. In another donor, MDMs were treated as in Fig. 3A and the gene level of ZIKV (E), ISG15 (F) and MxA (G) levels were assessed by RT-qPCR post treatment Data is presented as Mean±SD, n=2.

H-J. MDMs isolated from a healthy donor (same as in Fig. 3E) were mock infected or infected with DENV at MOI of 2 for 24 h and further treated with 4 µg/ml 2'3'-cGAMP for 6 h before being assessed for DENV replication by RT-qPCR at 30 hpi (H). ISG15 (I) and MxA (J) mRNA inductions were assessed by RT-qPCR. Data is presented as Genome equivalent (GE) per µg of total RNA. All figures were plotted from n=1 donor, 2 technical repeats, mean±SD.

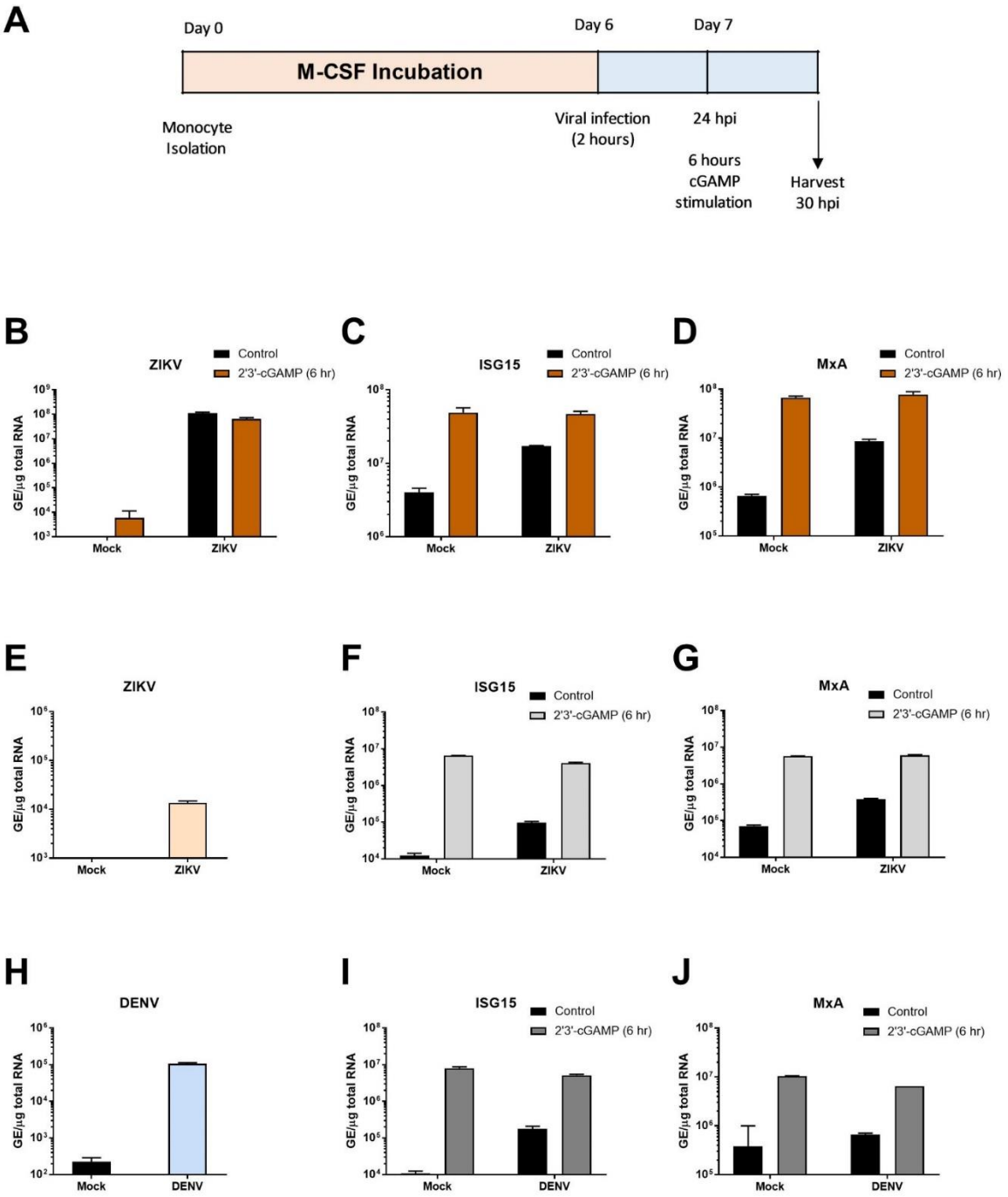
A
Day 0
Day 6
Day 7
M-CSF Incubation
Monocyte Isolation
Viral infection (2 hours)
24 hpi
6 hours cGAMP stimulation
Harvest 30 hpi
B
ZIKV
C
ISG15
D
MxA
E
ZIKV
F
ISG15
G
MxA
H
DENV
I
ISG15
J
MxA
Control
2'3'-cGAMP (6 hr)
GE/µg total RNA
Mock
ZIKV
DENV

STING regulated ZIKV/DENV infection in MDMs

Next, we investigated how STING contributes to the regulation of virus-induced ISG response. To address this, MDMs derived from two donors were transfected with STING suppressing siRNA (or control siRNA) followed by 24 h and 72 h of infection with either ZIKV or DENV virus (Fig. 4A). Due to the 48 h extension to the culture time for the siRNA treatment, an ISG response stimulated by 2'3'-cGAMP was tested in MDMs as a positive comparison to ascertain the induction of interferon response and the efficiency of *siSTING* (Supplementary Fig. 1A-B). Both ISG15 and MxA mRNA levels were induced by the ligand and were inhibited by STING downregulation, indicating that MDMs at day 8 post M-CSF incubation remain responsive to immune stimuli. Next, we investigated how *siSTING* impacts ISG expression. From our observation, we revealed that the downregulation of STING suppressed ISG expression of virus-infected macrophages in Donor 1 (Fig. 4B-C) but not in the donor 2 (Fig. 4D-E). This result suggests that cGAS/STING signalling might contribute to the induction of ISG response upon ZIKV/DENV infection, yet other pathways may still have a role depending on the donor and/or differentiation state of the MDMs and/or the level of viral replication. Moreover, consistent responses were found between the two viruses in terms of the induction of STING-ISG axis and the response to STING downregulation, indicating that these two viruses might similarly induce the antiviral host pathway.

Figure 4: STING regulated ZIKV/DENV infection in MDMs.

A. Schematic representation of experiment timeline.

B, C. MDMs isolated from Donor 1 were transfected with Control or siSTING and then mock infected or infected with ZIKV/DENV at MOI of 1 and ISG15 (B) and MxA (C) were assessed by RT-qPCR at 24 hpi and 72 hpi.

D, E. MDMs isolated from Donor 2 were transfected with Control or siSTING and then mock infected or infected with ZIKV/DENV at MOI of 1 and ISG15 (B) and MxA (C) were assessed by RT-qPCR at 24 hpi and 72 hpi. Data is presented as Genome equivalent (GE) per µg of total RNA. All figures were plotted from n=1 donor, 2 technical repeats, mean±SD.

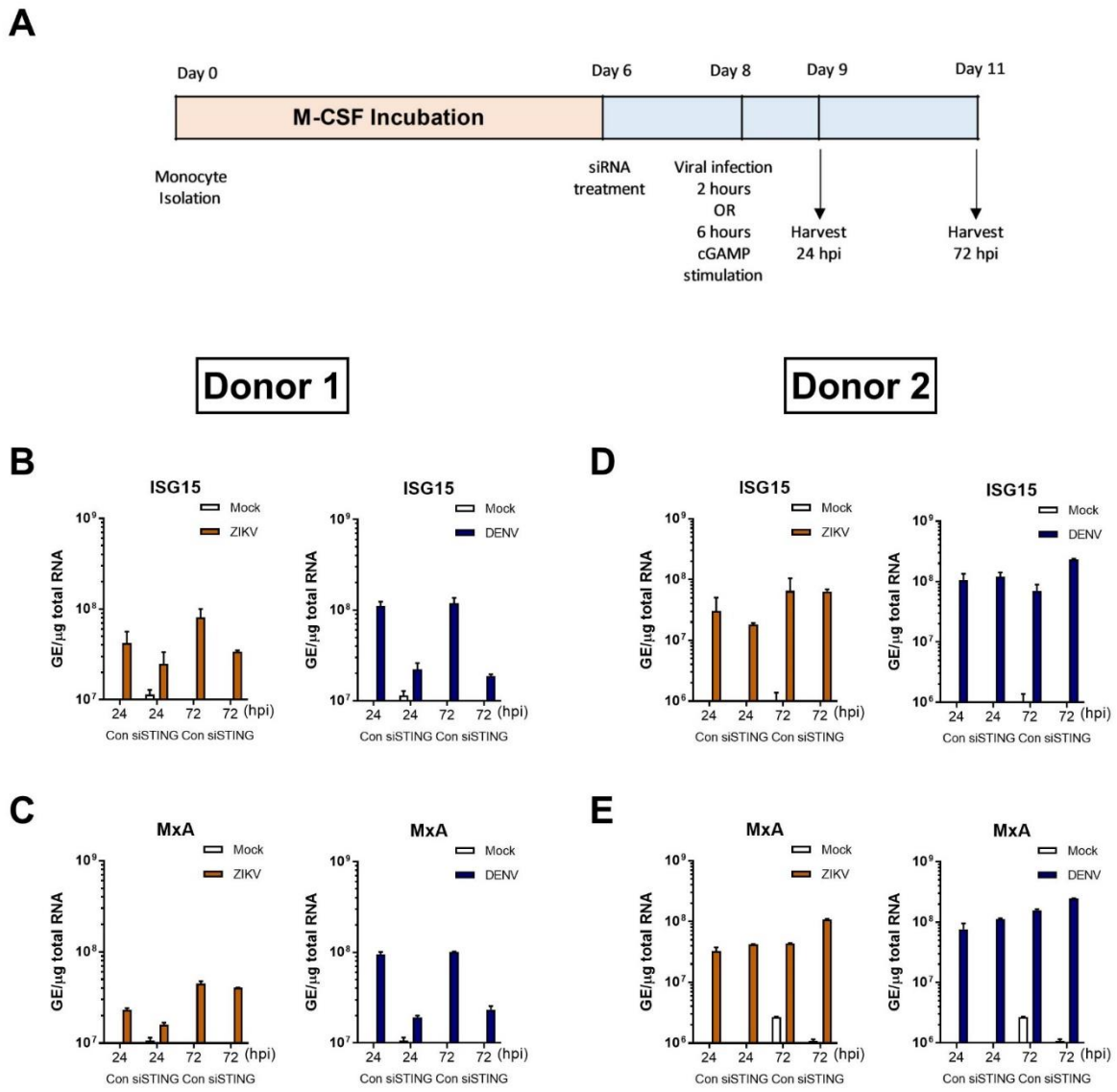
A
Day 0
Day 6
Day 8
Day 9
Day 11
M-CSF Incubation
Monocyte Isolation
siRNA treatment
Viral infection 2 hours OR 6 hours cGAMP stimulation
Harvest 24 hpi
Harvest 72 hpi
Donor 1
Donor 2
B
ISG15
Mock
ZIKV
DENV
GE/µg total RNA
24 24 72 72 (hpi)
Con siSTING Con siSTING
C
MxA
D
E

Discussion:

Species of the Flavivirus family pose a major infectious threat to the tropical world. Unlike Dengue and Yellow fever viruses, Zika virus is an emerging member of the family that came to the center of research due to its ability to uniquely invade the nerve system and to transmit *in utero*. From literature, type I interferons are critical for innate immune protection against viral infection, which are induced by the cytoplasmic sensing mechanism of viral nucleic acids or mis-localised host DNAs (in the context of cGAS/STING) [5–8]. Notably, the type I interferons (IFN-I) response acts against virtually all viruses and is often inhibited/manipulated by viruses to enhance their replication. One of the critical type I interferon-inducing pathway is mediated by the adaptor protein Stimulator of Interferon genes (STING) and its upstream cytosolic DNA sensor GMP-AMP synthase (cGAS). Since DENV is known to evade host response by targeting cGAS-STING for degradation, it is logical to assess whether the related Zika virus also regulates or is being regulated by STING activities.

DENV is known to infect a variety of myeloid cells, especially monocytes and T cells, whereas little was studied on ZIKV's infectivity in haematopoietic cells, except that it was discovered to invade human placental macrophages [16]. A number of DENV infection model adopt differentiation method using GM-CSF to enable macrophages to be more permissive to virus infection [9, 10, 27, 42]. However, the complexion of type I interferon and inflammasome signaling in this cell model [27, 28] can potentially influence with each other and thus interfere our analysis of STING activation and ISG response. In contrast, M-CSF is critical for the homeostasis of macrophage functions and it maintains the resting state of macrophages until immune challenge [26, 27]. Most importantly, M-CSF regulation is at the heart of maintaining placental development and the formation of immune defense by the local macrophages [43–45]. Therefore, to best address the role of STING regulation in DENV/ZIKV infected human macrophages, M-CSF has the superiority over the GM-CSF culture condition to address this question.

Given that M-CSF differentiated macrophages were used in few DENV studies [28], our work first aimed to characterise that these cells are permissive and sensitive to DENV and ZIKV infections, and they elicit considerable amount of type I interferon stimulated genes. We tested the dose and time upon which ZIKV infects MDMs and showed that the viral replication has rapidly occurred within 24 hours post infection. Resolution of infection was observed at 72 hpi but a high ISG mRNA level was maintained over this period. However, our observation of a potent induction of ISG expression was contradictory to previous research that suggested

STING inhibition by DENV [9, 10], still the MDM culture conditions by the different colony stimulating factor could largely influence the cells' ability to respond to virus infections. Thus, our method seemed to render macrophages DENV/ZIKV susceptibility for a longer period of time compared to Aguirre's model [9].

Secondly, we identified that the activation of ISG response by both ZIKV and DENV predominantly depends on active replication. Aguirre and Yu have reported that DENV antagonizes and evades STING and the subsequent type I interferon signaling [9, 10, 46] whilst other groups also showed that Dengue virus can induce the interferon axis in macrophages [27, 47]. In our study, at 24 hpi, neither ZIKV and DENV were able to intercept STING activation by its endogenous ligands, and consequently the ISG production remained significant with or without viral infection. Again, these observations contradicted to the STING cleavage model by DENV infection [9, 10] and thus confirmed that our M-CSF / MDM model has allowed the macrophages to be immune responsive to both virus infections. Additionally, evidence suggests that DENV and ZIKV block multiple components of the cGAS/STING/IFN cascade [9, 10, 20, 48–50], potentially because a single inhibition can be easily overcome by our immune amplification. Our challenge with cGAMP is a precise and potent activation mechanism of STING which bypasses the viral protease degradation of cGAS, which may thus counteract the prior viral antagonism. As a result, STING ligands is a highly effective tool of viral protection. However, degradation of STING by ZIKV may still occur at the protein level, which could be assessed as viral load establishes further.

Thirdly, our testing on STING downregulation in virus-infected MDMs showed a difference in donor responses to viral treatment as assessed by ISG expression. This difference may potentially be technical as a result of different efficiency of *siSTING* transfection or virus infection. Alternatively, evidence shows that a number of Toll-like receptors [51–53] and the RIG-I like receptor [54, 55] also interact and respond to Dengue virus, implying that immune signaling crosstalk and alternative interferon activation could give rise to this donor-variable interferon response. Nonetheless, this experiment has indicated that STING has a potential role in regulating ISG response to DENV and ZIKV, and that these two closely-related species are highly similar in their kinetics of immune activation. This may inform further investigations to compare their mechanisms of interaction with the host immunity.

In summary, even though our study has presented seemingly contradictory results to the report of DENV-mediated inhibition of STING-interferon signalling, we were pioneering in testing ZIKV and DENV infections in a M-CSF-cultured primary macrophage model. The observations showed a surprising activation of ISG response in MDMs stimulated by ZIKV/DENV viral nucleic acids. Following our work, two groups have published that non-structural proteins of ZIKV target cGAS, STING, TBK1, and Jak1-STAT pathways in multiple cell types [20, 50, 56]. These reports imply that both Dengue and Zika viruses induce STING-dependent interferon / ISG response, and possibly employ a conserved STING evasion strategy. Our research has revealed a basic similarity between ZIKV and DENV pathogenesis in the M-CSF –differentiated macrophages. This cell model has shown the advantage of displaying potent interferon-activated characteristics and thus could be expanded to study flavivirus infectivity and host-pathogen response in a wider donor population. The question of whether STING is similarly antagonized by ZIKV infection should also be address in future studies.

Material and Methods:

Cell cultures

Cytapheresis units from healthy adult human volunteers were obtained according to procedures approved by the “Etablissement Français du sang” (EFS) Committee. Peripheral blood mononuclear cells (PBMCs) were isolated from blood using Ficoll-Pague^{TM} density centrifugation method (GE Healthcare). Human CD14^{+} monocytes were isolated by positive selection using CD14+ microbeads (Miltenyi Biotech) according to the manufacturer’s guideline. CD14+ monocytes were differentiated into macrophages in complete RPMI 1640 (1% Pen-Strep, 1% L-glutamine, 10% low endotoxin fetal bovine serum) supplemented with 100 ng/ml human recombinant macrophage-colony stimulating factor (hr M-CSF, Peprotech) for 6 days.

Transfection & stimulation

Post M-CSF incubation, MDMs were transfected with hSTING ON-TARGETplus SMARTPool siRNA (Dharmacon #L-024333) to suppress *STING* expression, or with non-targeting siRNA pool (Dharmacon #L-001810) as negative control. 12.5 nM siRNA were delivered to MDMs using Viromer green (Lipocalyx, Germany) according to the manufacturer’s protocol. 48 hours post transfection, cells were further treated or harvested for gene expression assessment by RT-qPCR. MDMs were stimulated with 2’3’-cGAMP at 4 µg/ml in MDM culture medium to compare to the unstimulated control. Medium for MDMs was changed before each treatment.

Virus Preparation and Infection

Viral stocks of DENV-2 New Guinea C (NGC) strain (AF038403) [29] were produced as previously described [30]. The clinical isolate of epidemic strains of ZIKV including from Brazil (PE243_KX197192) [31] was kindly provided Alain Kohn (MRC-University of Glasgow Centre for Virus Research, UK) and Rafael Freitas de Oliveira Franca (FIOCRUZ, Recife, Brazil) and amplified using Vero cells (ATCC) by Décembre E using the same method as DENV-NGC [30]. All people involved in virus infection work have vaccine protection against various flavivirus species and virus stocks were kept in contained and isolated freezers to avoid damage to laboratory staffs.

Viruses were inactivated by UV radiation (4.75 J/cm^2) for 10 mins at a distance of 10 cm. Inactivation of viruses was carried out by Grass V. Monolayer of MDMs were infected with either DENV or ZIKV (active or UV-inactivated as indicated) for 2 hours at the indicated multiplicity of infection (MOI) in RPMI medium before being washed with PBS. MDMs were re-supplied with fresh culture medium and left for the indicated culture periods. For these experiments, mock control cells were replaced with fresh RPMI medium. By the end of

experiments, MDMs were washed twice with PBS and cells were harvested in guanidinium thiocyanate citrate (GTC) buffer for gene expression analysis as described below.

RNA, standard and Real-Time quantitative PCR

At the end of treatment, cells were washed with PBS and were lysed in guanidinium thiocyanate citrate (GTC) buffer for RNA isolation using the phenol/chloroform RNA isolation method [32]. 100 ng RNA was used to synthesis cDNA in 20 µl reaction volume using dNTPs and reverse transcriptase (life technologies). ZIKV, DENV, ISG15, MxA and glyceraldehyde-3-phosphate dehydrogenase (GAPDH) mRNA levels were determined by RT-qPCR using a Real-Time PCR SYBR Green Master Mix (Life Technologies). mRNA levels were normalised to *GAPDH* levels. The sequences of primers used in RT-qPCR are detailed below:

Genes	Primers (Forward / Reverse)
GAPDH	5'-AGGTGAAGGTCGGAGTCAACG-3' 5'-TGGAAGATGGTGATGGGATTTC-3'
ISG15	5'-GACAAATGCGACGAACCTCT-3' 5'-CGGCCCTTGTTATTCCTCA-3'
MxA	5'-ACAGGACCATCGGAATCTTG-3' 5'-CCCTTCTTCAGGTGGAACAC-3'
ZIKV-Brazil	5'-ATTGTTGGTGCAACACGACG-3' 5'-CCTAGTGGAATGGGAGGGGA-3'
DENV-NGC	5'-ACCTGGGAAGAGTGATGGTTATGG-3' 5'-ATGGTCTCTGGTATGGTGCTCTGG-3'

To calculate Genome equivalent (GE) number of mRNA expression, a stock of calibrator plasmid DNA at 10E9 copies per µl was diluted multiple times by ten folds to 10E8, 10E7, 10E6, 10E5, 10E4, 10E3, 10E2 and 10 copies per µl concentration. These standard DNA samples contain specific sites for each primer pairs to bind to and they were reacted in the same plate as the experiment samples. Each diluted standard DNA generates a Ct value which can form a linear relationship to calculate the copy number of genes in samples with a qPCR Ct value. GE is calculated as 2 copies (6.6 pg) /µl for a diploid genome.

Acknowledgements:

This work is supported by an EMBO short-term fellowship, ASTF 7459. We are grateful to Alain Kohn (MRC-University of Glasgow Centre for Virus Research, UK) and Rafael Freitas de Oliveira Franca (FIOCRUZ, Recife, Brazil) for providing us with ZIKV clinical isolate. We are grateful to Coléon S and Grass V for the technical assistance relating to virus infection and harvest.

Author Contributions:

YL, MD and EKT designed the experiments. YL carried out the *ex vivo* cell cultures, RNA and gene analysis work. ED carried out all the infection work. All authors were involved in the analysis and interpretation of the results, and the editing of the manuscript.

Conflict of interest:

Authors declare no conflict of interest.

References:

1. Merfeld E, Ben-Avi L, Kennon M, Cerveny KL. Potential mechanisms of Zika-linked microcephaly. Wiley Interdiscip Rev Dev Biol. 2017.

2. Brasil P, Sequeira PC, Freitas ADA, Zogbi HE, Calvet GA, De Souza RV, et al. Guillain-Barré syndrome associated with Zika virus infection. The Lancet. 2016.

3. Araujo AQC, Silva MTT, Araujo APQC. Zika virus-associated neurological disorders: A review. Brain. 2016.

4. Schneider WM, Chevillotte MD, Rice CM. Interferon-stimulated genes: a complex web of host defenses. Annu Rev Immunol. 2014;32:513–45. doi:10.1146/annurev-immunol-032713-120231.

5. Ishikawa H, Barber GN. STING is an endoplasmic reticulum adaptor that facilitates innate immune signalling. Nature. 2008;455:674–8. doi:10.1038/nature07317.

6. Tanaka Y, Chen ZJ. STING specifies IRF3 phosphorylation by TBK1 in the cytosolic DNA signalling pathway. Sci Signal. 2012;5:ra20.

7. Barber GN. STING: infection, inflammation and cancer. Nat Rev Immunol. 2015;15:760–70. doi:10.1038/nri3921.

8. Sun B, Sundström KB, Chew JJ, Bist P, Gan ES, Tan HC, et al. Dengue virus activates cGAS through the release of mitochondrial DNA. Sci Rep. 2017.

9. Aguirre S, Maestre AM, Pagni S, Patel JR, Savage T, Gutman D, et al. DENV Inhibits Type I IFN Production in Infected Cells by Cleaving Human STING. PLoS Pathog. 2012;8.

10. Aguirre S, Luthra P, Sanchez-Aparicio MT, Maestre AM, Patel J, Lamothe F, et al. Dengue virus NS2B protein targets cGAS for degradation and prevents mitochondrial DNA sensing during infection. Nat Microbiol. 2017.

11. Stabell AC, Meyerson NR, Gullberg RC, Gilchrist AR, Webb KJ, Old WM, et al. Dengue viruses cleave STING in humans but not in nonhuman primates, their presumed natural reservoir. Elife. 2018.

12. Carlin AF, Vizcarra EA, Branche E, Viramontes KM, Suarez-Amaran L, Ley K, et al. Deconvolution of pro- and antiviral genomic responses in Zika virus-infected and bystander macrophages. Proc Natl Acad Sci. 2018.

13. Ahn J, Gutman D, Saijo S, Barber GN. STING manifests self DNA-dependent inflammatory disease. Proc Natl Acad Sci U S A. 2012;109:19386–91.

doi:10.1073/pnas.1215006109.

14. Ohkuri T, Ghosh A, Kosaka A, Zhu J, Ikeura M, David M, et al. STING contributes to anti-glioma immunity via triggering type-I IFN signals in the tumor microenvironment. Cancer Immunol Res. 2014;2:1199–208.

15. Jønsson KL, Laustsen A, Krapp C, Skipper KA, Thavachelvam K, Hotter D, et al. IFI16 is required for DNA sensing in human macrophages by promoting production and function of cGAMP. Nat Commun. 2017.

16. Quicke KM, Bowen JR, Johnson EL, McDonald CE, Ma H, O'Neal JT, et al. Zika Virus Infects Human Placental Macrophages. Cell Host Microbe. 2016.

17. Ekins S, Liebler J, Neves BJ, Lewis WG, Coffee M, Bienstock R, et al. Illustrating and homology modeling the proteins of the Zika virus. F1000Research. 2016.

18. Priyamvada L, Hudson W, Ahmed R, Wrammert J. Humoral cross-reactivity between Zika and dengue viruses: Implications for protection and pathology. Emerging Microbes and Infections. 2017.

19. Barba-Spaeth G, Dejnirattisai W, Rouvinski A, Vaney MC, Medits I, Sharma A, et al. Structural basis of potent Zika-dengue virus antibody cross-neutralization. Nature. 2016.

20. Ding Q, Gaska JM, Douam F, Wei L, Kim D, Balev M, et al. Species-specific disruption of STING-dependent antiviral cellular defenses by the Zika virus NS2B3 protease. Proc Natl Acad Sci. 2018.

21. Weiskopf D, Sette A. T-cell immunity to infection with dengue virus in humans. Frontiers in Immunology. 2014.

22. Schmid MA, Diamond MS, Harris E. Dendritic cells in dengue virus infection: Targets of virus replication and mediators of immunity. Front Immunol. 2014.

23. Webster B, Werneke SW, Zafirova B, This S, Coléon S, Décembre E, et al. Plasmacytoid dendritic cells control dengue and chikungunya virus infections via IRF7-regulated interferon responses. Elife. 2018.

24. Marakalala MJ, Martinez FO, Plüddemann A, Gordon S. Macrophage heterogeneity in the immunopathogenesis of tuberculosis. Frontiers in Microbiology. 2018.

25. Laura C Miller YS. Macrophage Polarization in Virus-Host Interactions. J Clin Cell Immunol. 2015.

26. Hamilton JA. Colony-stimulating factors in inflammation and autoimmunity. Nature

Reviews Immunology. 2008.

27. Wu MF, Chen ST, Hsieh SL. Distinct regulation of dengue virus-induced inflammasome activation in human macrophage subsets. Journal of Biomedical Science. 2013.

28. Chen ST, Lin YL, Huang MT, Wu MF, Cheng SC, Lei HY, et al. CLEC5A is critical for dengue-virus-induced lethal disease. Nature. 2008.

29. Kroschewski H, Siew PL, Butcher RE, Thai LY, Lescar J, Wright PJ, et al. Mutagenesis of the dengue virus type 2 NS5 methyltransferase domain. J Biol Chem. 2008.

30. Décembre E, Assil S, Hillaire MLB, Dejnirattisai W, Mongkolsapaya J, Screaton GR, et al. Sensing of Immature Particles Produced by Dengue Virus Infected Cells Induces an Antiviral Response by Plasmacytoid Dendritic Cells. PLoS Pathog. 2014.

31. Donald CL, Brennan B, Cumberworth SL, Rezelj V V., Clark JJ, Cordeiro MT, et al. Full Genome Sequence and sfRNA Interferon Antagonist Activity of Zika Virus from Recife, Brazil. PLoS Negl Trop Dis. 2016.

32. Dreux M, Garaigorta U, Boyd B, Décembre E, Chung J, Whitten-Bauer C, et al. Short-range exosomal transfer of viral RNA from infected cells to plasmacytoid dendritic cells triggers innate immunity. Cell Host Microbe. 2012.

33. Gaidt MM, Ebert TS, Chauhan D, Ramshorn K, Pinci F, Zuber S, et al. The DNA Inflammasome in Human Myeloid Cells Is Initiated by a STING-Cell Death Program Upstream of NLRP3. Cell. 2017.

34. Paijo Jennifer, Döring Marius, Spanier Julia, Grabski Elena, Nooruzzaman Mohammed, Schmidt Tobias, Witte Gregor, Messerle Martin, Hornung Veit, Kaever Volkhard KU. cGAS Senses Human Cytomegalovirus and Induces Type I Interferon Responses in Human Monocyte-Derived Cells. PLoS Pathog. 2016;12:e1005546.

35. Murray PJ, Allen JE, Biswas SK, Fisher EA, Gilroy DW, Goerdt S, et al. Macrophage Activation and Polarization: Nomenclature and Experimental Guidelines. Immunity. 2014.

36. Chistiakov DA, Myasoedova VA, Revin V V., Orekhov AN, Bobryshev Y V. The impact of interferon-regulatory factors to macrophage differentiation and polarization into M1 and M2. Immunobiology. 2018.

37. Fleetwood AJ, Lawrence T, Hamilton JA, Cook AD. Granulocyte-Macrophage Colony-Stimulating Factor (CSF) and Macrophage CSF-Dependent Macrophage Phenotypes Display Differences in Cytokine Profiles and Transcription Factor Activities: Implications for CSF Blockade in Inflammation. J Immunol. 2007.

38. Paijo J, Döring M, Spanier J, Grabski E, Nooruzzaman M, Schmidt T, et al. cGAS Senses Human Cytomegalovirus and Induces Type I Interferon Responses in Human Monocyte-Derived Cells. PLoS Pathog. 2016.

39. Flipse J, Diosa-Toro MA, Hoornweg TE, Van De Pol DPI, Urcuqui-Inchima S, Smit JM. Antibody-Dependent Enhancement of Dengue Virus Infection in Primary Human Macrophages; Balancing Higher Fusion against Antiviral Responses. Sci Rep. 2016;6 July:1–13. doi:10.1038/srep29201.

40. West AP, Khoury-Hanold W, Staron M, Tal MC, Pineda CM, Lang SM, et al. Mitochondrial DNA stress primes the antiviral innate immune response. Nature. 2015;520:553–7. doi:10.1038/nature14156.

41. Lytle CD, Sagripanti J-L. Predicted inactivation of viruses of relevance to biodefense by solar radiation. J Virol. 2005.

42. Lo YL, Liou GG, Lyu JH, Hsiao M, Hsu TL, Wong CH. Dengue virus infection is through a cooperative interaction between a mannose receptor and CLEC5A on macrophage as a multivalent hetero-complex. PLoS One. 2016.

43. Pollard JW, Bartocci A, Arceci R, Orlofsky A, Ladner MB, Stanley ER. Apparent role of the macrophage growth factor, CSF-1, in placental development. Nature. 1987.

44. Hayashi M, Ohkura T, Inaba N. Increased Levels of Serum Macrophage Colony-Stimulating Factor before the Onset of Preeclampsia. Horm Metab Res. 2003.

45. Qiu X, Zhu L, Pollard JW. Colony-stimulating factor-1-dependent macrophage functions regulate the maternal decidua immune responses against Listeria monocytogenes infections during early gestation in mice. Infect Immun. 2009.

46. Yu CY, Chang TH, Liang JJ, Chiang RL, Lee YL, Liao CL, et al. Dengue virus targets the adaptor protein MITA to subvert host innate immunity. PLoS Pathog. 2012;8.

47. Chen Y-C, Wang S-Y. Activation of Terminally Differentiated Human Monocytes/Macrophages by Dengue Virus: Productive Infection, Hierarchical Production of Innate Cytokines and Chemokines, and the Synergistic Effect of Lipopolysaccharide. J Virol. 2002;76:9877–87. doi:10.1128/JVI.76.19.9877-9887.2002.

48. Best SM. The Many Faces of the Flavivirus NS5 Protein in Antagonism of Type I Interferon Signalling. J Virol. 2017.

49. Grant A, Ponia SS, Tripathi S, Balasubramaniam V, Miorin L, Sourisseau M, et al. Zika Virus Targets Human STAT2 to Inhibit Type i Interferon Signalling. Cell Host Microbe. 2016.

50. Zheng Y, Liu Q, Wu Y, Ma L, Zhang Z, Liu T, et al. Zika virus elicits inflammation to evade antiviral response by cleaving cGAS via NS1-caspase-1 axis. EMBO J. 2018.

51. Tsai YT, Chang SY, Lee CN, Kao CL. Human TLR3 recognizes dengue virus and modulates viral replication in vitro. Cell Microbiol. 2009.

52. Liang Z, Wu S, Li Y, He L, Wu M, Jiang L, et al. Activation of toll-like receptor 3 impairs the dengue virus serotype 2 replication through induction of IFN-β in cultured hepatoma cells. PLoS One. 2011.

53. Chen J, Ng MML, Chu JJH. Activation of TLR2 and TLR6 by Dengue NS1 Protein and Its Implications in the Immunopathogenesis of Dengue Virus Infection. PLoS Pathog. 2015.

54. Sprokholt JK, Kaptein TM, van Hamme JL, Overmars RJ, Gringhuis SI, Geijtenbeek TBH. RIG-I–like Receptor Triggering by Dengue Virus Drives Dendritic Cell Immune Activation and T_H 1 Differentiation. J Immunol. 2017.

55. Chazal M, Beauclair G, Gracias S, Najburg V, Simon-Lorière E, Tangy F, et al. RIG-I Recognizes the 5′ Region of Dengue and Zika Virus Genomes. Cell Rep. 2018.

56. Wu Y, Liu Q, Zhou J, Xie W, Chen C, Wang Z, et al. Zika virus evades interferon-mediated antiviral response through the co-operation of multiple nonstructural proteins in vitro. Cell Discov. 2017.

Supplementary figure 1: STING knockdown impairs 2'3'-cGAMP –induced ISG expressions.

A.&B. ISG15 (A) and MxA (B) inductions were assessed in control or siSTING transfected MDMs treated with +/- 6 h of 2'3'-cGAMP stimulation. Gene mRNA expression levels were assessed by RT-qPCR. Data is presented as Genome equivalent (GE) per µg of total RNA. All figures were plotted from n=2 donors, mean±SD.

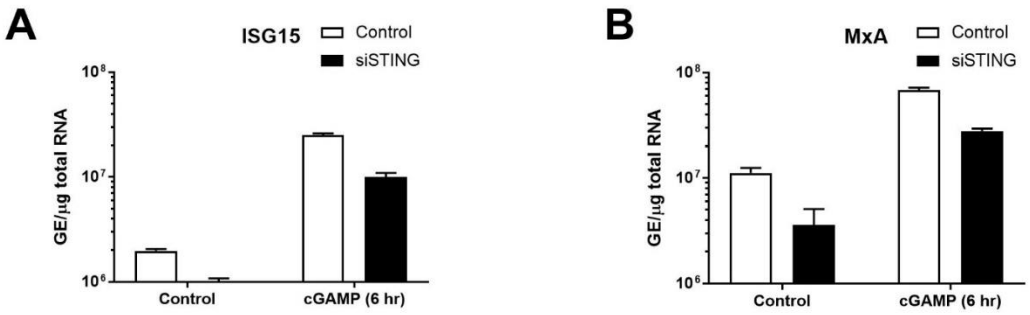

Chapter 5: Discussion and future work for STING regulation in response to Zika and Dengue virus infection.

Type I interferons, by name, have the primary function in interfering virus [134]. Most, if not all, viruses induce type I interferon response upon detection of their nucleic acid by the cytosolic sensors [233, 234, 281, 297–300]. These genetic materials are important for viruses to establish virulence in the host, and the survival and infectivity of a virus highly relies on its ability to minimise and block host immune reactions [301].

Members of the *Flaviviridae* family are a major threat to human health mainly due to their strong infectivity through mosquitos [302] and their widely known ability to evade immune defence via STING [232, 234, 300] and other antiviral adaptors [97, 303]. Dengue virus (DENV) is one of the most well-studies species of this family. Only humans and a few primates are susceptible to DENV infections whereas most rodents and primates can resist this virus predominantly because of the variations in the adaptor protein STING [232, 234, 304]. A mutation that resides in the third transmembrane domain of human STING is uniquely targeted by DENV-released non-structural (NS) protein/protease complex NS2B/3 [232, 305]. Particularly, the NS proteins are a potent weapon for flaviviruses to combat against human immune machineries. Flaviviruses release a variety of NS proteins to degrade multiple factors along the type I signalling axis, and these mechanisms of antagonism have been summarised in Chapter 1.5 [119]. Despite that these viruses have their specialties in infection, they share similarities in their interaction with the host and thus hypothesis can be made to research novel flavivirus species according to the knowledge of previous known viruses.

Zika virus (ZIKV) is a recently emerged flavivirus with its discovery in the 1940s and a notable outbreak after 2007 [306]. ZIKV is genetically close-related to DENV despite

that their symptoms of infection are different [236, 307]. DENV-infected patients are characterised by the flu-like “Dengue fever” [308] whereas ZIKV usually causes a self-resolving mild flu that will soon become asymptomatic [309]. However, ZIKV can reside in the host for more profound influence where it has been shown that the infection in pregnant women can transmit the virus to the foetus, which are often born with severe neurological defects such as microcephaly (reduced head circumference) and the Guillain–Barré syndrome (immune attack on the peripheral nerve system that causes rapid-onset of muscle weakness) [310–312]. Current research urgently seeks to identify host factors that respond to ZIKV establishment and *in utero* transmission. Due to the close relationship between ZIKV and DENV, a logical approach was to compare and contrast the infection machineries between these two flaviviruses, which may reveal some conserved targets for therapeutic design.

ZIKV is unique in its ability to transmit from mother to child during pregnancy [ref] potentially due to its long dormancy in the host to allow virulence to build up in the placental tissues. This also reflects that the virus can reside silently in certain cells and tissues without being detected. Quicke and colleagues [313] have reported that the placental tissue macrophages are the major target and niche for ZIKV to invade the foetus, although these cells were not previously identified as highly susceptible to flavivirus infection. One potential reason could be that the other flaviviruses such as DENV are more reactive to circulating dendritic cells and plasmacytoid cells [314–316], whereas ZIKV are more likely to “hide” longer to infect tissue-resident and resting immune cells like macrophages. Still, these two viruses may nonetheless induce the same immune regulator on initial encounter of host immunity and later inhibit it. As it is known that STING is a major regulator and degradation target of DENV [232, 234, 304], we thus wonder if it is the same for ZIKV, and most importantly whether such reaction occurs in macrophages.

Since live virus infection in human macrophages were analysed at 24h and days post infection, the first spike of type I interferon cannot be observed, and thus we have used type I interferon genes MxA and ISG15 as experimental readouts. Both genes are potently induced by virus-induced interferon signal and ISG15 is particularly known to

maintain the expression and functioning period of other ISG, such as RIG-I, PKR and MxA [317]. In our study, both ZIKV and DENV infects human primary macrophages at low MOI (multiplicity of infection = 1) and the replication could be detected as early as 24 hpi (hour post infection) (Paper 3 Fig. 1). This was in contrast to the result of Aguirre *et al*., [232] which not only showed that DENV induced little IFN-α production in their GM-CSF – macrophages but also the cleavage of STING protein at 48 hpi in STING-transfected HEK 293T cells. Although our study lacks a large population size and the result could be only representative of a single donor, still the major difference of interferon activation between our experiments could be the outcome of the culture conditions of macrophage differentiation. The growth factor GM-CSF (granulocyte-macrophage colony-stimulating factor) was used by Aguirre's group [232] in contrast to the M-CSF (macrophage colony-stimulating factor) condition used in our macrophage differentiation was a possible reason for this distinct result of virus-induced immune activation. The reason we have chosen M-CSF over GM-CSF in research was due to the fact that GM-CSF primes macrophages to activate both type I interferons and inflammasome-interleukin 1 pathways, whereas M-CSF – cultured macrophages predominantly release type I interferons upon viral challenges [28, 29]. Additionally, M-CSF tends to produce a more uniform and stable population of resting macrophages whereas GM-CSF (together with IL-4) is also used in differentiation of monocytes to dendritic cells [318, 319].

The effect of macrophage differentiation protocol should be investigated in future virus study with a large population size. This limitation of our study subject was mainly because that the white blood cells were eluted from 500 ml of blood donated in a hospital which was acquired only once each week. Thus, the small n number was inevitable in this time-limited project. In contrast, MDMs used in Paper 2 were isolated from 80 ml of whole blood from each donor so the isolation process can accommodate up to 3 donors a day. Therefore, a study population must be increased to understand the role of STING and MDMs in DENV/ZIKV infections.

In this preliminary study, we have also observed another distinction to the previous literature, the absence of ISG antagonism by DENV infection [232]. Again, this

difference is found in a single donor and it would not accurately represent the MDMs response in a large population. Additionally, we have tested virus infection for up to 72 h and it is likely that a longer period may be required by the viruses to establish STING antagonism. Although the reduction of ISG was not immediately seen at our designed time points, degradation of STING, or even cGAS, might still occur at the protein level.

Taken together, our M-CSF differentiated primary macrophage model presents a novel system in virus infection research due to its ability to show potent ISG inductions. Although our research was conducted in a limited population, we have observed a clear ISG response in macrophages infected with ZIKV and DENV, and that STING cleavage or ISG inhibition reported in previous research was absent in our studies. All these results should be repeated in more donors, and since ZIKV tend to reside in the host for a longer period of time, further time points could be looked into using our macrophage model. As viruses tend to induce type I interferons rapidly upon infection, a lower infection MOI (perhaps MOI=0.1) may potentially facilitate ZIKV/DENV to evade immune response and establish virulence better in cells. In addition to STING degradation, its upstream sensors (such as cGAS) and the downstream effectors (TBK1 and STAT) are also likely to be targeted by flaviviral proteases [304, 320, 321]. Even though macrophages are not as highly interferon-inducing to viruses as dendritic and plasmacytoid cells [322, 323], their signalling pathways are active and are perhaps even crucial for ZIKV to interact with to enable its survival in the host.

Chapter 6: Main conclusions

6.1 Paper 2: TMEM203 regulates the innate immune Type I interferon response via STING.

The novel proinflammatory mediator TMEM203 is a critical co-regulator of STING-activated type I interferon expression in human and mouse primary macrophages and murine macrophage cell lines. TMEM203 overexpression promotes STING translocation to lysosomes which resembles its active states. TMEM203 trafficking to lysosome membranes is likely to potentiate and promote ligand-independent STING translocation and activation. TMEM203 directly interacts with the N-terminal transmembrane domains of STING and such association can be further strengthened by STING's dimerization domain. TMEM203 selectively regulates cGAMP but not DMXAA -induced STING activity and these two ligands can distinctly alter TMEM203-STING association. Future research should aim to address the potential involvement of calcium signalling in the regulation of STING- type I interferon response via TMEM203. Additionally, LPS-induced TMEM203 signalling and TMEM203 polymorphism are areas to expand.

6.2 Paper 3: STING regulates type I interferon stimulated gene expression upon infection of Zika virus (ZIKV) and Dengue virus (DENV) in human monocyte-derived macrophages.

In our preliminary study, Zika virus and Dengue virus induce potent ISG expression in M-CSF differentiated human primary monocyte-derived macrophages. ISG induction in MDMs were viral replication dependent. Prior infection of ZIKV/DENV cannot impair cGAMP-induced STING activation at the tested dose and time, although STING-downregulation was associated with ISG reduction in ZIKV/DENV infected MDMs isolated from one donor.

References

(In addition to those listed in the papers)

1. Pate M, Damarla V, Chi DS, Negi S, Krishnaswamy G. Endothelial Cell Biology. In: Advances in Clinical Chemistry. 2010. p. 109–30. doi:10.1016/S0065-2423(10)52004-3.

2. Monks J, Rosner D, Jon Geske F, Lehman L, Hanson L, Neville MC, et al. Epithelial cells as phagocytes: apoptotic epithelial cells are engulfed by mammary alveolar epithelial cells and repress inflammatory mediator release. Cell Death Differ. 2005;12:107–14. doi:10.1038/sj.cdd.4401517.

3. Chaplin DD. Overview of the immune response. J Allergy Clin Immunol. 2010;125:S3–23. doi:10.1016/j.jaci.2009.12.980.

4. Davis MM, Tato CM, Furman D. Systems immunology: just getting started. Nat Immunol. 2017;18:725–32. doi:10.1038/ni.3768.

5. Brubaker SW, Bonham KS, Zanoni I, Kagan JC. Innate Immune Pattern Recognition: A Cell Biological Perspective. Annu Rev Immunol. 2015; 33:257-90. doi: 10.1146/annurev-immunol-032414-112240.

6. Chinen J, Fleisher TA, Shearer WT. Adaptive Immunity. In: Middleton's Allergy: Principles and Practice: Eighth Edition. 2013. p. 20–9.

7. Varol C, Mildner A, Jung S. Macrophages: Development and Tissue Specialization. Annu Rev Immunol. 2015;33:643–75. doi:10.1146/annurev-immunol-032414-112220.

8. Gordon S, Martinez-Pomares L. Physiological roles of macrophages. Pflugers Archiv European Journal of Physiology. 2017; 469(3-4):365-74. doi: 10.1007/s00424-017-1945-7.

9. Perdiguero EG, Geissmann F. The development and maintenance of resident macrophages. Nat Immunol. 2016;17:2–8. doi:10.1038/ni.3341.

10. Wynn TA, Chawla A, Pollard JW. Macrophage biology in development, homeostasis and disease. Nature. 2013; 496(7446): 445-55. doi: 10.1038/nature12034.

11. Okabe Y, Medzhitov R. Tissue-Specific Signals Control Reversible Program of Localization and Functional Polarization of Macrophages. Cell. 2014;157:832–44. doi:10.1016/j.cell.2014.04.016.

12. Doens D, Fernández PL. Microglia receptors and their implications in the response to amyloid β for Alzheimer's disease pathogenesis. Journal of Neuroinflammation. 2014; 11:48. doi: 10.1186/1742-2094-11-48.

13. Krause DL, Müller N. Neuroinflammation, microglia and implications for anti-inflammatory treatment in Alzheimer's disease. International Journal of Alzheimer's Disease. 2010; 2010:732806. doi: 10.4061/2010/732806.

14. Seneschal J, Clark RA, Gehad A, Baecher-Allan CM, Kupper TS. Human Epidermal Langerhans Cells Maintain Immune Homeostasis in Skin by Activating Skin Resident Regulatory T Cells. Immunity. 2012;36:873–84. doi:10.1016/j.immuni.2012.03.018.

15. Romani N, Clausen BE, Stoitzner P. Langerhans cells and more: langerin-expressing dendritic cell subsets in the skin. Immunol Rev. 2010;234:120–41. doi:10.1111/j.0105-2896.2009.00886.x.

16. West HC, Bennett CL. Redefining the Role of Langerhans Cells As Immune Regulators within the Skin. Front Immunol. 2018;8:1941. doi:10.3389/fimmu.2017.01941.

17. Bilzer M, Roggel F, Gerbes AL. Role of Kupffer cells in host defense and liver disease. Liver Int. 2006;26:1175–86. doi:10.1111/j.1478-3231.2006.01342.x.

18. Boyce EG, Fusco BE. Belimumab: Review of Use in Systemic Lupus Erythematosus. Clinical Therapeutics. 2012;34:1006–22.

19. Hussell T, Bell TJ. Alveolar macrophages: Plasticity in a tissue-specific context. Nature Reviews Immunology. 2014; 14(2):81-93. doi: 10.1038/nri3600.

20. Boyette LB, MacEdo C, Hadi K, Elinoff BD, Walters JT, Ramaswami B, et al. Phenotype, function, and differentiation potential of human monocyte subsets. PLoS One. 2017; 12(4): e0176460. doi: 10.1371/journal.pone.0176460.

21. Ziegler-Heitbrock L, Ancuta P, Crowe S, Dalod M, Grau V, Hart DN, et al. Nomenclature of monocytes and dendritic cells in blood. Blood. 2010;116:e74–80.

doi:10.1182/blood-2010-02-258558.

22. Patel AA, Zhang Y, Fullerton JN, Boelen L, Rongvaux A, Maini AA, et al. The fate and lifespan of human monocyte subsets in steady state and systemic inflammation. J Exp Med. 2017;214:1913–23. doi:10.1084/jem.20170355.

23. Serbina N V., Pamer EG. Monocyte emigration from bone marrow during bacterial infection requires signals mediated by chemokine receptor CCR2. Nat Immunol. 2006;7:311–7. doi:10.1038/ni1309.

24. Bain CC, Bravo-Blas A, Scott CL, Gomez Perdiguero E, Geissmann F, Henri S, et al. Constant replenishment from circulating monocytes maintains the macrophage pool in the intestine of adult mice. Nat Immunol. 2014; 15(10):929-37. doi: 10.1038/ni.2967.

25. Arnold L, Henry A, Poron F, Baba-Amer Y, van Rooijen N, Plonquet A, et al. Inflammatory monocytes recruited after skeletal muscle injury switch into antiinflammatory macrophages to support myogenesis. J Exp Med. 2007; 104(5): 1057-69.

26. Sprangers S, Vries TJ de, Everts V. Monocyte Heterogeneity: Consequences for Monocyte-Derived Immune Cells. J Immunol Res. 2016; Article ID 1475435.

27. Hamilton JA. Colony-stimulating factors in inflammation and autoimmunity. Nature Reviews Immunology. 2008; 8(7):533-44. doi: 10.1038/nri2356.

28. Wu MF, Chen ST, Hsieh SL. Distinct regulation of dengue virus-induced inflammasome activation in human macrophage subsets. Journal of Biomedical Science. 2013; 20:36. doi: 10.1186/1423-0127-20-36.

29. Hamilton JA. Colony-stimulating factors in inflammation and autoimmunity. Nat Rev Immunol. 2008;8:533–44. doi:10.1038/nri2356.

30. Swirski FK, Hilgendorf I, Robbins CS. From proliferation to proliferation: monocyte lineage comes full circle. Semin Immunopathol. 2014;36:137–48. doi:10.1007/s00281-013-0409-1.

31. Lin H, Lee E, Hestir K, Leo C, Huang M, Bosch E, et al. Discovery of a Cytokine and Its Receptor by Functional Screening of the Extracellular Proteome. Science (80-). 2008;320:807–11. doi:10.1126/science.1154370.

32. Yu W, Chen J, Xiong Y, Pixley FJ, Yeung Y-G, Stanley ER. Macrophage Proliferation Is Regulated through CSF-1 Receptor Tyrosines 544, 559, and 807. J Biol Chem. 2012;287:13694–704. doi:10.1074/jbc.M112.355610.

33. Shashkin P, Dragulev B, Ley K. Macrophage Differentiation to Foam Cells. Curr Pharm Des. 2005;11:3061–72. doi:10.2174/1381612054865064.

34. Andrés V, Pello OM, Silvestre-Roig C. Macrophage proliferation and apoptosis in atherosclerosis. Current Opinion in Lipidology. 2012; 23(5):429-38. doi: 10.1097/MOL.0b013e328357a379.

35. Robbins CS, Hilgendorf I, Weber GF, Theurl I, Iwamoto Y, Figueiredo JL, et al. Local proliferation dominates lesional macrophage accumulation in atherosclerosis. Nat Med. 2013; 19(9):1166-72. doi: 10.1038/nm.3258.

36. Weischenfeldt J, Porse B. Bone marrow-derived macrophages (BMM): Isolation and applications. Cold Spring Harb Protoc. 2008; 2008:pdb.prot5080. doi: 10.1101/pdb.prot5080..

37. Mills CD, Kincaid K, Alt JM, Heilman MJ, Hill AM. M-1/M-2 Macrophages and the Th1/Th2 Paradigm. J Immunol. 2000;164:6166–73. doi:10.4049/jimmunol.164.12.6166.

38. Mills C. M1 and M2 Macrophages: Oracles of Health and Disease. Crit Rev Immunol. 2012; 32(6):463-88.

39. Galván-Peña S, O'Neill LAJ. Metabolic Reprograming in Macrophage Polarization. Front Immunol. 2014;5:420. doi:10.3389/fimmu.2014.00420.

40. Rath M, Müller I, Kropf P, Closs EI, Munder M. Metabolism via Arginase or Nitric Oxide Synthase: Two Competing Arginine Pathways in Macrophages. Front Immunol. 2014;5:532. doi:10.3389/fimmu.2014.00532.

41. Geelhaar-Karsch A, Schinnerling K, Conrad K, Friebel J, Allers K, Schneider T, et al. Evaluation of arginine metabolism for the analysis of M1/M2 macrophage activation in human clinical specimens. Inflamm Res. 2013;62:865–9. doi:10.1007/s00011-013-0642-z.

42. Martinez FO, Gordon S. The M1 and M2 paradigm of macrophage activation: time for reassessment. F1000Prime Rep. 2014; 6:13. doi: 10.12703/P6-13.

43. Shapouri-Moghaddam A, Mohammadian S, Vazini H, Taghadosi M, Esmaeili S-A, Mardani F, et al. Macrophage plasticity, polarization, and function in health and disease. J Cell Physiol. 2018;233:6425–40. doi:10.1002/jcp.26429.

44. Chen J, Zhao Y, Liu Y. The Role of Nucleotides and Purinergic Signaling in Apoptotic Cell Clearance â€“ Implications for Chronic Inflammatory Diseases. Front Immunol. 2014;5:656. doi:10.3389/fimmu.2014.00656.

45. Ishikawa H, Barber GN. STING is an endoplasmic reticulum adaptor that facilitates innate immune signalling. Nature. 2008; 455(7213):674-8. doi: 10.1038/nature07317.

46. Pfeffer K, Matsuyama T, Kündig TM, Wakeham A, Kishihara K, Shahinian A, et al. Mice deficient for the 55 kd tumor necrosis factor receptor are resistant to endotoxic shock, yet succumb to L. monocytogenes infection. Cell. 1993;73:457–67.

47. Ehrt S, Schnappinger D, Bekiranov S, Drenkow J, Shi S, Gingeras TR, et al. Reprogramming of the Macrophage Transcriptome in Response to Interferon-γ and Mycobacterium tuberculosis. J Exp Med. 2001;194:1123–40. doi:10.1084/jem.194.8.1123.

48. Gog JR, Murcia A, Osterman N, Restif O, McKinley TJ, Sheppard M, et al. Dynamics of Salmonella infection of macrophages at the single cell level. J R Soc Interface. 2012; 9(75): 2696-2707. doi: 10.1098/rsif.2012.0163.

49. Lacoma A, Cano V, Moranta D, Regueiro V, Domínguez-Villanueva D, Laabei M, et al. Investigating intracellular persistence of Staphylococcus aureus within a murine alveolar macrophage cell line. Virulence. 2017;8:1761–75. doi:10.1080/21505594.2017.1361089.

50. Tate MD, Pickett DL, van Rooijen N, Brooks AG, Reading PC. Critical Role of Airway Macrophages in Modulating Disease Severity during Influenza Virus Infection of Mice. J Virol. 2010;84:7569–80. doi:10.1128/JVI.00291-10.

51. Ellermann-Eriksen S. Macrophages and cytokines in the early defence against herpes simplex virus. Virol J. 2005;2:59. doi:10.1186/1743-422X-2-59.

52. Wati S, Li P, Burrell CJ, Carr JM. Dengue Virus (DV) Replication in Monocyte-Derived Macrophages Is Not Affected by Tumor Necrosis Factor Alpha (TNF-), and

DV Infection Induces Altered Responsiveness to TNF- Stimulation. J Virol. 2007;81:10161–71. doi:10.1128/JVI.00313-07.

53. Jurado KA, Simoni MK, Tang Z, Uraki R, Hwang J, Householder S, et al. Zika virus productively infects primary human placenta-specific macrophages. JCI Insight. 2016;1. doi:10.1172/jci.insight.88461.

54. Quicke KM, Bowen JR, Johnson EL, McDonald CE, Ma H, O'Neal JT, et al. Zika Virus Infects Human Placental Macrophages. Cell Host Microbe. 2016; 20(1): 83-90. doi: 10.1016/j.chom.2016.05.015.

55. Rőszer T. Understanding the Mysterious M2 Macrophage through Activation Markers and Effector Mechanisms. Mediators Inflamm. 2015;2015:1–16. doi:10.1155/2015/816460.

56. Duluc D, Delneste Y, Tan F, Moles M-P, Grimaud L, Lenoir J, et al. Tumor-associated leukemia inhibitory factor and IL-6 skew monocyte differentiation into tumor-associated macrophage-like cells. Blood. 2007;110:4319–30. doi:10.1182/blood-2007-02-072587.

57. Beyer M, Mallmann MR, Xue J, Staratschek-Jox A, Vorholt D, Krebs W, et al. High-Resolution Transcriptome of Human Macrophages. PLoS One. 2012;7:e45466. doi:10.1371/journal.pone.0045466.

58. Xue J, Schmidt S V., Sander J, Draffehn A, Krebs W, Quester I, et al. Transcriptome-Based Network Analysis Reveals a Spectrum Model of Human Macrophage Activation. Immunity. 2014;40:274–88. doi:10.1016/j.immuni.2014.01.006.

59. Chistiakov DA, Bobryshev Y V., Orekhov AN. Changes in transcriptome of macrophages in atherosclerosis. J Cell Mol Med. 2015;19:1163–73. doi:10.1111/jcmm.12591.

60. Becker M, De Bastiani MA, Parisi MM, Guma FTCR, Markoski MM, Castro MAA, et al. Integrated Transcriptomics Establish Macrophage Polarization Signatures and have Potential Applications for Clinical Health and Disease. Sci Rep. 2015; 5:13351.

61. Boe DM, Curtis BJ, Chen MM, Ippolito JA, Kovacs EJ. Extracellular traps and macrophages: new roles for the versatile phagocyte. J Leukoc Biol. 2015;97:1023–

35. doi:10.1189/jlb.4RI1014-521R.

62. Liu H, Wu X, Gang N, Wang S, Deng W, Zan L, et al. Macrophage functional phenotype can be consecutively and reversibly shifted to adapt to microenvironmental changes. Int J Clin Exp Med. 2015;8:3044–53. http://www.ncbi.nlm.nih.gov/pubmed/25932281.

63. Hirayama D, Iida T, Nakase H. The phagocytic function of macrophage-enforcing innate immunity and tissue homeostasis. International Journal of Molecular Sciences. 2018; 19(1): pii:E92. doi: 10.3390/ijms19010092.

64. Hochreiter-Hufford A, Ravichandran KS. Clearing the dead: Apoptotic cell sensing, recognition, engulfment, and digestion. Cold Spring Harb Perspect Biol. 2013; 5(1): a008749. doi: 10.1101/cshperspect.a008748.

65. Schrijvers DM, De Meyer GRY, Herman AG, Martinet W. Phagocytosis in atherosclerosis: Molecular mechanisms and implications for plaque progression and stability. Cardiovascular Research. 2007; 73(3): 470-80.

66. Aderem A, Underhill DM. MECHANISMS OF PHAGOCYTOSIS IN MACROPHAGES. Annu Rev Immunol. 1999;17:593–623. doi:10.1146/annurev.immunol.17.1.593.

67. Warrell MJ. Intradermal rabies vaccination: the evolution and future of pre- and post-exposure prophylaxis. Curr Top Microbiol Immunol. 2012;351:139–57. doi:10.1007/82_2010_121.

68. Vergne I, Chua J, Singh SB, Deretic V. Cell biology of Mycobacterium Tuberculosis phagosome. Annu Rev Cell Dev Biol. 2004;20:367–94. doi:10.1146/annurev.cellbio.20.010403.114015.

69. Vandal OH, Pierini LM, Schnappinger D, Nathan CF, Ehrt S. A membrane protein preserves intrabacterial pH in intraphagosomal Mycobacterium tuberculosis. Nat Med. 2008;14:849–54. doi:10.1038/nm.1795.

70. Hume D a. Macrophages as APC and the Dendritic Cell Myth. J Immunol. 2008;181:5829–35. doi:10.4049/jimmunol.181.9.5829.

71. Soudja SMH, Chandrabos C, Yakob E, Veenstra M, Palliser D, Lauvau G. Memory-T-Cell-Derived Interferon-γ Instructs Potent Innate Cell Activation for

Protective Immunity. Immunity. 2014; 40(6): 974-88. doi: 10.1016/j.immuni.2014.05.005.

72. Harding C V., Geuze HJ. Class IIMHC molecules are present in macrophage lysosomes and phagolysosomes that function in the phagocytic processing of listeria monocytogenes for presentation to T cells. J Cell Biol. 1992; 119(3): 531-42.

73. Akira S, Uematsu S, Takeuchi O. Pathogen recognition and innate immunity. Cell. 2006; 124(4): 783-801.

74. Takeuchi O, Akira S. Pattern Recognition Receptors and Inflammation. Cell. 2010;140:805–20. doi:10.1016/j.cell.2010.01.022.

75. Hoving JC, Wilson GJ, Brown GD. Signalling C-Type lectin receptors, microbial recognition and immunity. Cell Microbiol. 2014;16:185–94. doi:10.1111/cmi.12249.

76. Akira S. Toll-like Receptor Signaling. J Biol Chem. 2003;278:38105–8. doi:10.1074/jbc.R300028200.

77. Uematsu S, Akira S. Toll-Like receptors (TLRs) and their ligands. Handb Exp Pharmacol. 2008;:1–20. doi:10.1007/978-3-540-72167-3_1.

78. Deguine J, Barton GM. MyD88: a central player in innate immune signaling. F1000Prime Rep. 2014;6:97. doi:10.12703/P6-97.

79. Ullah MO, Sweet MJ, Mansell A, Kellie S, Kobe B. TRIF-dependent TLR signaling, its functions in host defense and inflammation, and its potential as a therapeutic target. J Leukoc Biol. 2016;100:27–45. doi:10.1189/jlb.2RI1115-531R.

80. Takizawa H, Fritsch K, Kovtonyuk L V., Saito Y, Yakkala C, Jacobs K, et al. Pathogen-Induced TLR4-TRIF Innate Immune Signaling in Hematopoietic Stem Cells Promotes Proliferation but Reduces Competitive Fitness. Cell Stem Cell. 2017;21:225-240.e5. doi:10.1016/j.stem.2017.06.013.

81. Honda K, Takaoka A, Taniguchi T. Type I Inteferon Gene Induction by the Interferon Regulatory Factor Family of Transcription Factors. Immunity. 2006;25:349–60. doi:10.1016/j.immuni.2006.08.009.

82. Fowler JF. Brief summary of radiobiological principles in fractionated radiotherapy. Semin Radiat Oncol. 1992;2:16–21. doi:10.1016/S1053-

4296(05)80045-1.

83. Afonina IS, Müller C, Martin SJ, Beyaert R. Proteolytic Processing of Interleukin-1 Family Cytokines: Variations on a Common Theme. Immunity. 2015;42:991–1004. doi:10.1016/j.immuni.2015.06.003.

84. Matsuno H, Yudoh K, Katayama R, Nakazawa F, Uzuki M, Sawai T, et al. The role of TNF-α in the pathogenesis of inflammation and joint destruction in rheumatoid arthritis (RA): A study using a human RA/SCID mouse chimera. Rheumatology. 2002; 41(3): 329-37.

85. Dayer JM, Oliviero F, Punzi L. A brief history of IL-1 and IL-1 Ra in rheumatology. Frontiers in Pharmacology. 2017; 8:293. doi: 10.3389/fphar.2017.00293.

86. Shin SY, Katz P, Wallhagen M, Julian L. Cognitive impairment in persons with rheumatoid arthritis. Arthritis Care Res. 2012; 64(8): 1144-50. doi: 10.1002/acr.21683.

87. Raupach B, Peuschel SK, Monack DM, Zychlinsky A. Caspase-1-mediated activation of interleukin-1β (IL-1β) and IL-18 contributes to innate immune defenses against Salmonella enterica serovar typhimurium infection. Infect Immun. 2006; 74(8): 4922-6.

88. Latz E, Xiao TS, Stutz A. Activation and regulation of the inflammasomes. Nature Reviews Immunology. 2013; 13(6): 397-411. doi: 10.1038/nri3452.

89. Moreira LO, Zamboni DS. NOD1 and NOD2 Signaling in Infection and Inflammation. Front Immunol. 2012;3:328. doi:10.3389/fimmu.2012.00328.

90. Bauernfeind F, Bartok E, Rieger A, Franchi L, Nunez G, Hornung V. Cutting Edge: Reactive Oxygen Species Inhibitors Block Priming, but Not Activation, of the NLRP3 Inflammasome. J Immunol. 2011;187:613–7. doi:10.4049/jimmunol.1100613.

91. Loo YM, Gale M. Immune Signaling by RIG-I-like Receptors. Immunity. 2011; 34(5): 680-92. doi: 10.1016/j.immuni.2011.05.003.

92. Hornung V, Schlender J, Guenthner-Biller M, Rothenfusser S, Endres S, Conzelmann K-K, et al. Replication-Dependent Potent IFN-α Induction in Human Plasmacytoid Dendritic Cells by a Single-Stranded RNA Virus. J Immunol.

2004;173:5935–43. doi:10.4049/jimmunol.173.10.5935.

93. Lopez CB, Moltedo B, Alexopoulou L, Bonifaz L, Flavell RA, Moran TM. TLR-Independent Induction of Dendritic Cell Maturation and Adaptive Immunity by Negative-Strand RNA Viruses. J Immunol. 2004; 173(11): 6882-9.

94. Yoneyama M, Kikuchi M, Natsukawa T, Shinobu N, Imaizumi T, Miyagishi M, et al. The RNA helicase RIG-I has an essential function in double-stranded RNA-induced innate antiviral responses. Nat Immunol. 2004; 5(7): 730-7.

95. Broquet AH, Hirata Y, McAllister CS, Kagnoff MF. RIG-I/MDA5/MAVS Are Required To Signal a Protective IFN Response in Rotavirus-Infected Intestinal Epithelium. J Immunol. 2011;186:1618–26. doi:10.4049/jimmunol.1002862.

96. Errett JS, Suthar MS, McMillan A, Diamond MS, Gale M. The Essential, Nonredundant Roles of RIG-I and MDA5 in Detecting and Controlling West Nile Virus Infection. J Virol. 2013;87:11416–25. doi:10.1128/JVI.01488-13.

97. Dalrymple NA, Cimica V, Mackow ER. Dengue Virus NS Proteins Inhibit RIG-I/MAVS Signaling by Blocking TBK1/IRF3 Phosphorylation: Dengue Virus Serotype 1 NS4A Is a Unique Interferon-Regulating Virulence Determinant. MBio. 2015;6. doi:10.1128/mBio.00553-15.

98. Reikine S, Nguyen JB, Modis Y. Pattern Recognition and Signaling Mechanisms of RIG-I and MDA5. Front Immunol. 2014;5:342. doi:10.3389/fimmu.2014.00342.

99. Satoh T, Kato H, Kumagai Y, Yoneyama M, Sato S, Matsushita K, et al. LGP2 is a positive regulator of RIG-I- and MDA5-mediated antiviral responses. Proc Natl Acad Sci. 2010;107:1512–7. doi:10.1073/pnas.0912986107.

100. Li X, Ranjith-Kumar CT, Brooks MT, Dharmaiah S, Herr AB, Kao C, et al. The RIG-I-like receptor LGP2 recognizes the termini of double-stranded RNA. J Biol Chem. 2009; 284(20): 13881-91. doi: 10.1074/jbc.M900818200.

101. van der Veen AG, Maillard P V, Schmidt JM, Lee SA, Deddouche-Grass S, Borg A, et al. The RIG-I-like receptor LGP2 inhibits Dicer-dependent processing of long double-stranded RNA and blocks RNA interference in mammalian cells. EMBO J. 2018;37:e97479. doi:10.15252/embj.201797479.

102. Rodriguez KR, Bruns AM, Horvath CM. MDA5 and LGP2: Accomplices and

Antagonists of Antiviral Signal Transduction. J Virol. 2014;88:8194–200. doi:10.1128/JVI.00640-14.

103. Seth RB, Sun L, Ea CK, Chen ZJ. Identification and characterization of MAVS, a mitochondrial antiviral signaling protein that activates NF-κB and IRF3. Cell. 2005.

104. Zhou A, Hassel BA, Silverman RH. Expression cloning of 2-5A-dependent RNAase: A uniquely regulated mediator of interferon action. Cell. 1993; 122(5): 669-82.

105. Ben-Asouli Y, Banai Y, Pel-Or Y, Shir A, Kaempfer R. Human Interferon-γ mRNA Autoregulates Its Translation through a Pseudoknot that Activates the Interferon-Inducible Protein Kinase PKR. Cell. 2002;108:221–32. doi:10.1016/S0092-8674(02)00616-5.

106. Kristiansen H, Scherer CA, McVean M, Iadonato SP, Vends S, Thavachelvam K, et al. Extracellular 2'-5' Oligoadenylate Synthetase Stimulates RNase L-Independent Antiviral Activity: a Novel Mechanism of Virus-Induced Innate Immunity. J Virol. 2010;84:11898–904. doi:10.1128/JVI.01003-10.

107. Malathi K, Dong B, Gale M, Silverman RH. Small self-RNA generated by RNase L amplifies antiviral innate immunity. Nature. 2007; 448(7155): 816-9.

108. Balachandran S, Roberts PC, Brown LE, Truong H, Pattnaik AK, Archer DR, et al. Essential Role for the dsRNA-Dependent Protein Kinase PKR in Innate Immunity to Viral Infection. Immunity. 2000;13:129–41. doi:10.1016/S1074-7613(00)00014-5.

109. Hull CM, Bevilacqua PC. Mechanistic Analysis of Activation of the Innate Immune Sensor PKR by Bacterial RNA. J Mol Biol. 2015;427:3501–15. doi:10.1016/j.jmb.2015.05.018.

110. Schulz O, Pichlmair A, Rehwinkel J, Rogers NC, Scheuner D, Kato H, et al. Protein Kinase R Contributes to Immunity against Specific Viruses by Regulating Interferon mRNA Integrity. Cell Host Microbe. 2010;7:354–61. doi:10.1016/j.chom.2010.04.007.

111. Colgan DF, Manley JL. Mechanism and regulation of mRNA polyadenylation. Genes Dev. 1997;11:2755–66. doi:10.1101/gad.11.21.2755.

112. Rathinam VAK, Jiang Z, Waggoner SN, Sharma S, Cole LE, Waggoner L, et al.

The AIM2 inflammasome is essential for host defense against cytosolic bacteria and DNA viruses. Nat Immunol. 2010;11:395–402. doi:10.1038/ni.1864.

113. Zhang Z, Yuan B, Bao M, Lu N, Kim T, Liu Y-J. The helicase DDX41 senses intracellular DNA mediated by the adaptor STING in dendritic cells. Nat Immunol. 2011;12:959–65. doi:10.1038/ni.2091.

114. Sun L, Wu J, Du F, Chen X, Chen ZJ, O'Neill LA, et al. Cyclic GMP-AMP synthase is a cytosolic DNA sensor that activates the type I interferon pathway. Science. 2013;339:786–91. doi:10.1126/science.1232458.

115. Unterholzner L, Keating SE, Baran M, Horan KA, Jensen SB, Sharma S, et al. IFI16 is an innate immune sensor for intracellular DNA. Nat Immunol. 2010;11:997–1004. doi:10.1038/ni.1932.

116. Grieves JL, Fye JM, Harvey S, Grayson JM, Hollis T, Perrino FW. Exonuclease TREX1 degrades double-stranded DNA to prevent spontaneous lupus-like inflammatory disease. Proc Natl Acad Sci. 2015; 112(16): 5117-22. doi: 10.1073/pnas.1423804112.

117. Ho SSW, Zhang WYL, Tan NYJ, Khatoo M, Suter MA, Tripathi S, et al. The DNA Structure-Specific Endonuclease MUS81 Mediates DNA Sensor STING-Dependent Host Rejection of Prostate Cancer Cells. Immunity. 2016;44:1177–89. doi:10.1016/j.immuni.2016.04.010.

118. Barber GN. STING: Infection, inflammation and cancer. Nature Reviews Immunology. 2015; 15(12): 760-70.

119. Li Y, Wilson HL, Kiss-Toth E. Regulating STING in health and disease. Journal of Inflammation (United Kingdom). 2017; 14:11. doi: 10.1186/s12950-017-0159-2.

120. Liu Y, Jesus AA, Marrero B, Yang D, Ramsey SE, Montealegre Sanchez GA, et al. Activated STING in a vascular and pulmonary syndrome. N Engl J Med. 2014;371:507–18. doi:10.1056/NEJMoa1312625.

121. Jeremiah N, Neven B, Gentili M, Callebaut I, Maschalidi S, Stolzenberg MC, et al. Inherited STING-activating mutation underlies a familial inflammatory syndrome with lupus-like manifestations. J Clin Invest. 2014;124:5516–20.

122. Sharma S, Campbell AM, Chan J, Schattgen SA, Orlowski GM, Nayar R, et al.

Suppression of systemic autoimmunity by the innate immune adaptor STING. Proc Natl Acad Sci. 2015;112:E710-7. doi:10.1073/pnas.1420217112.

123. Wang J, Li P, Wu MX. Natural STING Agonist as an “Ideal” Adjuvant for Cutaneous Vaccination. J Invest Dermatol. 2016; 136(11): 2183-91.

124. Van Dis E, Sogi KM, Rae CS, Sivick KE, Surh NH, Leong ML, et al. STING-Activating Adjuvants Elicit a Th17 Immune Response and Protect against Mycobacterium tuberculosis Infection. Cell Rep. 2018; 23(5): 1435-47.

125. Blaauboer SM, Mansouri S, Tucker HR, Wang HL, Gabrielle VD, Jin L. The mucosal adjuvant cyclic di-GMP enhances antigen uptake and selectively activates pinocytosis-efficient cells in vivo. Elife. 2015; 4. doi: 10.7554/eLife.06670.

126. Hanson MC, Crespo MP, Abraham W, Moynihan KD, Szeto GL, Chen SH, et al. Nanoparticulate STING agonists are potent lymph node–targeted vaccine adjuvants. J Clin Invest. 2015;125:2532–46. doi:10.1172/JCI79915.

127. Fu J, Kanne DB, Leong M, Glickman LH, McWhirter SM, Lemmens E, et al. STING agonist formulated cancer vaccines can cure established tumors resistant to PD-1 blockade. Sci Transl Med. 2015;7:283ra52. doi:10.1126/scitranslmed.aaa4306.

128. Vadiveloo PK, Vairo G, Hertzog P, Kola I, Hamilton JA. Role of type I interferons during macrophage activation by lipopolysaccharide. Cytokine. 2000;12:1639–46. doi:10.1006/cyto.2000.0766.

129. Chow JC, Young DW, Golenbock DT, Christ WJ, Gusovsky F. Toll-like Receptor-4 Mediates Lipopolysaccharide-induced Signal Transduction. J Biol Chem. 1999;274:10689–92. doi:10.1074/jbc.274.16.10689.

130. Kiss-Toth E, Wyllie DH, Holland K, Marsden L, Jozsa V, Oxley KM, et al. Functional mapping and identification of novel regulators for the Toll/Interleukin-1 signalling network by transcription expression cloning. Cell Signal. 2006;18:202–14. doi:10.1016/j.cellsig.2005.04.012.

131. Wyllie DH, Søgaard KC, Holland K, Yaobo X, Bregu M, Hill AVS, et al. Identification of 34 novel proinflammatory proteins in a genome-wide macrophage functional screen. PLoS One. 2012;7(7): e42388.
doi: 10.1371/journal.pone.0042388.

132. Shambharkar PB, Bittinger M, Latario B, Xiong ZH, Bandyopadhyay S, Davis V, et al. TMEM203 is a novel regulator of intracellular calcium homeostasis and is required for spermatogenesis. PLoS One. 2015; 10(5): e0127480.

133. Ishikawa H, Barber GN. STING is an endoplasmic reticulum adaptor that facilitates innate immune signalling. Nature. 2008;455:674–8. doi:10.1038/nature07317.

134. Isaacs A, Lindenmann J. Virus Interference: I. The Interferon. CA Cancer J Clin. 1988; 38(5): 280-90.

135. De Andrea M, Ravera R, Gioia D, Gariglio M, Landolfo S. The interferon system: An overview. European Journal of Paediatric Neurology. 2002; 6 Suppl A:A41-6; discussion A55-8.

136. Le Page C, Génin P, Baines MG, Hiscott J. Interferon activation and innate immunity. Rev Immunogenet. 2000;2:374–86. http://www.ncbi.nlm.nih.gov/pubmed/11256746.

137. Bao Y, Liu X, Han C, Xu S, Xie B, Zhang Q, et al. Identification of IFN-γ-producing innate B cells. Cell Res. 2014;24:161–76. doi:10.1038/cr.2013.155.

138. Colonna M, Krug A, Cella M. Interferon-producing cells: on the front line in immune responses against pathogens. Curr Opin Immunol. 2002;14:373–9. doi:10.1016/S0952-7915(02)00349-7.

139. Trinchieri G. Type I interferon: friend or foe? J Exp Med. 2010;207:2053–63. doi:10.1084/jem.20101664.

140. Schindler C, Levy DE, Decker T. JAK-STAT signaling: From interferons to cytokines. Journal of Biological Chemistry. 2007; 282(28): 20059-63.

141. Steimle V, Siegrist CA, Mottet A, Lisowska-Grospierre B, Mach B. Regulation of MHC class II expression by interferon-γ mediated by the transactivator gene CIITA. Science (80-). 1994; 265(5168): 106-9.

142. Giroux M, Schmidt M, Descoteaux A. IFN- -Induced MHC Class II Expression: Transactivation of Class II Transactivator Promoter IV by IFN Regulatory Factor-1 is Regulated by Protein Kinase C-. J Immunol. 2003;171:4187–94. doi:10.4049/jimmunol.171.8.4187.

143. Vremec D, O'Keeffe M, Hochrein H, Fuchsberger M, Caminschi I, Lahoud M, et al. Production of interferons by dendritic cells, plasmacytoid cells, natural killer cells, and interferon-producing killer dendritic cells. Blood. 2006;109:1165–73. doi:10.1182/blood-2006-05-015354.

144. Bastos KRB, Barboza R, Sardinha L, Russo M, Alvarez JM, Lima MRD. Role of Endogenous IFN-γ in Macrophage Programming Induced by IL-12 and IL-18. J Interf Cytokine Res. 2007;27:399–410. doi:10.1089/jir.2007.0128.

145. Frucht DM, Fukao T, Bogdan C, Schindler H, O'Shea JJ, Koyasu S. IFN-γ production by antigen-presenting cells: mechanisms emerge. Trends Immunol. 2001;22:556–60. doi:10.1016/S1471-4906(01)02005-1.

146. Wu C, Xue Y, Wang P, Lin L, Liu Q, Li N, et al. IFN-γ Primes Macrophage Activation by Increasing Phosphatase and Tensin Homolog via Downregulation of miR-3473b. J Immunol. 2014;193:3036–44. doi:10.4049/jimmunol.1302379.

147. Zhou Z, Hamming OJ, Ank N, Paludan SR, Nielsen AL, Hartmann R. Type III Interferon (IFN) Induces a Type I IFN-Like Response in a Restricted Subset of Cells through Signaling Pathways Involving both the Jak-STAT Pathway and the Mitogen-Activated Protein Kinases. J Virol. 2007;81:7749–58. doi:10.1128/JVI.02438-06.

148. Abed NS, Chace JH, Fleming AL, Cowdery JS. Interferon-γ Regulation of B Lymphocyte Differentiation: Activation of B Cells Is a Prerequisite for IFN-γ-Mediated Inhibition of B Cell Differentiation. Cell Immunol. 1994;153:356–66. doi:10.1006/cimm.1994.1034.

149. Ramana C V., Gil MP, Schreiber RD, Stark GR. Stat1-dependent and -independent pathways in IFN-γ-dependent signaling. Trends Immunol. 2002;23:96–101. doi:10.1016/S1471-4906(01)02118-4.

150. Lew DJ, Decker T, Darnell JE. Alpha Interferon and Gamma Interferon Stimulate Transcription of a Single Gene through Different Signal Transduction Pathways. Mol Cell Biol. 1989;9:5404–11.

151. Decker T, Lew DJ, Mirkovitch J, Darnell JE. Cytoplasmic activation of GAF, an IFN-gamma-regulated DNA-binding factor. EMBO J. 1991; 10(4): 927-32.

152. Sheppard P, Kindsvogel W, Xu W, Henderson K, Schlutsmeyer S, Whitmore

TE, et al. IL-28, IL-29 and their class II cytokine receptor IL-28R. Nat Immunol. 2003;4:63–8. doi:10.1038/ni873.

153. Kotenko S V., Gallagher G, Baurin V V., Lewis-Antes A, Shen M, Shah NK, et al. IFN-λs mediate antiviral protection through a distinct class II cytokine receptor complex. Nat Immunol. 2003;4:69–77. doi:10.1038/ni875.

154. Prokunina-Olsson L, Muchmore B, Tang W, Pfeiffer RM, Park H, Dickensheets H, et al. A variant upstream of IFNL3 (IL28B) creating a new interferon gene IFNL4 is associated with impaired clearance of hepatitis C virus. Nat Genet. 2013;45:164–71. doi:10.1038/ng.2521.

155. Kessler DS, Veals SA, Fu XY, Levy DE. Interferon-alpha regulates nuclear translocation and DNA-binding affinity of ISGF3, a multimeric transcriptional activator. Genes Dev. 1990;4:1753–65. doi:10.1101/gad.4.10.1753.

156. Stark GR, Darnell JE. The JAK-STAT Pathway at Twenty. Immunity. 2012;36:503–14. doi:10.1016/j.immuni.2012.03.013.

157. Rengachari S, Groiss S, Devos JM, Caron E, Grandvaux N, Panne D. Structural basis of STAT2 recognition by IRF9 reveals molecular insights into ISGF3 function. Proc Natl Acad Sci. 2018; 115(4): E601-609.

158. DUMOUTIER L, LEJEUNE D, HOR S, FICKENSCHER H, RENAULD J-C. Cloning of a new type II cytokine receptor activating signal transducer and activator of transcription (STAT)1, STAT2 and STAT3. Biochem J. 2003;370:391–6. doi:10.1042/bj20021935.

159. Pott J, Mahlakoiv T, Mordstein M, Duerr CU, Michiels T, Stockinger S, et al. IFN- determines the intestinal epithelial antiviral host defense. Proc Natl Acad Sci. 2011;108:7944–9. doi:10.1073/pnas.1100552108.

160. Jewell NA, Cline T, Mertz SE, Smirnov S V., Flano E, Schindler C, et al. Lambda Interferon Is the Predominant Interferon Induced by Influenza A Virus Infection In Vivo. J Virol. 2010; 84(21): 11515-22. doi: 10.1128/JVI.01703-09.

161. Okabayashi T, Kojima T, Masaki T, Yokota S, Imaizumi T, Tsutsumi H, et al. Type-III interferon, not type-I, is the predominant interferon induced by respiratory viruses in nasal epithelial cells. Virus Res. 2011;160:360–6.

doi:10.1016/j.virusres.2011.07.011.

162. Odendall C, Kagan JC. The unique regulation and functions of type III interferons in antiviral immunity. Curr Opin Virol. 2015;12:47–52. doi:10.1016/j.coviro.2015.02.003.

163. Chen K, Liu J, Cao X. Regulation of type I interferon signaling in immunity and inflammation: A comprehensive review. J Autoimmun. 2017;83:1–11. doi:10.1016/j.jaut.2017.03.008.

164. Uematsu S, Akira S. Toll-like Receptors and Type I Interferons. J Biol Chem. 2007;282:15319–23. doi:10.1074/jbc.R700009200.

165. Fang R, Jiang Q, Zhou X, Wang C, Guan Y, Tao J, et al. MAVS activates TBK1 and IKKε through TRAFs in NEMO dependent and independent manner. PLoS Pathog. 2017; 13(11): e1006720. doi: 10.1371/journal.ppat.1006720.

166. Tanaka Y, Chen ZJ. STING specifies IRF3 phosphorylation by TBK1 in the cytosolic DNA signaling pathway. Sci Signal. 2012;5:ra20.

167. Abe T, Barber GN. Cytosolic-DNA-Mediated, STING-Dependent Proinflammatory Gene Induction Necessitates Canonical NF-κB Activation through TBK1. Journal of virology. 2014;88:5328–41. doi:10.1128/JVI.00037-14.

168. Tailor P, Tamura T, Kong HJ, Kubota T, Kubota M, Borghi P, et al. The Feedback Phase of Type I Interferon Induction in Dendritic Cells Requires Interferon Regulatory Factor 8. Immunity. 2007;27:228–39. doi:10.1016/j.immuni.2007.06.009.

169. Tamura T, Yanai H, Savitsky D, Taniguchi T. The IRF Family Transcription Factors in Immunity and Oncogenesis. Annu Rev Immunol. 2008;26:535–84. doi:10.1146/annurev.immunol.26.021607.090400.

170. RYALS J, DIERKS P, RAGG H, WEISSMANN C. A 46-nucleotide promoter segment from an IFN-α gene renders an unrelated promoter inducible by virus. Cell. 1985;41:497–507. doi:10.1016/S0092-8674(85)80023-4.

171. Thanos D, Maniatis T. Virus induction of human IFNβ gene expression requires the assembly of an enhanceosome. Cell. 1995; 83(7): 1091-100.

172. Yarilina A, Park-Min K-H, Antoniv T, Hu X, Ivashkiv LB. TNF activates an IRF1-

dependent autocrine loop leading to sustained expression of chemokines and STAT1-dependent type I interferon–response genes. Nat Immunol. 2008;9:378–87. doi:10.1038/ni1576.

173. Venkatesh D, Ernandez T, Rosetti F, Batal I, Cullere X, Luscinskas FW, et al. Endothelial TNF Receptor 2 Induces IRF1 Transcription Factor-Dependent Interferon-β Autocrine Signaling to Promote Monocyte Recruitment. Immunity. 2013;38:1025–37. doi:10.1016/j.immuni.2013.01.012.

174. Ivashkiv LB, Donlin LT. Regulation of type I interferon responses. Nat Rev Immunol. 2013;14:36–49. doi:10.1038/nri3581.

175. Perry AK, Chen G, Zheng D, Tang H, Cheng G. The host type I interferon response to viral and bacterial infections. Cell Research. 2005; 15(6): 407-22.

176. Schoggins JW, Wilson SJ, Panis M, Murphy MY, Jones CT, Bieniasz P, et al. A diverse range of gene products are effectors of the type I interferon antiviral response. Nature. 2011;472:481–5. doi:10.1038/nature09907.

177. Brierley MM, Marchington KL, Jurisica I, Fish EN. Identification of GAS-dependent interferon-sensitive target genes whose transcription is STAT2-dependent but ISGF3-independent. FEBS J. 2006;273:1569–81. doi:10.1111/j.1742-4658.2006.05176.x.

178. Jaks E, Gavutis M, Uzé G, Martal J, Piehler J. Differential Receptor Subunit Affinities of Type I Interferons Govern Differential Signal Activation. J Mol Biol. 2007;366:525–39. doi:10.1016/j.jmb.2006.11.053.

179. Platanias LC. Mechanisms of type-I- and type-II-interferon-mediated signalling. Nat Rev Immunol. 2005;5:375–86. doi:10.1038/nri1604.

180. Ho HH, Ivashkiv LB. Role of STAT3 in Type I Interferon Responses. J Biol Chem. 2006;281:14111–8. doi:10.1074/jbc.M511797200.

181. Liu X-Y, Chen W, Wei B, Shan Y-F, Wang C. IFN-Induced TPR Protein IFIT3 Potentiates Antiviral Signaling by Bridging MAVS and TBK1. J Immunol. 2011;187:2559–68. doi:10.4049/jimmunol.1100963.

182. Der SD, Zhou A, Williams BRG, Silverman RH. Identification of genes differentially regulated by interferon apha, beta, or gamma using oligonucleotide

arrays. Proc Natl Acad Sci. 1998;95:15623–8. doi:10.1073/pnas.95.26.15623.

183. Decker T, Kovarik P. Serine phosphorylation of STATs. Oncogene. 2000;19:2628–37. doi:10.1038/sj.onc.1203481.

184. Varinou L, Ramsauer K, Karaghiosoff M, Kolbe T, Pfeffer K, Müller M, et al. Phosphorylation of the Stat1 Transactivation Domain Is Required for Full-Fledged IFN-γ-Dependent Innate Immunity. Immunity. 2003;19:793–802. doi:10.1016/S1074-7613(03)00322-4.

185. Ramsauer K, Sadzak I, Porras A, Pilz A, Nebreda AR, Decker T, et al. p38 MAPK enhances STAT1-dependent transcription independently of Ser-727 phosphorylation. Proc Natl Acad Sci. 2002;99:12859–64. doi:10.1073/pnas.192264999.

186. Uddin S, Sassano A, Deb DK, Verma A, Majchrzak B, Rahman A, et al. Protein Kinase C-δ (PKC-δ) Is Activated by Type I Interferons and Mediates Phosphorylation of Stat1 on Serine 727. J Biol Chem. 2002;277:14408–16. doi:10.1074/jbc.M109671200.

187. Nair JS, DaFonseca CJ, Tjernberg A, Sun W, Darnell JE, Chait BT, et al. Requirement of Ca2+ and CaMKII for Stat1 Ser-727 phosphorylation in response to IFN-. Proc Natl Acad Sci. 2002;99:5971–6. doi:10.1073/pnas.052159099.

188. de Veer MJ, Holko M, Frevel M, Walker E, Der S, Paranjape JM, et al. Functional classification of interferon-stimulated genes identified using microarrays. J Leukoc Biol. 2001;69:912–20.

189. Sato M, Hata N, Asagiri M, Nakaya T, Taniguchi T, Tanaka N. Positive feedback regulation of type I IFN genes by the IFN-inducible transcription factor IRF-7. FEBS Lett. 1998;441:106–10. doi:10.1016/S0014-5793(98)01514-2.

190. Marie I. Differential viral induction of distinct interferon-alpha genes by positive feedback through interferon regulatory factor-7. EMBO J. 1998;17:6660–9. doi:10.1093/emboj/17.22.6660.

191. Schoggins JW, Rice CM. Interferon-stimulated genes and their antiviral effector functions. Curr Opin Virol. 2011;1:519–25.

192. Schneider WM, Chevillotte MD, Rice CM. Interferon-stimulated genes: a

complex web of host defenses. Annu Rev Immunol. 2014;32:513–45. doi:10.1146/annurev-immunol-032713-120231.

193. Kotenko S V. IFN-λs. Curr Opin Immunol. 2011;23:583–90. doi:10.1016/j.coi.2011.07.007.

194. Weiss G, Maaetoft-Udsen K, Stifter SA, Hertzog P, Goriely S, Thomsen AR, et al. MyD88 Drives the IFN- Response to Lactobacillus acidophilus in Dendritic Cells through a Mechanism Involving IRF1, IRF3, and IRF7. J Immunol. 2012;189:2860–8. doi:10.4049/jimmunol.1103491.

195. Vazquez C, Horner SM. MAVS Coordination of Antiviral Innate Immunity. J Virol. 2015;89:6974–7. doi:10.1128/JVI.01918-14.

196. Xu H, He X, Zheng H, Huang LJ, Hou F, Yu Z, et al. Structural basis for the prion-like MAVS filaments in antiviral innate immunity. Elife. 2014;3:e01489. doi:10.7554/eLife.01489.

197. Wu B, Peisley A, Tetrault D, Li Z, Egelman EH, Magor KE, et al. Molecular Imprinting as a Signal-Activation Mechanism of the Viral RNA Sensor RIG-I. Mol Cell. 2014;55:511–23. doi:10.1016/j.molcel.2014.06.010.

198. Shi Z, Zhang Z, Zhang Z, Wang Y, Li C, Wang X, et al. Structural Insights into Mitochondrial Antiviral Signaling Protein (MAVS)-Tumor Necrosis Factor Receptor-associated Factor 6 (TRAF6) Signaling. J Biol Chem. 2015;290:26811–20. doi:10.1074/jbc.M115.666578.

199. Dixit E, Boulant S, Zhang Y, Lee ASY, Odendall C, Shum B, et al. Peroxisomes Are Signaling Platforms for Antiviral Innate Immunity. Cell. 2010; 141(4): 668-81. doi: 10.1016/j.cell.2010.04.018.

200. Romling U, Galperin MY, Gomelsky M. Cyclic di-GMP: the First 25 Years of a Universal Bacterial Second Messenger. Microbiol Mol Biol Rev. 2013;77:1–52. doi:10.1128/MMBR.00043-12.

201. Zhang X, Shi H, Wu J, Zhang X, Sun L, Chen C, et al. Cyclic GMP-AMP containing mixed Phosphodiester linkages is an endogenous high-affinity ligand for STING. Mol Cell. 2013;51:226–35.

202. Davies BW, Bogard RW, Young TS, Mekalanos JJ. Coordinated regulation of

accessory genetic elements produces cyclic di-nucleotides for V. cholerae virulence. Cell. 2012;149:358–70.

203. Ablasser A, Goldeck M, Cavlar T, Deimling T, Witte G, Röhl I, et al. cGAS produces a 2′-5′-linked cyclic dinucleotide second messenger that activates STING. Nature. 2013;498:380–4. doi:10.1038/nature12306.

204. Diner EJ, Burdette DL, Wilson SC, Monroe KM, Kellenberger CA, Hyodo M, et al. The Innate Immune DNA Sensor cGAS Produces a Noncanonical Cyclic Dinucleotide that Activates Human STING. Cell Rep. 2013;3:1355–61.

205. Nazmi A, Mukhopadhyay R, Dutta K, Basu A. STING Mediates Neuronal Innate Immune Response Following Japanese Encephalitis Virus Infection. Sci Rep. 2012;2:1–10.

206. Zevini A, Olagnier D, Hiscott J. Crosstalk between Cytoplasmic RIG-I and STING Sensing Pathways. Trends Immunol. 2017;38:194–205. doi:10.1016/j.it.2016.12.004.

207. Chiu YH, MacMillan JB, Chen ZJ. RNA Polymerase III Detects Cytosolic DNA and Induces Type I Interferons through the RIG-I Pathway. Cell. 2009;138:576–91.

208. Su C, Zheng C. Herpes Simplex Virus 1 Abrogates the cGAS/STING-Mediated Cytosolic DNA-Sensing Pathway via Its Virion Host Shutoff Protein, UL41. J Virol. 2017;91. doi:10.1128/JVI.02414-16.

209. Wang Y, Wang X, Li J, Zhou Y, Ho W. RIG-I activation inhibits HIV replication in macrophages. J Leukoc Biol. 2013;94:337–41. doi:10.1189/jlb.0313158.

210. Yan N, Regalado-Magdos AD, Stiggelbout B, Lee-Kirsch MA, Lieberman J. The cytosolic exonuclease TREX1 inhibits the innate immune response to human immunodeficiency virus type 1. Nat Immunol. 2010;11:1005–13. doi:10.1038/ni.1941.

211. Gao D, Wu J, Wu Y-T, Du F, Aroh C, Yan N, et al. Cyclic GMP-AMP synthase is an innate immune sensor of HIV and other retroviruses. Science. 2013;341:903–6.

212. Castanier C, Garcin D, Vazquez A, Arnoult D, Ablasser A, Bauernfeind F, et al. Mitochondrial dynamics regulate the RIG-I-like receptor antiviral pathway. EMBO Rep. 2010;11:133–8. doi:10.1038/embor.2009.258.

213. Marchetti M, Monier M-N, Fradagrada A, Mitchell K, Baychelier F, Eid P, et al. Stat-mediated Signaling Induced by Type I and Type II Interferons (IFNs) Is Differentially Controlled through Lipid Microdomain Association and Clathrin-dependent Endocytosis of IFN Receptors. Mol Biol Cell. 2006;17:2896–909. doi:10.1091/mbc.e06-01-0076.

214. Malakhova OA, Kim KII, Luo J-K, Zou W, Kumar KGS, Fuchs SY, et al. UBP43 is a novel regulator of interferon signaling independent of its ISG15 isopeptidase activity. EMBO J. 2006;25:2358–67. doi:10.1038/sj.emboj.7601149.

215. François-Newton V, de Freitas Almeida GM, Payelle-Brogard B, Monneron D, Pichard-Garcia L, Piehler J, et al. USP18-based negative feedback control is induced by type I and type III interferons and specifically inactivates interferon α response. PLoS One. 2011; 6(7): e22200.

216. Piganis RAR, De Weerd NA, Gould JA, Schindler CW, Mansell A, Nicholson SE, et al. Suppressor of Cytokine Signaling (SOCS) 1 Inhibits Type I Interferon (IFN) Signaling via the Interferon α Receptor (IFNAR1)-associated Tyrosine Kinase Tyk2. J Biol Chem. 2011;286:33811–8. doi:10.1074/jbc.M111.270207.

217. Li Y, Li C, Xue P, Zhong B, Mao A-P, Ran Y, et al. ISG56 is a negative-feedback regulator of virus-triggered signaling and cellular antiviral response. Proc Natl Acad Sci. 2009; 106(19): 7945-50.

218. Gale M, Sen GC. Viral Evasion of the Interferon System. J Interf Cytokine Res. 2009;29:475–6. doi:10.1089/jir.2009.0078.

219. Schulz KS, Mossman KL. Viral Evasion Strategies in Type I IFN Signaling - A Summary of Recent Developments. Front Immunol. 2016;7:498. doi:10.3389/fimmu.2016.00498.

220. García-Sastre A. Ten Strategies of Interferon Evasion by Viruses. Cell Host and Microbe. 2017; 22(2): 176-84.

221. Maringer K, Fernandez-Sesma A. Message in a bottle: Lessons learned from antagonism of STING signalling during RNA virus infection. Cytokine and Growth Factor Reviews. 2014; 25(6): 669-79.

222. Valadão ALC, Aguiar RS, de Arruda LB. Interplay between inflammation and

cellular stress triggered by Flaviviridae viruses. Frontiers in Microbiology. 2016; 7:1233. doi: 10.3389/fmicb.2016.01233.

223. Maximova OA, Faucette LJ, Ward JM, Murphy BR, Pletnev AG. Cellular inflammatory response to flaviviruses in the central nervous system of a primate host. J Histochem Cytochem. 2009; 57(10): 973-89.

224. Murray CL, Jones CT, Rice CM. Architects of assembly: roles of Flaviviridae non-structural proteins in virion morphogenesis. Nat Rev Microbiol. 2008;6:699–708. doi:10.1038/nrmicro1928.

225. Zhang Y. Structures of immature flavivirus particles. EMBO J. 2003;22:2604–13. doi:10.1093/emboj/cdg270.

226. Bollati M, Alvarez K, Assenberg R, Baronti C, Canard B, Cook S, et al. Structure and functionality in flavivirus NS-proteins: Perspectives for drug design. Antiviral Res. 2010;87:125–48. doi:10.1016/j.antiviral.2009.11.009.

227. Maruyama SR, Castro-Jorge LA, Ribeiro JMC, Gardinassi LG, Garcia GR, Brandão LG, et al. Characterisation of divergent flavivirus NS3 and NS5 protein sequences detected in Rhipicephalus microplus ticks from Brazil. Mem Inst Oswaldo Cruz. 2014; 109(1): 38-50.

228. Geiss BJ, Stahla H, Hannah AM, Gari HH, Keenan SM. Focus on flaviviruses: current and future drug targets. Future Med Chem. 2009;1:327–44. doi:10.4155/fmc.09.27.

229. García LL, Padilla L, Castaño JC. Inhibitors compounds of the flavivirus replication process. Virol J. 2017;14:95. doi:10.1186/s12985-017-0761-1.

230. Scaturro P, Trist IML, Paul D, Kumar A, Acosta EG, Byrd CM, et al. Characterization of the Mode of Action of a Potent Dengue Virus Capsid Inhibitor. J Virol. 2014;88:11540–55. doi:10.1128/JVI.01745-14.

231. Lim SP, Wang Q-Y, Noble CG, Chen Y-L, Dong H, Zou B, et al. Ten years of dengue drug discovery: Progress and prospects. Antiviral Res. 2013;100:500–19. doi:10.1016/j.antiviral.2013.09.013.

232. Aguirre S, Maestre AM, Pagni S, Patel JR, Savage T, Gutman D, et al. DENV Inhibits Type I IFN Production in Infected Cells by Cleaving Human STING. PLoS

Pathog. 2012; 8(10): e1002934.

233. Aguirre S, Luthra P, Sanchez-Aparicio MT, Maestre AM, Patel J, Lamothe F, et al. Dengue virus NS2B protein targets cGAS for degradation and prevents mitochondrial DNA sensing during infection. Nat Microbiol. 2017; 2:17037. doi: 10.1038/nmicrobiol.2017.37.

234. Stabell AC, Meyerson NR, Gullberg RC, Gilchrist AR, Webb KJ, Old WM, et al. Dengue viruses cleave STING in humans but not in nonhuman primates, their presumed natural reservoir. Elife. 2018; 7; pii:e31919.

235. Priyamvada L, Hudson W, Ahmed R, Wrammert J. Humoral cross-reactivity between Zika and dengue viruses: Implications for protection and pathology. Emerging Microbes and Infections. 2017; 6(5): e33.

236. Ekins S, Liebler J, Neves BJ, Lewis WG, Coffee M, Bienstock R, et al. Illustrating and homology modeling the proteins of the Zika virus. F1000Research. 2016; 5:275. doi: 10.12688/f1000research.8213.2

237. Rockstroh A, Moges B, Barzon L, Sinigaglia A, Palù G, Kumbukgolla W, et al. Specific detection of dengue and Zika virus antibodies using envelope proteins with mutations in the conserved fusion loop. Emerg Microbes Infect. 2017; 6(11): e99.

238. Granger D, Hilgart H, Misner L, Christensen J, Bistodeau S, Palm J, et al. Serologic testing for zika virus: Comparison of three zika virus IgM screening enzyme-linked immunosorbent assays and initial laboratory experiences. J Clin Microbiol. 2017; 55(7): 2127-36.

239. Premkumar L, Collins M, Graham S, Liou G-JA, Lopez CA, Jadi R, et al. Development of Envelope Protein Antigens To Serologically Differentiate Zika Virus Infection from Dengue Virus Infection. J Clin Microbiol. 2017;56. doi:10.1128/JCM.01504-17.

240. de Araújo TVB, Ximenes RA de A, Miranda-Filho D de B, Souza WV, Montarroyos UR, de Melo APL, et al. Association between microcephaly, Zika virus infection, and other risk factors in Brazil: final report of a case-control study. Lancet Infect Dis. 2018;18:328–36. doi:10.1016/S1473-3099(17)30727-2.

241. Christian KM, Song H, Ming G. A previously undetected pathology of Zika virus

infection. Nat Med. 2018; 24(3): 258-9.

242. Yockey LJ, Jurado KA, Arora N, Millet A, Rakib T, Milano KM, et al. Type I interferons instigate fetal demise after Zika virus infection. Sci Immunol. 2018;3:eaao1680. doi:10.1126/sciimmunol.aao1680.

243. Grant A, Ponia SS, Tripathi S, Balasubramaniam V, Miorin L, Sourisseau M, et al. Zika Virus Targets Human STAT2 to Inhibit Type i Interferon Signaling. Cell Host Microbe. 2016; 19(6): 882-90.

244. Bowen JR, Quicke KM, Maddur MS, O'Neal JT, McDonald CE, Fedorova NB, et al. Zika Virus Antagonizes Type I Interferon Responses during Infection of Human Dendritic Cells. PLOS Pathog. 2017;13:e1006164. doi:10.1371/journal.ppat.1006164.

245. Ashour J, Laurent-Rolle M, Shi P-Y, Garcia-Sastre A. NS5 of Dengue Virus Mediates STAT2 Binding and Degradation. J Virol. 2009;83:5408–18. doi:10.1128/JVI.02188-08.

246. Best SM. The Many Faces of the Flavivirus NS5 Protein in Antagonism of Type I Interferon Signaling. J Virol. 2017; 91(3), pii:e01970.

247. Moreira-Teixeira L, Mayer-Barber K, Sher A, O'Garra A. Type I interferons in tuberculosis: Foe and occasionally friend. J Exp Med. 2018;215:1273–85. doi:10.1084/jem.20180325.

248. McNab F, Mayer-Barber K, Sher A, Wack A, O'Garra A. Type I interferons in infectious disease. Nature Reviews Immunology. 2015; 15(2): 87-103.

249. Luker KE, Hutchens M, Schultz T, Pekosz A, Luker GD. Bioluminescence imaging of vaccinia virus: Effects of interferon on viral replication and spread. Virology. 2005;341:284–300. doi:10.1016/j.virol.2005.06.049.

250. Murphy AA, Rosato PC, Parker ZM, Khalenkov A, Leib DA. Synergistic control of herpes simplex virus pathogenesis by IRF-3, and IRF-7 revealed through non-invasive bioluminescence imaging. Virology. 2013;444:71–9. doi:10.1016/j.virol.2013.05.034.

251. Jørgensen SE, Christiansen M, Ryø LB, Gad HH, Gjedsted J, Staeheli P, et al. Defective RNA sensing by RIG-I in severe influenza virus infection. Clin Exp

Immunol. 2018;192:366–76. doi:10.1111/cei.13120.

252. Ruiz-Moreno JS, Hamann L, Jin L, Sander LE, Puzianowska-Kuznicka M, Cambier J, et al. The cGAS/STING Pathway Detects Streptococcus pneumoniae but Appears Dispensable for Antipneumococcal Defense in Mice and Humans. Infect Immun. 2018;86:pii:e00849-17. doi:10.1128/IAI.00849-17.

253. Ruiz-Moreno JS, Hamann L, Shah JA, Verbon A, Mockenhaupt FP, Puzianowska-Kuznicka M, et al. The common HAQ STING variant impairs cGAS-dependent antibacterial responses and is associated with susceptibility to Legionnaires' disease in humans. PLOS Pathog. 2018;14:e1006829. doi:10.1371/journal.ppat.1006829.

254. Welsh RM, Bahl K, Marshall HD, Urban SL. Type 1 Interferons and Antiviral CD8 T-Cell Responses. PLoS Pathog. 2012;8:e1002352. doi:10.1371/journal.ppat.1002352.

255. Le Bon A, Schiavoni G, D'Agostino G, Gresser I, Belardelli F, Tough DF. Type I Interferons Potently Enhance Humoral Immunity and Can Promote Isotype Switching by Stimulating Dendritic Cells In Vivo. Immunity. 2001;14:461–70. doi:10.1016/S1074-7613(01)00126-1.

256. Jego G, Palucka AK, Blanck J-P, Chalouni C, Pascual V, Banchereau J. Plasmacytoid Dendritic Cells Induce Plasma Cell Differentiation through Type I Interferon and Interleukin 6. Immunity. 2003;19:225–34. doi:10.1016/S1074-7613(03)00208-5.

257. Critchley-Thorne RJ, Simons DL, Yan N, Miyahira AK, Dirbas FM, Johnson DL, et al. Impaired interferon signaling is a common immune defect in human cancer. Proc Natl Acad Sci. 2009;106:9010–5. doi:10.1073/pnas.0901329106.

258. Moriyama M, Arakawa Y. Treatment of interferon-α for chronic hepatitis C. Expert Opin Pharmacother. 2006;7:1163–79. doi:10.1517/14656566.7.9.1163.

259. Murira A, Lamarre A. Type-I Interferon Responses: From Friend to Foe in the Battle against Chronic Viral Infection. Front Immunol. 2016;7:609. doi:10.3389/fimmu.2016.00609.

260. Rong L, Perelson AS. Treatment of hepatitis C virus infection with interferon

and small molecule direct antivirals: viral kinetics and modeling. Crit Rev Immunol. 2010;30:131–48. doi:5603dbb41ca52347,1a5c5f2936a724f3 [pii].

261. Utay NS, Douek DC. Interferons and HIV Infection: The Good, the Bad, and the Ugly. Pathog Immun. 2016;1:107. doi:10.20411/pai.v1i1.125.

262. Weder N, Zhang H, Jensen K, Yang BZ, Simen A, Jackowski A, et al. Child Abuse, Depression, and Methylation in Genes Involved With Stress, Neural Plasticity, and Brain Circuitry. J Am Acad Child Adolesc Psychiatry. 2014;53:417-424.e5. doi:10.1016/j.jaac.2013.12.025.

263. Cheng L, Ma J, Li J, Li D, Li G, Li F, et al. Blocking type I interferon signaling enhances T cell recovery and reduces HIV-1 reservoirs. J Clin Invest. 2017; 127(1): 269-79.

264. Takeuchi T, Genovese MC, Haraoui B, Li Z, Xie L, Klar R, et al. Dose reduction of baricitinib in patients with rheumatoid arthritis achieving sustained disease control: results of a prospective study. Ann Rheum Dis. 2019;78:171–8. doi:10.1136/annrheumdis-2018-213271.

265. Wang P, Zheng SG. Regulatory T cells and B cells: implication on autoimmune diseases. Int J Clin Exp Pathol. 2013;6:2668–74. http://www.ncbi.nlm.nih.gov/pubmed/24294353.

266. Giltiay N V., Chappell CP, Clark EA. B-cell selection and the development of autoantibodies. Arthritis Res Ther. 2012;14 Suppl 4:S1. doi:10.1186/ar3918.

267. Hooks JJ, Moutsopoulos HM, Geis SA, Stahl NI, Decker JL, Notkins AL. Immune Interferon in the Circulation of Patients with Autoimmune Disease. N Engl J Med. 1979; 301(1): 5-8.

268. Barbalat R, Ewald SE, Mouchess ML, Barton GM. Nucleic Acid Recognition by the Innate Immune System. Annu Rev Immunol. 2011; 29: 185-214.

269. Higgs BW, Liu Z, White B, Zhu W, White WI, Morehouse C, et al. Patients with systemic lupus erythematosus, myositis, rheumatoid arthritis and scleroderma share activation of a common type I interferon pathway. Ann Rheum Dis. 2011; 70(11): 2029-36.

270. Marro BS, Ware BC, Zak J, de la Torre JC, Rosen H, Oldstone MBA.

Progression of type 1 diabetes from the prediabetic stage is controlled by interferon-α signaling. Proc Natl Acad Sci. 2017;114:3708–13. doi:10.1073/pnas.1700878114.

271. Postal M, Sinicato N, Peliçari K, Marini R, Costallat L, Appenzeller S. Clinical and serological manifestations associated with interferon-α levels in childhood-onset systemic lupus erythematosus. Clinics. 2012;67:157–62. doi:10.6061/clinics/2012(02)11.

272. Crow MK. Type I interferon in the pathogenesis of lupus. J Immunol. 2014;192:5459–68. doi:10.4049/jimmunol.1002795.

273. Lodato F. Systemic lupus erythematosus following virological response to peginterferon alfa-2b in a transplanted patient with chronic hepatitis C recurrence. World J Gastroenterol. 2006;12:4253. doi:10.3748/wjg.v12.i26.4253.

274. Ho V, McLean A, Terry S. Severe systemic lupus erythematosus induced by antiviral treatment for hepatitis C. J Clin Rheumatol. 2008; 14(3): 166-8.

275. O'Neill LAJ, Golenbock D, Bowie AG. The history of Toll-like receptors — redefining innate immunity. Nat Rev Immunol. 2013;13:453–60. doi:10.1038/nri3446.

276. Seth RB, Sun L, Ea CK, Chen ZJ. Identification and characterization of MAVS, a mitochondrial antiviral signaling protein that activates NF-kB and IRF3. Cell. 2005;122:669–82.

277. Ishikawa H, Barber GN. STING is an endoplasmic reticulum adaptor that facilitates innate immune signalling. Nature. 2008;455:674–8. doi:10.1038/nature07317.

278. Pourcelot M, Zemirli N, Silva Da Costa L, Loyant R, Garcin D, Vitour D, et al. The Golgi apparatus acts as a platform for TBK1 activation after viral RNA sensing. BMC Biol. 2016;14:69. doi:10.1186/s12915-016-0292-z.

279. Gonugunta VK, Sakai T, Pokatayev V, Yang K, Wu J, Dobbs N, et al. Trafficking-Mediated STING Degradation Requires Sorting to Acidified Endolysosomes and Can Be Targeted to Enhance Anti-tumor Response. Cell Rep. 2017;21:3234–42. doi:10.1016/j.celrep.2017.11.061.

280. Dobbs N, Burnaevskiy N, Chen D, Gonugunta VK, Alto NM, Yan N. STING Activation by Translocation from the ER Is Associated with Infection and

Autoinflammatory Disease. Cell Host Microbe. 2015;18:157–68. doi:10.1016/j.chom.2015.07.001.

281. Sun L, Wu J, Du F, Chen X, Chen ZJ. Cyclic GMP-AMP synthase is a cytosolic DNA sensor that activates the type I interferon pathway. Science (80-). 2013; 339(6121): 786-91.

282. Mukai K, Konno H, Akiba T, Uemura T, Waguri S, Kobayashi T, et al. Activation of STING requires palmitoylation at the Golgi. Nat Commun. 2016;7 May:11932. doi:10.1038/ncomms11932.

283. Saitoh T, Fujita N, Hayashi T, Takahara K, Satoh T, Lee H, et al. Atg9a controls dsDNA-driven dynamic translocation of STING and the innate immune response. Proc Natl Acad Sci U S A. 2009;106:20842–6. doi:10.1073/pnas.0911267106\r0911267106 [pii].

284. Kim S, Koch P, Li L, Peshkin L, Mitchison TJ. Evidence for a role of calcium in STING signaling. bioRxiv. 2017;:10.1101/145854.

285. Shi H, Wu J, Chen ZJ, Chen C. Molecular basis for the specific recognition of the metazoan cyclic GMP-AMP by the innate immune adaptor protein STING. Proc Natl Acad Sci. 2015;112:8947–52. doi:10.1073/pnas.1507317112.

286. Gao P, Ascano M, Zillinger T, Wang W, Dai P, Serganov AA, et al. Structure-function analysis of STING activation by c[G(2’,5’) pA(3’,5’)p] and targeting by antiviral DMXAA. Cell. 2013;154:748–62.

287. Tsuchiya Y, Jounai N, Takeshita F, Ishii KJ, Mizuguchi K. Ligand-induced Ordering of the C-terminal Tail Primes STING for Phosphorylation by TBK1. EBioMedicine. 9:87–96.

288. Huang Y-H, Liu X-Y, Du X-X, Jiang Z-F, Su X-D. The structural basis for the sensing and binding of cyclic di-GMP by STING. Nat Struct Mol Biol. 2012;19:728–30. doi:10.1038/nsmb.2333.

289. Yi G, Brendel VP, Shu C, Li P, Palanathan S, Cheng Kao C. Single Nucleotide Polymorphisms of Human STING Can Affect Innate Immune Response to Cyclic Dinucleotides. PLoS One. 2013; 8(10): e77846.

290. de Almeida LA, Carvalho NB, Oliveira FS, Lacerda TLS, Vasconcelos AC,

Nogueira L, et al. MyD88 and STING Signaling Pathways Are Required for IRF3-Mediated IFN-β Induction in Response to Brucella abortus Infection. PLoS One. 2011;6:e23135. doi:10.1371/journal.pone.0023135.

291. Hamdan N, Kritsiligkou P, Grant CM. ER stress causes widespread protein aggregation and prion formation. J Cell Biol. 2017;216:2295–304. doi:10.1083/jcb.201612165.

292. Oslowski CM, Urano F. Measuring ER Stress and the Unfolded Protein Response Using Mammalian Tissue Culture System. In: Methods in Enzymology. 2011. p. 71–92. doi:10.1016/B978-0-12-385114-7.00004-0.

293. Hashimoto J, Watanabe T, Seki T, Karasawa S, Izumikawa M, Seki T, et al. Novel In Vitro Protein Fragment Complementation Assay Applicable to High-Throughput Screening in a 1536-Well Format. J Biomol Screen. 2009;14:970–9. doi:10.1177/1087057109341406.

294. Morell M, Ventura S, Avilés FX. Protein complementation assays: Approaches for the in vivo analysis of protein interactions. FEBS Lett. 2009;583:1684–91. doi:10.1016/j.febslet.2009.03.002.

295. Rochette S, Diss G, Filteau M, Leducq J-B, Dubé AK, Landry CR. Genome-wide protein-protein interaction screening by protein-fragment complementation assay (PCA) in living cells. J Vis Exp. 2015;:doi: 10.3791/52255. doi:10.3791/52255.

296. Jin L, Xu L-G, Yang I V, Davidson EJ, Schwartz DA, Wurfel MM, et al. Identification and characterization of a loss-of-function human MPYS variant. Genes Immun. 2011;12:263–9. doi:10.1038/gene.2010.75.

297. Dell'Oste V, Gatti D, Gugliesi F, De Andrea M, Bawadekar M, Lo Cigno I, et al. Innate nuclear sensor IFI16 translocates into the cytoplasm during the early stage of in vitro human cytomegalovirus infection and is entrapped in the egressing virions during the late stage. J Virol. 2014;88:6970–82. doi:10.1128/JVI.00384-14.

298. Gao D, Wu J, Wu Y-T, Du F, Aroh C, Yan N, et al. Cyclic GMP-AMP Synthase Is an Innate Immune Sensor of HIV and Other Retroviruses. Science (80-). 2013;341:903–6. doi:10.1126/science.1240933.

299. Diner BA, Lum KK, Toettcher JE, Cristea IM. Viral DNA Sensors IFI16 and

Cyclic GMP-AMP Synthase Possess Distinct Functions in Regulating Viral Gene Expression , Immune Defenses , and Apoptotic Responses during Herpesvirus Infection. MBio. 2016;7:1–15.

300. Nitta S, Sakamoto N, Nakagawa M, Kakinuma S, Mishima K, Kusano-Kitazume A, et al. Hepatitis C virus NS4B protein targets STING and abrogates RIG-I-mediated type I interferon-dependent innate immunity. Hepatology. 2013;57:46–58.

301. Lytle CD, Sagripanti J-L. Predicted inactivation of viruses of relevance to biodefense by solar radiation. J Virol. 2005; 79(22): 14244-52.

302. Huang Y-J, Higgs S, Horne K, Vanlandingham D. Flavivirus-Mosquito Interactions. Viruses. 2014;6:4703–30. doi:10.3390/v6114703.

303. Castillo Ramirez JA, Urcuqui-Inchima S. Dengue Virus Control of Type I IFN Responses: A History of Manipulation and Control. J Interf Cytokine Res. 2015;35:421–30. doi:10.1089/jir.2014.0129.

304. Ding Q, Gaska JM, Douam F, Wei L, Kim D, Balev M, et al. Species-specific disruption of STING-dependent antiviral cellular defenses by the Zika virus NS2B3 protease. Proc Natl Acad Sci. 2018; 115(27): E6310-8.

305. Yu CY, Chang TH, Liang JJ, Chiang RL, Lee YL, Liao CL, et al. Dengue virus targets the adaptor protein MITA to subvert host innate immunity. PLoS Pathog. 2012; 8(6): e1002780.

306. Paixão ES, Barreto F, da Glória Teixeira M, da Conceição N. Costa M, Rodrigues LC. History, Epidemiology, and Clinical Manifestations of Zika: A Systematic Review. Am J Public Health. 2016;106:606–12. doi:10.2105/AJPH.2016.303112.

307. Priyamvada L, Hudson W, Ahmed R, Wrammert J. Humoral cross-reactivity between Zika and dengue viruses: Implications for protection and pathology. Emerging Microbes and Infections. 2017; 6(5): e33.

308. Martina BEE, Koraka P, Osterhaus ADME. Dengue virus pathogenesis: An integrated view. Clinical Microbiology Reviews. 2009; 22(4): 564-81.

309. Miner JJ, Diamond MS. Zika Virus Pathogenesis and Tissue Tropism. Cell Host Microbe. 2017;21:134–42. doi:10.1016/j.chom.2017.01.004.

310. Merfeld E, Ben-Avi L, Kennon M, Cerveny KL. Potential mechanisms of Zika-linked microcephaly. Wiley Interdiscip Rev Dev Biol. 2017; 6(4). doi: 10.1002/wdev.273.

311. Brasil P, Sequeira PC, Freitas ADA, Zogbi HE, Calvet GA, De Souza RV, et al. Guillain-Barré syndrome associated with Zika virus infection. The Lancet. 2016; 74(3): 253-5.

312. Araujo AQC, Silva MTT, Araujo APQC. Zika virus-associated neurological disorders: A review. Brain. 2016; 139(Pt 8): 2122-30.

313. Quicke KM, Bowen JR, Johnson EL, McDonald CE, Ma H, O'Neal JT, et al. Zika Virus Infects Human Placental Macrophages. Cell Host Microbe. 2016;20:83–90. doi:10.1016/j.chom.2016.05.015.

314. Schmid MA, Diamond MS, Harris E. Dendritic cells in dengue virus infection: Targets of virus replication and mediators of immunity. Front Immunol. 2014; 5:647.

315. Webster B, Werneke SW, Zafirova B, This S, Coléon S, Décembre E, et al. Plasmacytoid dendritic cells control dengue and chikungunya virus infections via IRF7-regulated interferon responses. Elife. 2018; 7, pii:e34273.

316. Gary-Gouy H, Lebon P, Dalloul AH. Type I Interferon Production by Plasmacytoid Dendritic Cells and Monocytes Is Triggered by Viruses, but the Level of Production Is Controlled by Distinct Cytokines. J Interf Cytokine Res. 2002;22:653–9. doi:10.1089/10799900260100132.

317. Zhao C, Denison C, Huibregtse JM, Gygi S, Krug RM. Human ISG15 conjugation targets both IFN-induced and constitutively expressed proteins functioning in diverse cellular pathways. Proc Natl Acad Sci. 2005; 102(29): 10200-5.

318. van de Laar L, Coffer PJ, Woltman AM. Regulation of dendritic cell development by GM-CSF: molecular control and implications for immune homeostasis and therapy. Blood. 2012;119:3383–93. doi:10.1182/blood-2011-11-370130.

319. Chapuis F, Rosenzwajg M, Yagello M, Ekman M, Biberfeld P, Gluckman JC. Differentiation of human dendritic cells from monocytesin vitro. Eur J Immunol. 1997;27:431–41. doi:10.1002/eji.1830270213.

320. Zheng Y, Liu Q, Wu Y, Ma L, Zhang Z, Liu T, et al. Zika virus elicits inflammation to evade antiviral response by cleaving cGAS via NS1-caspase-1 axis. EMBO J. 2018; 37(18); pii:e99347.

321. Wu Y, Liu Q, Zhou J, Xie W, Chen C, Wang Z, et al. Zika virus evades interferon-mediated antiviral response through the co-operation of multiple nonstructural proteins in vitro. Cell Discov. 2017; 3:17006.

322. Webster B, Assil S, Dreux M. Cell-Cell Sensing of Viral Infection by Plasmacytoid Dendritic Cells. J Virol. 2016; 90(22): 10050-3.

323. Fernandez-Garcia M-D, Mazzon M, Jacobs M, Amara A. Pathogenesis of Flavivirus Infections: Using and Abusing the Host Cell. Cell Host Microbe. 2009;5:318–28. doi:10.1016/j.chom.2009.04.001.

324. Hornung V, Bauernfeind F, Halle A, Samstad EO, Kono H, Rock KL, et al. Silica crystals and aluminum salts activate the NALP3 inflammasome through phagosomal destabilization. Nat Immunol. 2008;9:847–56. doi:10.1038/ni.1631.

325. Rzeniewicz K, Newe A, Rey Gallardo A, Davies J, Holt MR, Patel A, et al. L-selectin shedding is activated specifically within transmigrating pseudopods of monocytes to regulate cell polarity in vitro. Proc Natl Acad Sci U S A. 2015;112:E1461-70. doi:10.1073/pnas.1417100112.

326. Yildiz S, Alpdundar E, Gungor B, Kahraman T, Bayyurt B, Gursel I, et al. Enhanced immunostimulatory activity of cyclic dinucleotides on mouse cells when complexed with a cell-penetrating peptide or combined with CpG. Eur J Immunol. 2015; 45(4): 1170-9.

327. Burdette DL, Monroe KM, Sotelo-Troha K, Iwig JS, Eckert B, Hyodo M, et al. STING is a direct innate immune sensor of cyclic di-GMP. Nature. 2011;478:515–8.

328. Woodward JJ, Iavarone AT, Portnoy DA. c-di-AMP secreted by intracellular Listeria monocytogenes activates a host type I interferon response. Science. 2010;328:1703–5. doi:10.1126/science.1189801.

329. Eder K, Guan H, Sung HY, Ward J, Angyal A, Janas M, et al. Tribbles-2 is a novel regulator of inflammatory activation of monocytes. Int Immunol. 2008;20:1543–50. doi:10.1093/intimm/dxn116.

330. Guan H, Shuaib A, Leon DD De, Angyal A, Salazar M, Velasco G, et al. Competition between members of the tribbles pseudokinase protein family shapes their interactions with mitogen activated protein kinase pathways. Sci Rep. 2016; 6: 32667. doi: 10.1038/srep32667.

331. Schindelin J, Arganda-Carreras I, Frise E, Kaynig V, Longair M, Pietzsch T, et al. Fiji: An open-source platform for biological-image analysis. Nature Methods. 2012; 9(7): 676-82. doi: 10.1038/nmeth.2019.

Appendix 1: Supplementary data for Paper 2

A1.1 Relative mRNA expression levels of TMEM203, STING, and MAVS in human monocyte-derived macrophages (A-C); Linear correlation was discovered between STING vs TMEM203 but not between MAVS vs TMEM203.

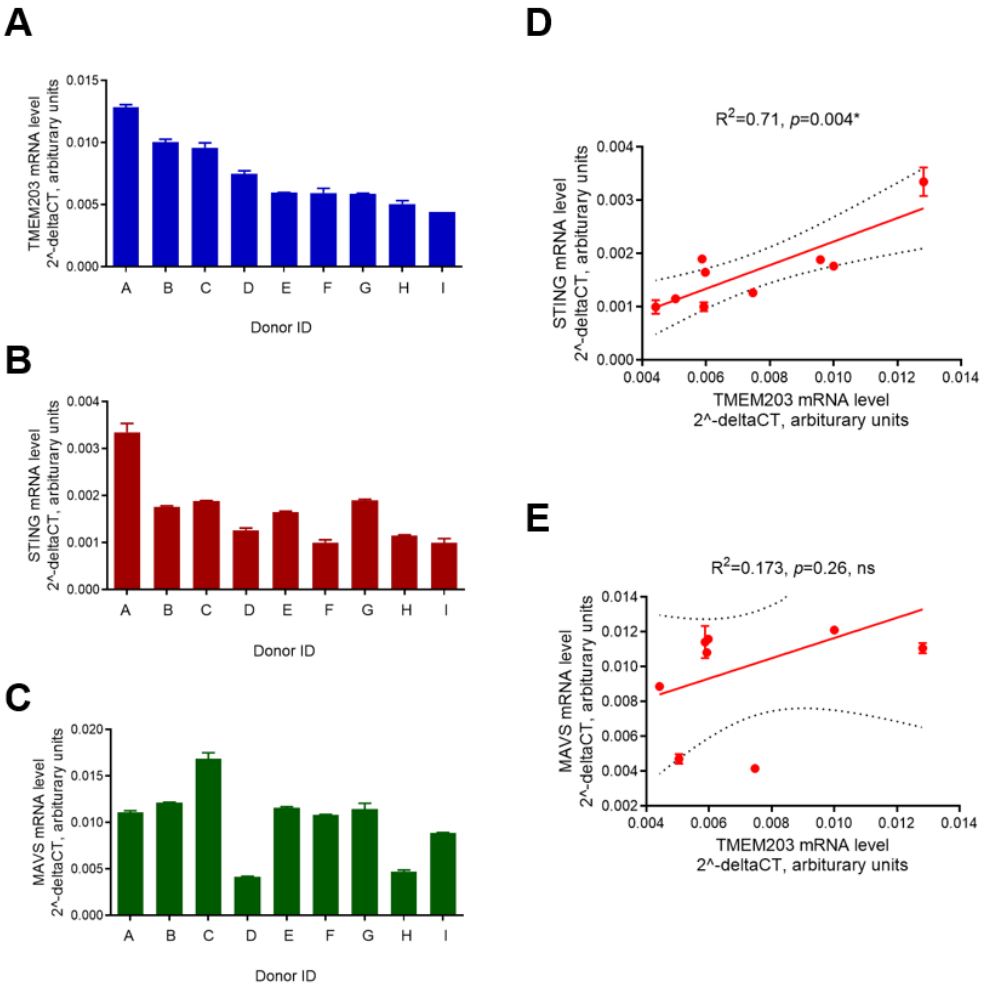

Figure A1. A strong correlation of mRNA levels was identified between TMEM203 and STING but not TMEM203 and MAVS in primary monocyte-derived macrophages. Basal mRNA expression level of TMEM203 (A), STING (B), and MAVS (C) in primary human monocyte-derived macrophages isolated from 9 donors (letter coded identities). Spearman correlation coefficient of STING mRNA expression (D) and MAVS mRNA expression (E) were measured against TMEM203 mRNA expression in donors (95% confidence interval: dash lines). Sample macrophages isolated from each donor were analysed by qPCR in duplicates. Data is presented as mean ± SD, n=2 technical replicates.

A1.2 siRNA transfection does not activate *IFN-β* and *IL-8* mRNA upregulation

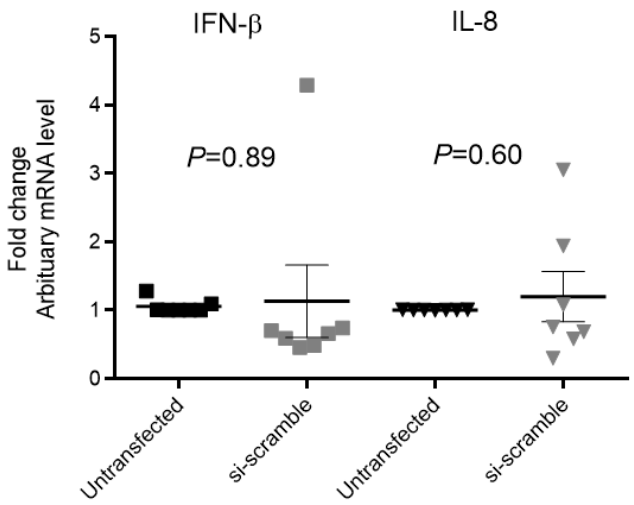

Figure A2. Control siRNA transfection does not induce significant inflammatory activation in primary monocyte-derived macrophages. MDMs were left untransfected or transfected with scrambled siRNA sequences at 12.5 nM using Viromer green transfection method. 48 hours post transfection mRNA expressions of *IFN-β* and *Cxcl8* (IL-8) were assessed by RT-qPCR. Data is presented as mean ± SEM with n=7 donors.

A1.3 Optimising siRNA-directed knockdown in human MDMs

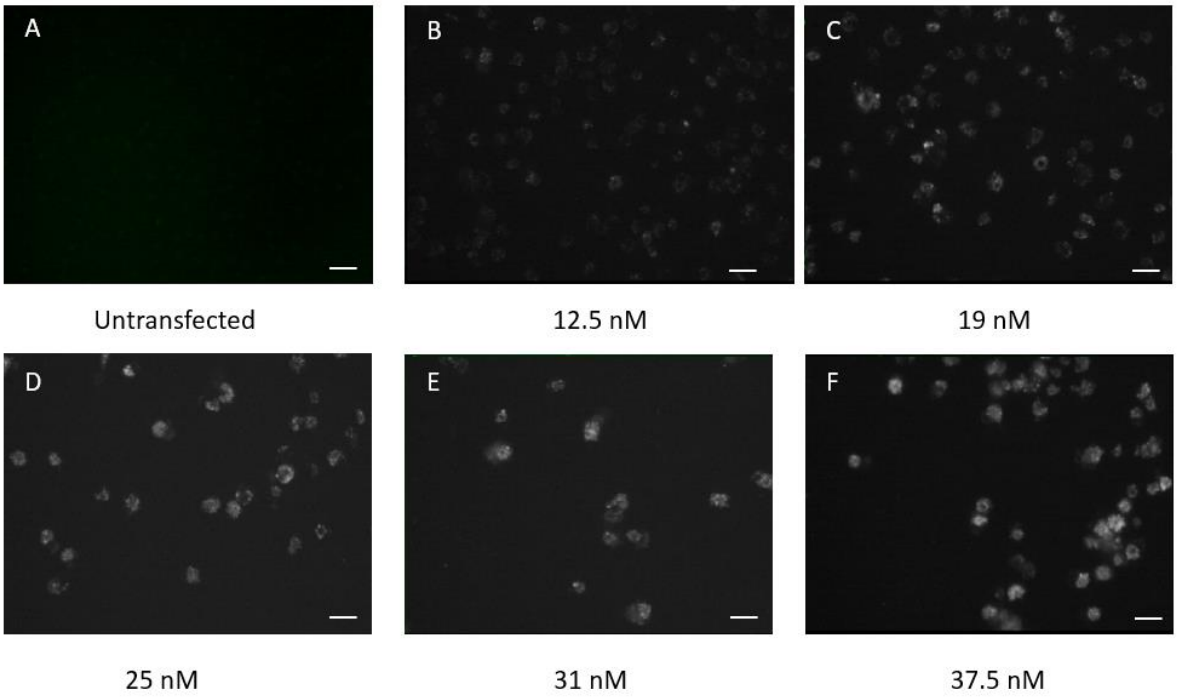

Figure A3. Assessment of cell viability and siRNA transfection efficiency in primary monocyte-derived macrophages. The lowest dose of siRNA transfection showed consistent siGlo signal in cells and no significantly reduction of cell numbers. Representative images were taken 48 hrs post-transfection of green transfection indicator siGlo in MDMs isolated from Donor #94, and visualised under green fluorescent microscope (magnification x20). Concentration of siRNA for each transfection was indicated below each graph. Scale bar 25μm.

A1.4 Site-directed mutagenesis for the generation of STING mutants

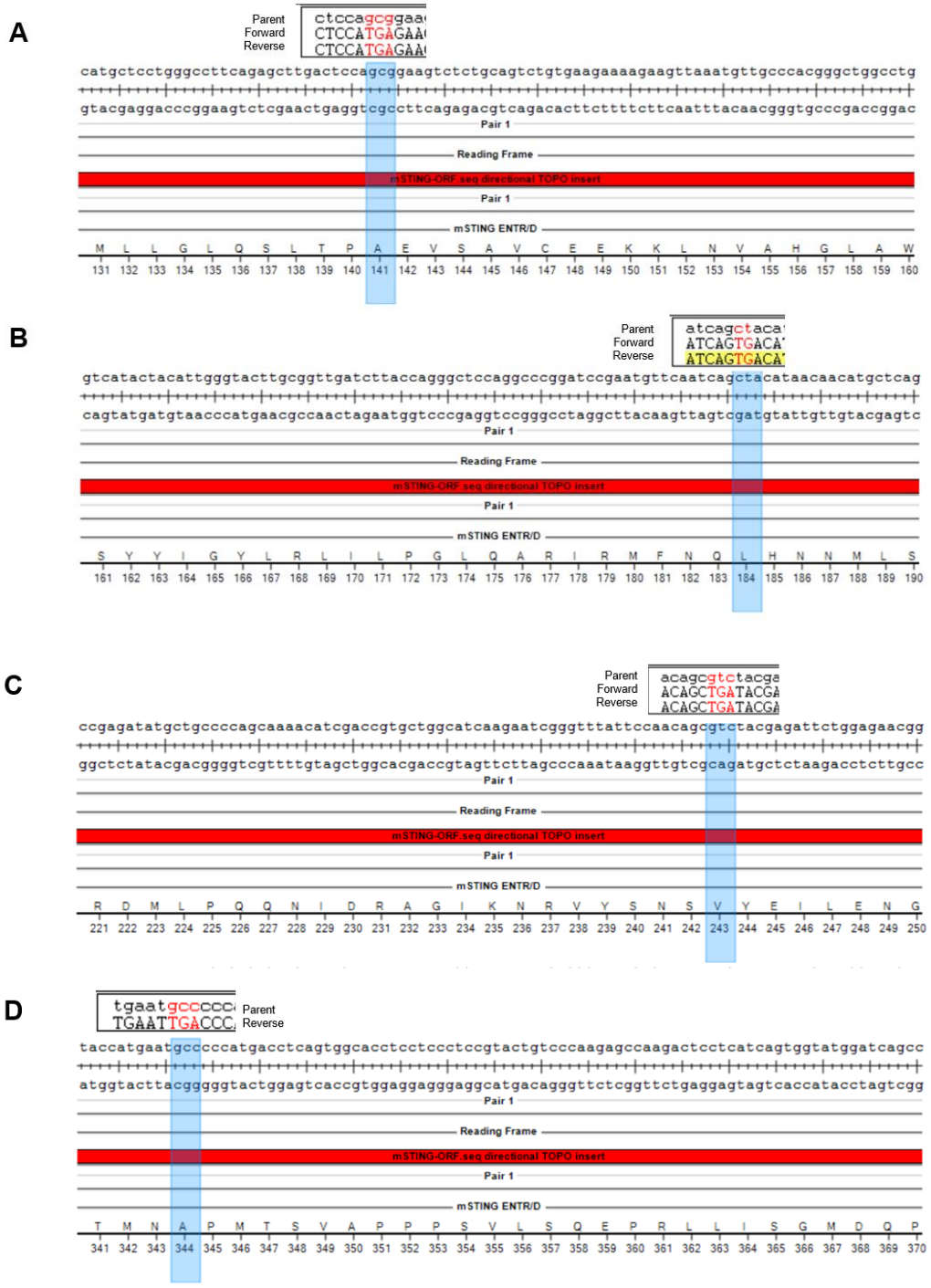

Figure A4. Sequence confirmation of Sting mutagenesis. Site-directed mutagenesis of Sting truncations at (A) 141A, (B) 184L, (C) 243V, and (D) 344A were confirmed by both forward and reverse Sanger sequencing. Amino acid residues were replaced with a stop codon in the sense transcription strand to result in truncations.

A1.5 Optimising ER staining in HeLa cells.

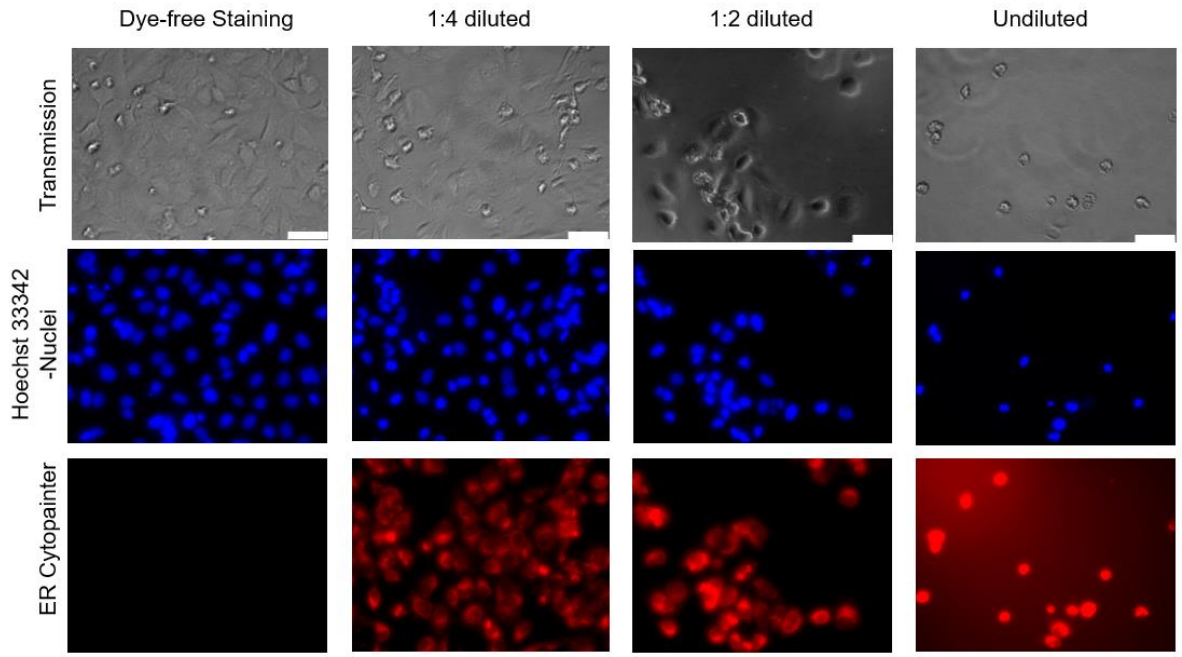

Figure A5. ER staining in HeLa cells. Adherent HeLa cells were stained with ER Cytopainter dyes (Abcam) reconstituted in staining buffer according to the manufacturer's protocol. The staining reagent was further diluted by mixing the recommended dose with 1xPBS. Hoechst 33342 was mixed with ER staining buffer at 1:1000 dilution to counterstain the nuclei, and the control was incubated with dye-free staining buffer diluted 1:4 with PBS. Cells were imaged under the Leica AFI6000 Time-Lapse microscopy at 40X magnification. Scale bar is 50 µm.

A1.6 Optimising lysosome staining in HeLa cells.

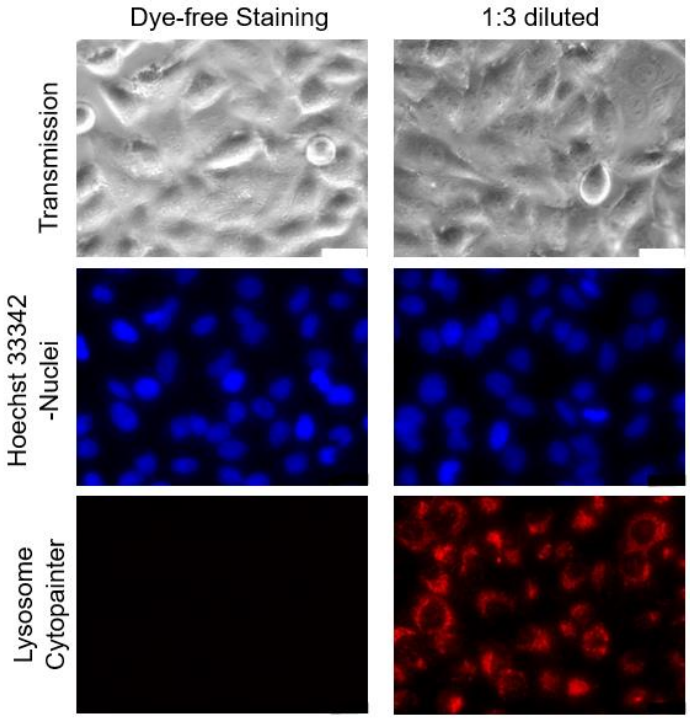

Figure A6. Lysosome staining in HeLa cells. Adherent HeLa cells were stained with Lysosome Cytopainter dyes (Abcam) reconstituted in staining buffer according to the manufacturer's protocol. The staining reagent is further diluted by mixing 1:3 with 1xPBS and this concentration was tested by Bukhari A to be the optimal dose for lysosome visualisation. Hoechst 33342 was mixed with lysosome staining buffer at 1:1000 dilution to counterstain the nuclei, and the control was incubated with dye-free staining buffer diluted 1:3 with PBS. Cells were imaged under the Leica AFI6000 Time-Lapse microscopy at 63X magnification. Scale bar is 25 µm.

A1.7 Optimising co-transfection of protein complementation fluorescence for confocal imaging.

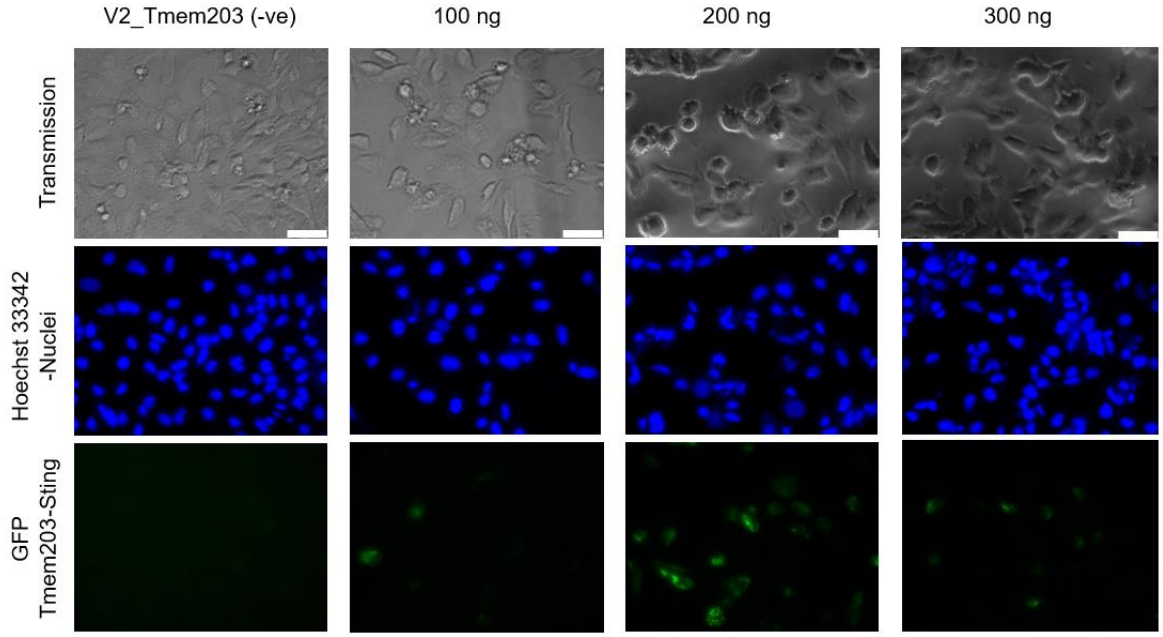

Figure A7. Protein complementation transfection in HeLa cells. Adherent HeLa cells were (co) transfected with plasmids designed for V1 and V2 reporter protein complementation assay for Tmem203 and Sting interaction. The total amount of V1_Sting and V2_Tmem203 plasmids transfected into 20,000 cells in 100 µl culture medium were indicated. The negative control was transfected with 100 ng of V2_Tmem203 plasmid only. 24 hours post transfection, HeLa cells were stained with Hoechst 33342 (1:1000) and were imaged under the Leica AFI6000 Time-Lapse microscopy at 40X magnification. Scale bar is 50 µm.

A1.8 Summary of assay development

The following work has helped to develop assays to complete the work presented in paper 2, although these did not produce displayable data.

1. Adjusting voltage for analysing HEK293 and monocyte population by FACS. Testing TOPRO-3 staining concentration to indicate cell viability.
2. Adjusting cell concentration for HeLa cells imaging using 10mm/35mm glass bottom culture dish. We tested cell density from 300,000 / 100 µl to 150,000 / 100 µl and the best concentration was the highest, which gives a monolayer of HeLa cells for microscopy after plasmid DNA transfection.
3. Testing concentrations for DMXAA, 3'-3' cGAMP and 2'-3' cGAMP stimulation in primary macrophages. We tested 2'-3' cGAMP at 1 µg/ml, 2 µg/ml and 4 µg/ml and the highest concentration gave the maximal IFNβ response. 3'-3' cGAMP was used at 1 µg/ml in consistent to our colleagues in Singapore. DMXAA was used at 4 µg/ml and 10 µg/ml and the high concentration gave the optimal response.
4. Testing transfection method for 3'-3' cGAMP stimulation in MDMs. Digitonin-permeabilization buffer was used to incubate MDMs with and without 3'-3' cGAMP for 15 mins to 30 mins. Incubation longer than 20 mins gives excessive cell death.
5. Optimising the annealing temperature (Tm) for each site-directed mutagenesis. Tm for each PCR reaction is determined by the predicted Tm of each primer pair.
6. Optimising antibody concentration for protein detection in Western blots.
7. Testing and optimising NonBIT live cell luciferase assay system (Promega), including substrate concentrations, 1.1/2.1 gene tagging orientations (1.1_Tmem203 + 1.2_Sting, 1.1_Tmem203 + Sting_1.2, Tmem203_1.1 + 1.2_Sting, and Tmem203_1.1 + Sting_1.2), Hoechst 33342 staining concentration, and plating strategy. Katherine Pye was also involved in the optimisation process.

Appendix 2: Materials for Paper 2

A2.1 List of Reagents

Reagent	Catalog Number	Company
Agarose	1.01236	Sigma Aldrich
ATP (Adenosine 5'-triphosphate disodium salt hydrate)	A26209	Sigma Aldrich
Anhydrous Ampicillin	A9393	Sigma Aldrich
Anhydrous DMSO	276855	Sigma Aldrich
Bovine Serum Albumin	A7906	Sigma Aldrich
CD14 Microbeads, human	130-050-201	Miltenyl Biotec
CytoPainter ER staining kit – red fluorescence	Ab139482	Abcam
CytoPainter Lysosomal staining kit – red fluorescence	Ab112137	Abcam
DAPI (4',6-Diamidino-2-2Phenylindole, Dihydrochloride)	D1306	Thermo Fisher
DharmaFECT 1 Transfection Reagent	T-2001-03	Dharmacon, Horizon - Discovery
Digitonin	Ab141501	Abcam
DMXAA (5,6-dimethylxanthenone-4-acetic acid)	tlrl-dmx	Sigma Aldrich
DTT (DL-Dithiothreitol)	3154	Tocris
ECL Select Western Blotting detection reagent	RPN2235	GE-Healthcare
EDTA (Ethylenediamine Tetraacetate acid)	BP2482-500	Thermo Fisher
Ethidium Bromide	46067	Sigma Aldrich
FBS (Fetal Bovine Serum)	10500	Life Technologies
FBS Ultralow endotoxin	S1860-500	VWR
Ficoll-Pague PLUS	17-1440-03	GE Healthcare

Gateway™ LR Clonase™ II Enzyme mix	11791100	Thermo Fisher
GenElute™ Plasmid Miniprep kit	PLN350-1KIT	Sigma Aldrich
GenElute™ HP Plasmid Midiprep kit	NA0200	Sigma Aldrich
GeneRuler 100bp plus DNA ladder	SM0321	Thermo Fisher
Glycerol	G5516	Sigma Aldrich
GTP (Guanosine 5'-trophosphate sodium salt hydrate)	G8877	Sigma Aldrich
Hoechst 33342 Trihydrochloride nuclear stain	H3570	Thermo Fisher
iScript cDNA Synthesis kit	170-8891	Biorad
Kanamycin sulfate	60615	Sigma Aldrich
L-glutamine	BE17-605E	Lonza
Lipofectamine™ 3000 Transfection reagent	L3000008	Thermo Fisher
LPS from *E.coli*, Serotype R515	ALX-581-007-L002	Enzo
LS columns	130-042-401	Miltenyl Biotec
MEM Non-essential amino acids solution (100X)	1114050	Thermo Fisher
Nano-Glo® Live Cell Assay System	N2012	Promega
NEB 5-alpha Competent *E.coli* (High Efficiency)	C2987/ Lot 205	New England Biolabs
NuPAGE™ Antioxidant	NP0005	Life Technologies
NuPAGE MES running buffer (20X)	NP0002	Life Technologies
NuPAGE Transfer buffer (20X)	NP0006-1	Life Technologies
NuPAGE® Novex® 4-12% Bio-Tris Protein Gels, 1.0mm, 10 well	NP0321BOX	Life Technologies

ON-TARGETplus Non-targeting Pool control siRNA	D-001810-10	Dharmacon
ON-TARGETplus SMARTpool TMEM173 (STING) siRNA	L-024333-02	Dharmacon
ON-TARGETplus SMARTpool Tmem173 (mouse Sting) siRNA	L-055528-00	Dharmacon
ON-TARGETplus SMARTpool TMEM203 siRNA	L-015191-01	Dharmacon
ON-TARGETplus SMARTpool Tmem203 (mouse) siRNA	L-057116-01	Dharmacon
Penicillin / Streptomycin	15140-122	Life Technologies
Pierce™ BCA Protein Assay kit	23227	Life Technologies
PolyFECT Transfection reagent	301105	Qiagen
PrecisionPLUS SYBR mastermix	PrecisionPLUS-iC-SY	Primerdesign
Protease inhibitor cocktail (100X)	P8340	Sigma Aldrich
QuikChange II Site-Directed Mutagenesis kit	200523	Agilent
ReBlot Plus Strong Antibody Stripping Solution, 10X	2504	Merk Millipore
Recombinant human M-CSF	300-25	Peprotech
ReliaPrep™ RNA Minoprep system	Z6012	Promega
RIPA Lysis buffer	R0278	Sigma Aldrich
Restriction Endonucleases	NA	Promega
Restriction buffers	NA	Promega
RPMI-1640 media	31870-025	Life Technologies
siGLO Green Transfection indicator	D-001630	Thermo Fisher
Thapsigargin	T9033	Sigma Aldrich
TO-PRO®-3 Iodide	T3605	Life Technologies

Tris Acetate-EDTA (TAE) Buffer 50X concentrate	SRE0033	Sigma Aldrich
Triton X-100	T8787	Sigma Aldrich
Trypsin-EDTA	25200056	Life Technologies
Viromer Green Transfection reagent	VG-01LB-01	Lipocalyx
B-mercaptoethanol	M3701	Sigma Aldrich
2’-3’ cGAMP	tlrl-nacga23	Invivogen
3’-3’ cGAMP	tlrl-nacga	Invivogen

A2.2 List of Antibodies

Antibody	Target / Clone	Catalog number	Company
CD3 monoclonal antibody, PE	SK7	12-0036-42	eBioscience™
CD14 anti-human Alexa Fluor®700	61D3	56-0149	Affymetrix eBioscience
CD14 anti-human FITC	M5E2	301803	BioLegend
CD19 monoclonal antibody, PE-Cyanine7	HIB19	25-0199-41	eBioscience™
CD62L (L-Selectin) anti-human APC	DREG56	17-0629	Affymetrix eBioscience
CD68 monoclonal antibody unconjugated	PG-M1	MA5-12407	eBioscience™
TMEM173 anti-human rabbit monoclonal unconjugated	TMEM173 aa 250 to the C-terminus	Ab181125/ EPR13130	Abcam
GFP/YFP mouse monoclonal antibody unconjugated	Whole protein	CSB-MA000283	Cusabio
PDHX (E3BP) mouse monoclonal antibody unconjugated	H-6	Sc-377255	Santa Cruz
Polyclonal goat anti-mouse IgG-HRP	NA	P0447	Dako
Polyclonal goat anti-rabbit IgG-HRP	NA	P0448	Dako

A2.3 List of plasmid DNA

The list below describes plasmid DNA used by the primary author (myself). Additional plasmid DNA used in paper 2 can be found in the new manuscript in PNAS, 2019.

Site-directed mutagenesis were carried out by myself using gene-carrying entry vectors as input backbones. After mutation, genes were gateway cloned into pcDNA3.1-DEST vectors or NonBIT Renilla vectors containing either N or C terminal tags.

Vector	Source
pcDNA3.1 gateway destination vector	Empty vector acquired from Invitrogen. Split Venus tag and YFP tag insertions at the N or C terminal of attR cloning sites were produced by E. Kiss-Toth. The WT Tmem203 and Sting were inserted into V1, V2, YFP tagged pcDNA3.1 vector by E. Kiss-Toth. Gateway cloning of mutant Sting insertions into these vectors were made by myself.
pENTR/D entry vector	Empty vector acquired from Invitrogen. The WT Tmem203 and Sting insertions were produced by D. Wyllie. pE-Sting mutants were made by myself.
1.1/2.1 BIT	Empty vector acquired from Promega, NonBIT PPI system, by E. Kiss-Toth. The WT or mutant Tmem203 and Sting insertion between the attR sites were produced by myself and with help from Vera Kiss-Toth.
pEGFP-N2	Plasmid DNA acquired by E. Kiss-Toth.

Appendix 3: Methodology for Chapter 2

A3.1 Bioinformatics

Nucleotide sequences for TMEM203 (human), TMEM173 (human STING), Tmem203 (mouse), Tmem173 (mouse STING) and Tbk1 (mouse TANK-binding kinase, mTBK1) were obtained from GeneBank, NCBI (National Center for Biotechnology Information). Gene and protein accession numbers were obtained from Ensembl and Uniprot, respectively. DNASTAR® Lasergene 14 SeqBuilder was used to create gene maps, predict amino acid sequences, identifying endonuclease restriction sites and design primers for single amino acid mutations. The program SeqMan Pro 14 was used to align nucleotide sequences to verify mutations of plasmids. Uniprot was used to identify the predicted molecular weight of proteins. Genes are listed below in Table 1.

Table 1. List of genes.

Gene	Species	Gene ID	mRNA ID	Protein ID
TMEM203	Human	ENSG00000187713	NP_444273.1	Q969S6
TMEM173 / STING (Canonical)	Human	ENSG00000184584	NP_938023.1	Q86WV6
Tmem203	Mouse	ENSMUSG00000078201	NP_796318.2	Q8R235
Tmem173 / *Sting* (Canonical)	Mouse	ENSMUSG00000024349	NP_082537.1	Q3TBT3

A3.2 Established cell line cultures

RAW 264.7 mouse macrophage cell line is maintained in Dulbecco's Modified Eagle medium (DMEM) supplied with 1% Penicillin-Streptomycin (100 U/ml, P-S), 1% L-Glutamine (0.05 mM, L-G), 10% low endotoxin heat-inactivated fetal bovine serum (LE-HI-FBS); HeLa human cervical cancer cell line is maintained in DMEM supplied with 1% P-S, 1% L-G and 10% HI-FBS; HEK293 T human embryonic kidney cell line is maintained in DMEM supplied with 1% PS, 1% nonessential amino acids (NEAA) and 10% HI-FBS; immortalised bone marrow derived macrophage (iBMDM) cell line is maintained in DMEM supplied with 1% PS, 1% L-G and 10% LE-HI-FBS. All cells lines were purchased from ATCC except for the iBMDM cell line (C57BL/6 background) which was generated as described in [324] and kindly given by David Brough's lab (University of Manchester). All cell lines were maintained in a 37℃ incubator with 5% CO_2. Cells were plated at densities listed below (Table 2) on the day before transfection or treatment to allow attachment.

Table 2. Cell plating format.

Cell line	Cell density	Volume of medium (ml)	Plate format
RAW 264.7	500,000	2	6
HeLa	250,000	1	12
HEK293 T	125,000	0.5	24
	25,000	0.1	96
iBMDM	200,000	2	6
	100,000	1	12
	50,000	0.5	24
	10,000	0.1	96

A3.3 Human primary cell isolation and culture

A 3.3.1 Isolation of PBMC

Healthy and unrelated adult donors (aged 20 to 50 years old) were recruited to provide blood for isolation of peripheral blood mononuclear cells (PBMCs). All blood donors were given written and informed consent under regulation stated in the ethical approval SMBRER310 and in accordance to the Declaration of Helsinki.

PBMC and CD14+ monocyte isolation protocol follows method stated by Hadadi E (PhD Thesis submitted in 2015, University of Sheffield). In essence, blood was collected in 50ml tubes with sterile sodium citrate in a ratio of 9:1 to prevent clotting, and was then carefully transferred into 50 ml tube in 2:1 ratio to and on top of Ficoll-Pague^{TM} Plus (GE Healthcare, Life Sciences). Overlaid blood-Ficoll gradient was centrifuged for 20 min at 900 x g with low acceleration and deceleration rates to separate PBMC layer by buoyancy. The PBMC layer which appears just below the top plasma layer was collected into a clean 50 ml tube and washed with 50 ml cold 1x phosphate-buffered saline (PBS)-ethylenediaminetetraacetic acid (EDTA, 2 mM) (PBS-EDTA; PBSE). The cells were centrifuged (5 mins 1500 rpm) and the pellet was resuspended and incubated for 5 mins at room temperature in 10 ml 1x red blood cell (RBC) lysis buffer (155 mM NH_4Cl, 10 mM $KHCO_3$ and 0.1 mM EDTA) to lyse the erythrocytes by hypotonic pressure. After incubation, cells were washed in 50 ml 1x PBSE and centrifuged for 5 mins at 1500 rpm. The supernatants containing RBC debris was removed and the cells were resuspended in 30 ml 1 x PBSE. Cell number was counted using a haemocytometer (C-Chip, Digital Bio) and the cells were then centrifuged for 5 mins at 1500 rpm to acquire the PBMC pellet for further purification steps.

A3.3.2 Isolation of CD14 positive (+) monocytes

CD14 proteins are abundantly expressed on the cellular surface and are vital for the activation of innate immune responses in mammalian myeloid cells typically monocytes. Thus, they are often used as selection markers for monocyte purification. To isolate monocytes from PBMCs, positive selection was used to tag CD14-expressing monocytes with magnetic microbeads (Miltenyi Biotec). To do so, every 10

million pelleted PBMCs were resuspended in 90 µl magnetic cell sorting (MACS) buffer (1 x PBS, 2% (w/v) low endotoxin bovine serum albumin (BSA), 2 mM EDTA) supplemented with 10 µl CD14 microbeads (Miltenyi Biotech), and incubated for 15 mins at 4 °C to allow microbeads binding to CD14+ cells. The PBMCs were washed in 2 ml additional MACS buffer, centrifuged (5 mins at 1200 rpm), and resuspended in 500 µl MACS buffer to be added to pre-washed (3ml MACS buffer) LS column (Miltenyi Biotec). For magnetic selection, the column was washed with 3 x 3 ml MACS buffer to remove non-magnetic bound cells, and the microbeads-bound cells were immediately flushed down the column with 5 ml cold MACS buffer into a clean collection tube. Cell number was counted again using a haemocytometer and spun down (5 mins 1500 rpm) to acquire a cell pellet for further experimental purposes.

A3.3.3 Determine monocyte purity and viability by FACS

To assess the purity of CD14+ monocytes after isolating all CD14+ cells, samples were prepared in MACS buffer. A sample of 750,000 cells was taken for analysis by fluorescence-activated cell sorting (FACS) using a LSR II flow cytometer (BD Bioscience), and data was analysed by FlowJo_V10 software. Both pre-purified PBMC samples and post-purified CD14+ selected cells were prepared as described in Table 3. Pre-purification PBMCs were singly stained with anti-human CD3-PE (, clone SK7), anti-human CD19-PECyanine7 (eBioscience, clone HIB19), or anti-human CD14-Alexa Fluor®700 (eBioscience, clone 61D3), For each sample, 10,000 cell events were recorded on an arbitrary gate created on a bivariate scatterplot of forward (FSC) vs. side (SSC) to separate cells by sizes and granularities, respectively. The forward and side scattered lights were both adjusted to 275 volts to allow best display of subpopulations of CD14+ cells. Gates were drawn around the subpopulations close to the population boundaries and monocyte population was identified according to gating strategies suggested by Hadadi E (PhD Thesis submitted in 2015, University of Sheffield). An average of over 90% monocytes were identified in total CD14+ population with minor proportions of cell debris, lymphocytes, granulocytes and CD14+ monocyte doublets (Fig. 13). Monocyte responsiveness to immune challenge was tested by phorbol 12-myristate 13-acetate (PMA) treatment which indicates the ability to become active and induce shedding of L-selection (Fig. 14) [325].

Table 3. PBMC and monocyte staining.

Samples	Staining Antibodies	Clone	Fluorophore
Figure 13/ Monocyte purity assay			
Total population	Unstained	N/A	N/A
Dead cells	Hoechst 33342	N/A	Hoechst 33342
T lymphocytes	Anti-CD3	SK7	PE
B lymphocytes	Anti-CD19	HIB19	PE- Cyanine7
Canonical monocytes	Anti-CD14	61D3	Alexa Fluro® 700
Figure 14/ Monocyte activation assay			
Total population	Unstained	N/A	N/A
Dead cells	Hoechst 33342	N/A	Hoechst 33342
Canonical monocytes	Anti-CD14	M5E2	FITC
L-selectin	Anti-CD62L (L-selectin)	DREG56	APC

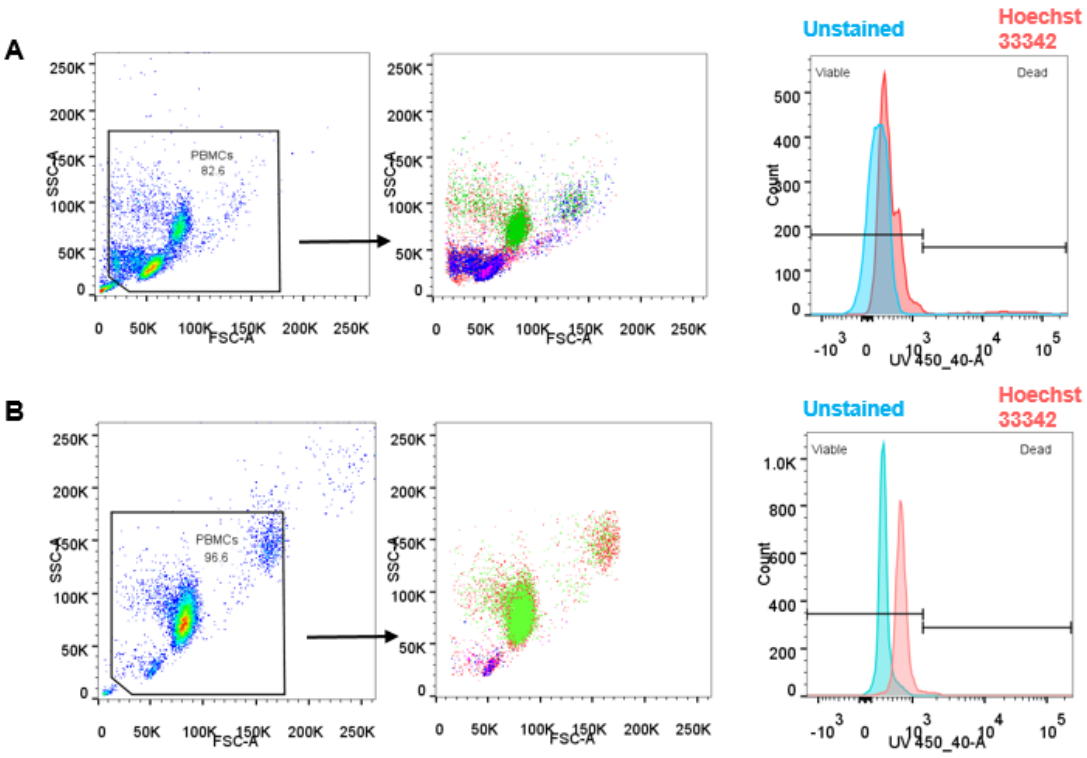

C

		(A) Pre CD14 positive Column Selection		(B) Post CD14 positive Column Selection	
	Sample Name	Count	Frequency of Parent (PBMCs)	Count	Frequency of Parent (PBMCs)
	Unstained_Total PBMCs	11556	100%	10735	100%
	Hoechst 33342_Dead cells	1019	8.82%	424	3.95%
	CD14_Monocytes	2755	23.8%	9681	90.2
	CD19_B lymphocytes	455	3.9%	151	1.4%
	CD3_T lymphocytes	6150	53.2%	200	1.9%

Figure A8. Monocyte identification in peripheral blood mononuclear cells (PBMCs). PBMCs pre (A) and post (B) CD14 positive column selection were analysed by flow cytometry to indicate monocyte purity. PBMCs were left unstained or stained with Hoechst 33342 (UV_450nm activated) to indicate cell death. Hoechst negative (viable) cells were stained with fluorescence-conjugated antibodies against CD14, CD19 and CD3 to identify populations of monocytes, B lymphocytes and T lymphocytes, respectively. Green colour indicates the monocyte population in the forward (FSC) and side (SSC) scatter plot. (C) Frequency of subpopulation of cells were calculated and a reduced ratio of T and B lymphocyte in PBMCs has resulted in over 90% of monocyte purity post CD14 selection. Experiments conducted in monocytes isolated from two donors and the result is representative from a healthy Donor.

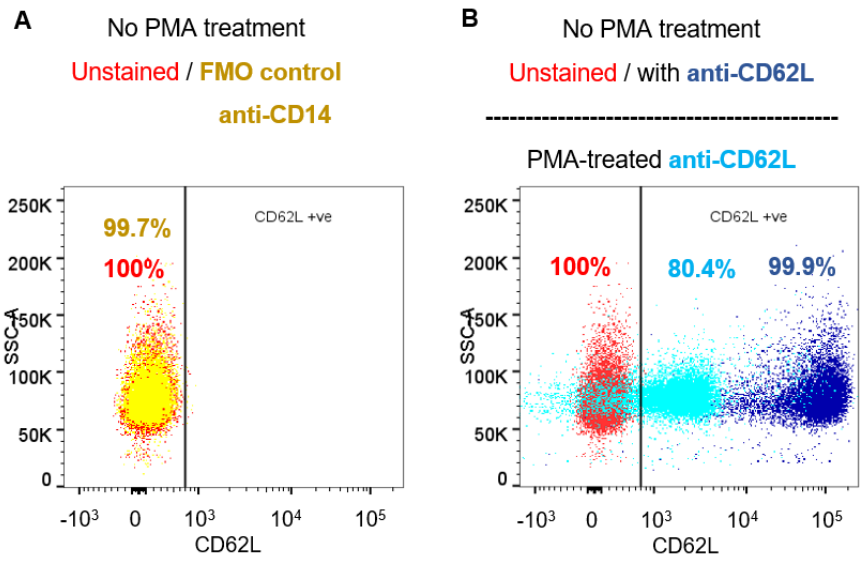

Figure A9. PMA-activated human primary monocytes.

Post CD14 selection, viable monocytes (Hoechst negative) were tested by CD62L (L-selectin) shedding to indicate the ability of activation. (A) Fluorescence minus one (FMO) control: Fluorescence-conjugated CD14 antibodies (Yellow) identifies the total monocyte population (Red) which is CD62L negative (unstained). (B) Total monocyte population (Red) was stained with anti-CD62L (Dark Blue) before PMA treatment; PMA stimulation was able to induce CD62L shedding/reduction in monocytes (Dark Blue to Light Blue), suggesting monocyte activation post CD14 column selection. Experiment conducted in collaboration with Kajus Baidzajevas using monocytes isolated from two donors and the result is representative from a healthy Donor.

A3.3.4 Monocyte maintenance and macrophage differentiation

Primary CD14+ monocytes were temporarily cultured in complete RPMI-1640 medium supplemented with 10% (v/v) LE-HI-FBS (Biowest), 1% PS (Gibco) and 1% L-glutamine before differentiation. Primary monocytes were seeded in 12 well plates at 250,000 ± 5% cells (1.5 ml) per well density to be differentiated into monocyte-derived macrophages (MDMs). Monocytes were differentiated into human monocyte-derived macrophages (MDMs) with RPMI-1640 monocyte medium supplied with 100 ng/ml human recombinant macrophage-colony stimulating factor (hrM-CSF; PeproTech) for 7 days (medium was not changed during incubation). Fresh medium was supplied before further cell treatment.

A3.4 Mouse primary cell isolation and culture

WT and Tmem203 knockout (-/-) C57BL/6 mice were generated by Harwell Institute (Oxford) by CrispR-Cas9 method, and the hind limbs were given to our lab. Genome of Tmem203 was confirmed by Sanger sequencing indicated by MRC Harwell (indicated in Paper 2, Fig. S2F). Femur and Tibia of mouse hind limbs were cleared out from muscles and were truncated at both end so that bone marrow can be eluted and collected using RPMI (10% LE-HI-FBS and 1% P-S) without Phenol Red for visualising in the tube. Bone marrow was centrifuged and replaced with fresh complete DMEM medium (10% LE-HI-FBS, 1% P-S and 10% L929 conditioned medium) to grow for 5 days in T75 flasks in a humid 37 ℃ incubator containing 5% CO_2. Bone marrow-derived macrophages were re-seeded in cell culture plates containing fresh medium before further treatments. BMDMs were seeded at a density of 100,000 cells in 1 ml medium in 12 well plates. Experiments were conducted in duplicate or triplicate wells.

A3.5 STING stimulation

A3.5.1 2’-3’ cGAMP

The endogenous STING ligand 2’-3’ cGAMP was reconstituted in 1xPBS to a concentration of 1µg/µl. Stimulation was performed by mixing the indicated concentrations of ligand with fresh cell culture medium and incubate for indicated periods. Unstimulated control was replaced with fresh medium without 2’-3’ cGAMP.

A3.5.2 3’-3’ cGAMP

the bacterial STING ligand 3’-3’ cGAMP was reconstituted in 1xPBS to a concentration of 1µg/µl. Bacterial cyclic dinucleotides carry two negatively-charged phosphate groups that reduce their ability to penetrate the plasma membrane [326], and thus 3’-3’ cGAMP was aided with the previously suggested Digitonin-permeabilisation method [120, 286, 289, 327]. Stimulation procedure was performed according to Woodward JJ. *et al* [328]. Post differentiation, macrophages were washed twice with ice-cold PBS and pre-incubated with 10 x Digitonin permeabilisation buffer (50 mM HEPES pH 7.0, 100 mM KCl, 3 mM MgCl2, 0.1 mM DTT, 85 mM sucrose, 0.2% BSA, 1 mM ATP, 0.1 mM GTP, with or without 10 µg/ml digitonin) with or without 1 µg/ml 3’-3’ cGAMP for 15-20 mins. Digitonin buffer was thoroughly washed twice with PBS and cells were then supplemented with fresh complete medium and incubated for indicated period of time since initial addition of ligand. Incubation of cells was always at 37°C with 5% CO_2.

A3.5.3 DMXAA

The synthetic STING ligand DMXAA was reconstituted by mixing 10 mg DMXAA in 1 ml solvent 100% dimethyl sulfoxide (DMSO). Stimulation was performed by mixing DMXAA/DMSO in complete cell culture medium and apply to cells. Unstimulated control was replaced with fresh medium containing only DMSO at the same dose as DMXAA stimulation complex.

A3.6 Transfection and stimulation

Each cell type transfection was performed by a specific protocol which has been optimised by our precious laboratory members or myself.

A3.6.1 siRNA Transfection into MDMs and iBMDMs

As STING is an anti-viral adaptor protein, all the virus-derived transfection methods can likely induce STING-dependent antiviral response prior to our investigations, we therefore choose non-microbial derived delivery method that is potent nucleic acid vehicle and is less likely to induce type I interferon response. Delivery of small-interfering RNA (siRNA) into MDMs uses the transfection reagent Viromer Green (Lipocalyx) according to the manufacturer's guidelines. For optimisation of siRNA transfection, siGlo green transfection indicator (Dharmacon, #D-001620-01) was used at the indicated concentrations (Chapter 2 Fig. 4 & Appendix 1.3, page 270). ON-TARGETplus smartpool control non-targeting siRNA and siRNA against human and mouse *TMEM203* / *Tmem203* and STING (*TMEM173* / *Tmem203*) were purchased from Dharmacon. siRNA was diluted to 20µM before being used to transfect cells. For optimised siRNA transfection in MDMs and iBMDMs the concentration was 12.5 nM. For this, 1.4 µl siRNA (20 µM) was mixed with 8.6 µl and added to Viomer green mixture (Buffer green 90 µl added to Viromer green 1 µl) and incubated for 15 mins at room temperature. The transfection complex was applied to 1 well of 2 ml cell culture in 6 well format and the transfected cells are maintained at 37°C in humid 5% CO_2 incubator for 48 hrs before being used in further experiments.

A3.6.2 RAW 264.7 cells

RAW 264.7 macrophages were transfected with plasmids or siRNA using DharmaFECT reagent according to the manufacturer's guidelines. 0.4 µl of DharmaFECT was required to deliver 100 ng plasmid DNA into 25,000 cells in 100 µl transfection volume in a 96 well plate format. The same protocol delivers 20 µM siRNA into RAW 264.7 cells.

A3.6.3 HEK293 cells

HEK 293 cells were transfected with plasmids using PolyFECT reagent according to the manufacturer's guidelines. 1 µl of PolyFECT was required per 100 ng plasmids for transfection into 25,000 cells in 100 µl transfection volume in a 96 well plate format.

A3.6.4 HeLa cells

HeLa cells were seeded in the centre of glass-bottom imaging dish (35 mm diameter, glass area 10 mm diameter) at 300,000 cells in 100 µl DMEM medium (10% LE-HI-FBS and 1% P-S) and incubated for 1 h to allow adherence. After this, cells were further supplied with 1.5 ml complete medium and leave overnight before transfection. A total of 1.5 µg of plasmid DNA was resuspended in 490 µl of serum-free medium and incubated with 10 µl P3000 and 3 µl 3000 Reagent, provided in Lipofectamine3000 transfection kit, for 30 mins at room temperature. The mixture was supplied with 1 ml complete medium to transfect HeLa cells for 24 hrs before further studies.

A3.7 Gene expression analysis

A3.7.1 RNA isolation

Total RNA isolation from cells was preformed using ReliaPrep™ RNA Cell miniprep system (Promega). Post treatment, cell medium was aspirated and cells were washed twice with PBS before being lysed with BL-TG buffer and isolated according to the manufacturer's protocols. RNA concentrations were determined using NanoDrop™ 1000 microvolume Spectrometer (Thermo Fisher).

A3.7.2 Complementary (c)DNA synthesis

Complementary DNA was produced from total RNA using iScript™ cDNA synthesis kit (Biorad). 500 ng total RNA was mixed with 1 µl Reverse Transcriptase and 4 µl reaction master mix in a total volume of 25 µl. The mixture was reacted on a Bioer LifeECO™ PCR Thermal Cycler at 25℃ for 5 mins, 46℃ for 20 mins, 95℃ for 1 min and maintained at 4℃ until it is used for further treatment.

A3.7.3 Quantitative Real-Time Polymerase Chain Reaction (qPCR)

Quantitative PCR was performed in triplicate wells and quantified in CFX384 Touch™ real-time PCR iCycler (Biorad). Reaction mixture contains 4.4 µl cDNA (0.5 ng/ml), 5 µl mastermix, 0.3 µl forward primer (10 µM) and 0.3 µl reverse primer (10 µM). Mixture was reacted with hot start (95℃ 2 mins) followed by 40 cycles of amplification (95℃ 10 secs + 60℃ 60 secs), and a final melt curve was determined by an additional amplification process. The primer sequences used for mRNA level quantification were shown in Table 4. Primers are designed with Blast primer design tool (NCBI) and all sequences were generated by Sigma-Aldrich unless otherwise specifies.

For analysis of relative gene expressions, C_t values of interest genes were normalised to the C_t values (expression levels) of β-actin and were calculated using the $2^{(-Ct)}$ method. Gene expressions were compared to the indicated control group designed for each experiment. Analysis of gene expression by genome equivalent method is described in Chapter 4, Material and Methods, RNA, standard and Real-Time quantitative PCR.

Table 4. List of primers used in qPCR reaction.

Human Gene	Primer sequences
β-ACTIN	Forward 5' - GGATGACAGAAGGAGATCACT G – 3' Reverse 5' - CGATCCACACGGAGTACTTG – 3'
Cxcl8 (IL-8 gene)	Forward 5' - TGCCAAGGAGTGCTAAAG – 3' Reverse 5' - CTCCACAACCCTCTGCAC – 3'
IFN- β	Forward 5' - AAGCAGCAATTTTCAGTGTCAGA – 3' Reverse 5' - CCTCAGGGATGTCAAAGTTCA – 3'
TMEM203	Forward 5' - GTCTTCGAGATGCTGTTGTGC – 3' Reverse 5' - ACGTAATGAGGCCGAACCAG – 3'
STING	Forward 5' - TCTCGCAGGCACTGAACATC – 3' Reverse 5' - GGGCCACGTTGAAATTCCCT – 3'
MAVS	Forward 5' - TGCCTCACAGCAAGAGACCA – 3' Reverse 5' - CCGCTGAAGGGTATTGAAGAGA – 3'

Mouse Gene	Primer Sequences
β-actin	Forward 5' - GGGACCTGACAGACTACCTCATG - 3' Reverse 5' – GTCACGCACGATTTCCCTCTCAGC – 3'
Tmem203	Forward 5' – CCCTGTTGGTGTTCTCCGTA - 3' Reverse 5' – GCACAAAGACGTTCCACCAG - 3'
Sting	Forward 5' – GCTGGCATCAAGAATCGGGT - 3' Reverse 5' – TACTCCAGGATACAGACGCC - 3'
Ifnb1	Forward 5' – TGTCCTCAACTGCTCTCCAC - 3' Reverse 5' – CATCCAGGCGTAGCTGTTGT - 3'
Cxcl2	Forward 5' – ATCCAGAGCTTGAGTGTGACG - 3' Reverse 5' – TTTGACCGCCCTTGAGAGTG - 3'

A3.8 Western blot

A3.8.1 BCA protein concentration assay

To prepare protein samples, cells were washed with 1x PBS and lysed with RIPA buffer (Sigma Aldrich) containing 10% protease inhibitor. Every 250,000 cells were then lysed by 200µl RIPA-protease inhibitor mixture on ice for >30 mins with multiple vigorous vortexing, and 15 min sonication. Samples were centrifuged for 10 mins (14,000 rpm at 4℃) to remove membrane debris and supernatants were collected for protein assay. Pierce BCA protein assay (Thermofisher) was performed to determine protein concentration in the lysate according to the manufacturer's guideline. Lysates were diluted to a concentration of 5 µg per 10 µl with 1x Laemmli buffer (4% SDS, 10% 2-mercaptoethanol, 20% glycerol, 0.004% bromophenol blue, 0.125 M Tris-HCl, pH 6.8).

A3.8.2 SDS-PAGE

Total protein separation was performed by SDS-PAGE (Sodium Dodecyl Sulfate PolyAcrilamide Gel Electrophoresis). 5 µg (in 10 µl) of each protein sample or 5 ul of protein ladder was loaded into each well of the pre-cast NuPAGE 4%-12% Bis-Tris Protein Gels, 1.0 mm, 12-well (Thermo Fisher). Empty wells were filled with 10 µl of 1x Laemmli buffer. The gel was transferred to the electrophoresis tank filled with 1x NuPAGE MES SDS Running Buffer to run for 1.5 - 2 h at 150-200 V.

A3.8.3 Western blot

Following electrophoresis, proteins were transferred to methanol-activated positively charged PVDF nylon membrane followed by antibody detextion. Protein-blot transfer sandwich (negative electrode – 2 sponges / 2 filer papers / Gel / PVDF membrane / 2 filter papers / 5 sponges – positive electrode) was placed in the Western blot tank filled with 1x NuPAGE Transfer Buffer supplemented with 10% (v/v) methanol and 1 ml NuPAGE antioxidant. Proteins were transfer for 1 h at 40 V.

To blot for specific proteins, membranes were rinsed with 1X Tris buffered saline (TBS) – 0.1% (v/v) Tween-20 (TBST) and then blocked with 10% (w/v) skimmed milk in TBST for 1 h at room temperature. Post blocking, membrane was rinsed 4 times with TBST

for 5 mins and then incubated with primary antibodies diluted in 5% milk-TBST on 4°C overnight. Primary antibodies were rinse off the next day with 5 mins – 4 times TBST, and the HRP conjugated secondary antibodies were applied in 5% milk-TBST to incubate the membrane at room temperature for 1 h. At the end, secondary antibodies were rinsed by 5 mins - 4 times with TBST. Antibody concentrations were listed in Table 5.

To detect proteins, the membrane was incubated for 2 mins with chemiluminescence followed by visualisation under a C-DiGit ® Western Blot Scanner (LI-COR). Signal of secondary antibodies can be strapped off by incubation in 1x ReBlot Plus Strong antibody stripping solution (Merk Millipore) for 10 mins at room temperature. The membrane can be re-blocked and blotted with another primary and secondary antibody to detect different proteins. Protein bands were quantified using Image Studio Digit Version 5. Data were normalised to the loading control.

Table 5. Antibody concentrations used in Western blotting.

Antibody	Concentration
GFP/YFP mouse monoclonal antibody unconjugated	1:4000
PDHX (E3BP) mouse monoclonal antibody unconjugated	1:8000
Polyclonal goat anti-mouse IgG-HRP For YFP detection	1:2000
Polyclonal goat anti-mouse IgG-HRP For PDHX detection	1:4000

A3.9 Molecular cloning

A3.9.1 Site-directed mutagenesis

Single-amino acid mutation was performed using QuikChange II Site-Directed Mutagenesis kit (Agilent) following the manufacturer's protocol. The Wildtype gene has already been cloned into pENTR/D-TOPO® vector (Thermo Fisher) between the attL1/attL2 region. The entry clone also contains Kanamycin resistance gene for bacterial selection. In brief, each mutagenesis was reacted with 100 ng entry plasmid vector, 125 ng of each oligonucleotide primer, and the rest of the reagents provided by the kit. Forward and reverse primers were designed for each mutation with the tri-nucleotide substitution in the middle to change single amino acid, and 15-nucleotide long sequence at each side of mutation (total 33 bp in length). Primers were generated by Sigma Aldrich and were used at the recommended concentration as according to the Mutagenesis kit protocol. Primer sequences for Sting truncation mutants were stated in Chapter 2 Materials and Methods: Site-directed Mutagenesis and molecular cloning. Polymerase chain reaction (PCR) cycling condition is detailed in Table 6 (modified from the manufacturer's protocol). The resulting plasmid products were transformed into XL10-Gold ultra-competent cells following the manufacturer's instructions (Agilent). Mutations of Sting was confirmed by Sanger sequencing as shown in Appendix 1.4 (page 271).

Table 6. Agilent site-directed mutagenesis guideline protocol for polymerase chain reaction.

Segment	Cycles	Temperature	Time
1	1	95℃	2 mins
2	25-30	95℃	20 sec
		60℃	10 sec
		68℃	1 min/ kb of plasmid length*
3	1	68℃	5 mins

*For example, a 5 kb plasmid requires 5 mins per cycle at 68℃. The temperature of this step can be optimised to help the amplification of desired plasmids.

A3.9.2 Ligase recombination

Mutated genes inside the Gateway Entry clones were further cloned into a Gateway Destination vector [329] containing split Venus tag, or Yellow Fluorescence Protein (YFP) tag [330], or split Renilla BIT tags (modified from the commercially available BIT system, Promega) which are later used for expression in mammalian cells. Ligase recombination of gene cloning into Gateway Destination vectors uses Gateway™ LR Clonase™ II Enzyme Mix (Invitrogen). Reaction was performed according to the manufacturer's protocol. In brief, 10 ng (1 µl) of entry clone plasmid carrying the designed gene was mixed with 100 ng (1 µl) Gateway Destination vector and 0.5 µl of LR Clonase II to incubate for 1 h at 25 °C. Reaction was terminated by mixing with 1 µl proteinase K and incubating for 10 mins at 37 °C. Destination vectors were transformed into one vial of 45 µl of NEB 5-alpha Competent *E. coli* (High Efficiency) (New England Biolabs) according to the manufacturer's (New England Biolabs) protocol.

A3.9.3 Bacteria transformation and plasmid preparation

To transform Gateway Entry Clones into XL10-Gold ultracompetent cells, a vial of 45 µl *E.coli* was taken out of -80°C freezer and immediately and gently thawed on ice. Cells were treated with 2 µl of β-mercaptoethanol (provided with the kit) for 10 mins, and were further added 2 µl of Dpn I-treated plasmid products (enzyme provided with the kit, 1µl Dpn I was used to digest 1 tube of PCR reaction for 15 mins at 37 °C). Mixture was gently swirled and incubated on ice for 30 mins followed by an exact 30 sec heat-shock at 42°C before being recovered on ice for 2 mins. Mixture was then transferred to a 15 ml Falcon tube containing 0.5 ml of warm SOC growth medium (Super Optimal Broth, Invitrogen) and incubated at 37 °C for 1 hour with shaking at 240 rpm. By the end, 100 µl of bacterial culture was plated onto a warm LB-Kanamycin (50 µg/ml) agar plate and incubated upside down (to avoid drying the agar by water evapouration) at 37 °C for a further 16-20 hours before colonies were selected for further use.

To transform Gateway Destination clones into NEB 5-alpha Competent *E.coli* (High Efficiency), plasmids were mixed and incubated with one unit (45 µl) of bacteria pre-thawed on ice. This is followed by exactly 30 sec of heat-shock at 42 °C and 2-5 mins

recovery on ice. Cells were then supplemented with 1 ml warm SOC growth medium and cultured at 30℃ for 90 mins. 150 µl of bacteria were evenly spread on a warm LB-Ampicillin agar plate (100 µg/ml) and incubated upside down at 30 °C for 16 – 20 hours before bacteria colonies were selected for further use.

Post transformation, six colonies per mutation were selected for amplification in 3 ml SOB broth (Super Optimal broth, 32 g Tryptone + 20 g Yeast extract+ 5 g NaCl heat-dissolved in 1 L ddH_2O) containing the appropriate antibiotics) at 30 °C for 18-24 hours to obtain enough cells for plasmid isolation (Sigma Aldrich).

A3.9.4 Plasmid sequence verification

To ascertain the correct plasmids were amplified, plasmid DNA was digested with restriction endonucleases (Promega) in the suggested digestion buffer for 1 to 1.5 hours at 37 °C. Briefly, 5 µl of plasmids (over 500 ng) were used in each digestion with 1 or multiple enzymes at a total volume of 10 µl or 15 µl according to the manufacturer's suggestions. Plasmid digestion was checked by DNA gel electrophoresis. Plasmid samples were diluted 1:5 with sample loading dye (0.25% bromophenol blue, 30% glycerol in ddH_2O) and loaded into the wells of a 10% agarose gel (1:50 ddH_2O diluted 50x TAE (Tris Acetate-EDTA) with 10% w/v agarose powder, both Sigma Aldrich) containing 0.5 µg/ml ethidium bromide, with 1x TAE as the running buffer. The GeneRuler 100bp plus DNA ladder was used to indicate the size of the digested DNA products. DNA was separated at 80-90 V for 40 to 50 mins and the gel was visualised and captured under the UV lamp in InGenius3 gel imaging and analysis system (SYNGENE). Once DNA fragments were confirmed at the expected lengths, plasmid samples were sent for sequence confirmation at Sanger sequencing labs of Source Bioscience (Nottingham). Reaction primers were provided by the sequencing lab according to the construct. Specific primers designed for plasmids constructed for split-Renilla protein complementary assay were purchased from Sigma Aldrich.

Primer used for sequencing genes in the Entry Clones were (5'-3'):
Forward: M13F, TGT AAA ACG ACG GCC AGT
Reverse: M13R, CAG GAA ACA GCT ATG ACC

Primers used for sequencing genes in the V1 and YFP fusion Destination Clones were (5'-3'):
Forward: CMVF_pCDNA3, CAA CGG GAC TTT CCA AAA TG
Reverse: BGH Reverse, TAG AAG GCA CAG TCG AGG

Primers used for sequencing genes in the BIT fusion Destination clones were (5'-3'):
Forward: CCC TGT TGG TGT TCT CCG TA
Reverse: GCA CAA AGA CGT TCC ACC AG

One correct Entry Clone per mutation was selected for further cloning process and one correct Destination Clone per mutation was selected for transformation and amplification.

A3.9.5 Bacteria amplification and stock

To maintain bacteria culture for further use, 0.5 ml of overnight bacteria culture is thoroughly mixed with 40% glycerol and kept at -80 °C for later use.

To amplify plasmids, bacteria colonies or glycerol stock (20% glycerol in growth medium) were added to 3-5 ml SB buffer for small quantity plasmids preparation or to 50 ml LB buffer (10 g Tryptone + 5 g Yeast extract + 5 g NaCl heat-dissolve in 1 L ddH_2O) for medium quantity plasmid preparation. All bacteria cultures were supplied with 50 µg / ml Kanamycin or 100 µg / ml Ampicillin according to the plasmid antibiotics selection condition and cells were incubated at 30℃ for 18 – 24 h.

A3.9.6 Plasmid isolation

Small quantity plasmid purification was carried out using GenElute™ plasmid Miniprep kit and medium quantity plasmid purification was carried out using GenElute™ HP Plasmid Midiprep kit, both from Sigma Aldrich. Plasmid concentration was determined using NanoDrop™ 1000 microvolume Spectrometer (Thermo Fisher) and were at least 80 ng/ml.

A3.9.7 Plasmid maps

Plasmid maps are shown in Figure 15. The split Renilla fusion plasmids were constructed using NanoBiT ® PPI MCS Starter system vectors (Promega, UK) which allowed the Tmem203 and Sting genes in the entry clones to recombine into the multiple cloning sites by LR Recombinase reaction (Invitrogen), creating either the N terminal or C terminal fusion of LgBiT (2.1) or SmBiT (1.1). The plasmids were selected on 100 µg / ml Ampicillin according to the manufacturer's protocol.

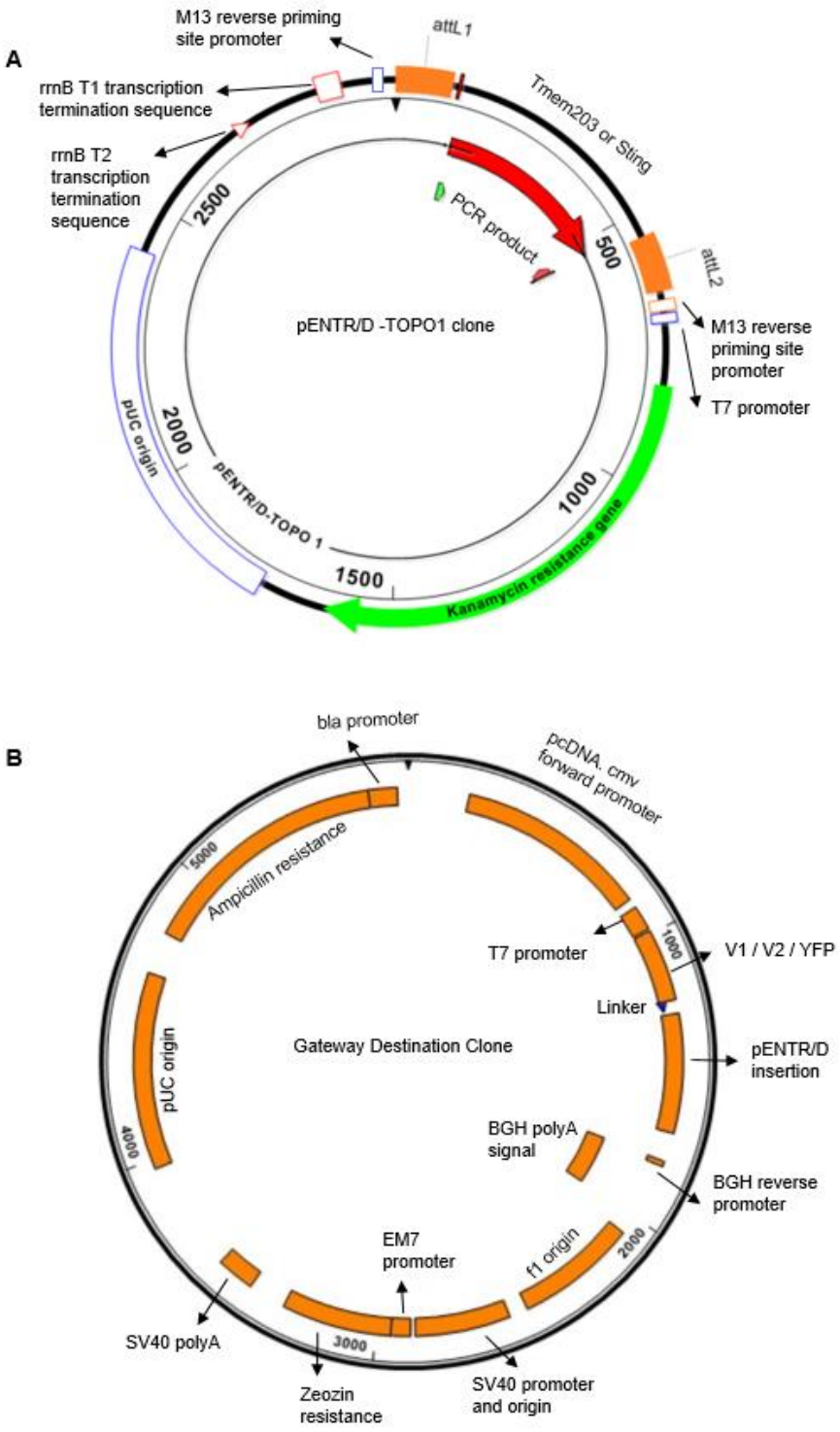

Figure A10. Circular map for (A) pENTR/D-TOPO1 clone and (B) Venus and Yellow fluorescence protein fusion Gateway Destination clones.

Desired genes such as Tmem203 and Sting are cloned from pENTR/D vectors into the pENTR/D insertion site in the Gateway Destination vector.

A3.10 Protein complementation assay (PCA)

A3.10.1 Split Venus fluorescence system

Venus protein is a derivative of Green Fluorescent Protein (GFP) with enhanced fluorescence. The Venus is split into a large part V1 and a small part V2. Each tag was expressed in the Gateway Destination vectors which are clones with the desirable genes to create fusion proteins. For Venus-reporter PCA, HEK293 T cells were plated and transfected with the indicated methods described in Appendix 3.6.3. Cells were transfected with the recommended amount of a single plasmid per well, or half amount of each plasmid for co-transfections. A single transfection of V1 fusion protein was used as control transfection. 18 - 24 h post transfection, cells were washed with 1x PBS before further treatment.

Flow cytometry was performed to identify Venus fluorescence-positive cell population. Post treatment, HEK293 cells were gently and thoroughly washed with PBS and detached by resuspending in 0.5 ml FACS buffer (5% (v/v) FBS in PBS). Samples were maintained on ice until process. Samples were run on a bivariate forward (FSC) vs. side (SSC) scatterplot using BD^{TM} LSRII Flow Cytometer (BD Bioscience). After identifying the major cell population, 2 µl of the nuclear dye TO PRO-3 (0.2mM, Red 660nm laser, Thermo Fisher) was added to 0.5 ml cells to identify cell death (TO PRO-3 positivity). Blue 530nm laser was used to excite Venus fluorescence expressed in cells. Successful interaction between proteins would result in the formation of GFP signal from V1 and V2 tags, and should result in a positive shift of GFP signal in the histogram. 10,000 cell events were recorded for each sample. Geometric mean for the histogram of GFP expression was used to determine signal strength.

Venus PCA transfected into HeLa cells for imaging Tmem203-Sting localisation on intracellular organelles were transfected as described in Appendix 2.6.4, and the images were acquired and analysed by confocal microscopy as described below (Appendix 3.11.2).

A3.10.2 Split Renilla luciferase reporter system

Renilla signal is split into a large part named 2.1 and a small part named 1.1. For split Renilla-reporter PCA, HEK293 T cells were seeded at a density of 25,000 cells per 100 µl in 96 well plates the day before transfection to allow attachment. Cells were transfected with a total of 100 ng of plasmid DNA per well, or 50ng each for co-transfections using PolyFECT transfection method as described in Appendix 3.6.3. Empty vector Nano-BIT was used as negative control plasmid. 2.1 N RelA and 1.1 C IκBα was transfected as positive control. Cells were used in experiments 18 - 24 h post transfection.

To assess protein interaction from Renilla PCA, old medium was aspirated from the cell culture and the plate was washed with 50 µl of PBS. Each well was detached by resuspension in 50 µl of colourless sterile trypsin-EDTA (0.25% in PBS) and were transferred to a non-transparent white 96 well plate. Plate was sealed and centrifuged at 1000 rpm for 3 mins, and PBS was replaced with 50 µl colourless DMEM (10% HI-FBS) to attach cells to the bottom. To measure Renilla activity, 25 µl of Renilla substrate mixture (1:19 Substrate to buffer ratio as suggested by Nano-Glo live assay system, Promega) was added to each well with 5 mins incubation at 37℃ prior to stimulation and luciferase assessment. Renilla-catalysed substrate breakdown and luminescence was measured by 37℃ -controlled Varioskan plate reader (Thermo Fisher, version: 4.00.53) in the absence of ligands and were measured repeatedly with stimulations at the indicated times. DMXAA and 2'-3'cGAMP were added in 5 µl volume per well to achieve the total concentration of 50 µg/ml and 10 µg/ml, respectively. Interaction between 2.1 N RelA and 1.1 C IκBα was measured at the time points to indicate the rate of signal deterioration. By the end, cells were stained with Hoechst 33342 (0.002 nM) for 5 min to indicate cell numbers, which is used for Renilla normalisation. Measurement lasts a maximum of 30 mins to prevent extensive cell death.

To calculate Renilla luciferase activity of each well:

$$\text{Renilla luciferase activity} = \frac{(\text{luminescence of treatment} - \text{luminescence of NanoBIT})}{(\text{Hoechst of treatment} - \text{Hoechst of unstained cells})}$$

A3.11 Fluorescent microscopy

A3.11.1 Fluorescent imaging for human macrophages

To determine green indicator siGlo transfection efficiency into human primary monocyte-derived macrophages (MDM), macrophages were transfected with the indicated amount of siGlo (Dharmacon, GE Healthcare) using Viromer Green transfection reagent as instructed by the manufacturer (Lipocalyx). 48 hours post transfection, culture medium was aspirated and replaced with warm colourless RPMI (1% PS and 10% LE-FBS). MDMs were imaged using a Leica AF6000 time lapse fluorescent microscope with 37℃ temperature control.

To identify macrophage marker CD68 expression, primary monocytes were seeded in 8 well chamber slides at a density of 200,000 cells per 400µl RPMI-1640 (1% PS and 10% LE-FBS) and differentiated into macrophages with 100 ng/ml human recombinant M-CSF as described previously. Differentiated MDMs were washed twice with PBS and fixed with 4% formalin for 30 mins at 37℃. Cells were again washed three times with PBS and permeabilised with 0.1% Triton x100 in PBS for 15 mins. Cells were washed five times with 1x PBS to thoroughly remove Triton, and then blocked with 2% BSA-PBS for 45 mins at room temperature. After blocking, macrophages were changed into 1% BSA-PBS mixed with either 2 µg/ml primary mouse anti-CD68 (Dako) for specific binding, or 2 µg/ml anti-CD68 isotype (Dako) for non-specific binding control, or 1% BSA-PBS only for secondary antibody only control. Macrophages were incubated at 4℃ overnight. On the next day, cells were washed 3 times with PBS and incubated with 2 µg/ml goat anti-mouse secondary antibodies in 1% BSA-PBS for 1 h at room temperature. Macrophages were washed five times with PBS, mounted with vector shield containing DAPI, and dried at room temperature in dark for at least 30 mins before imaging. Samples were imaged under Leica AF6000 time lapse fluorescent microscope.

Images of each experiment were acquired at the indicated and consistent magnification, light exposure, gain and intensity.

A3.11.2 Imaging for protein complementation assay

For organelle staining, HeLa cells were plated into glass-bottom petri dish and transfected with plasmids as stated in Appendix 3.6.4. Post transfection, cells were washed three times with PBS and incubated with either CytoPainter ER staining kit – red fluorescence (Abcam) or CytoPainter Lysosomal staining kit – red fluorescence (Abcam) for 10 min at 1:5 and 1:3 dilutions (with 1x PBS), respectively. Cells were then washed three times with PBS and recovered at 37℃ for 30 mins in warm colourless DMEM (1% PS and 10% HI-FBS). Control cells were maintained in warm colourless DMEM until imaging. Cells were then imaged with confocal microscopy on a Zeiss LSM 510 META with 40X inverted water-lens (Molecular Probes) with 30℃ temperature control. Both ER and lysosomal staining were excited at light wavelength of 565/615 nm, and Venus fluorescence obtained from Tmem203-Sting interaction PCA expression was excited at 500/520 nm.

To image Tmem203-Sting localisation on the ER and lysosomes, HeLa cells were attached, transfected with plasmids, and stained with organelle dyes as described in Appendix 3.6.4 and 3.10.1. HeLa cells were imaged with confocal microscopy on a Zeiss LSM 510 META with 40X inverted water-lens (Molecular Probes) with 30℃ temperature control. A tilescan of GFP signal (Venus reconstitution) was produced for each sample so that 12 to 15 areas could be selected for better analysis (a demonstration of a tilescan is shown in Figure 16). Fifteen images were captured per sample and two independent experiments were carried for each condition. Images were analysed with Fiji_ImageJ [331]. Individual cells were analysed as shown in Figure 17.

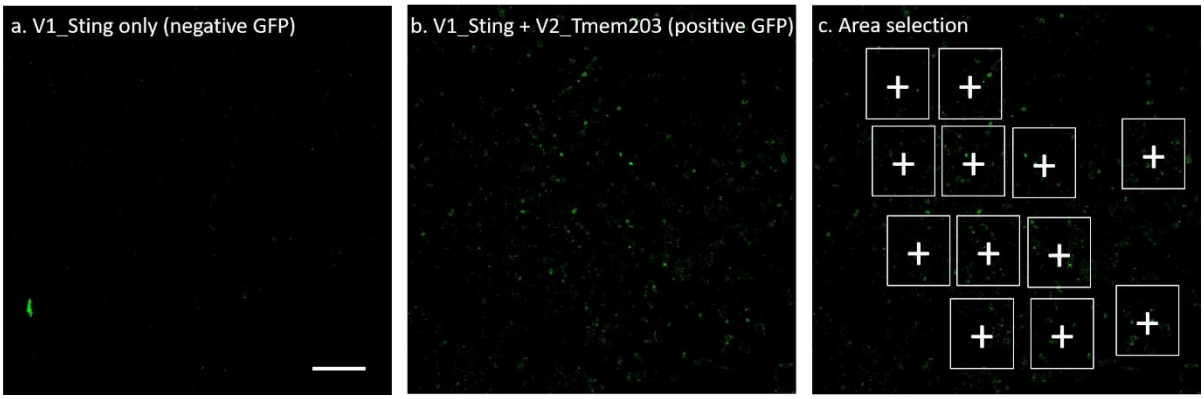

Figure A11. Area selection for confocal microscopy of split Venus protein complementation assay of Sting - Tmem203 interaction.

Glass-bottom culture dish with HeLa cells was scaned under a Zeiss confocal microscope. A 5x5 area was selected for tilescan to produce a map of cells with weak but clear GFP signal. Transmission light phase was omitted to avoid fluorescence bleaching for later steps. Little and non-specific GFP signal shown in a. demonstrates a negative V1_Sting single transfection whereas positive GFP generated from V1_Sting and V2_Tmem203 interaction was shown in b. To prevent bias of result interpretation, 12 – 15 non-overlaping areas per dish were selected to be analysed in higher magnifications and resolutions, such as in c. Each selection area provides a view of 10-20 HeLa cells (although some were on the edge of view) which were captured for image analysis as shown in Figure 17. Scale bar is 100 µm.

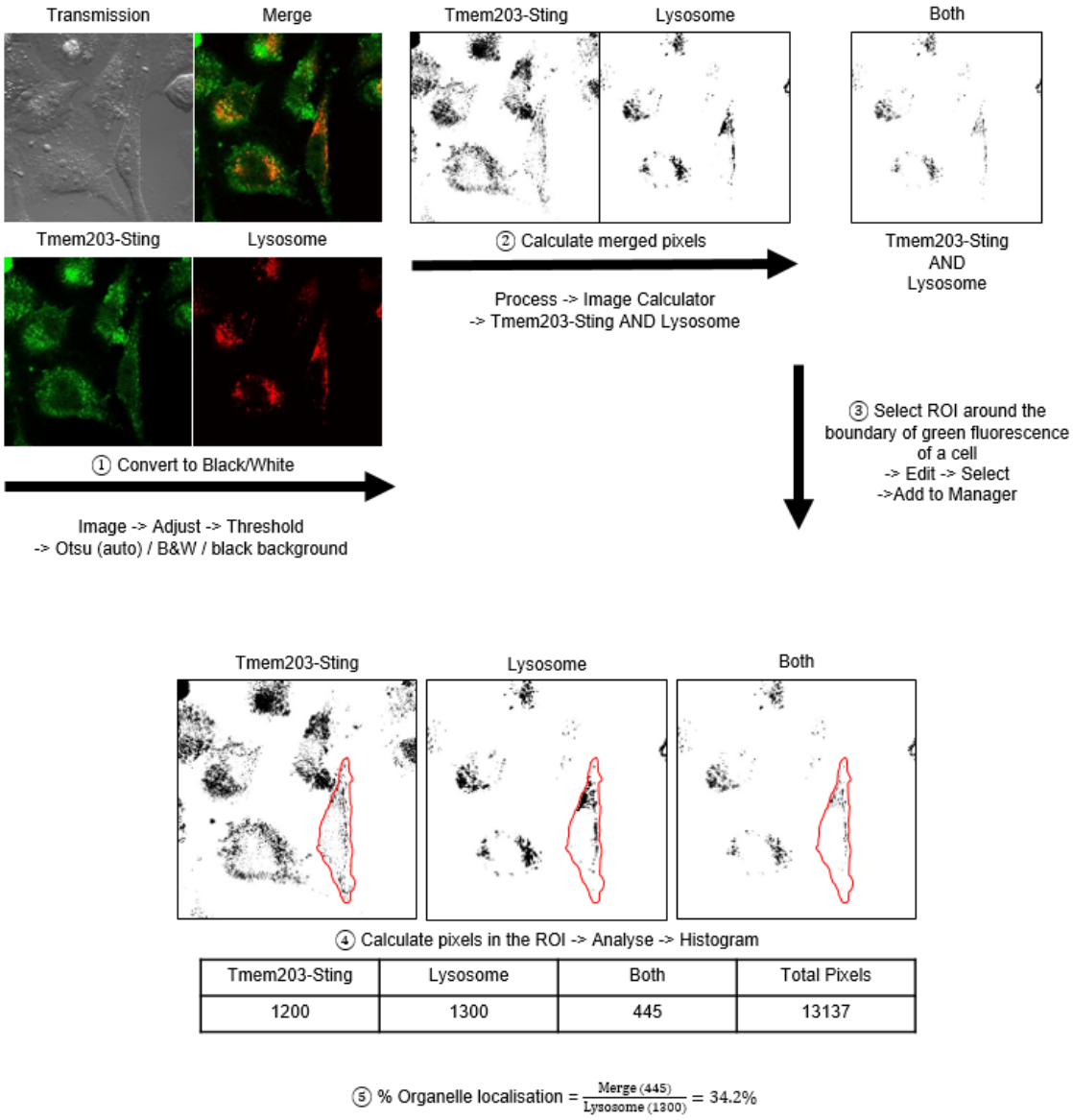

Tmem203-Sting	Lysosome	Both	Total Pixels
1200	1300	445	13137

Figure A12. Demonstration of imaging analysis using Fiji.

① After acquiring images, the transmission (Cell), green (Tmem203-Sting), red (Lysosome) and the merged images were created. Convert the green and red channels to Black/White for analysis. ② Calculate the common (Both) pixels of the green and red channels. ③ Analyse cells individually. Select the region of interest (ROI) around the boundary of green fluorescence (Tmem203-Sting co-expression) of a cell and add the selection to ROI manager. ④ Calculate the number of pixels for each channel and the Both pixels in the ROI. ⑤ Calculate the ratio of Tmem203-Sting expression on the lysosome (Both)) over the detection of lysosome to obtain the percentage of lysosomal expression of Tmem203-Sting. Only the whole-bodied cells were analysed to avoid generation of false-positive results and over-calculation.